The role of urotensin-II in atherosclerosis and ischemic cardiomyopathy

Nicolas Bousette
Department of Experimental Medicine
McGill University, Montreal, Quebec, Canada
January 2007

A thesis submitted to the faculty of graduate studies and research as partial fulfillment of requirements for the degree of Doctor of Philosophy (Ph.D)

Your file Votre référence
ISBN: 978-0-494-32295-6
Our file Notre référence
ISBN: 978-0-494-32295-6

Abstract

Atherosclerosis, a vascular disease which may lead to coronary artery occlusion and consequent myocardial infarction is primarily caused by dyslipidemia. Ischemic cardiomyopathy due to atherosclerosis is the leading cause of morbidity and mortality in the western world today. Vasoactive factors are increasingly being recognized not only as contributors to atherosclerotic plaque formation, but also to cardiac function and remodeling following ischemic cardiac injury. Urotensin II (UII) is one such vasoactive factor. UII possesses a wide range of cardiovascular effects, from contraction of the rat aorta to complete cardiovascular collapse in cynomolgus monkeys. UII binds a seven transmembrane spanning G-protein coupled receptor termed UT. Expression of UII is significantly elevated in the hearts of patients with congestive heart failure (CHF). Recent reports have also shown increased plasma levels of the peptide in patients with CHF, and these levels correlated with the severity of the disease. This project was designed to investigate the role of UII and UT in both atherosclerosis and CHF. To this end, UII expression was evaluated both in a model of CHF in the rat, and in human atherosclerosis of the carotid arteries and aortae. Furthermore, the pathophysiological role of urotensin-II in CHF was investigated, with the use of a selective UII antagonist, SB-611812. Finally, genetically modified mice deficient in either ApoE, UT, or both genes, were evaluated to study the role of UII/UT signaling in a model of atherosclerosis. We found that UII and its receptor, UT, were both significantly elevated in a model of CHF induced by coronary artery ligation. UII antagonism significantly

attenuated mortality, cardiac dysfunction, and hypertrophy. This was associated with a significant decrease in cardiac fibrosis. We next went on to demonstrate that UII and UT were significantly elevated in human atherosclerotic carotid arteries and aortae. Finally, we demonstrated that deletion of the UT gene in mice deficient for ApoE exacerbates atherosclerosis of the aorta. Furthermore, this was associated with significantly increased hyperlipidemia and organ hypertrophy as well as significantly reduced body mass, liver mass, and hepatic steatosis.

In conclusion we were the first to demonstrate a pathophysiological role for UII in cardiovascular diseases which may lead to a breakthrough in the management of CHF and may also give more insight into the pathogenesis of atherosclerosis.

Resume

Athérosclérose, une maladie vasculaire qui peut conduire a une obstruction de l'artère coronaire, et, par conséquent, une infraction myocardite, est causée principalement par des niveaux élevés de lipides. La cardiomyopathie ischémique due a l'athérosclérose est la cause principale de l'état morbide et mortalité dans les pays occidentaux d'aujourd'hui. Cependant, les facteurs vasoactifs sont de plus en plus reconnus, non seulement comme contributeurs a la formation de plaques d'athérosclérose, mais également un facteur de la fonction cardiaque et a la reconstitution suivant une lésion cardiaque. Urotensin II(UII) est l'un de ces facteurs vasoactifs. UII possède une large variété d'effets cardiovasculaires, depuis la contraction de l'aorte chez le rat jusqu'à l'affaissement cardiovasculaire total chez le singe cynomolgus.

UII s'associe avec le récepteur UT, qui est un récepteur du type serpentine. L'existence de l'UII est élevée de façon signifiante dans le coeur des patients souffrant de congestion insuffisance cardiaque. De récents rapports ont aussi démontré un accroissement des niveaux de UII dans le plasma chez les patients ayant une défaillance cardiaque (DC), et, ces niveaux correspondent avec la sévérité de la maladie. Ce projet était destine a la recherche du rôle de UII et l'UT dans les cas de l'athérosclérose et DC.

De ce fait, UII expression fut évaluée a la fois dans un modèle de DC chez le rat, ainsi que l'athérosclérose des artères carotides et aorte chez l'humain. De plus, le rôle pathophysiologique de l'urotensin-II dans le DC fut le sujet d'une investigation, avec l'utilisation d'un antagoniste selectif UII, SB-611812.

Finalement, Les souris, modifiées génétiquement, déficientes en ApoE, UT ou dans chacun des gènes, furent évaluées afin d'étudier le rôle de signal UII/UT dans un modèle d'atherosclerose.

Nous avons découvert que UII et son récepteur UT étaient tout deux élevés dans un modèle de DC occasionner par une ligature de l'artère coronaire. L'antagonisme UII a atténué de façon signifiante la mortalité, mal fonction cardiaque et d'hypertrophie. Ceci était associe a une diminution significative de la fibrose cardiaque. Ensuite, nous avons démontré que UII et UT étaient élevés de façon significative dans l'athérosclérose des artères carotides et aorte chez l'humain. Finalement, nous avons démontré que la suppression du gène UT chez la souris ayant une déficience pour ApoE, augmente l'athérosclérose de l'aorte. De plus,ceci était associe avec une augmentation significative lipides du sang et d'hypertrophie d'organe ainsi que la réduction de la masse corporelle, le volume du foie et la stéatoses hépatique.

En conclusion, Nous ete les premiers a montre que UII joue un rôle pathophysiologique dans le DC et l'athérosclérose. UII peut-etre un objectif intéressant dans le champ pharmaceutique pour le traitement de DC. De plus, nous fournissons la première description de UII et UT élevés dans l'athérosclérose chez l' humain. Finalement, nous avons découvert que le fait de bloquer le signal UII/UT par la disparition du gène UT accroît plutôt que diminue l' athérosclérose chez la souris déficient pour ApoE. Alors, on a potentiellement trouver un autre cle au mechanisme de athérosclérose.

Acknowledgements

First and foremost I would like to thank Dr. Adel Giaid for being my supervisor, mentor, and friend. It is his generous and creative support that made my doctoral training possible. I have the utmost respect for him as a scientist.

I would also like to express a great deal of gratitude for my thesis committee members, Dr. Danuta Radzioch, Dr. Jamie Engert, and Dr. Jaques Genest. They provided invaluable insight into my research and were always available to help with questions and concerns that arose during my training.

I would also like to Thank Dr. Rob Sladek and Dr. Tomi Pastinen, Pierre Fiset, and Dr. Séverine Létuvé for teaching me much of the practical details necessary for RT-PCR and western blotting. In addition, I thank Dominique Besso and Marylin Linhares for all their help with the administrative matters.

Finally I would like to thank, my other half, Lauren, for understanding that regular working hours do not apply to graduate students. Last but not least, I would like to thank my family for all their loving support without which this pursuit would not have been possible. A special thank-you goes out to my mother for translating my abstract.

Preface

This PhD thesis was written in accordance with the "guidelines for thesis preparation" from the department of graduates studies and research at McGill University. This thesis is in the manuscript based format. Text was duplicated from published and submitted manuscripts. Peer-reviewed manuscripts incorporated into this thesis, in which the candidate was directly involved are as follows:

Chapter 2.

- Bousette N, Hu F, Ohlstein EH, Dhanak D, Douglas SA, Giaid A. Urotensin-II blockade with SB-611812 attenuates cardiac dysfunction in a rat model of coronary artery ligation. J Mol Cell Cardiol. 2006;41:285-95.

- Bousette N, Pottinger J, Ramli W, Ohlstein EH, Dhanak D, Douglas SA, Giaid A. Urotensin-II receptor blockade with SB-611812 attenuates cardiac remodeling in experimental ischemic heart disease. Peptides. 2006; [Epub ahead of print]

Chapter 3.

- Bousette N, Patel L, Douglas SA, Ohlstein EH, Giaid A. Increased expression of urotensin II and its cognate receptor GPR14 in atherosclerotic lesions of the human aorta. Atherosclerosis 2004 ;176:117-23.

Chapter 4

- Bousette N; Ramli W:Hu F; Ohlstein E.H.; Douglas S.A; Giaid A.Urotensin-II Receptor Knockout Increases Plasma Lipids and Atherosclerosis in ApoE Knockout Mice. (Submitted to *Journal of Clinical Investigation*)

The candidate carried out the majority of the work for the research presented in chapters 2-4.

Other manuscripts which are not part of this thesis but with which the candidate was directly involved with includes:

- Bousette, N & Giaid A. Urotensin-II and Cardiovascular disease; A Review Current Hypertension Reports; 2006 Invited review (publication date 12/2006).
- Qureshi ST, Zhang X, Aberg E, Bousette N, Giaid A, Shan P, Medzhitov RM, Lee PJ. Inducible Activation of TLR4 Confers Resistance to Hyperoxia-Induced Pulmonary Apoptosis.J Immunol. 2006;176(8):4950-8.
- Bousette N, Giaid A. Endothelin-1 in atherosclerosis and other vasculopathies. Can J Physiol Pharmacol. 2003 Jun;81(6):578-87.

Table of Contents

List of Figures & Tables

Chapter 1

Chapter 2

Chapter 3

Chapter 4

List of abbreviations

1. AA.....Amino acid
2. ACAT.....Acyl-CoA-Cholesterol Acyltransferase
3. ACE.....Angiotensin converting enzyme
4. AngII.....Angiotensin-II
5. ApoE.....Apolipoprotein-E
6. AT-1.....Angiotensin type I receptor
7. AU.....Arbitrary units
8. BNP.....Brain natriuretic peptide
9. BP.....Blood Pressure
10. BSA.....Bovine serum albumin
11. CAD.....Coronary artery disease
12. Ca_i.....Intracellular calcium
13. cDNA.....Complimentary DNA
14. CHO.....Chinese hamster ovary
15. CHF.....Congestive heart failure
16. CNS.....Central nervous sysytem
17. CO.....Cardiac output
18. cTnI.....Cardiac troponin I
19. CVP.....Central venous pressure
20. DMEM.....Dulbecco's modified eagles medium
21. +dP/dt....The first derivative of the rate in positive pressure change
22. -dP/dt...The first derivative of the rate in negative pressure change

23. ECM.....Extracellular matrix

24. eNOS.....Endothelial nitric oxide synthase

25. EGF.....Epidermal growth factor

26. ELISA.....Enzyme linked immunosorbent assay

27. ERK.....Extracellular regulated kinase

28. ET-1.....Endothelin-1

29. GFR.....Glomerular filtration rate

30. GPCR.....G-protein coupled receptor

31. HDL.....High density lipoprotein

32. HR.....Heart rate

33. ICV.....Intracerebroventricular

34. IL-6.....Interleukin-6

35. iNOS.....Inducibe nitric oxide synthase

36. JNK.....c-Jun amino terminal kinase

37. KCl.....Potassium chloride

38. IV.....Intravenous

39. LAD.....Left anterior descending

40. LDL.....Low density lipoprotein

41. L-NAME..... nitro-L-arginine methyl ester

42. LRP.....Low density lipoprotein related peptide

43. LV.....Left ventricle

44. LVEDD.....Left ventricle end-diastolic dimension

45. LVEDP..... left ventricular end-diastolic pressure

46. LVSP.....Left ventricular systolic pressure

47. Lys.....Lysine

48. MAP... .....Mean arterial pressure

49. MAPK.....Mitogen activated protein kinase

50. MEK.....MAPK and ERK kinase

51. MI.....Myocardial infarction

52. MLC_2.....Myosin light chain regulatory protein

53. MMP.....Matrix metalloproteinase

54. mRNA.....Messenger RNA

55. NADPH.....Nicotinamide adenine dinucleotide phosphate

56. NCDC.....phenyl-N,N-diphenylcarbamate

57. NGS.....Normal Goat serum

58. NO.....Nitric oxide

59. NYHA.....New York heart association

60. ORN.....Ornithine

61. PBS.....Phosphate buffered saline

62. PCWP.....Pulmonary capillary wedge pressure

63. Pdiast.....Diastolic arterial pressure

64. PKC.....Protein kinase C

65. Psyst.....systolic arterial pressure

66. PVDF.....Polyvinilidine difluoride

67. RT-PCR.....Reverse transcriptase-polymerase chain reaction

68. RVSP.....Right ventricular systolic pressure

69. SDS-PAGE.....Sodium dodecyl sulphate-polyacrylamide gel electrophoresis

70. SMC.....Smooth muscle cell

71. TIMP.....Tissue inhibitor of Matrix metaloproteinase

72. TPR.....Total peripheral resistance

73. Trp.....Tryptophan

74. TTBS.....Tris buffered saline with Tween-20

75. Tyr.....Tyrosine

76. UII.....Urotensin-II

77. UT.....Urotensin-II receptor

78. VLDL.....Very low density lipoprotein

Chapter I

Background & Literature review

1.1 Background

1.1.1 Heart failure

Clinical heart failure has various etiologies including ischemic, idiopathic and valvular cardiomyopathy. However, for purposes of brevity only ischemic cardiomyopathy will be addressed here. Ischemic cardiomyopathy is the end result of reduced or absent blood flow to the myocardium. The cause of this is predominantly atherosclerosis of coronary arteries but can also occur as a result of coronary vasospasm. With severe prolonged ischemia, myocardial tissue undergoes cell death by both necrotic and apoptotic mechanisms.

The resulting myocardial infarct undergoes tissue repair processes in which the infarcted tissue is replaced by fibrotic tissue. Although there is evidence of adult human cardiac cell proliferation. [Beltrami et al. 2001] This mechanism is obviously not adequate for total wound repair, hence the resultant formation of scar tissue following myocardial infarction.

In the early stages following coronary occlusion there is a large degree of fibrin/fibrinogen deposition which forms a provisional matrix. This is followed by mature scar formation in which the fibrin is replaced predominantly by collagen. [Dobaczewski et al 2006] The mature scar is constantly being remodeled by matrix metalloproteases which in some instances of severe infarction predispose the ventricular wall to aneurysm. [Baron, 1971]

Although necessary to prevent ventricular aneurysm and rupture, this fibrosis can expand beyond the infarct, leading to fibrillar collagen deposition throughout the viable myocardium. Indeed, several studies have described

this reactive fibrosis as the increase in degree of collagen deposition in regions remote from infarct scar. [Frimm et al. 1996; Sun et al. 1998; Cittadini et al. 2002; See et al. 2005] This remote fibrosis is disadvantageous in that it stiffens the heart and thus decreases ventricular compliance and increases filling pressures. This, in turn causes diastolic dysfunction which can lead to lung edema and consequent cardiac dyspnea.

Of late, attention has been focused not only on the degree of collagen accumulation within and remote from the myocardial infarct, but also on the type of collagens expressed. Initially following myocardial infarction both collagen type I and type III are increased. However, while high expression of collagen type I persists, collagen type III returns to normal levels much earlier. [Cleutjens et al. 1995] Indeed, Bishop et al. (1990) report that in both ischemic and dilated cardiomyopathy there is an increase in absolute levels of both type I and III collagen, however, there was a significant reduction in the proportion of type III collagen.

Collagen type I is more rigid while collagen type III provides more elasticity. Thus an increase in collagen type I:III ratio is associated with a decrease in myocardial compliance which may lead to diastolic dysfunction. [Mukherjee et al. 1990; Nishikawa et al. 2001] In addition, the increase in fibrosis has been shown to decrease oxygen diffusion in the myocardium, thus increasing the hypoxia of an already ischemic tissue. [Sabbah et al. 1995]

The necrosis of functional cardiomyocytes decreases the pumping capacity of the heart. The heart compensates by at least two different

mechanisms. Firstly, the heart dilates thereby increasing end-diastolic volume and maintaining stroke volume even in the face of reduced ejection fraction. This is detrimental to the heart since chamber dilatation increases chamber radius and thus increases wall stress as described by the Laplace relationship.

$$\text{Wall stress} = \frac{P \times R}{2Th}$$

P: Intrachamber pressure; R: Chamber radius; Th: Wall thickness

The increased wall stress increases the workload for the heart and therefore increases oxygen demand. This compensatory mechanism thus perpetuates cardiac dysfunction in ischemic cardiomyopathy.

The second mechanism that the heart uses to compensate for reduced functional units following myocardial infarction is cardiac hypertrophy. [Zaino et al. 1963] That is, individual cardiac myocytes increase protein content to form more contractile units. Cardiac hypertrophy has been classified as either eccentric or concentric, in which, sarcomeres are added in series or in parallel, respectively. [Grossman et al. 1975] The former is generally stimulated by circulatory volume overload while the latter is generally stimulated by pressure overload. Cardiac hypertrophy is also detrimental to heart function for several reasons. For example, it decreases myocardial compliance and thus increases filling pressures. In addition, cardiac hypertrophy decreases the capillary-to-sarcomere ratio thus reducing oxygen

availability to working myocardium and thus increasing cardiac ischemia. [Tomanek et al. 1986] Although the heart has compensatory methods for maintaining function in the short term these changes ultimately damage the heart irreversibly resulting in end-stage heart failure.

Importantly, circulating vasoactive factors such as endothelin -1 are elevated in heart failure patients, [McMurray et al. 1992] and have been demonstrated to contribute to cardiac pathology. [Iwanaga et al. 1998] Indeed, the inhibition of endothelin has shown therapeutic benefit. [Mylona et al. 1999] Also, there is an enormous amount of data demonstrating the contribution of angiotensin-II (AngII) to cardiac pathology hence the development and widespread use of ACE inhibitors and Angiotensin receptor blockers. Another more recently described endothelial derived vasoactive peptide with potential contribution to cardiac pathology is Urotensin-II (UII). Therefore, studies evaluating the role of UII in the cardiovascular field are warranted.

1.1.2 Atherosclerosis

Atherosclerosis, is a vascular disease which involves mostly large conducting and elastic arteries. Lesion formation is a process which can occur over a period of decades in humans. Dyslipidemia, is the main contributing factor to atherosclerotic disease. Indeed, populations with serum total cholesterol less than 150 mg/dL have a very low incidence of atherosclerotic events even in if other major risk factors are present. [Roberts. 1995] Dyslipidemia is characterized

as either high plasma levels of very-low density and low density lipoproteins (VLDL and LDL) and/or low plasma levels of high density lipoproteins (HDL).

Prone areas for lesion development include sites of curvature, such as the aortic arch, as well as arterial branch points such as in the carotid artery. In addition, coronary arteries including the left anterior descending coronary artery are commonly afflicted with atherosclerotic lesions. Lesion development is a dynamic process but for simplicity's sake it will be described here in steps. Initially, there may be the development of a thickened intima, although this is not absolutely necessary for lesion development. This thickened intima largely occurs where laminar blood flow is disturbed such as at curvatures and branch points within arteries. Stary et al. 1992 This thickened intima is predominantly the result of smooth muscle cell (SMC) migration and proliferation, hence the importance of proliferative effects of circulating vasoactive factors. These sites of thickened intima are thought to provide "fertile soil" for lesion development. Schwartz et al. 1995

A prerequisite for lesion formation is the accumulation of extracellular lipid, which is delivered to the intima via circulating lipoproteins. Following lipoprotein entry into the intima it is believed to bind to negatively charged proteoglycans. Camejo et al. 2002 There is evidence that the extracellular matrix (ECM) produced by proliferating SMCs has more affinity for lipoproteins than does the ECM produced by quiescent SMCs. Camejo et al. 1993

The presence of intra-intimal lipids is believed to induce the secretion of chemokines which attract monocytes. Chen et al. 1999 Upon entering the

intimal space the lipids are taken up by specific lipoprotein receptors, including the LDL receptor and the LDL like receptor protein (LRP), as well as by scavenger receptors. The latter are important for foam cell formation because they are not down-regulated by lipids. [Hurt et al. 1990] Therefore lipids are taken up by these scavenger receptors until the monocyte derived macrophages become lipid filled foam cells. Foams cells accumulate within the intimal space, and develop into what are described histologically, as fatty streaks. These fatty streaks have been demonstrated even in fetuses, [Napoli et al. 1997] however they are not raised and are not symptomatic. Continued accumulation of intimal lipids ultimately causes foam cell death and release of intracellular lipids. These lipids coalesce to form small pools of extracellular lipid. At the same time fibrosis of the overlying intima commences. This fibro-proliferative response continues until a necrotic fatty core is covered by a fibrous cap, which is referred to as a fibroatheroma.

These lesions can remain clinically silent as long as they are not large enough to cause significant stenosis of the coronary artery. However, these lesions are also prone to vasospasm which can cause acute ischemic attacks. Eventually, these lesions can become complicated by either endothelial denudation and/or plaque rupture. The latter leads to thrombo-embolic episodes which are believed to be the main cause of myocardial infarction.

Therefore, the process of atherosclerotic lesion development starts early in life and continues for decades ultimately causing coronary stenosis

with a fixed lesion or coronary occlusion via plaque rupture and subsequent thrombosis. Alternatively the same pathology is observed in the cranial vasculature in which ischemia leads to strokes of the brain. Together, mortality ultimately due to atherosclerotic disease in either the brain or heart account for the most deaths per annum in North America.

1.2 Literature review

1.2.1 Urotensin-II.

Urotensin-II (UII) is a small protein with pleiotropic effects; however it is generally referred to as a vasoactive factor. Originally isolated from a species of fish known as Gillichthys mirabilis in 1980, [Pearson et al, 1980] it has since been cloned from frog, mice, rats, pigs, monkeys and man. [Oshako et al., 1986; Conlon et al., 1992; Coulouarn et al., 1998; Coulouarn et al., 1999; & Elshourbagy et al., 2002] It was first described to be a somatostatin-like peptide based on structural homology with somatostatin-1,[Pearson, 1980] and has since been described as a paralogue of somatostatin, arising from the same ancestral gene. [Tostivint, 2006]

UII has been demonstrated to be the most potent vasoconstictor identified to date. Indeed, being in the range of an order of magnitude more potent than endothelin-1. [Ames et al. 1999] However, it has also been shown to be an endothelial dependent vasodilator. [Gibson, 1987] This dual vasoactivity of UII is reminiscent of endothelin-1, a well known vasoactive peptide implicated in a variety of cardiovascular diseases. However unlike endothelin-1 which binds to at least two different receptors, UII is specific for only one receptor. [Sakurai et al. 1992; Douglas et al. 2004] This receptor was originally known as the orphan G-protein coupled receptor GPR-14 or the sensory epithelium neuropeptide-like receptor, but has now been termed UT, by The International Union of Pharmacology (IUPHAR). [Douglas et al. 2000]

1.2.2 Physiological UII expression

UII was first isolated from the caudal neurosecretory region of the teleost fish (Table 1) [Pearson et al., 1980]. In frogs, prepro UII mRNA was shown to be primarily expressed in the spinal cord, rhombencephalon, and mesencephalon [Coulouarn et al., 1998]. In mice and rats UII is expressed most abundantly in the central nervous system (CNS), specifically in the spinal cord, cerebellum, and medulla oblongata, but also in the rat epididimis and mouse thymus [Coulouarn et al., 1999]. Elshourbagy et al.[2002] found that mouse prepro-UII mRNA was also prominently expressed in the heart, thoracic aorta, skeletal muscle, kidney, spleen, and testis. In monkeys prepro-UII mRNA was found to be expressed in the heart, including both atria and ventricles, the thoracic aorta, as well as kidney, liver, spleen, skeletal muscle and of course in the spinal cord [Elshourbagy et al.2002]. In humans, dot blot analysis showed that UII mRNA expression was strongest in spinal cord but was also evident in several other tissues including the kidneys, small intestine, thymus, pituitary gland, and adrenal gland as well as the stomach, and liver [Coulouarn et al., 1998]. Nothacker et al.[1999] found that human prepro-UII mRNA was expressed at highest levels in human kidney with lower levels in spinal cord and medulla oblongata. On the other hand, UII protein was demonstrated using immunohistochemical techniques in human vascular and endocardial endothelium as well as the renal epithelium. [Maguire et al., 2004; Shenouda et al.,2002] Endothelial cells of human renal capillaries exhibited moderate U-II immunoreactivity, with little expression in the normal glomeruli. [Shenouda et al.,2002]

Table 1. Summary of species and organ specific expression of UII and UT.

	Fish & frogs	Mouse	Rat	Monkey	Human
CNS	UII (Pearson et al. 1980, Coulouarn et al., 1998)	UII (Coulouarn et al., 1999) UT (Elsourbagy et al., 2002)	UT (Gartlon et al. 2001)	UII (Coulouarn et al., 2002) UT (Elshourbagy et al. 2002)	UII (Coulouarn et al., 1998) Nothacker et al.1999
Heart		UII (Coulouarn et al., 2002)	UT (Gartlon et al. 2001, Gong et al. 2004)	UII (Coulouarn et al., 2002) UT (Elshourbagy et al. 2002, Ames et al. 1999)	UT (Matsushita et al., 2001)
Aorta		UII (Coulouarn et al., 2002) UT (Elsourbagy et al., 2002)	UT (Nothacker et al.1999)	UII (Coulouarn et al., 2002) UT (Elshourbagy et al. 2002)	
Skeletal Muscle		UII (Coulouarn et al., 2002)		UII (Coulouarn et al., 2002)	
Kidney		UII (Coulouarn et al., 2002)	UT (Song et al. 2006)	UII (Coulouarn et al., 2002)	UII (Coulouarn et al., 1998) Nothacker et al.1999 Shenouda et al.,2002 UT (Matsushita et al., 2001)
Spleen		UII (Coulouarn et al., 2002)		UII (Coulouarn et al., 2002)	
Liver				UII (Coulouarn et al., 2002)	UII (Coulouarn et al., 1998)
Testis		UII (Coulouarn et al., 2002)			
Small intestine					UII (Coulouarn et al., 1998)
Stomach					UII (Coulouarn et al., 1998)
Adrenal gland					UII (Coulouarn et al., 1998)
Pancreas		UT (Elsourbagy et al., 2002)		UT (Ames et al. 1999	

In the Sprague-Dawley rat kidneys immunoreactive UII was more intense in the proximal rather than distal convoluted tubules, with negligible expression in either glomeruli or arterioles.[Song et al. 2006]

UII is also found circulating in the plasma suggesting it may have endocrine effects. In a study investigating the source of circulating UII, Charles et al. [2005] found that there were arteriovenous gradients in UII levels across the heart, liver and kidneys in normal anesthetized sheep indicating these organs as sources of circulating UII.

1.2.3 Physiological UT expression

UT was discovered to be the cognate receptor for UII by three separate groups in late 1999 [Nothacker et al., 1999; Mori et al., 1999; Liu et al., 1999]. In mice, UT prepro-mRNA was demonstrated to be abundantly expressed in the heart followed by lesser expression in the thoracic aorta, bladder, and pancreas [Elsourbagy et al., 2002]. Nothacker et al.[1999] found that UT is expressed in rat heart, pulmonary artery and thoracic aorta. While, Gartlon et al. [2001] found that UT mRNA was abundantly expressed in the rat brain but highest expression was in the heart. Using immunohistochemical techniques Gong et al. [2004] showed that UT was expressed only in cardiomyocytes of the left ventricle, but not in the right ventricle or atria of normal rats. In the kidney, UT is expressed in both glomerular arterioles as well as the inner medullary collecting ducts and ascending thin loops of Henle of the rat [Song et al. 2006].

In the monkey prepro-UT mRNA was most abundantly expressed in the thoracic aorta, with less but still prominent expression in the ventricles of the heart and in the spinal cord. Interestingly Ames et al.[1999] demonstrated that UT was most prominently expressed in the heart and pancreas of humans. Using RT-PCR Ames et al.[1999] revealed expression in human cardiac and aortic tissue, as well as in endothelial cells and smooth muscle cells from coronary arteries. Although, others still, have found that UT mRNA was abundantly, yet equally expressed in both human cardiovascular and renal tissues [Matsushita et al., 2001]. In support of this Aiyar et al.[2005] and Disa et al.[2005] demonstrated UT mRNA expression in the cat kidney and UII radioligand binding in the rat kidney, respectively.

1.2.4 UII Synthesis and Structure

In mice UII is synthesized from a gene with four exons and three introns that spans 4799 nucleotides [Elshourbagy et al., 2002]. From this a 371 nucleotide mRNA transcript is spliced, which in turn encodes a 123 amino acid prepropeptide. This prepropeptide is ultimately cleaved to form a mature 14 amino acid peptide in mice. In humans UII is first synthesized as a 124 amino acid prepropeptide which is then cleaved at a dibasic site to form an 11 amino acid mature peptide (Figure 1) [Coulouarn et al., 1998]. Analysis of the prepropeptide indicates several mono/polybasic cleavage sites, [Chartrel et al., 2004] that would produce UII of 11, 16 and/or 19 amino acids long.

Figure 1. Schematic of mature UII protein from several species with the conserved cyclic hexapeptide in black (adapted from Douglas et al. 2004)

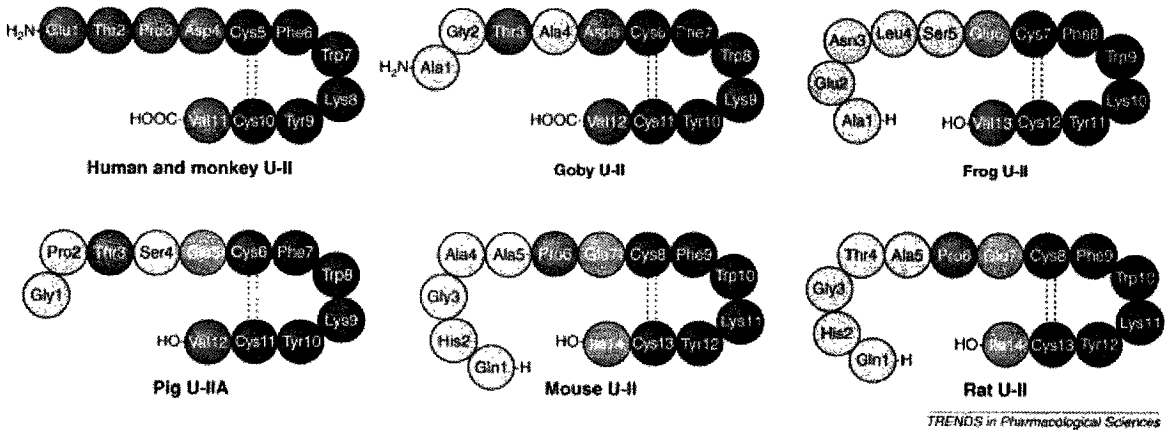

Therefore perhaps UII circulates as a peptide of varying lengths, although there has been no published observation for either the 16 or 19 AA long UII peptide. Analysis of cDNAs for UII from various species demonstrates large differences in the amino terminal region of the proprotein, yet all species have a conserved cyclic hexapeptide at the C-terminus of the gene. The sequence of this hexapeptide is CFWKYC and is cyclic because of the disulphide bridge formed between the two cysteine resides. Human preproUII has a predicted molecular weight of 13.9 KDa, while its mature form in humans is quite small at 1.3 KDa. Several species express more than 1 prepro-UII transcript believed to be the result of alternative splicing, however mature forms are conserved.[Mori et al., 1999; Ohsako et al., 1986]

The maturation of human UII from the prepropeptide is catalyzed by an as of yet unknown enzyme. However both calcium dependent furin and aprotonin sensitive trypsin have shown urotensin converting enzyme activity in cell based and plasma based assays, respectively.[Russell et al., 2004]

Sugo et al. [2003] discovered urotensin related peptide (URP). An 8 amino acid peptide (ACFWKYCV) with the conserved cyclic hexapaptide yet transcribed from a distinct gene from that of UII in both humans and rats. The physiological significance of this UII-like peptide remains to be elucidated. URP has comparable binding affinity for UT and also demonstrates identical in vivo effects as UII, supporting the fact that it is the cyclic hexapeptide that is required for UII biological activity. Also, URP is

expressed in the same tissues as UII in rat and human but at lower levels. [Mori et al. 2004]

1.2.5 UT Synthesis and Structure

UT protein (Figure 2), on the other hand, is synthesized from an intronless gene with an open reading frame 1158 and 1167 nucleotides long which produce proteins of 386 and 389 amino acids, in mouse and man, respectively [Elshourbagy et al., 1999]. UT has a predicted molecular weight of ~42 KDa. However it has several potential glycosylation sites and as such has been shown to have a molecular weight ~60KDa [Boucard et al., 2003].

1.2.6 UII/UT signaling

UII isopeptides originating from either mammalian, amphibian, or piscine species were all equipotent agonists at recombinant UT receptors. [Elshourbagy et al. 2002] This is explained by the fact that biological activity is maintained in all UII isopeptides containing the cyclic hexapeptide. [Itoh et al. 1988] In fact, structure activity relationships in a calcium mobilization assay using UT transfected CHO cells have demonstrated that the side chains of the residues Trp-7, Lys-8, and Tyr-9 of UII are most important for receptor binding and activation. [Flohr et al. 2002] UII has been shown to bind the fourth transmembrane domain including specific interaction with methionine residues at positions 184 and 185. [Boucard et al., 2003] Intracellularly, UT is believed to be coupled to the class of G-proteins known as $G_{\alpha q}$. The latter,

Figure 2 UT Schematic.

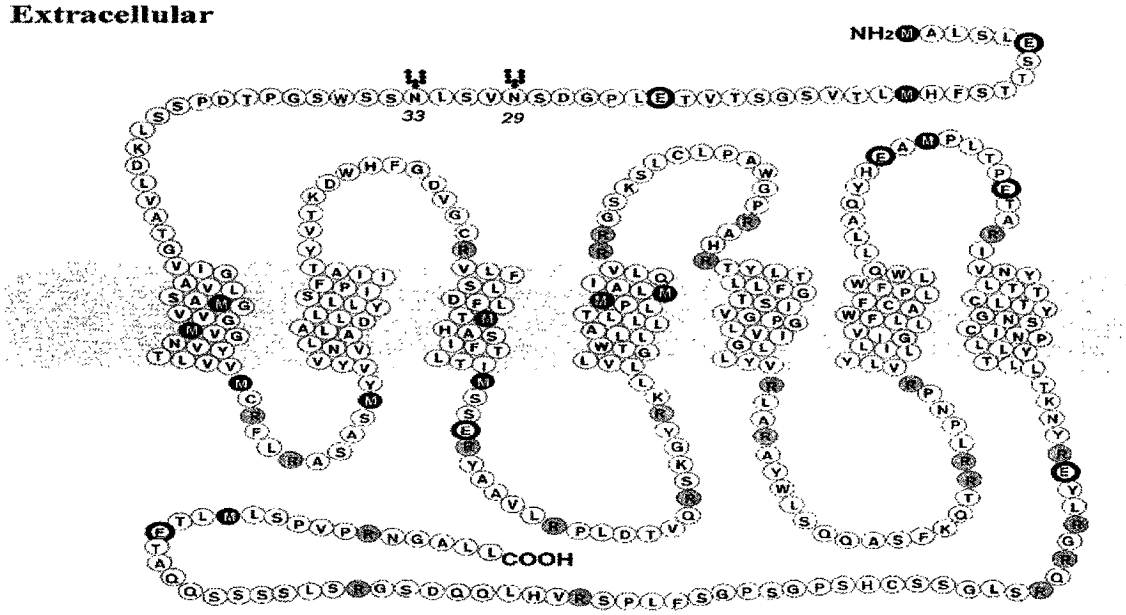

when activated, is known to activate phospholipase C, which in turn catalyzes the production of diacylglycerol and inositol triphosphate. The former can activate certain isoforms of PKC, while the latter can induce the release of intracellular calcium from the endoplasmic reticulum. Indeed, UII has been shown to induce an increase in intracellular calcium in UT expressing cells. Nothacker et al., 1999; Liu et al., 1999 Moreover, UII induced phosphoinositide hydrolysis and this effect was inhibited by an inhibitor of phospholipase C (NCDC). Saetrum-Opgaard et al.2000 In addition, several studies have provided evidence that UII induces the activation of ERK 1/2 and protein kinase C (PKC). Birker-Robaczewska et al. 2003; Tasaki et al.2004; Shi et al., 2005 ; Chen et al.2004 and Watanabe et al.2001

UII signaling may also be mediated by phospholipase A_2 dependent arachidonic acid production. Indeed, CHO cells transfected with rat UT were induced to synthesize arachidonic acid metabolites upon administration of UII. Mori et al., 1999 In addition, both Gray et al.[2001] and Gardiner et al.[2004] have demonstrated inhibition of UII mediated vasodilation with indomethacin, a non-selective inhibitor of cyclooxygenase enzymes, which catalyzes the formation of prostaglandins from the precursor arachidonic acid. Also, UII mediated contraction of guinea pig ileum was inhibited with the use of indomethacin.Horie et al. 2003 In a follow-up study Horie et al.[2005] demonstrated attenuation of UII induced contraction of guinea pig ileum with the use of a phospholipase A_2 inhibitor.

Ligand/receptor mediated signaling cessation can occur by a variety of mechanisms including ligand release, receptor desensitization, and/or

receptor internalization. In fact, there are several established models for receptor internalization including clathrin-coated pit endocytosis.

Ligand release is likely not the most efficient mechanism for signaling termination since UII has been described to have psuedo-irreversible binding qualities. Indeed, similarly to endothelin-1, UII was shown to be a pseudo-irreversible ligand demonstrating significantly longer washout times compared to other vasoactive compounds including angiotensin, serotonin, and noradrenalin. [Douglas et al., 2000]

However, UT receptor internalization has been observed following ligand binding in COS-7 cells.[Proulx et al., 2005] This process was shown to be mediated at least in part by clathrin-coated pit endocytosis, and dependent on phosphorylation of specific residues in the cytoplasmic tail. Of note is the fact that the latter study showed that the UT containing endocytic vesicles contained β-Arrestin-1 and β-Arrestin-2. Giebing et al. [2005] demonstrated that UII binding to UT receptor induced recruitment of Arrestin-3 to the plasma membrane but not arrestin-2. Furthermore, internalized receptors were associated with early endosomal antigen and the transferrin receptor indicating their localization to early and recycling endosomes. In fact, they demonstrated that although 70% of UT receptors were internalized after 30 minutes exposure to UII, these receptors were quantitatively recycled to the membrane within 60 minutes. However, β-arrestin proteins were not associated with these UT containing endosomes. In addition, UT internalization was not hindered in cells lacking expression of either Arrestin

2 or Arrestin-3, clearly demonstrating their independence from these molecules for internalization. However, the latter study did not investigate arrestin-1 and therefore these discrepant findings may be explained by varying isoforms of arrestin being utilized in different cell types.

1.2.7 Vasoactivity

UII was initially demonstrated to be a mammalian vasoactive factor in rats using an aortic bio-assay. Specifically, UII of fish origin induced endothelium dependent vasorelaxation and endothelium independent vasoconstriction in aortic strips [Gibson, 1987]. In fact, rat aortic contraction is now commonly utilized as an assay for UII activity. Since then numerous studies describing the varying nature of this vasoactive peptide have been published. The most studied species, with regard to UII vasoactivity, is the rat. Gibson [1987] originally demonstrated that UII induced vasorelaxation of the preconstricted rat aorta at low doses (0.1-0.5nM), while higher doses (1-10nM) induced vasoconstriction. Of note was that the low dose induced vasorelaxation only occurred when the endothelium was intact. Indeed, upon denudation, UII only induced vasoconstriction of the rat aorta. [Gibson, 1987] Of note, UII had a much stronger effect in the rat thoracic aorta compared to the abdominal aorta [Itoh et al., 1988]. A later study by Gendron et al.[2004] demonstrated that maximal contraction in aortae induced by UII increases with age in both Wistar-Kyoto rats as well as spontaneously hypertensive rats. Oddly, Ishihata et al.[2005] demonstrated that efficacy of UII mediated contraction, with

or without an intact endothelium, was reduced in aged (25-27 months) Fischer 344 rats compared to young (2-3 months) rats, indicating strain variablility.

The UII induced aortic contraction of the rat aorta was found to be mediated via the uptake of extracellular calcium and was sensitive to pretreatment with nitredipine, a dihydropyridine receptor blocker.[Gibson et al., 1988] A later study designed to elucidate the mechanism of UII induced rat aortic contraction showed that UII vasoconstriction is mediated by the Ca(2+)/calmodulin/Myosin Light chain kinase system. [Tasaki et al.2004] In addition, they also demonstrated that UII induced aortic contraction was attenuated by inhibitors of PKC, p38MAPK, and ERK1/2, suggesting a considerable degree of intracellular signaling crosstalk. This study is complemented by the findings of Rossowski et al.[2002] which demonstrated that UII induced aortic ring contractions were inhibited with calcium channel blockers, as well as inhibitors of phospholipase C, PKC, Rho kinase, and tyrosine kinase. This endothelium independent vasoconstriction indicates that UII has contractile effects on vascular smooth muscle cells (SMC). Indeed, Sauzeau et al. [2001] demonstrated that UII induces cultured SMC contraction and that this is mediated by RhoA and Rho-kinase.

Itoh et al.[1987] also showed that UII had vasoconstrictive activity in the carotid artery of the rat, while Maclean et al.[2000] found UII induced vasoconstriction of rat main pulmonary arteries. The latter study showed that the maximal vasoconstrictive effect was significantly enhanced in the

presence of L-NAME (nitro-L-arginine methyl ester), and in vessels from pulmonary hypertensive rats exposed to chronic hypoxia for 2 weeks.

In the rat coronary vasculature UII vasoactivity appears to have a strong endothelial component. For instance, 2 different groups demonstrated that UII (0.1nM) elicited a biphasic response of coronary flow, namely an initial phase of vasoconstriction followed by sustained vasodilatation. [Katano et al., 2000 & Gray et al., 2001] This biphasic vasoactivity is likely explained by endothelial effects. Indeed when gray et al.[2001] administered L-NAME, an inhibitor of endothelial nitric oxide synthase, or indomethacin, in addition to the UII in the perfusate of the isolated heart, the result was sustained vasoconstriction lacking the later vasodilation.

Noteworthy, are the findings of Ishihata et al.[2005] who demonstrated that the UII induced coronary vasodilation in perfused heart was mediated by both NO and prostaglandins in young fisher 344 rats while it was mediated primarily by prostaglandins in aged rats. Indeed, hearts from aged rats released significantly less NO metabolites following UII administration than did hearts from young rats.

Remarkably, Bottrill et al.[2000] found that UII induced contraction in "some" endothelium intact left anterior descending coronary arteries, while endothelium removal significantly enhanced the vasoconstriction.

In other arteries of the rat UII appears to have a strong vasodilatory action. In fact, Zhang et al. [2003] demonstrated vasodilation of isolated endothelium intact small renal arteries of the rat. However, denuded vessels

or vessels preincubated with L-NAME lacked vasoactivity. Therefore UII must induce vasodilation at least in part by induction of nitric oxide (NO) synthesis in the endothelium. Another study demonstrated that UII induced calcium independent NO production in the rat aortic adventitia, and that this was significantly attenuated with a specific inhibitor of inducible nitric oxide synthase (iNOS). [Lin et al. 2004] However, this likely has a small physiological impact since the main action of UII on the aorta is vasoconstriction.

Importantly, UII intravenous (IV) bolus injection *in vivo* induces a decrease in mean arterial pressure in rats [Gibson et al., 1986; Gardiner et al., 2001 Hassan et al., 2003]. This is characterized as a sustained mesenteric and hindquarter vasodilation. This vasodilation can be inhibited with indomethacin and L-NAME, indicating that UII activates signaling pathways involving both cyclooxygenase and eNOS enzymes. [Gardiner et al., 2004; Abdelrahman et al., 2002] The effect of IV UII in rats has also been described as biphasic, with an initial decrease in MAP followed by a modest increase in blood pressure. [Gardiner et al., 2004] In contrast, IV injection in conscious ewes induced a transient increase in MAP followed by a sustained decrease in pressure, as well as a reflex tachycardia. [Watson et al., 2003] Of note, UII mediated hypotensive effects were significantly more pronounced in spontaneously hypertensive rats than their normotensive counterparts. [Gendron et al.2005] Oddly, in the latter study, the use of neither L-NAME nor meclofenac, a non-selective inhibitor of cyclooxygenase, had any effect on UII mediated hypotension and yet sulfaphenazole and phalloidin, a CYP2C9 inhibitor and a cytoskeletal fixation agent, respectively

were able to attenuate the UII mediated hypotension. Importantly, the latter study did not indicate whether these substances were tested alone and therefore effects independent from UII cannot be ruled out.

The UII mediated in vivo vasodilation is further supported in a study by Ovcharenko et al.[2006] who demonstrated that UII induced a significant decrease in mean arterial pressure and renal vascular resistance in rats in vivo. In this study the authors showed that this effect on renal vascular resistance was significantly more pronounced in rats with congestive heart failure (CHF) due to aortocaval shunting. Furthermore, while normal rats showed a small yet insignificant decrease in glomerular filration rate (GFR) following bolus UII administration, CHF rats showed a significant increase in GFR. Unfortunately, whether this increase in GFR was due to afferent vasodilation or efferent vasoconstriction was not evaluated in this study.

However the most pronounced effect of UII on the vasculature is in Cynomolgus monkeys. Ames et al. [1999] showed a decrease in mean arterial pressure at low doses (3pM) but a drastic rise in total peripheral resistance (TPR) leading to cardiovascular collapse and death at higher doses (300pM). This cardiovascular collapse was associated with a small decrease in MAP but a substantial decrease in cardiac contractility (dP/dt), stroke volume and cardiac output. Also, left ventricular end-diastolic pressure (LVEDP) was dose dependently increased. The authors attribute this massive increase in TPR following bolus injection of UII in the cynomolgus monkey to systemic vasoconstriction. Indeed the authors also demonstrated extremely potent

and consistent U-II induced contraction in all isolated arterial vessels of the cynomolgus monkey, including both elastic and muscular arteries. Of note, UII exhibited potency 6–28-fold more than endothelin-1 (ET-1). However, the UII induced vasoconstriction was restricted to arteries, as veins showed no vasoactivity to UII. The decrease in cardiac function following UII administration was believed to be the result of myocardial ischemia from intense coronary vasoconstriction. Indeed the authors observed ST segment elevations, indicative of cardiac ischemia, in the electrocardiogram with the highest dose.

The only other animal model that shows consistent vasoconstriction in all arterial segments is the cat. [Behm et al. 2004] In fact all feline isolated arteries evaluated including the aorta, renal, femoral, and carotid arteries, as well as both conduit and resistance mesenteric arteries exhibited UII induced vasoconstriction. Importantly, UII did not significantly alter heart rate or stroke volume; therefore since the pumping capacity of the heart was unaltered both MAP as well as systemic vascular resistance increased significantly following bolus IV injection of UII. This "true" hypertensive effect is in contrast to the monkey whom developed arterial vasoconstriction but a small decrease in MAP due to cardiac failure.

In humans, Stirrat et al.[2001] found that UII exhibited potent vasodilatory activity on endothelium intact small pulmonary and abdominal arteries. In contrast, Camarda et al.[2002] showed that UII induces potent, yet low efficacious vasoconstriction in the human umbilical artery and vein. Similarly,

in isolated human coronary, mammary, and radial arteries as well as saphenous and umbilical veins, UII demonstrated more potent yet less efficacious vasoconstriction compared to endothelin-1. Maguire et al., 2000. In an interesting study by Maguire et al.2004 UII demonstrated potent vasoconstriction of atherosclerotic epicardial arteries. Of note was the fact that they revealed that small coronary arteries responded much more to UII with a significantly stronger constrictive response than the larger coronary arteries and therefore may influence blood pressure by constricting resistance arteries more so than conduit arteries. Although, a major caveat of the latter studies was the fact that all isolated vessels were denuded of endothelium, thereby eliminating endothelium mediated vasorelaxation.

A disparity was found when another study failed to demonstrate any UII vasoactivity in human small resistance arteries, mammary arteries, nor veins. Hillier et al., 2001 The varying nature of UII vasoactivity in human vessels is underscored by a study which showed that only 38% of mammary arteries tested and 66% of radial arteries tested were reactive to UII. Paysant et al. 2001

Human in vivo studies, using normal volunteers have shown conflicting results as well, with one study showing brachial artery vasoconstriction Bohm et al., 2002, and two other studies showing no effect Affolter et al., 2002; and Wilkinson et al., 2002. In contrast, two studies have shown that UII induces vasodilation in the microcirculation of normal volunteers while it induces vasoconstriction in patients with either congestive heart failure Lim et al., 2004 or essential

hypertension [Sondermeijer et al., 2005]. Such paradoxical vasonconstriction is an established phenomenon in diseased vessels. [Ludmer et al., 1986]

1.2.8 Mitogenic effects

In addition to its well established vasoactivity UII has also demonstrated mitogenic effects in endothelial cells, smooth muscle cells and cell lines, as well as hypertrophic effects in cardiomyocytes. In endothelial cells, UII induced dose dependent proliferation as well as dose dependent anti-apoptotic effects.[Shi et al., 2005] The authors also demonstrated that UII (10nM) induced the phosphorylation of mitogen-activated protein kinase p42/44 (MAPKp42/44). Accordingly, the proliferation and anti-apoptotic effects were shown to be dependent on MAPK p42/44, since pretreatment of cells with the MEK inhibitor (PD98059, 10uM) prevented this effect.

Several groups have demonstrated UII mitogenic activity in smooth muscle cells (SMCs).[Chen et al., 2004; Sauzeau et al., 2001; Watanabe et al., 2001; & Tamura et al., 2003] The mechanism of UII induced SMC proliferation has not yet been completely delineated. For instance, both Chen et al.[2004] and Watanabe et al.[2001] demonstrate UII induced proliferation is abolished with PKC and MAPK inhibitors. However, Sauzeau et al.[2001] Showed that UII induced RhoA and Rho kinase and that inhibition of the latter two enzymes also inhibited UII mediated SMC proliferation. Therefore, once more there is evidence of a great deal of intracellular cross talk following UT activation. This is further exemplified by the fact that c-Src tyrosine kinase, calcineurin, and EGF

receptor inhibitors also attenuated UII induced SMC proliferation. [Chen et al., 2004; & Watanabe et al., 2001] Of note, Tamura et al. [2003] found that UII failed to activate ERK 1/2 in suspended cells, but did so in cells adhered to fibronectin, suggesting a dependence on integrin signaling in the UII cascade.

UII's widespread mitogenic role is further supported by the findings of Matsushita et al. [2003] whom demonstrated a mitogenic role for UII in a renal cell line. The latter study also showed that UII induced proliferation exhibited PKC, MAPK, and calcium dependency. Furthermore, UII has also been shown to induce proliferation of several tumor cell lines of varying origin. Takahashi et al., 2003

In addition to its hyperplasic activity in several cell types, UII has exhibited hypertrophic activity as well. UII induced cardiomyocyte hypertrophy has been demonstrated by several groups. [Johns et al., 2004; Onan et al., 2004; Tzanidis et al., 2003] The latter has been shown in both neonatal rat cardiomyocytes and in a cardiomyocyte cell line (H9c2 cells). Interestingly, both cell types required up-regulation of the receptor via an adenoviral vector, in order to demonstrate a hypertrophic response from UII. Notably, Onan et al [2004] demonstrated that the hypertrophic effect was dependent on the MAPKs, ERK1/2 and p38, but also on the phosphorlylation of the EGF receptor.

The necessity for receptor up-regulation to elicit the hypertrophic response suggests that in the "normal" physiologic state UII does not act as a hypertrophic factor. Perhaps only following up-regulation of the receptor, as

Tzanidis et al [2003] demonstrated in the infarcted rat myocardium, does the hypertrophic role become apparent.

The mechanism of UII induced cardiomyocyte hypertrophy may involve Calcineurin, a phosphatase believed to be integral factor in the development of cardiac hypertrophy. Indeed, Li et al.[2005] demonstrated that UII increased calcineurin activity significantly in human right ventricular trabeculae from failed hearts.

1.2.9 Cardiac effects

In light of the relative abundant expression of UT in the heart of several species it is not surprising that UII may have some cardiac effects in the basal state. *In vivo* cardiac response to intravenous (IV) bolus UII includes a sustained tachycardia in the rat, although this is likely a baroreceptor reflex response to the decrease in mean arterial pressure (MAP) that occurs with IV UII injection in rats. However, a positive inotropic response has been demonstrated with UII in both human and rat cardiac preparations. Russell et al., 2001; Gong et al., 2004. Indeed, Russell et al. [2001] demonstrated that UII exerted a potent, yet low efficacious inotropic effect on isolated right atrial trabeculae. Similarly, Gong et al. [2004] also demonstrated increased contractile force in a rat left ventricular papillary muscle preparation with UII administration. In a later study Russell et al. [2004] investigated the mechanism of UII inotropic activity in cardiac tissue. Specifically, UII induced an inotropic response in atrial trabeculae which was associated with phosphorylation of myosin light

chain regulatory protein (MLC-2), as well as PKC isoforms. Inhibition of PKC with chelerythrine inhibited the inotropic response but did not affect the MLC-2 phosphorylation, suggesting that UII inotropy is mediated via PKC but MLC-2 phosphorylation is not required.

In contrast, Hassan et al. [2003] found that UII IV bolus administration to rats led to a significant decrease in cardiac contractility. In this latter study the authors observed a decrease in mean arterial pressure but no difference in heart rate which conflicts with previous reports. [Gibson et al., 1986; Gardiner et al., 2001]

UII is an activator of eNOS production in the vascular endothelium however, UII reduced eNOS mRNA expression and activity in rat neonatal cardiomyocytes, resulting in a reduction in cardiomyocyte NO production. [Li et al., 2002] Oddly the same group followed up with a study in which adult male rat hearts were perfused retrogradely with UII, in a Lagendorff working heart model, which led to a UII induced increase in eNOS protein content in the heart. These discrepant findings may be explained by the difference in receptor density between neonatal and adult cardiomyocytes. Alternatively, the difference may be attributable to the model used, i.e. cell culture vs. ex vivo tissue study.

1.2.10 Central nervous system effects

Intracerebroventricular (ICV) administration of UII in rats induced some interesting behavioral and endocrine effects. For instance, ICV administration of 3-10μg UII in Sprague-Dawley rats increased rearing and

grooming in these animals. [Gartlon et al., 2001] In addition, plasma prolactin and thyroid stimulating hormone levels were increased following ICV dosing. This is supported by the findings of Matsumoto et al. [2004] who showed that ICV injection of UII induced anxiogenic or stress related effects.

Injection of UII into specific brain areas resulted in divergent cardiovascular effects. [Lu et al., 2002] Specifically, microinjection into brain area A1 produced depressor response reducing systemic blood pressure (BP) and decreasing heart rate (HR). Conversely, UII (10pmol) injection into paraventricular and arcuate nuclei resulted in a pressor response with tachycardia. This study is supported by the findings of lin et al. [2003] who showed that ICV injection of UII induced a significant increase in blood pressure and heart rate in the rat. However, administration of pentolinium, a ganglionic blocking agent, to the rats prior to UII injection attenuated the pressor and tachycardic response indicating that ICV injection of UII activates the sympathetic nervous system. Similarly to the mechanism of UII action in isolated blood vessels and cultured smooth muscle cells, when rats were pretreated with either, the MEK inhibibitor, PD 98059, or the Rho kinase inhibitor Y-27362, prior to ICV administration of UII, rats exhibited an attenuated pressor response. However, the tachycardic effect on the heart was only slightly attenuated with PD 98059 or Y-27362 pretreatment and did not reach statistical significance suggesting separate mechanisms for UII induced pressor and tachycardiac effects following ICV infusion.

This pressor effect of ICV UII injection was further evaluated in spontaneously hypertensive rats. [Lin et al., 2003] Remarkably, the UII induced pressor response was significantly exaggerated in these animals compared to Wistar-Kyoto rats, while the tachycardic response was comparable between rat strains.

Similarly in conscious ewes ICV injection led to a significant increase in MAP, HR, and Cardiac output (CO), and cardiac contractility. [Watson et al., 2003] In this study the authors also observed significant increases in plasma epinephrine, adrenocorticotropic hormone, as well as glucose following ICV administration of UII. In agreement with the notion that ICV injection of UII activates the sympathetic nervous system, prior administration of propanolol to sheep prevented the cardiac responses due to ICV injection of UII. [Hood et al. 2005]

A study evaluating UII signaling in choline acetyltransferase-positive neurons demonstrated that UII induces an increase in intracellular calcium (Ca_i). [Filipeanu et al., 2002] The increase in Ca_i was due to calcium influx from the extracellular space. PKC inhibition had no effect, but PKA inhibition attenuated the rise in Ca_i suggesting alternate signaling pathways utilized in neuronal cells. Another study showed that UII induces c-FOS, a transcriptional regulator, in the rat brain following ICV injection suggesting UII may have an indirect role in gene induction in the brain. [Gartlon et al. 2004]

1.2.11 Antagonists

With the increasing reports of elevated levels of UII in various diseases the mechanistic pathways are inevitably sought. An important tool for such research is a potent selective receptor blocker. Various compounds have been investigated for their capacity to inhibit UII signaling. Originally, Somatostatin receptor antagonists were evaluated based on the structural similarity of UII and somatostatin, most of these, however, had only moderate affinity for human and rat UT. Rossowski et al., 2002 Behm et al. 2002 further characterized a somatostatin antagonist, SB-710411. This compound inhibited U-II induced vasoconstriction in a competitive and surmountable manner in a rat aortic bioassay. However SB-710411 also potentiated ET-1 mediated vasoconstriction, a characteristic common to somatostatin receptor antagonists, and therefore was not suitable for study as a UII antagonist. Furthermore, in a later study, Behm et al.2004 showed that SB-710411 had potent agonist effects in monkeys inducing strong vasoconstriction while it maintained relatively potent antagonistic activity in rat aortic bioassay. Thus, concluding it is a species dependent effector.

Next, [Orn(8)]U-II was developed by replacing the Lysine residue at position 8 of UII with an ornithine residue. Camarda et al., 2002 This compound acted as competitive and selective antagonist in the rat aortic bioassay however it was a full agonist in HEK293 cells expressing recombinant human and rat UT. The divergent effects of this compound in the two assays were ascribed to differences in receptor density.

The Neuromedin B receptor antagonist BIM-23127, was then assayed for its capacity for UT antagonism because of its structural similarity to the somatostatin antagonist SB-710411.[Herold et al.2003] BIM-23127 exhibited potent and competitive antagonistic activity in both UT expressing cell lines (calcium mobilization assays) and in the rat aortic bioassay. In addition, Johns et al.[2004] demonstrated that UII induced cardiomyocyte hypertrophy was significantly attenuated with the use of this compound. However based on the fact that it was a somatostatin antagonist it could not be used specifically for UT antagonism studies. Although, it may be exploited as a lead compound for the development of more specific UT antagonists.

Urantide was next to be evaluated and it was found to be a very potent and highly selective antagonist in a rat aortic bioassay and therefore may be suitable for the study of UII mechanistic pathways. [Patacchini et al., 2003] However, a later study by Camarda et al. [2004] found while urantide acted as a specific antagonist in the rat aortic bioassay; it showed potent agonistic effects in a calcium mobilaization assay using CHO cells expressing recombinant UT. The authors attribute the divergent effects to the degree of receptor density with the high receptor number in the cell assay exaggerating the effect of urantide. Another caveat is that urantide is a peptidic compound and as such is not suitable for in vivo studies in which it is absorbed via the gastrointestinal tract due to its susceptibility to degradation by endogenous peptidases.

The first non-peptidic antagonist developed specifically for UII antagonism was ACT-058362; 1-[2-(4-benzyl-4-hydroxy-piperidin-1-yl)-ethyl]-3-(2-methyl-quinolin-4-yl)-urea sulfate salt), also referred to as Palosuran. This compound antagonizes binding of (125)I-labeled U-II on cells endogenously expressing human UT and cells carrying the recombinant human UT receptor with a high affinity in the low nanomolar range. Of note is the fact that Palosuran has 10 fold less affinity for rat recombinant UT receptors compared to human UT receptors. ACT-058362 inhibits U-II-induced calcium mobilization and mitogen-activated protein kinase phosphorylation. This compound proved efficacious in a kidney ischemia reperfusion model which demonstrated attenuated ischemia induced acute renal failure and decreased histologically apparent kidney lesions with pretreatment of ACT-058362.[Clozel et al. 2004]

The next non-peptidic antagonist to be characterized was SB-706375.[Douglas et al. 2005] This compound potently inhibited [$^{(125)}$I]hU-II binding to cells expressing rodent, feline and monkey recombinant UT receptors and SJRH30 cells expressing 'native' UT receptors. SB-706375 was a potent, competitive U-II antagonist in rat isolated aorta (inhibition of contraction). It also demonstrated 100-fold selectivity for the human UT receptor compared to 86 distinct receptors, ion channels, enzymes, transporters and nuclear hormones. In addition, vasoconstriction induced in isolated aortae by KCl, phenylephrine, angiotensin II and endothelin-1 were unaffected by SB-706375. Therefore, SB-706375 is a high-affinity, selective, reversible

antagonist that may be utilized in animal models to delineate pathophysiological roles for UII.

1.3 Urotensin-II in disease

1.3.1 Heart failure

Although UII is most prominently expressed in the CNS of most species in the non-diseased state, its expression is up-regulated substantially in the heart in the presence of cardiac disease. This increased expression of UII and UT in the heart due to heart failure was originally evaluated in humans by Douglas et al.[2002] UII immunoreactivity was found to be significantly elevated in patients with end-stage CHF due to either dilated or ischemic cardiomyopathy. Importantly, this study showed that UII levels were significantly correlated with left ventricular end-diastolic dimension and inversely correlated with ejection fraction. In addition, to the significantly elevated UII protein expression, they also found that UII binding sites, a surrogate marker to UT levels, was significantly increased in end stage CHF tissue independent of the etiology of cardiac disease.

This landmark study was followed up with studies using animal models of heart failure. Tzanidis et al. [2003] used a rat heart failure model in which ligation of the left anterior coronary artery induced elevated expression of both UII and UT in the heart. This study showed that UII peptide and UT mRNA were increased in both infarcted and non-infarcted portions of the LV. Notably, these authors also demonstrated that UII had a hypertrophic effect

on cardiomyocytes, although the hypertrophic effect could only be established after adenovirus mediated up-regulation of the receptor in cultured neonatal cardiomyocytes. The latter finding underscores the low expression levels of UT in the non-diseased state. In addition to demonstrating the hypertrophic effect Tzanidis et al. also showed that UII acted as a fibrotic factor, inducing the synthesis of pro-collagens type I and III as well as fibronectin mRNA in cardiac fibroblasts. Interestingly He et al. [2004] also demonstrated UII induced collagen type I mRNA synthesis in fibroblasts, while Wang et al. [2004] demonstrated similar effects in an endothelial cell culture.

Similarly to Tzanidis et al. [2003] a study by Johns et al. [2004] demonstrated in an identical model that both UII and UT mRNA was significantly elevated following coronary ligation. The latter group also showed that UII induced the production of IL-6, an inflammatory cytokine in cultured cardiomyocytes, indicating UII may have pro inflammatory effects in heart failure. In addition, this study also demonstrated UII mediated cardiomyocyte hypertrophy following adenovirus mediated up-regulation of UT in H9c2 cardiomyocytes.

In a model of hypoxia induced pulmonary hypertension, Zhang et al.[2002] found that UII was significantly elevated by 97% in the right ventricle and by 33% in the left ventricle. In addition, radioligand binding studies showed that UT expression was also increased significantly in both the right and left ventricle following 4 weeks of hypoxia.

The increased expression of UII and UT in failing hearts is further supported by several studies demonstrating increased plasma levels of UII in adult human heart failure.[Ng et al., 2002; Richards et al., 2002; Russell et al., 2003; Lapp et al., 2004; Gruson et al., 2005] as well as in children with congenital heart disease.[Simpson et al. 2005]

UII is believed to be secreted prominently by the heart because of the plasma gradient in UII levels between the pulmonary artery and aortic root described by Russell et al. [2003], although the lungs cannot be excluded as the source of increased UII.

Lapp et al.[2004] demonstrated significantly increased UII plasma levels in patients with ischemic cardiomyopathy and these levels correlated significantly with LVEDP, brain natriuretic peptide (BNP) levels, and New York heart association (NYHA) functional class and tended to correlate inversely with ejection fraction. Similarly, Gruson et al.[2005] demonstrated that the UII levels in CHF patients correlated negatively with ejection fraction and positively with neurohormonal factors including endothelin-1 and BNP.

Conversely, both Dschietzig et al [2002] and Kruger et al. [2005] found no difference in UII plasma and tissue levels in patients with CHF compared to normal controls. The reason for this discrepancy is unknown. Conceivably, these differences may be attributed to different assays or patient populations used.

The functional significance of elevated UII levels in heart failure is presently unknown and may simply represent an indirect effect. However,

the demonstration that patients with CHF exhibit microcirculatory vasoconstriction, while normal volunteers reveal vasodilation following UII administration, suggests that increased UII plasma levels may contribute to vascular tone, especially in the diseased state.[Lim et al., 2004]

The profibrotic effect observed by Tzanidis et al. [2003] has been further supported by Kompa et al. 2004, who showed that chronic infusion of UII in the rat for 2 weeks led to a 40% increase in left ventricular end-diastolic pressure (LVEDP) which is indicative of increased myocardial stiffness. Indeed they went on to show that the 40% increase in LVEDP was associated with a significant increase in fibrosis as determined by an increased collagen type I:III ratio. UII has also shown fibrotic effects in an endothelial cell culture, inducing collagen Type I expression as well as inhibiting matrix metalloproteinase (MMP)-1 activity.[Wang et al.2004] This fibrotic effect was also shown to be ERK 1/2 dependent.

1.3.2 Systemic and Pulmonary Hypertension

Although UII induced vasoactivity in humans may be variable at best, its potent nature has prompted some research in hypertensive patients. UII was significantly elevated in hypertensive patients compared to normotensive controls, and the increase in UII plasma levels in these patients were correlated with systolic blood pressure and age [Cheung et al. 2004]. In addition, Rdzanek et al.[2005] found that UII plasma levels were significantly elevated in post MI survivors with hypertension compared to post MI survivors without hypertension following exercise stress. Another study which evaluated UII levels in the cerebrospinal fluid demonstrated that UII levels positively correlated with MAP in a cohort of patients undergoing surgery for non-cardiovascular causes. [Thompson et al., 2003] The association of increased plasma levels of UII in hypertension seems to be widespread. Indeed, Balat et al. [2005] found significantly increased UII plasma levels in patients with preeclampsia, a condition in which pregnant females present with new onset systemic hypertension. Another study which also compared UII plasma levels between preeclamptic and normotensive pregnant women found no difference in plasma samples. [Cowley et al. 2005] The inconsistency between the findings of Balat et al. [2005] who showed significantly elevated UII plasma levels in preeclamptic patients vs. the findings of Cowley et al. [2005] may be due to the effect of sample size. Indeed Balat et al. recruited 60 patients while Cowley et al. only evaluated 20 patients.

The UII plasma level difference observed in hypertensive vs. normal controls was found to potentially have a pathophysiological relevance in a study which showed that patients with idiopathic hypertension exhibited vasoconstriction, while a normal control cohort exhibited vasodilation, following UII injection into the microcirculation. Sondermeijer et al., 2005

Qi et al.[2004] demonstrated in a model of pulmonary hypertension induced by aorto-caval shunting that UII up-regulation was associated with muscularization of the pulmonary arteries. Another study evaluating the effects in pulmonary arterial SMCs showed that UII induced the expression of NADPH oxidase. Djordjevic et al. 2004 Specifically UII induced the protein expression of subunits p22phox and NOX4 and increased the levels of reactive oxygen species in pulmonary arterial SMCs. This was associated with an increase in the phosphorylated forms of ERK1/2, p38MAPK, JNK, and Akt, again demonstrating a considerable degree of intracellular signaling cross-talk.

1.3.3 Atherosclerosis

Atherosclerosis, the primary cause of ischemic cardiomyopathy and ultimately the major contributing factor to death in the Western world today is obviously an enormous burden on society and as such is the focus of a considerable amount of research. In light of the vasoactive properties of UII, its role in atherosclerosis has been investigated. Hassan et al.[2005] demonstrated that UII protein and mRNA levels were significantly increased

in arteries of patients with coronary atherosclerosis compared to normal coronary arteries. Greatest expression of U-II was observed in endothelial cells of lesions, especially inflammatory lesions or those with a fibrofatty core. Myointimal cells, smooth muscle cells and foam cells also expressed U-II. Thus, these findings suggested a potential role for U-II in the pathogenesis of coronary atherosclerosis.

Furthermore, Maguire et al.[2004] found prominent UII immunoreactivity in atherosclerotic plaques of coronary arteries as well as in the thickened intima of failed saphenous vein grafts of explanted human hearts. Notably, CD68+ macrophages showed a similar distribution pattern in adjacent sections suggesting a macrophage origin of UII in atherosclerotic lesions. In addition to increased UII levels in atherosclerotic lesions, increased UII levels in plasma of patients with atherosclerotic disease has also been demonstrated. [Heringlake et al. 2004, Lapp et al. 2004] Specifically, Heringlake et al. [2004] found that patients with documented coronary artery disease (CAD) had significantly elevated UII plasma levels compared to normal volunteers, and that the levels increased with severity of CAD. In addition, they also demonstrated that UII plasma levels correlated significantly with pulmonary capillary wedge pressure (PCWP), a surrogate marker for left ventricular filling pressures, and inversely with left ventricular ejection fraction. The demonstration of increased UII levels in patients with atherosclerotic disease is in sharp contrast to the findings of Joyal et al. [2006] who showed that in patients with acute coronary events, UII levels were significantly lower

compared to patients with stable coronary artery disease and normal controls. Furthermore, UII levels correlated inversely with systemic arterial pressure in these patients. This latter report is supported by a study which evaluated fatal and non-fatal cardiovascular events in a cohort of patients with end-stage renal disease.[Zoccali et al. 2006] The cohort exhibited double the plasma levels of UII compared to normal volunteers. However, the patients within this cohort who experienced cardiovascular events had significantly reduced UII plasma levels compared to the patients who did not have any cardiovascular events. Although this issue of decreased levels in the face of acute events is as of yet unresolved, one could speculate that there is a sudden increase in receptor expression and therefore a sequestration of UII from plasma, especially since UII is a pseudo-irreversible ligand. However further studies are warranted.

UT mRNA was shown to be significantly up-regulated in the aortae of ApoE KO mice, an established animal model for the study of atherosclerosis. [Wang et al., 2005] This was complemented by the demonstration of significantly increased UII radioligand binding in these same aortae. Therefore, UII and UT are increased in atherosclerotic vessels of both mice and humans.

Intimal thickening is one earliest stages of the atherosclerotic process. Indeed, it is these sites of increased intimal thickening that have the greatest predilection for atherosclerotic plaque formation. Intima-media thickness has been shown to correlate with unfavourable levels of established cardiovascular risk factors. [Salonen et al. 1991] As such, smooth muscle cell

proliferation is integral to the patho-physiology of atherosclerosis. SMCs migrate into the intima and proliferate producing the thickened neointima, an early characteristic of atherosclerotic lesions. As mentioned before, UII has shown proliferative effects in cultured vascular smooth muscle cells. [Chen et al., 2004; Sauzeau et al., 2001; & Watanabe et al., 2001] In addition, Watanabe et al.[2001] demonstrated a synergistic effect of UII on proliferation of SMCs when administered with either serotonin or oxidized LDL. In support of the latter study lysophosphatidylcholine, an oxidized phospholipid, also synergistically enhanced UII mediated SMC proliferation. [Watanabe et al., 2002] This has potentially serious pathological implications since oxidized lipids are a major contributor to atherosclerotic lesion formation. This synergistic activity may explain the observed associations between UII plasma levels and clinical atherosclerotic disease.

The mitogenic role of UII in SMCs is supported by a study which showed significantly increased UII expression in the neointima of a rat carotid artery restenosis. [Rawkowski et al., 2005] Specifically, balloon mediated injury in the carotid artery of the rat led to a substantial increase in intima:media thickness ratio and this was associated with significantly increased UII expression. Treatment of rats subjected to angioplasty with a UII antagonist, SB-611812, led to significantly reduced neointimal formation as evidenced by reduced intima:media ratio compared to rats receiving placebo. Thus UII may actively participate in atherosclerosis progression by inducing the proliferation of vascular smooth muscle cells.

Macrophages are also important contributors in the pathophysiology of atherosclerosis. In fact they are present in the earliest form of atherosclerotic lesions termed fatty streaks. Macrophages take up low density lipoprotein (LDL) and oxidized LDL via scavenger receptors and ultimately become foam cells. These foam cells accumulate initially forming fatty streaks but with time contribute to the formation of the necrotic fibrofatty core of large atherosclerotic lesions. UII has been shown to promote the formation of foam cells. Specifically monocyte derived macrophages demonstrated significantly increased Acyl CoA: Cholesterol Acyl Transferase (ACAT) activity and expression following incubation with 25nM UII. This effect was completely inhibited by urantide, a selective UT receptor antagonist; rottlerin, a PKC inhibitor; PD98059 a MEK inhibitor; Y27632, a Rho kinase (ROCK) inhibitor; PP2, a c-Src protein tyrosine kinase inhibitor; and GDP-beta-S, a G-protein inactivator. This demonstrates that there is substantial degree of intracellular signaling crosstalk in the monocyte/macrophage population as well. The latter study also showed that this increase in ACAT activity and expression was associated with a significant increase in acetylated LDL induced cholesterol uptake.

The liver is integral to serum lipid homeostasis and as such potentially affects the development of atherosclerotic disease. This is especially interesting in light of the finding that UII induces triglyceride lipase activity and lipid mobilization from the coho salmon liver.[Sheridan et al., 1986] However whether this effect is extrapolated to humans is as of yet still unknown.

Circulating lipoproteins are known to cross the endothelium and enter the intima often binding reversibly to negatively charged proteoglycans of the extracellular matrix. Thus any factor that increases endothelial permeability presumably may increase lipid entry into the intima and therefore increase susceptibility to intravascular lesion formation. UII has been shown to increase plasma extravasation in rat aortae.[Gendron et al. 2004] The latter study is supported by the findings of Vergura et al.[2004] who demonstrated increased plasma extravasation in several tissues in mice following IV injection of 10pM-10nM UII. UII induced plasma extravasation was significantly attenuated in this study with pre-injection of [Orn(8)]U-II, a UT antagonist.

1.4 Rationale

UII, a small protein with vasoactive properties was first isolated from the caudal neurosecretory region of the teleost fish. In most species UII is most predominant in the central nervous system, while UT is predominant in heart and kidneys. UT is a seven transmembrane spanning G-protein coupled receptor which associates with the $G_{\alpha q}$ protein. UII binds UT in a pseudo-irreversible manner and elicits activation of a broad spectrum of intracellular signaling molecules including PKC and ERK 1/2.

UII is a vasoactive factor inducing vasoconstriction of some arteries such as the rat aorta, while inducing endothelial mediated vasodilation of other vessels. UII induces proliferation of endothelial cells, and smooth muscle cells, as well as hypertrophy of cardiac myocytes. Furthermore, UII

elicits inotropic responses in ex vivo heart preparations. IV injection of UII results in a decrease in mean arterial blood pressure with reflexive tachycardia in the rat while it causes cardiovascular collapse in monkeys. On the other hand, intracerebral injection of UII causes a pressor response and tachycardia in both rats and sheep. Physiological functions of UII are summarized in table below.

UII expression is increased in failing human hearts as well as in plasma of patients with heart failure and hypertension. Similarly, UII is increased in plasma of patients with documented coronary atherosclerosis. UII and UT are up-regulated in atherosclerotic arteries of humans, in arteries of rats with balloon angioplasty mediated arterial injury, and in aortae of hypercholesterolemic mice. Also UII induces SMC proliferation alone and in a synergistic fashion with oxidized LDL, a major contributor to atherosclerosis. In addition, UII promotes foam cell formation and finally increases vessel wall permeability potentially increasing lipid accumulation in the intimal space. Thus UII is widely expressed in cardiovascular disease and therefore may have a pathophysiological role.

Table 2. Physiological effects of UII in various organs.

Organ	**Physiological effects**
Heart	1. Cardiac inotropic effects. 2. Cardiomyocyte hypertrophy. 3. Cardiac fibroblast mediated collagen and fibronectin synthesis. 4. Coronary vasoactivity.
Vasculature	1. Endothelial cell dependent vasodilator. 2. Endothelial cell independent vasoconstrictor. 3. Smooth muscle cell mitogen. 4. Endothelial cell mitogen. 5. Foam cell inducer. 6. Plasma extravasation.
Kidneys	1. May increase or decrease GFR.
Liver	1. Induces Depot Lipase activity thereby channeling glucose into free fatty acid synthesis.*
CNS	1. Anxiogenic effects. 2. Induces the release of Epinephrine, ACTH, Glucose, & prolcatin.

* Only demonstrated in Coho salmon.

1.5 Hypothesis and Aims

Elevated levels of UII in cardiovascular diseases is well documented. However, the role UII plays in these diseases is presently unknown. Moreover, are the elevated levels a cause or effect of cardiovascular pathologies? Therefore, the objectives of the following study were to evaluate the degree of UII expression in atherosclerosis and ischemic cardiomyopathy. Furthermore we aimed to evaluate the mechanistic role of UII in the latter diseases with both pharmacological and genetic approaches. Specifically, the aims of the present study were as follows:

(1) To evaluate UII and UT expression in a rat model of congestive heart failure and to elucidate a mechanistic role for this system using a selective UII receptor antagonist.

(2) To assess the degree of UII and UT expression in human carotid and aortic atherosclerosis.

(3) To evaluate the role of UII/UT signaling via UT gene deletion in a well established model of atherosclerosis using ApoE knockout mice.

Chapter II

Urotensin-II receptor blockade with the non-peptide antagonist SB-611812 improves cardiac function and remodeling in experimental heart failure

2.1 Preface

This chapter presents our findings of UII and UT expression in a rat model of heart failure. We also demonstrate the effects of UII antagonism with SB-611812, on cardiac function and remodeling. SB-611812, a non-peptidic UII receptor antagonist, is a parent compound of the SB-706375 described in the literature review. This is the first *in vivo* study published demonstrating the efficacy of UT blockade in an experimental model of CHF using a selective non-peptidic UT receptor antagonist. The results presented here demonstrate a beneficial effect with the use of this compound and hence proposes UII as a possible target for cardiovascular therapy. The work presented in this chapter resulted in two manuscripts published in the *Journal of Molecular and Cellular Cardiology* and *Peptides*. The following text is taken from the two published manuscripts.

2.2 Abstract

Background: Expression of urotensin II (UII) is significantly elevated in the hearts of patients with congestive heart failure (CHF). Recent reports have also shown increased plasma levels of UII in patients with CHF, and these levels correlated with the severity of disease. We therefore hypothesized that blockade of UII signaling would improve cardiac function and remodeling.

Methods and results: CHF was induced in rats by ligating the left coronary artery. Animals were then administered a specific UT receptor antagonist, SB-611812, or vehicle for 8 weeks (30mg/kg/day, UID by gavage). We measured cardiac function and evaluated the levels of mRNA expression for mediators of CHF. In addition, we evaluated UII, UT, collagen type I and type III levels using Western blotting. Cardiomyocyte hypertrophy was evaluated by measuring cardiomyocyte cross-sectional area. Cardiac fibrosis was analyzed histologically using Masson's Trichrome stain while collagen deposition was analyzed with Picrosirius red staining. Finally, cardiac fibroblast proliferation was evaluated. Animals with CHF showed increased UII and UT expression as evidenced by immunohistochemistry and Western blotting. Treatment with SB-611812 significantly reduced overall mortality, left ventricular end-diastolic pressure by 72%, lung edema by 71%, right ventricular systolic pressure by 92%, central venous pressure by 59%, and cardiomyocyte hypertrophy by 54% ($P<0.05$). SB-611812 also significantly reduced collagen type I:III ratio ($P<0.01$) compared to the vehicle group. Treatment also led to a significant reduction in fibrosis in the viable left

ventricle and collagen deposition in the viable endocardium. 1nM UII induced proliferation of cardiac fibroblasts and this mitogenic effect was significantly inhibited with 1μM of SB-611812 ($P<0.05$).

Conclusion: Blockade of the UII receptor reduced mortality, improved cardiac function and cardiac remodeling associated with this model of myocardial infarction and CHF, suggesting an important role for UII in the pathogenesis of these diseased conditions.

2.3 Introduction

Urotensin-II (UII) a relatively novel peptide, originally isolated from fish spinal cords, has prompted some substantial interest in the field of cardiovascular medicine. UII is an 11 amino acid peptide in humans and has an intramolecular ring structure connected by two cysteine residues.[Coulouarn et al. 1998] The cyclic portion is essential for UII activity.[Kinney et al. 2002] Accordingly, it is conserved throughout all species.[Coulouarn et al. 1998 & Coulouarn et al. 1999] UII binds to a 389 amino acid G-protein coupled receptor termed UT.[Ames et al. 1999] The G-protein associated with the UT receptor is of the Gq class, which is the same class of G-proteins that bind to angiotensin, endothelin and α-adrenoceptors. UII induced both endothelium-independent vasoconstriction and endothelium-dependent vasorelaxation, the order and magnitude of which was dependent on the species tested and anatomical location.[Douglas et al., 2000; Camarda et al., 2002; Bohm et al., 2002] UII induced vasoconstriction of the coronary vasculature in a variety of animals including rat, dog, monkey as well as in man.[Ames et al., 1999; Bottrill et al., 2000; Douglas et al., 2000] Notably, Bottrill et al,[2000] demonstrated that UII induced vasoconstriction of the rat coronary vasculature was enhanced with removal of the endothelium which is especially interesting in light of the endothelial dysfunction that commonly accompanies CHF. This is supported by the findings of Lim et al,[2004] who demonstrated that UII induced vasodilation in the microvasculature of normal subjects while it induced vasoconstriction in the microvasculature of patients with CHF. UII also exerted inotropic effects on the isolated human atrial

trabeculea,[Russell et al., 2001] mitogenic effects on smooth muscle cells, [Sauzeau et al., 2001 & Watanabe et al., 2001] and induced collagen and fibronectin synthesis by cardiac fibroblasts. [Tzanidis et al., 2003] The latter study also showed that UII induced hypertrophy of rat neonatal cardiomyocytes, as does both endothelin-1 (ET-1) and angiotensin-II (Ang-II). [Sadoshima et al., 1993 & Bogoyevitch et al., 1994] Bolus injection of UII into cynomolgus monkeys resulted in the development of cardiovascular collapse. [Ames et al., 1999]

The heart is one of the tissues with the highest degree of UT expression, further supporting its role in cardiovascular physiology. [Ames et al., 1999] Indeed, UT mRNA was found in both atrial and ventricular tissue. [^{125}I] U-II binding sites were noted in human left ventricle using quantitative receptor autoradiography, [Maguire et al., 2000] and mRNA transcripts for the receptor were also shown in the heart using in situ hybridization. [Liu et al., 1999] We have previously demonstrated increased myocardial expression of UII in CHF patients, and this increase was significantly correlated with the increase in left ventricular end-diastolic dimension (LVEDD). [Douglas et al., 2002] Our findings were followed by several reports of increased plasma levels of UII in CHF. [Richards et al., 2002 & Ng et al., 2002] Of note, is the finding of increased plasma levels of UII which correlated with left ventricular end-diastolic pressure. [Lapp et al., 2004]

Recently, Johns et al, [2004] demonstrated in a model of CHF in the rat, that cardiac ventricular mRNA expression of U-II and UT receptor were increased, and that this increase was associated with increased expression

of the cytokines interleukin-1β (IL-1) and IL-6 in a time dependent manner. In addition this study demonstrated that a competitive peptidic UT receptor antagonist, BIM-23127, inhibited U-II-induced hypertrophy in H9c2 cardiomyocytes.

Fibrosis, a fundamental characteristic of cardiac remodeling following infarction, increases myocardial stiffness in large part by interstitial collagen deposition. UII, has been previously shown to have a pro-fibrotic effects. For example, Tzanidis et al. [2003] demonstrated that UII induced collagen type I, collagen type III, and fibronectin mRNA expression in rat neonatal cardiac fibroblasts. Furthermore, Wang et al. [2004] demonstrated that UII induced collagen type I mRNA and protein while decreasing expression and activity of matrix metalloproteinase-1 (MMP-1) in endothelial cells.

Based on the cardiovascular actions of UII and our own findings in CHF patients, we hypothesized that UII is up-regulated in an experimental CHF model of myocardial infarction, and that UT receptor antagonism may lead to improvement in cardiac function and structure. Thus, a non-peptidic selective UT antagonist SB-611812, that has been shown to effectively to block the vasoconstrictive effects of U-II in renal arteries, was administered to rats prior and after coronary artery ligation; and evaluated for its effects on mortality, infarct size, hemodynamics, and gene/ protein expression.

2.4 Methods

2.4.1 Details of SB-611812

SB-611812, an arylsulfonamide UT antagonist (2,6-dichloro-N-(4-chloro-3-{[2-(dimethylamino)ethyl]oxy}phenyl)-4-(trifluoromethyl)benzenesulfonamide), was synthesized at GlaxoSmithKline, King of Prussia, PA. [Dhanak et al., 2001] SB-611812, potently binds the rat recombinant UT receptor (K_i 121nM) and antagonizes UII in both isolated vascular tissue (rat aortic contraction) and cell based (inhibition of $[Ca2+]_i$-mobilization in rat UT-HEK293 cells) assays (pA2s of 6.59 and 6.60, respectively). SB-611812 has approximately 100% bioavailability, and has a 4-5h half life in the rat by oral gavage. Specificity of SB-611812 was demonstrated by the fact that pretreatment of the rat isolated aorta with 10 μM SB-611812 (which is 40-fold higher concentration than the pA_2 of this compound in the aortic vasoactivity bioassay) did not inhibit the contraction induced by KCl, Phenylephrine, Endothelin-I, or Angiotensin-II. In a separate study, we found that 1nM exogenous UII induced a significant increase in renal vascular resistance which was 90% inhibited with the dose utilized in the present study (30mg/kg/day) (data not shown). Dosing experiments in healthy animals showed no acute or chronic effects for the drug on hemodynamics or cardiac function.

2.4.2 Surgical methodology

Throughout the study male Lewis rats weighing ~250 grams obtained from Charles River laboratories were used. Animals were initially divided into a

sham group (n=9) and a myocardial infarction (MI) group. The MI group was further subdivided randomly into 5 groups including: MI only group (n=22), an MI + treatment group (Day 0) in which treatment was administered by gavage (30 mg/kg/day; once a day) 30 minutes prior to surgery (n=22); MI + vehicle group (day 0) in which the drug vehicle (0.1% methylcellulose) was administered by gavage 30 minutes prior to surgery (n=28); MI + treatment group (Day 10) in which treatment was administered by gavage 10 days after surgery (n=12); MI + vehicle group (Day 10) in which the drug vehicle (0.1% methylcellulose) was administered by gavage 10 days after surgery (n=15). Animals were administered either SB-611812, or vehicle once a day for the duration (8 weeks) of the study period.

All animals receiving a coronary ligation underwent a left thoracotomy followed by dissection of the pericardial sac and exposure of the left anterior ventricular free wall. The left anterior descending coronary artery (LAD) was then visualized and a suture was placed in the myocardium surrounding the LAD and the suture was ligated. Pallor of the anterior free wall was verified before wound closure.

The sham group underwent the same procedure except the suture was not ligated but was cut at both ends at the epicardial border. Following surgical intervention rats were allowed to recover for 8 weeks before sacrifice.

Just prior to sacrifice, animals were subjected to measurements of hemodynamics and cardiac functions. Experiments were performed in

accordance with the Guide for the Care and Use of Laboratory Animals (National Institutes of Health Publication 86 to 23, revised 1996), and with approval of the Animal Care Committee of the McGill University Health Center.

2.4.3 Hemodynamic and cardiac function measurements.

Rats were catheterized via the carotid artery. The polyethylene tubing (PE50 from Intramedic, Montreal, Canada) catheter (0.58mm), which was connected to a pressure transducer measured systolic arterial pressure (Psyst.), diastolic arterial pressure (Pdiast.), and mean arterial pressure (MAP). The catheter was then passed into the left ventricle for measurements of left ventricular end-systolic pressure (LVESP), left ventricular end-diastolic pressure (LVEDP), +dP/dt (the first derivative of the rate in positive pressure change in the ventricle), and -dP/dt (the first derivative of the rate in negative pressure change in the ventricle). Using a jugular vein approach, central venous pressure and right ventricular systolic pressure (RVSP) was determined by insertion of the catheter into the right atrium and ventricle, respectively.

2.4.4 Tissue collection

Animals were sacrificed by exsanguination, and the hearts were collected and snap frozen in liquid nitrogen and stored at -80°C, or fixed in 4% paraformaldehyde and embedded in paraffin for histological and

immunohistochemical analysis. Lungs were also harvested and weighed. They were allowed to dry in a 40°C oven for 1 week and weighed again until there were three consecutive identical weights. These values were then used to calculate the lung wet/dry weight ratio.

2.4.5 Infarct analysis

Heart tissue embedded in paraffin was cut at 5μm slices and stained with the histological stain, Masson's trichrome which allowed one to discern infarct from non-infarcted myocardial tissue. Following this, pictures were taken of the sections and downloaded into an image analysis program for infarct size analysis, (Image ProPlus, Media Cybernetics, CA, USA). All sections were examined in a blinded fashion.

2.4.6 Assessment of cardiomyocyte hypertrophy

Myocyte cross sectional area analysis was carried out by taking photomicrographs of the endocardial region of heart sections stained with hematoxylin & eosin (at 400X magnification). These photomicrographs (4/animal; sham n=6, vehicle n=8, and treatment n=8) were then analyzed by the image analysis program, *Image ProPlus*. The latter enables the users to demarcate individual myocytes and quantify their area using arbitrary units.

2.4.7 Immunohistochemistry

Immunohistochemical staining for UII and UT was performed using the avidin-biotin peroxidase method. Paraffin sections were dewaxed in toluene for 20 minutes, and rehydrated through 100%, 90%, 70%, and 50% alcohol for two minutes each. All sections were then immersed in PBS solution for five minutes and then 3% hydrogen peroxide solution to block endogenous peroxidase activity for 30 minutes. The sections were then washed three times in PBS solution for five minutes. The sections were permeabilized in 0.2% Triton in 0.1M PBS (pH 7.4) for 30 minutes and washed three times in PBS for five minutes. Sections were then incubated in 10% normal goat serum (NGS) for 30 minutes at room temperature after which they were incubated overnight at 4°C with the primary antibody. The sections were washed three times in PBS for five minutes following the cold storage, and incubated for 45 minutes with biotinylated goat-anti rabbit-IgG (1:200) at room temperature. They were then washed three times again in PBS for five minutes, and incubated with the avidin-biotin-peroxidase complex (Vectastain Elite Kit, Vector Laboratories, Burlingame, CA, U.S.A.) for 45 minutes at room temperature. Sections were then washed three times in PBS solution for five minutes. Following this, sections were incubated in 3'3 diaminobenzidene solution (0.025%) for 2 minutes for chromogenesis. Sections were covered using permount (Fischer Scientific, New Jersey, USA) and glass coverslips and were allowed to dry. Negative control sections were incubated with the antisera:antigens mixture or a normal serum only. The antibody against UII

utilized in this study has been previously described. [Douglas et al. 2002] The antibodies against UT were raised in rabbit using epitopes from the 1st extracellular, 1st intracellular, and 2nd extracellular loops.

2.4.8 Real Time RT-PCR

Left ventricular myocardial samples (for n values see Table 2) were retrieved from storage for RNA extraction using Trizol (Invitrogen, Ontario, Canada) and performed as per the manufacturer's instructions. RNA integrity was then verified for all samples by evaluating the clarity of the 28S and 18S bands and verifying that the bands were 28S>18S by gel electrophoresis. Following this, 2 μg of each RNA sample was reverse transcribed to synthesize cDNA using the Omniscript reverse transcriptase kit from Qiagen (Ontario, Canada). From this, 1 μl of cDNA was used to amplify target genes using specific primers (Table 3). Genes were amplified individually in the LightCycler (Roche, Montreal, Canada) using Quantitect SYBR Green reagent (Qiagen, Ontario, Canada) with the following amplification conditions: DNA polymerase activation, 15 minutes at 95 ° C followed by 40 cycles of denaturation, annealing and extension for 15 seconds at 94 ° C, 20 seconds at 50-60 ° C (depending on primer T_m) and 20-30 seconds at 72 ° C (depending on amplicon size), respectively. Primers were designed using PrimerQuest biotool [www.idtdna.com] (Table 3). All values for mRNA expression determined by RT-PCR are expressed as the ratio of the copy number of the mRNA transcript of interest to the copy number of the mRNA

transcript of the housekeeping gene RPL32. A homogeneous amplification of the products was rechecked by analyzing the melting curves of the amplified products.

2.4.9 Western Blotting

Protein samples were assayed with specific antibodies against UII, UT, collagen type I, collagen type III, (Santa-Cruz Biotechnology, California). Briefly, protein samples were extracted from left ventricular tissue using an extraction buffer containing 50mM Tris/HCl, pH 7.2; 150mM NaCl; 1% (v/v) Triton X-100; 1mM sodium orthovanadate; 50 mM sodium pyrophosphate; 100 mM sodium fluoride; and a complete protease inhibitor cocktail tablet (Roche, Montreal, Canada; 1 tablet /50 ml buffer). The extracted protein was then snap frozen in liquid nitrogen and stored at –80°C. Protein concentrations were determined using the Bio-Rad modified Bradford protein assay. 50µg of protein were then diluted 1:2 with Laemmli sample buffer (Bio-Rad, CA, USA) and electrophoresed on a 6% or 10% SDS-PAGE gel at 120 volts (V) for 1 hour. Following this, proteins were transferred to a PVDF membrane at 100 V for 90 minutes. The membrane was then blocked with 5% skim milk powder in Tris-buffered saline (TTBS; 0.05M Tris, 0.15M NaCl; pH 7.6) with 0.1% Tween-20 for 90 minutes. This was followed by an overnight incubation with the primary antibody. The following day, the membrane was then washed with TTBS and incubated with secondary antibody-conjugated to horse radish peroxidase for 60 minutes. The

membrane was then washed in TTBS and then incubated with Lumi-Light chemiluminescent substrate (Roche, Montreal, Canada) for 5 minutes and then exposed on radiographic film. Protein bands were then quantified using arbitrary units (AU) with the image analysis program, *Image ProPlus* (Media Cybernetics, CA. USA).

2.4.10 Histological and morphological analysis.

All hearts were sectioned across the ventricles for histological, morphological, and immunohistochemical analyses. The extent of fibrosis in both the viable left ventricle and infarcted region was quantified by analysis of Masson's Trichome stained heart sections (cut in transverse fashion). Specifically, for analysis of fibrosis in the viable left ventricle, 6 random photomicrograghs were taken in the viable left ventricular myocardium at 400X magnification for each animal (sham n=6, vehicle n=9, and treatment n=9). The amount of fibrosis in these photomicrographs were then quantified by *Image ProPlus*. For analysis of fibrosis within the infarcted region three photomicrographs from each animal were taken and blue staining was quantified. Histological assessment of fibrillar collagen deposition was carried out using picrosirius red staining. The latter was evaluated (in both viable myocardium and in the infarct region) in same fashion as the fibrosis analysis with Masson's trichrome stained heart sections described above.

LV chamber area analysis was carried out by determining the intra chamber area of the LV from histological sections cut in the transverse plane.

Using the latter sections we also measured wall thicknesses in both viable and non-viable regions of hearts with *Image ProPlus.*

2.4.11 Fibroblast culture and proliferation assay

The effect of SB-611218 on UII stimulated ventricular fibroblast proliferation was investigated on neonatal rat cardiac fibroblasts that were purchased from Cell applications (CA, USA). Initially, cardiac fibroblasts from passage 5 were plated at an equal density of 10^4 cells /well in a 96 well plate in DMEM with 10% bovine serum (with 50 U/ml penicillin, 50 μg/ml streptomycin) for 48 hours (37°C) followed by serum starvation in DMEM/0.01% bovine serum albumin (BSA) (with 50 U/ml penicillin, 50 μg/ml streptomycin) for 48 hours. Following this cells were incubated with either DMEM/10% serum media, DMEM/0.01% BSA media, DMEM/0.01% BSA media with either 1pM, 1nM, 100 nM UII (peptide institute, Osaka, Japan), or DMEM/0.01% BSA media with 100nM UII + 1μM SB-611812, for 48 hours. Proliferation was quantified using the colorimetric BrDU ELISA proliferation assay from Roche (Montreal, Canada). Protocol was carried out as per manufacturer's instructions.

2.4.12 Statistical analysis

All parameters were evaluated using either one-way ANOVA test (with the Tukey post-hoc test), student's t-test (for two group comparisons), or Kaplan-Meier analysis for mortality, with the aid of the statistical program *SPSS 11.5.* A P value of <0.05 was considered statistically significant.

2.5 Results

2.5.1 Characteristics of the MI/CHF Model

Several anatomical and functional parameters were evaluated in the CHF model including hemodynamics, cardiac function, heart and lung weights and also mRNA and protein expression of markers and mediators of CHF. Specifically, there was a significant increase in LVEDP (165%), RVSP (19%), CVP (98%), and a significant decrease in ±dP/dt (32%) in vehicle-treated MI rats compared to sham rats (Table 1). There was a significant increase in the heart weight to body weight ratio (36%; $P<0.05$) (Table 1), cardiomyocyte hypertrophy (61%; $P<0.005$), LV chamber size/body weight (110%; $P<0.001$), as well as the lung wet-to-dry weight ratio in the vehicle group compared to the sham group (11%; $P<0.001$) (Table 1). LVSP was decreased (15%) compared to the sham group but this did not reach statistical significance (Table 1). There was no significant difference in systolic and diastolic blood pressure, mean arterial pressure and heart rate between the two groups (Table 1). Also, left ventricular wall thicknesses were measured in both scar and non-scar regions although no statistically significant differences were observed. To verify the lack of effect by the drug vehicle we included a group of animals in which MI was induced but there was no administration of either drug or vehicle. Accordingly parameters were virtually indistinguishable between the group of animals which were subjected to MI and administered drug vehicle compared to those in which MI was induced without administration of either drug or vehicle (data not shown).

The mRNA expression of both BNP and AT-1 were significantly increased in the vehicle-treated MI group compared to the sham group (9% and 8%, respectively; $P<0.05$) (Table 2). Conversely, cardiac troponin I (cTnI) levels were significantly decreased in the vehicle-treated MI group compared to the sham group (7%; $P<0.005$) (Table 2). The mRNA levels for factors believed to be integral to the fibrotic process of CHF including the extracellular proteins collagen type I, collagen type III, and fibronectin were determined. The mRNA levels of all three extracellular matrix (ECM) proteins evaluated were significantly increased in the vehicle group compared to the sham group (10%, 11%, and 7% respectively; $P<0.01$) (Table 2). Also, the mRNA expression of TIMP-1 was significantly elevated in the vehicle group compared to the sham group (8%; $P<0.01$) (Table 2). Together, these data confirm the presence of CHF secondary to MI in this animal model.

2.5.2 Increased Myocardial Expression of UII in heart failure

Immunohistochemistry revealed the presence of little to no UII expression in cardiomyocytes and only weak UII expression in intramyocardial vascular smooth muscle cells of normal hearts (Figure 1A). Also, no UII expression was observed in endothelial cells of the myocardial vasculature. In contrast, there was strong expression of UII in CHF animals. Especially in the surviving cardiomyocytes and myofibroblasts of the infarcted left ventricular endocardium (Figure 1B-C). Immunoreactivity was strong in the viable left ventricle, particularly at the peri-infarct border zone (Figure 1D-E). Also,

there was abundant expression of UII in intramyocardial vessels of the left ventricle (Figure 1F). In the right ventricle of CHF animals, moderate expression of UII in cardiomyocytes and intramyocardial smooth muscle cells was observed (Figure 1G). The ventricular septa only showed weak UII expression. All negative control sections showed no immunoreactivity for UII (Figure 1H).

UII protein content was also quantified using Western blot analysis. Here we show that the level of UII protein expression is significantly increased in the hearts, specifically, the left ventricles of CHF animals compared to sham operated controls (1705 ± 103 Arbitrary Units (AU) vs. 1346 ± 96 AU; $P<0.05$) (Figure 2). Rat prepro-UII consists of 123 amino acid residues with a predicted molecular weight of 13.7 KDa. In accordance with this, the Western blot shows a band corresponding to protein with a molecular weight of approximately 14 KDa.

2.5.3 Increased Myocardial Expression of UT in heart failure

There was moderate diffuse UT immunoreactivity in the normal control hearts (Figure 3A). Specifically, UT immunoreactivity was seen in cardiomyocytes, vascular and endocardial endothelial cells, and in vascular smooth muscle cells. In animals with myocardial infarction, like UII, UT protein expression was much more pronounced in the viable cardiomyocytes within the infarct region although perhaps to a slightly lesser degree compared to UII (Figure 3B-D). In addition, pronounced immunoreactivity was observed in the

endocardial endothelium, especially in the infarct region (Figure 3B-D). There was marked and intense UT immunoreactivity in the myocardial vasculature, both in the infarcted and non-infarcted zones (Figure 3E-F). The vascular UT immunoreactivity was stronger in small vessels. The interventricular septum showed diffuse immunoreactivity though it was less intense than the right ventricle of CHF animals which showed diffuse, yet pronounced immunoreactivity (Figure 3G). Right ventricular vasculature also exhibited UT immunoreactivty although this was less intense than in the infarcted LV. There was no detectable immunoreactivity in negative control sections in which the primary anti-sera was omitted or preabsorbed with the antigen (Figure 3H).

Western blot analysis was also performed to determine UT protein content. Of note, the band corresponding to UT at 60 KDa was comparable between normal and CHF hearts (Figure 4). However there were two bands at approximately 150 and 200 KDa which were significantly increased in the CHF hearts compared to the normal controls. Specifically, the band at ~200 KDa was significantly increased [1241 ± 164 AU vs. 356 ± 56 AU; $P<0.001$] in CHF hearts compared to normal hearts. The band at ~150 KDa was virtually nonexistent in normal hearts while it was quite prominent in CHF hearts. This indicates that UT forms either a hetero- or homo-oligomeric complex in heart failure. The specificity for UT was verified by the presence of these bands

using three different antibodies raised against three different epitopes of UT (data not shown).

Subsequently, we quantified UT mRNA levels by RT-PCR in the left and right ventricles of control and CHF animals (Table 2). UT mRNA was increased in the left ventricle of the CHF compared to control animals, however it did not reach statistical significance. UT mRNA was significantly increased in the right ventricle of CHF animals compared to that of control animals ($P<0.05$).

2.5.4 Effect of UII Antagonist on Mortality, Cardiac morphology and function

Treatment with the UT receptor antagonist starting on day 0 significantly reduced overall (0 hr-8 weeks) mortality compared to the vehicle-treated MI group ($P=0.024$; Figure 5). Infarct analysis demonstrated a small, non-significant, decrease in infarct size in the treatment group compared to the vehicle group ($P = 0.14$). However, treatment (starting on day 0) led to a significant (54%) reduction in cardiomyocyte hypertrophy ($P < 0.01$) (Table 1) and ventricular dilatation (79%; Fig. 6; $P < 0.001$). Early treatment with SB-611812 also significantly improved cardiac function and reduced lung edema (Fig. 7 and Table 1). Specifically, the treatment group had a significantly reduced LVEDP (72%; $P < 0.001$) and RVSP (92%; $P < 0.05$) compared to the vehicle group. CVP was also significantly reduced in the treatment compared to the vehicle group (58%; $P < 0.05$). The UII receptor antagonist

also significantly improved the degree of lung edema as determined by the wet-to-dry weight ratio of the lungs (71%, $P < 0.001$). Heart weight to body weight ratio was also improved by treatment but this did not reach statistical significance ($P = 0.099$). Cardiac contractility indices ±dP/dt showed improvement compared to vehicle but this did not reach statistical significance (Table 1). There was no notable effect for the drug on either systolic, diastolic or mean arterial pressure, nor was there a difference in heart rate in the treatment group compared to the vehicle group.

2.5.5 Fibrosis analysis

In addition to the marked improvement observed for the hemodynamic and cardiac functional parameters we also observed a significant difference in protein and gene expression. Specifically, analysis of the protein levels for collagen types I and III indicated a significant reduction (83%) in the collagen type I:III ratio in the treatment group compared to the vehicle group ($P<0.05$) (Figure 8A, D). This significant decrease in collagen I:III ratio was the result of a significant decrease in collagen type I in treated animals compared to untreated ($P<0.05$) (Figure 8B), and a non-significant decrease in collagen type III protein levels (Figure 8C).

Masson's trichrome analysis demonstrated significantly increased interstitial fibrosis in the non-infarct zone of the left ventricle of vehicle compared to sham animals (113,640 ± 4,615 vs 52,747 ± 3,737; $P<0.001$). In the same zone, the SB-611812 group had significantly reduced interstitial

fibrosis compared to vehicle (86,928 ± 6,031 vs. 113,640 ± 4,615; P=0.004) (figure 9). In the infarct zone, there was no difference in the extent of fibrosis between vehicle and treatment groups (265,851 ± 11,749 vs. 267,511 ± 9,277).

Analysis of picrosirius red staining demonstrated that the non-infarct zone of the left ventricle of vehicle group exhibited significantly increased collagen deposition compared to sham animals (152,416 ± 32,426 vs. 29,702 ± 3,765; P=0.003). In the same region, the treatment group exhibited significantly reduced picrosirius red staining compared to the vehicle group (74,398 ± 9,141 vs. 152,416 ± 32,426; P=0.03) (Figure 10). Picrosirius red staining in the infarct region was comparable between vehicle and treatment groups (521,311 ± 18,690 vs. 495,798 ± 24,481).

2.5.6 Fibroblast proliferation assay

UII demonstrated potent low efficacy mitogenic effects on cardiac fibroblasts as it significantly induced proliferation of these cells at 1nM UII and 100nM UII following incubation for 48 hours (P<0.05; Figure 11). The potency of UII is underscored by the fact that it tended to induce proliferation even at 1pM UII, although this did not reach statistical significance (P=0.076). Administration of the UII antagonist SB-611812 at a concentration of 1 μM completely inhibited the 100nM UII-induced neonatal cardiac fibroblast proliferation (P<0.01; Figure 11).

2.5.7 Sub-study: effect of delayed treatment

Two additional groups, which were given either the antagonist or vehicle starting on day 10 post-MI were also evaluated. Similarly to the group in which treatment was administered on day 0, delayed SB-611812 administration was also able to afford a significant reduction in LVEDP (10.38 ± 1.65 mmHg vs. 21.5 ± 72.31 mmHg; $P<0.01$). Also, both RVSP and CVP were significantly reduced in the delayed treatment group compared to the vehicle group (22.37 ± 3.33 mmHg vs. 35.43 ± 2.43 mmHg and 3.87 ± 0.515 mmHg vs. 6.86 ± 0.705 mmHg, respectively; $P<0.05$). Finally, treatment started on day 10 led to a significant reduction in lung wet-to-dry weight ratio (4.77 ± 0.067 vs. 5.03 ± 0.093; $P<0.05$). There was no significant difference between treatment and vehicle (started on day 10) for other parameters including LVSP, ± dP/dt, MAP nor heart weight to body weight ratio. Infarct sizes were slightly smaller in treatment group compared to vehicle group, however this was not statistically significant (38.2 ± 2.7 vs. 32.1 ± 2.7; $P=0.15$). Finally, although delayed treatment led to a decrease in mortality compared to vehicle group, this did not reach statistical significance by Kaplan-Meier analyses ($P=0.29$). Based on these findings, it is evident that there was no detrimental effect of early treatment and thus the delayed treatment study arm was not pursued further.

2.6 Discussion

The present study demonstrated increased expression of UII and UT in the myocardium of rats with CHF secondary to myocardial infarction. Hence based on these findings, the efficacy of UII blockade using a specific UT antagonist, SB-611812 was evaluated in the rat CHF model. This is the first in vivo study demonstrating the efficacy of UT blockade in an experimental model of CHF using a selective nonpeptidic UT receptor antagonist, SB-611812. This antagonist is highly selective for the UT receptor and is devoid of any agonist activity, which has been a hindrance with previous UT antagonists described in the literature. [Behm et al. 2004] Importantly, SB-611812 led to a decrease in mortality. However, due to the small number of animals in this study, we must use caution when interpreting the survival benefit of this drug. In addition to the reduced mortality, treatment showed an improvement in CHF as evidenced by significantly reduced LVEDP, lung edema, RVSP, and CVP when compared to the control group receiving only the drug vehicle, methylcellulose. Furthermore, our data showed that the improvement in cardiac function observed with SB-611812 treatment was the result of attenuated cardiac remodeling following infarction. Indeed, we have demonstrated here that blockade of UII with SB-611812 led to a significant decrease in myocardial and endocardial fibrosis as well as a reduction in collagen deposition. In addition, we show that UII has a mitogenic effect of cardiac fibroblasts which may contribute to myocardial fibrosis post-coronary ligation. These findings demonstrate an important role for UII in

cardiovascular function and structure, and suggest a potential therapeutic significance for selective UT antagonism in the treatment of CHF.

Comparison of SB-611812 with other receptor antagonists in similar models indicates a large therapeutic potential for this antagonist. Of note, endothelin receptor antagonists have actually shown increased mortality and adverse ventricular remodeling following coronary ligation in the rat when administered early after infarction however, delayed administration of the antagonists significantly improved cardiac function and survival [Nguyen et al. 1998 & Mulder et al. 1997] Interestingly, our study demonstrates that there is no detrimental effect of early UT antagonism following myocardial infarction.

On the other hand, the use of angiotensin converting enzyme (ACE) inhibitors showed an improvement in cardiac function similar to the one reported here for the UT antagonist SB-611812 [Pfeffer et al. 1991; Jain et al. 1994; Lapointe et al. 2002]. Although drug efficacies cannot be directly compared in such a manner because of variations in study parameters it can still be appreciated that SB-611812 improves cardiac dysfunction associated with coronary artery ligation in a manner that is comparable to other therapeutic modalities including ACE inhibition which is a mainstay in cardiovascular therapy today.

The loss of functional contractile units following MI causes a reduction in pumping capacity of the heart. As a compensatory mechanism, the heart dilates to increase stroke volume. Here we show that treatment led to a significant reduction in ventricular dilatation compared to vehicle treated

animals. Ventricular dilatation increases wall stress and the heart compensates by increasing cardiomyocyte size. Indeed, cardiac hypertrophy is an important prognostic determinant in heart disease and thus its attenuation is an important therapeutic mechanism. This study demonstrates that CHF in the rat is associated with a significant increase in cardiac hypertrophy and that treatment with SB-611812 significantly attenuated this hypertrophy. This finding is supported by others who showed that UII induced cardiomyocyte hypertrophy [Tzanidis et al., 2003 & Johns et al., 2004]. Recently, Johns et al, [2004] showed that the UII-induced cardiomyocyte hypertrophy was inhibited with the administration of a competitive peptidic UT receptor antagonist, BIM-23127.

Previous studies have suggested that UII does not have a spare receptor reserve, [Douglas et al., 2004] therefore UII activity is regulated, at least in part, by altering the UII receptor expression. Therefore in addition to demonstrating increased UII expression in heart failure which is well established in a variety of cardiovascular diseases, we also sought to evaluate if UT is differentially expressed in heart failure. We demonstrated that UT protein expression is significantly increased using immunohistochemistry and Western blotting. Rat UT has a molecular weight (MW) of 42.7 KDa. However this protein has several glycosylation sites and as such has been demonstrated to have a MW ~60KDa. [Boucard et al., 2003] Interestingly, we found using western blotting, that the bands corresponding

to ~60KDa proteins were comparable between normal and CHF hearts. However there were two bands corresponding to proteins of MW of ~150 KDA and ~200 KDa that were significantly increased in CHF hearts. Interestingly, these same bands were seen with all three different antibodies raised against three different UT epitopes. Therefore the high molecular weight proteins are likely homo or hetero protein oligomers. Oligomerization of G-protein coupled receptors (GPCR) is actually quite a prominent phenomenon and is now known to affect receptor specificity, pharmacology and trafficking. [Prinster et al., 2005] Therefore the high MW bands that are significantly increased in CHF hearts demonstrated in the present study are likely to demonstrate receptor homo- or hetero oligmerization with GPCRs.

There is evidence that collagen type I is more rigid while collagen type III has more elastic properties [Marijianowski et al. 1995]. Therefore an increase in the ratio of collagen type I:III, as occurs in heart failure, [Huang et al. 2004; Wei et al. 2004] would increase the rigid type collagen to the elastic type collagen thus explaining the increased myocardial stiffness observed in CHF. In fact Nishikawa et al.[2001] showed that a decrease in LVEDP, following amlodipine administration was associated with a decrease in the collagen type I:III ratio. Interestingly, Kompa et al. [2004] demonstrated that chronic infusion of UII in the rat led to a 40% increase in LVEDP and that this was associated with a significant increase in the collagen type I:III ratio. Here, we show that the treatment with the UT receptor antagonist SB-611812 led to a significant

decrease in LVEDP and the collagen type I:III ratio. This difference in ratio was due to a significant decrease in collagen type I protein levels and a non-significant decrease in collagen type III protein levels in the treatment compared to the vehicle group.

These findings are further supported by the demonstration of reduced reactive fibrosis in the viable myocardium as determined by Masson's trichrome staining as well as reduced endocardial collagen deposition as evidenced by reduced picrosirius red staining in the treatment group compared to the vehicle group. The mechanism of SB-611812 mediated inhibition of collagen type I synthesis will require further studies. In addition, it is of interest that collagen type I and fibronectin mRNA levels of the treatment group were not significantly different from the control sham group.

Myocardial fibrosis, a prominent characteristic of ventricular remodeling in CHF, is the result of increased deposition of extracellular matrix (ECM) proteins including collagens and fibronectin. [Wei et al. 2000] Notably, Tzanidis et al. [2003] have demonstrated UII induced collagen production from cardiac fibroblasts. Also Wang et al. [2004] utilizing an endothelial cell culture, found that UII increased expression of collagen type I mRNA and protein and conversely decreased the expression of MMP-1mRNA and protein as well as decreased the activity of MMP-1. UII activity in cardiac fibroblasts was further substantiated by He et al. [2004] who demonstrated UII induced proliferation of cardiac fibroblasts. We also sought to determine if UII possessed mitogenic activity in neonatal cardiac fibroblasts. To this end, we show that UII induced

cardiac fibroblast proliferation. Furthermore, we complemented these findings by demonstrating that UII induced proliferation of rat cardiac fibroblasts was inhibited with the use of the UT antagonist SB-611812.

In conclusion, we have demonstrated, in a rat model of CHF induced by coronary ligation, up-regulation of myocardial UII and UT, and that blocking the UT receptor pathway with the specific UT antagonist SB-611812 leads to decreased mortality and improved parameters of cardiac function including decreased LVEDP, lung edema, RVSP and CVP, and reduces cardiac remodeling. These findings suggest that SB-611812 shows substantial therapeutic potential for the treatment of myocardial infarction and CHF.

Figure 1. Representative photomicrographs of UII immunohistochemistry. Panel A demonstrates weak diffuse UII immunoreactivity of left ventricular myocardium of normal rats (200X magnification). Panel B shows intense UII immunoreactivity in surviving cardiomyocytes (thin arrow) in the endocardial region of the left ventricle of an infarcted (thick arrow) myocardium (200X magnification). Panel C is a greater magnification of the same section as panel B (thin arrow indicating surviving cardiomyocyte; 400X magnification). Panel D demonstrates intense immunoreactivity in the viable cardiomyocytes (thin arrow) in the border zone of the peri-infarct region of the left ventricle of CHF animals (thick arrow indicates scar region; 200X magnification). Panel E is greater magnification of panel D (thin arrow indicating viable myocardium and thick arrow indicating infarcted tissue; 400X magnification). Panel F shows strong UII immunoreactivity of the microvasculature (dashed arrows) in the infarcted myocardium (400X magnification). Panel G demonstrates moderate diffuse UII immunoreactivity in the right ventricle of CHF animals (300X magnification). Panel H is a negative control demonstrating no immunoreactivity of the same section as panel D (thin arrow indicating viable myocardium and thick arrow indicating scar tissue) when the primary serum is omitted. All sections were counterstained with hematoxylin. Scale bars represent 75 μm.

Figure 1

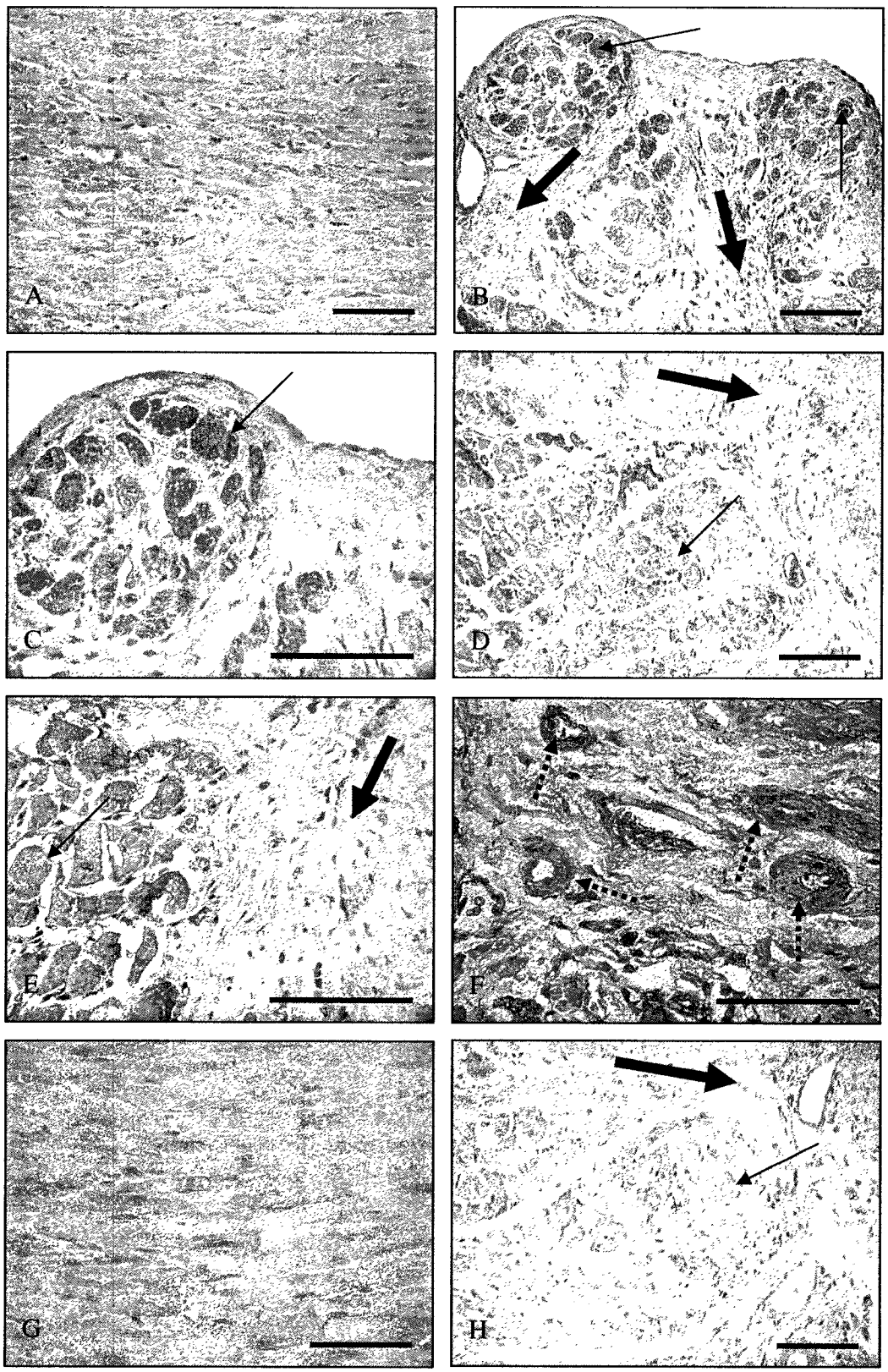

Figure 2. Prepro-UII protein quantification. Representative Western blot demonstrating prepro-UII protein levels with a molecular weight of 13.7 KDa from left ventricular protein homogenates of normal and CHF hearts.

Figure 2

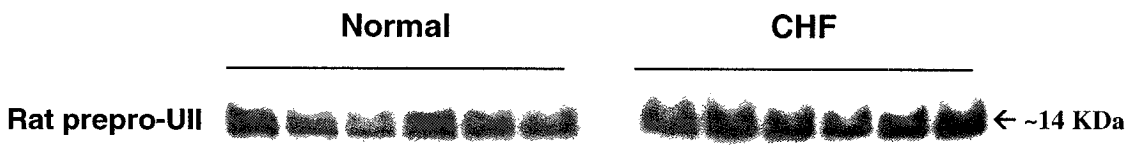

Figure 3. Representative photomicrographs of UT immunohistochemistry. Panel A demonstrates moderate diffuse UT immunoreactivity of left ventricular myocardium of normal rats (300X magnification). Panel B shows strong UT immunoreactivity in the endocardial region of the left ventricle of a CHF animal, with staining in the endocardial endothelium (short arrows), and viable cardiomyocytes (long thin arrow, thick arrow indicates infarct scar; 200X magnification). Panel C is a greater magnification of the same section as panel B demonstrating strong UT immunoreactivity in both the endocardial endothelial cells (short arrows) and the surviving cardiomyocytes (long thin arrows) in the endocardial region of the left ventricle (thick arrow indicates infarct scar; 400X magnification). Panel D demonstrates intense immunoreactivity in the viable cardiomyocytes (long thin arrow), endothelial cells (short arrow), and microvasculature (dashed arrow) in the infarct zone of the left ventricle of a CHF animal (400X magnification). Panels E & F show intense UT immunoreactivity in the microvasculature (dashed arrows) of both the infarct and peri-infarct zone respectively (400X magnification). Panel G demonstrates moderate to strong diffuse UT immunoreactivity in the right ventricle of CHF animals (300X magnification). Panel H is a negative control demonstrating no immunoreactivity of the same section as panel D (thin arrow indicating viable myocardium and dashed arrow indicating myocardial vessel) when the primary serum is omitted. All sections were counterstained with hematoxylin. Scale bars represent 75 μm.

Figure 3

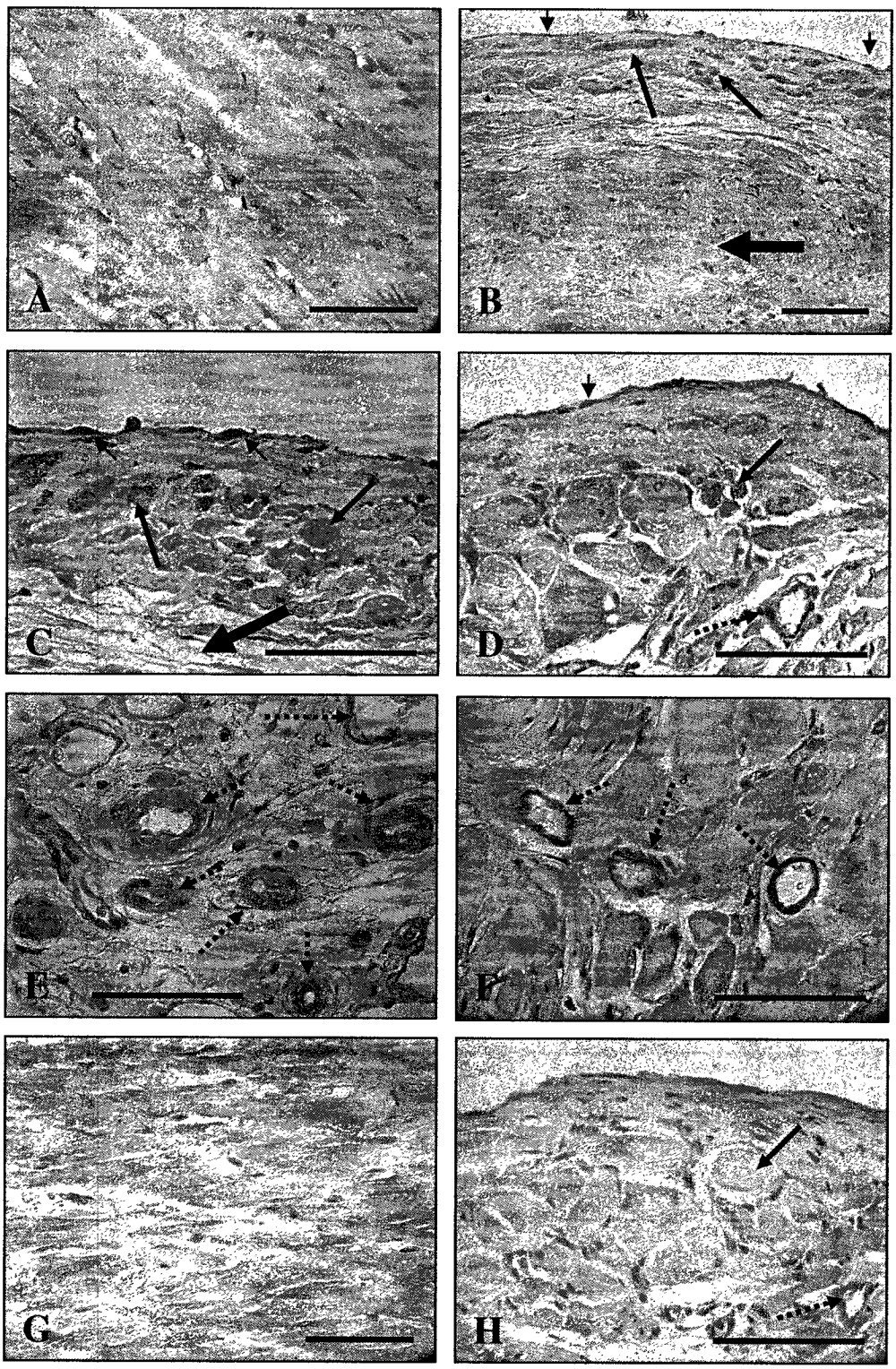

Figure 4. UT quantification

Representative Western blot demonstrating UT protein levels from left ventricular protein homogenates of normal and CHF hearts. Bands represent proteins with molecular weights of ~30KDa ~60KDa ~100KDa ~150KDa ~200KDa.

Figure 4

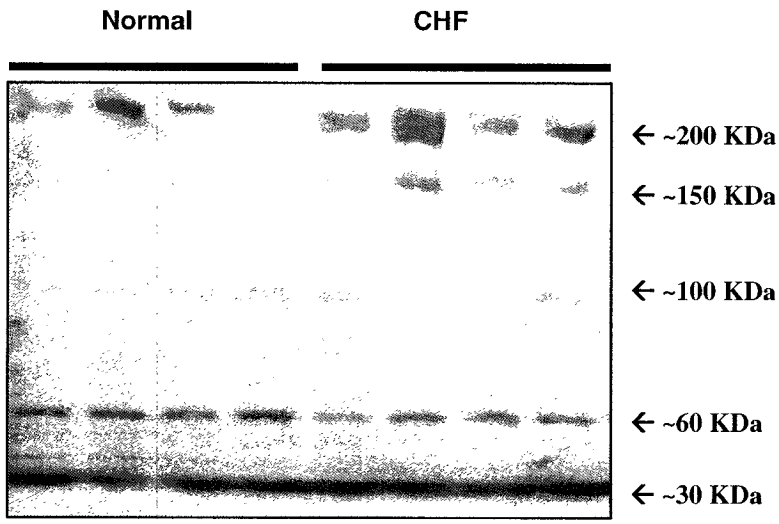

Figure 5. Kaplan-Meier Survival plots.

Figure shows survival plot in which overall mortality is significantly reduced (P=0.0244).

Figure 5

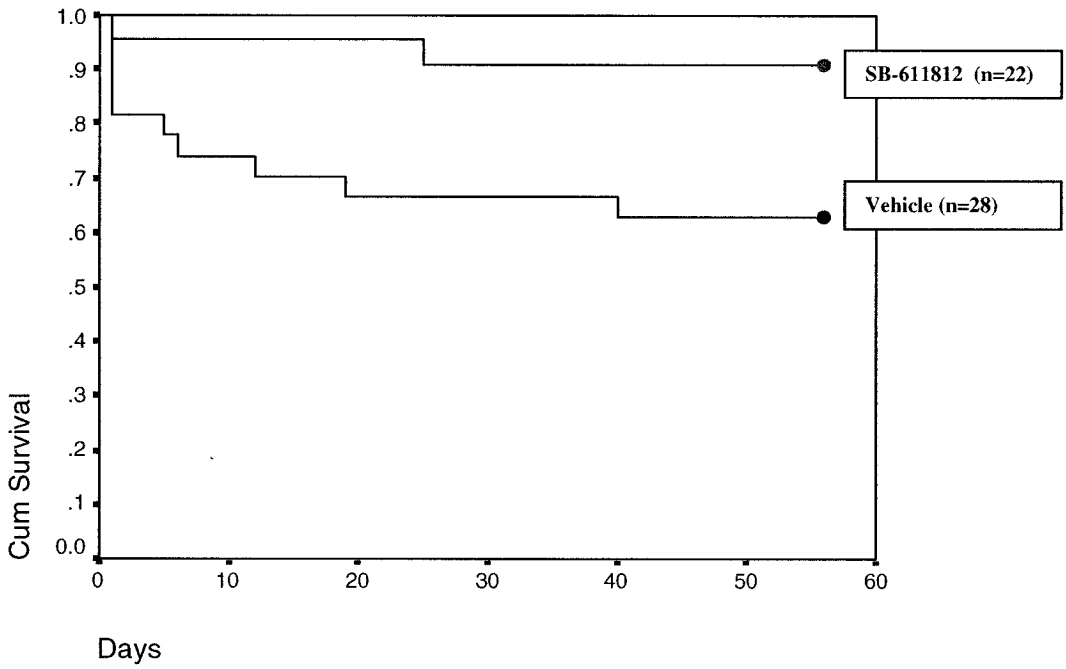
1.0
.9
.8
.7
.6
.5
.4
.3
.2
.1
0.0
Cum Survival
0
10
20
30
40
50
60
Days
SB-611812 (n=22)
Vehicle (n=28)

Figure 6. Analysis of left ventricular chamber size.

Representative photomicrographs of transversely cut hearts from sham (A), vehicle (B), and treatment (C) groups stained with Masson's trichrome. D, Graph representing quantification left ventricular chamber area in sham (N=6), Vehicle (N=9), and treatment (N=9) groups. * indicates $P<0.001$ vs. sham; # indicates $P<0.001$ vs.vehicle.

Figure 6.

A

B

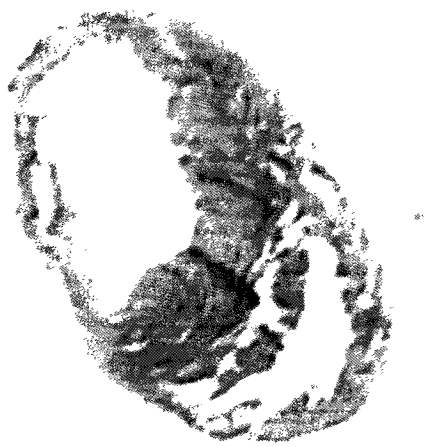

C

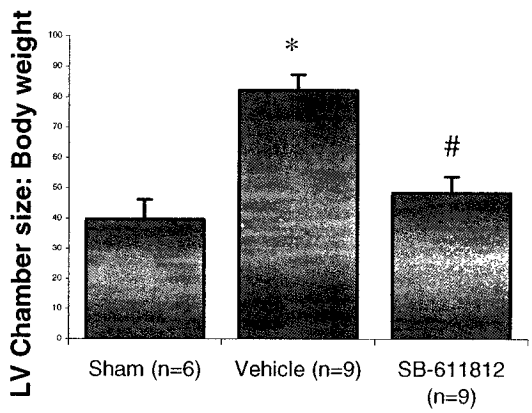

D

Figure 7. Effect of UT receptor blockade on cardiac function and lung edema. Panel A demonstrates a significant reduction in LVEDP in the treatment compared to the vehicle group. Similarly, panels B and C show a significant reduction in RVSP and CVP, respectively in the treatment compared to the vehicle group. Panel D shows a significant reduction in lung wet-to-dry weight ratio in the treatment compared to the vehicle group. * indicates $P < 0.05$ vs; sham # indicates $P < 0.05$ vs. vehicle.

Figure 7

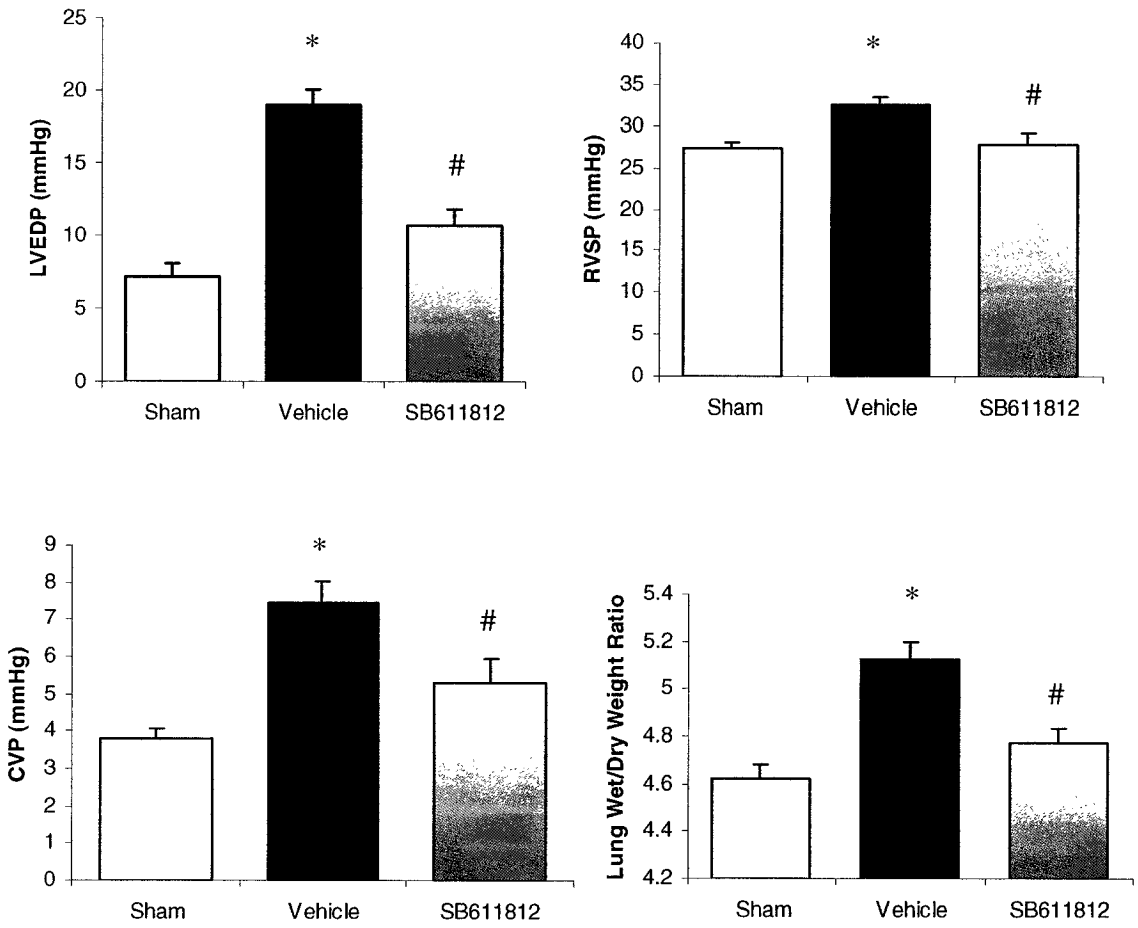
LVEDP (mmHg)
25
20
15
10
5
0
*
#
Sham
Vehicle
SB611812
RVSP (mmHg)
40
35
30
25
20
15
10
5
0
*
#
Sham
Vehicle
SB611812
CVP (mmHg)
9
8
7
6
5
4
3
2
1
0
*
#
Sham
Vehicle
SB611812
Lung Wet/Dry Weight Ratio
5.4
5.2
5
4.8
4.6
4.4
4.2
*
#
Sham
Vehicle
SB611812

Figure 8. Effect of SB-611812 of collagen protein expression. Panel A, representative Western blots demonstrating collagen type I and type III protein levels in the sham, vehicle and SB-611812 treatment groups. Panel B, a graph demonstrating the quantification of collagen type I protein levels in the sham (n=6), vehicle (n=8) and SB-611812 (n=9) treatment groups. Panel C, a graph demonstrating quantification of collagen type III protein levels in the sham (n=6), vehicle (n=8) and SB-611812 (n=9) treatment groups. Panel D, a graph demonstrating collagen type I to type III ratio in the sham (n=6), vehicle (n=8) and SB-611812 (n=9) treatment groups. * indicates $P< 0.05$ vs. sham; # indicates $P< 0.05$ vs. vehicle.

Figure 8

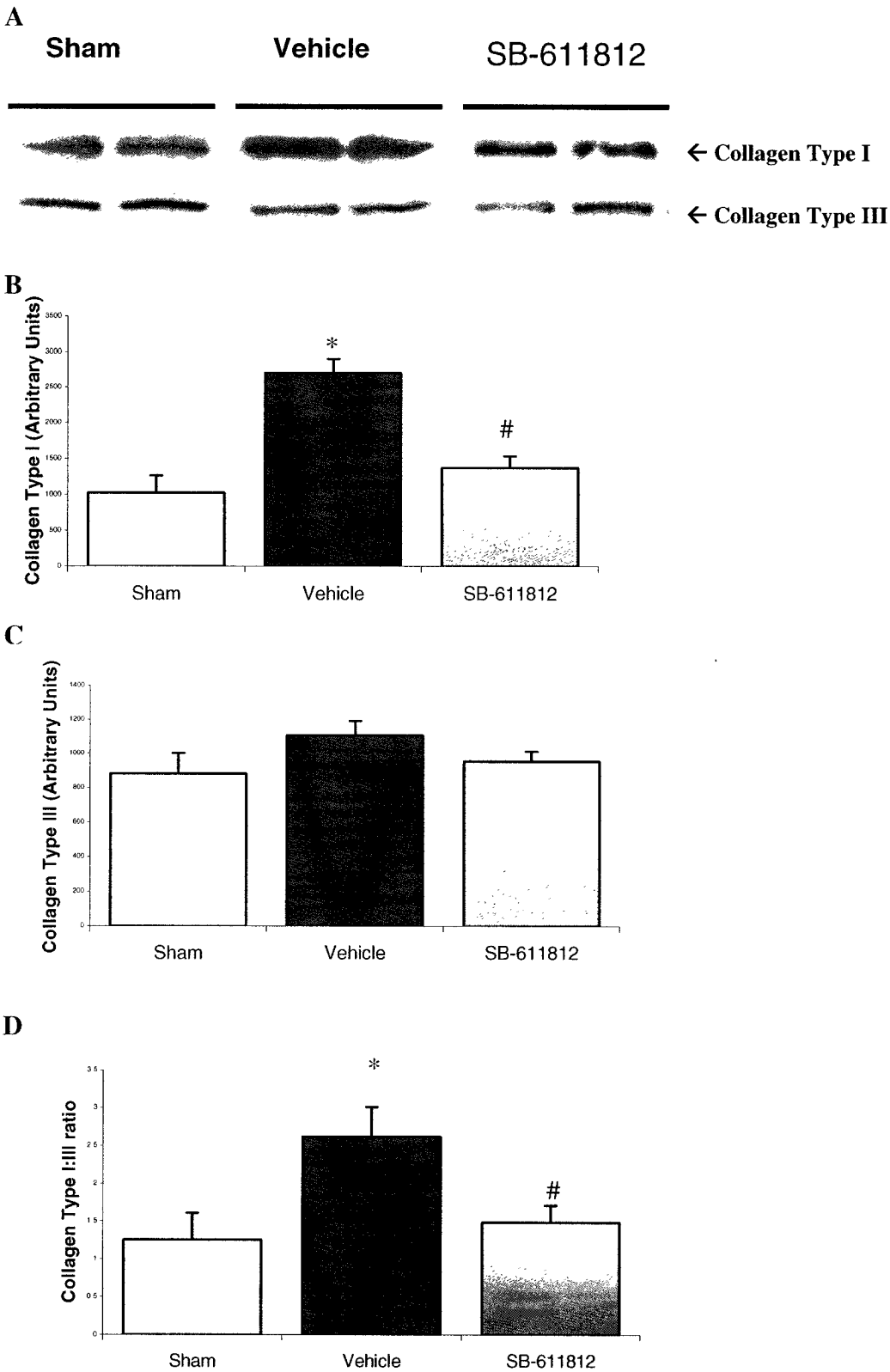
A
Sham
Vehicle
SB-611812
← Collagen Type I
← Collagen Type III
B
Collagen Type I (Arbitrary Units)
*
#
Sham
Vehicle
SB-611812
C
Collagen Type III (Arbitrary Units)
Sham
Vehicle
SB-611812
D
Collagen Type I:III ratio
*
#
Sham
Vehicle
SB-611812

Figure 9. Analysis of interstitial fibrosis.

Representative photomicrographs of viable left ventricle from sham (A), vehicle (B), and treatment (C) groups stained with Mason's trichrome. Short arrow indicates interstitial fibrosis (stained blue). Dashed long arrow indicates viable cardiomyocytes (stained red). D, Graph representing quantification of interstitial fibrosis in sham (N=6), Vehicle (N=9), and treatment (N=9) groups. * indicates $P<0.001$ vs. sham; # indicates $P=0.004$ vs. vehicle.

Figure 9

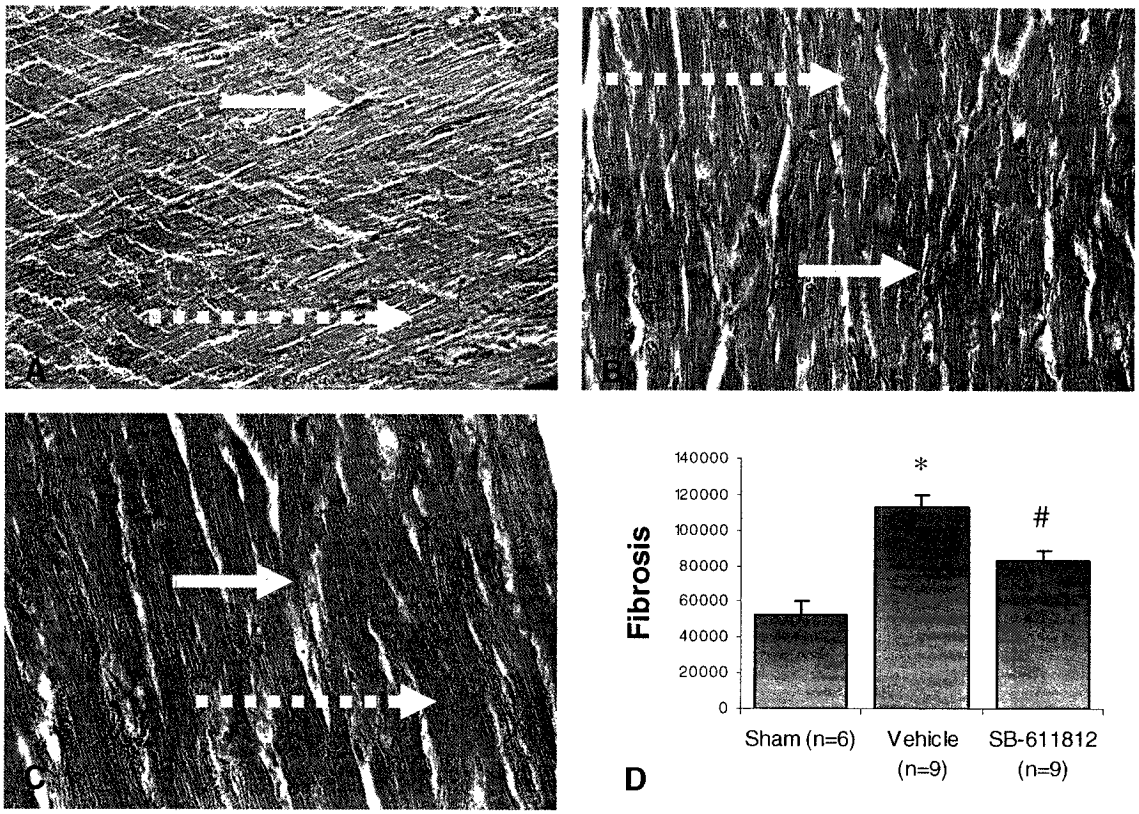
A
B
C
D
Fibrosis
140000
120000
100000
80000
60000
40000
20000
0
*
#
Sham (n=6)
Vehicle (n=9)
SB-611812 (n=9)

Figure 10. Analysis of collagen deposition.

Representative photomicrographs of viable endocardial left ventricle from sham (A), vehicle (B), and treatment (C) groups stained with picrosirius red. Short arrow indicates endocardial collagen deposition (stained red). Dashed long arrow indicates viable cardiomyocytes (stained yellow). D, Graph representing quantification of collagen deposition in sham (N=6), vehicle (N=9), and treatment (N=9) groups. * indicates P=0.003 vs. sham; # indicates P<0.037 vs. vehicle.

Figure 10

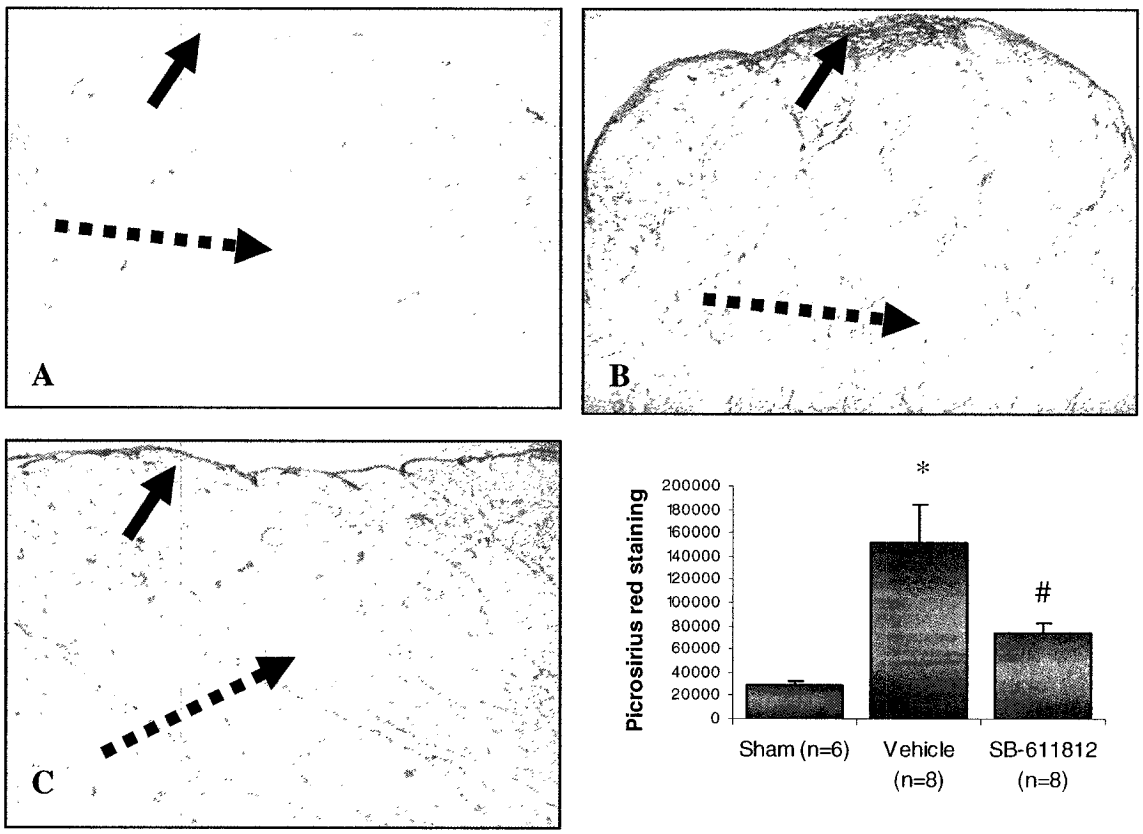
A
B
C
Picrosirius red staining
200000
180000
160000
140000
120000
100000
80000
60000
40000
20000
0
*
#
Sham (n=6)
Vehicle (n=8)
SB-611812 (n=8)

Figure 11. Urotensin-II induced rat fibroblast proliferation is inhibited by SB-611812. Dose-response curve demonstrating that UII acted as a potent, low efficacious mitogen for rat cardiac fibroblasts, which significantly increased proliferation at 1nM and 100 nM UII. Antagonism with 1μM SB-611812 inhibited this effect at the highest UII concentration. * indicates $P<0.05$ vs serum-free media, # indicates $P<0.01$ vs 100 nM UII.

Figure 11

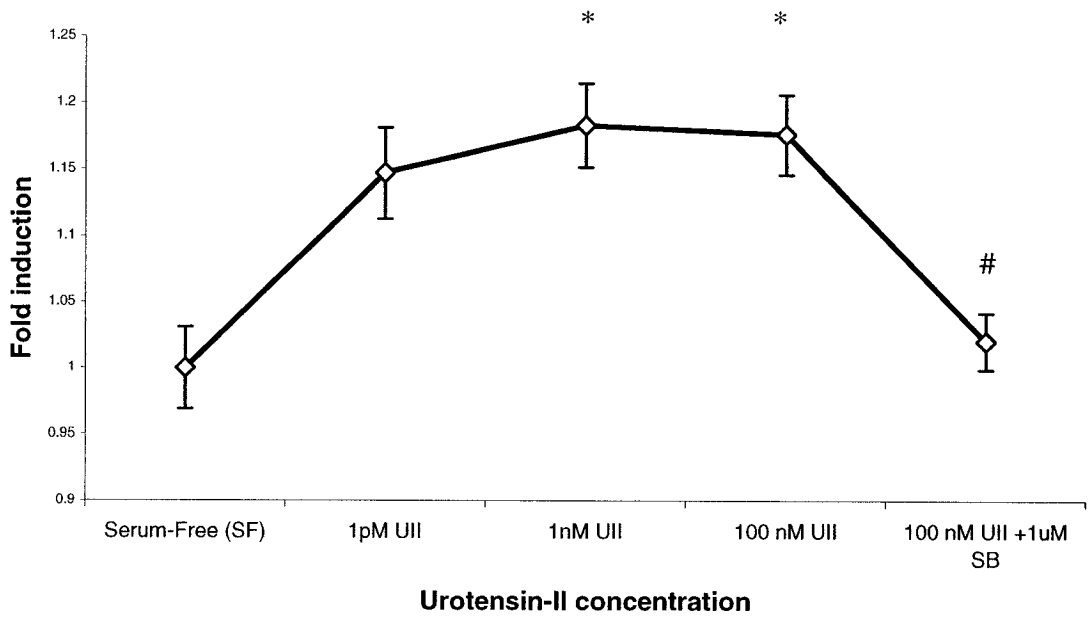
*
*
#
1.25
1.2
1.15
1.1
1.05
1
0.95
0.9
Fold induction
Serum-Free (SF)
1pM UII
1nM UII
100 nM UII
100 nM UII +1uM SB
Urotensin-II concentration

Table 1. Hemodynamic parameters, cardiac function, heart weight and lung edema for the three study groups.

Parameters	Sham (n=9)	Vehicle (n=16)	SB611812 (n=17)
LVEDP (mmHg)	7.18 ± 0.91	19.0 ± 1.06 *	10.6 ± 1.10 #
RVSP (mmHg)	27.3 ± 0.78	32.6 ± 0.79 *	27.7± 1.50 #
CVP (mmHg)	3.78 ± 0.28	7.47 ± 0.56 *	5.31 ± 0.62 #
+dP/dt	4050 ± 273	2765 ± 241*	3162 ± 184 *
-dP/dt	4210.0 ± 258.1	2870 ± 249 *	3183 ± 206 *
LVSP (mmHg)	108.1 ± 4.59	91.8 ± 4.89	92.1 ± 4.48
Psystolic (mmHg)	103.9 ± 4.54	95.1 ± 5.76	98.8 ± 4.85
Pdiastolic (mmHg)	65.89 ± 4.48	70.7 ± 5.59	72.9 ± 4.53
MAP (mmHg)	78.4 ± 3.85	78.8 ± 5.60	81.5 ± 4.29
HW/BW % (g/g)	0.241 ± 0.008	0.300 ± 0.016 *	0.267± 0.005
Lung wet/dry ratio	4.62 ± 0.055	5.13 ± 0.064 *	4.77 ± 0.066 #
Infarct size	N/A	38.2% ± 2.2	33.06% ± 1.7
CM Area AU	199977 ± 8324	321897 ± 10390 *	256382 ± 7705 #
Chamber size	39.8 ± 4.9	82.1 ± 6.2 *	48.4 ± 4.9 #
LV WT (non-scar; AU)	606 ± 39	636 ± 32	622 ± 32
LV WT (scar; AU)	N/A	235 ± 67	279 ± 63

LVSP (Left Ventricular Systolic Pressure), Psystolic (Systolic blood pressure), Pdiastolic (Diastolic blood pressure), MAP (Mean Arterial Pressure), LVEDP (Left Ventricular End-Diastolic Pressure), RVSP (Right Ventricular Systolic Pressure), CVP (Central Venous Pressure), +dP/dt (the first derivative of the rate in positive pressure change in the ventricle), -dP/dt (the first derivative of the rate in negative pressure change in the ventricle), HW/BW (heart weight to body weight ratio),lung wet:dry weight ratio, infarct size, CM Area AU (cardiomyocyte area in arbitrary units), LV WT (left ventricular wall thicknesses (non-scar and scar regions);. * indicates $P<0.05$ vs. sham; # indicates $P<0.05$ vs vehicle.

Table 2. Relative expression of genes determined by RT-PCR.

Genes	Sham (n=8)	Vehicle (n=12)	SB611812 (n=8)
RPL32 ($1/C_t$)	0.059 ± 0.09	0.060 ± 0.09	0.060 ± 0.14
UT LV	0.519 ± 0.217	0.591 ± 0.028	N/A
UT RV	0.525 ± 0.024	0.563 ± 0.016 *	N/A
BNP	0.938 ± 0.014	1.021 ± 0.008 *	1.022 ± 0.011 *
AT-1	0.522 ± 0.009	0.560 ± 0.008 *	0.576 ± 0.015 *
cTnI	1.21 ± 0.02	1.13 ± 0.03 *	1.16 ± 0.06
Collagen Type 1	0.864 ± 0.012	0.948 ± 0.014 *	0.927 ± 0.025
Collagen Type III	0.910 ± 0.007	1.013 ± 0.015 *	0.994 ± 0.021 *
Fibronectin	0.782 ± 0.004	0.837 ± 0.011 *	0.820 ± 0.014
MMP-2	0.383 ± 0.005	0.395 ± 0.006	0.392 ± 0.007
MMP-9	0.493 ± 0.007	0.529 ± 0.013	0.536 ± 0.019
MMP-14	0.674 ± 0.004	0.691 ± 0.008	0.681 ± 0.010
TIMP-1	0.695 ± 0.005	0.748 ± 0.007 *	0.739 ± 0.012 *
TIMP-2	0.884 ± 0.004	0.919 ± 0.006	0.901 ± 0.008
TIMP-3	0.804 ± 0.005	0.799 ± 0.008	0.786 ± 0.012

RPL32 (Ribosomal protein L32); Ct (threshold cycle); UT (urotensin-II receptor), LV (left ventricle), RV (right ventricle), BNP (brain natriuretic peptide), AT-1 (angiotensin type 1 receptor), cTnI (cardiac troponin I), MMP (matrix metalloproteinase), TIMP (tissue inhibitor of MMP). * indicates $P<0.05$ vs. sham.

Table 3. Primer sequences for RT-PCR mRNA expression analysis.

Genes	Primer sequences
AT-1 F:	5' CCG TGA CTG TGA ATT TGC TG 3'
AT-1 R:	5' GGA ATG TAT TTC AGA AGC TGG AG 3'
BNP F:	5' ACA GCT CTC AAA GGA CCA 3'
BNP R:	5' ATC CGG TCT ATC TTC TGC 3'
Collagen type I F:	5' GCA ACA GTC GAT TCA CCT ACA GCA 3'
Collagen type I R:	5' AAT GTC CAA GGG AGC CAC ATC 3'
Collagen type III F:	5' AGA AGT CTC TGA AGC TGA TGG 3'
Collagen type III R:	5' GCT CCA TTC ACC AGT TGT 3'
c TnI F:	5' CTG ACC CAG AAG ATC TAT GAC 3'
cTnI R:	5' TCC TTC TTC ACC TGC TTG A 3'
Fibronectin F:	5' CAG TGG CAG AAA GAG TAT CTC G 3'
Fibronectin R:	5' GTA TAC TGG TTG TAG GTG TGG 3'
MMP-2 F:	5' GGG TCT ATT CTG CCA GCA CTC 3'
MMP-2 R:	5' CTC CAG AAC TTG TCT CCT GCA A 3'
MMP-9 F:	5' TCT CGA ATC ACG GAG GAA 3'
MMP-9 R:	5' TTT GCG CCC AGA GAA GAA 3'
MMP-14 F:	5' GAT TGA TGC AGC TCT CTT CTG 3'
MMP-14 R:	5' CCT TCC CAG ACT TTG ATG 3'
RPL32 F:	5' ATC CTG ATG CCC AAC ATT GGT TAC 3'
RPL32 R:	5' GTT GCA CAT CAG CAG CAC TTC CAG 3'
TIMP-1 F:	5' GTA AAG ACC TAT AGT GCT GGC TG 3'
TIMP-1 R:	5' GAG GAT CTG ATC TGT CCA CAA 3'
TIMP-2 F:	5' GGT CAC AGA GAA GAG CAT CAA TG 3'
TIMP-2 R:	5' GTC CTC GAT GTC AAG AAA CTC 3'
TIMP-3 F:	5' GAT CAA GTC CTG CTA CTA CTT GC 3'
TIMP-3 R:	5' CGT AGT GTT TGG ACT GAT AGC 3'
UT F:	5' GGG CAT GGT GGG AAA TGT A 3'
UT R:	5' AGA CGT ACA TGG AGG CCG AG 3'

AT-1, Angiotensin type 1 receptor; BNP, brain natriuretic peptide; cTnI, cardiac troponin-I; MMP, matrix metalloprotease; RPL32, ribosomal protein L32; and TIMP, tissue inhibitors of MMPs.

Chapter III

Increased Expression of Urotensin II and its Cognate Receptor, UT, in Atherosclerotic Lesions of the Human Aorta.

3.1 Preface

In the previous chapter we investigated the role of UII in a model of heart failure in the rat. We found that UII is increased in heart failure and that blockade of UII signaling could ameliorate cardiac function and remodeling. Thus here we aimed at determining whether this factor is increased in human atherosclerosis, the most prominent cause of ischemic cardiomyopathy and hence heart failure in North America. This work resulted in a manuscript published in the journal *Atherosclerosis,* which was the first published report of increased UII and UT expression in human atherosclerosis.

3.2 Abstract

Urotensin II (UII), a novel vasoactive peptide, possesses a wide range of cardiovascular effects. UII binds a seven transmembrane spanning G-protein coupled receptor termed UT. In the present study, we have characterized UII expression in both carotid and aortic atherosclerotic plaques. Using immunohistochemistry, we demonstrated UII immunoreactivity in endothelial, smooth muscle and inflammatory cells of both carotid and aortic plaques, with a clear propensity for intimal staining. Using quantitative real-time RT-PCR we observed both increased UII and UT mRNA expression in tissue extracts from abdominal aortic aneurysms. We also extended our PCR analysis to include leukocyte expression of UII and UT. We found that lymphocytes were by far the largest producers of UII mRNA. In contrast monocytes and macrophages were the largest producers of UT mRNA, with relatively little expression in foam cells, lymphocytes, and platelets. Our findings qualitatively and quantitatively demonstrate increased expression of UII in atherosclerosis with a large degree of inflammatory cell involvement. These findings suggest a possible role for UII in the pathophysiology of atherosclerosis.

3.3 Introduction

Atherosclerosis, the leading cause of myocardial infarction and stroke, generally affects muscular and elastic arteries. Of these, carotid arteries and aortae are common targets. Many vasoactive factors are now known to play an important role in the pathophysiology of atherosclerosis. A novel vasoactive peptide, termed Urotensin-II (UII), has been shown to have many properties reminiscent of endothelin-1. Human UII is an 11 amino acid peptide [Coulouarn etal., 1998], with a molecular weight of ~1388 [Matsushita et al. 2001]. Expression of U-II has been shown throughout the cardiovascular, nervous and urogenital systems [Ames et al. 1999; Maguire et al. 2000; Douglas et al. 2002; & Shenouda et al. 2002]. We have recently shown increased myocardial expression of UII in patients with congestive heart failure [Douglas et al. 2002]. Others have reported expression of UII in the heart and aorta of man, monkeys and mice [Matsushita et al. 2001;& Elshourbagy et al. 2002]. Pharmacologic studies have shown that UII is the most potent vasoconstrictor peptide isolated to date, however the vasoactive properties of UII depend on the anatomical site and the type of species [Ames et al. 1999; Maguire et al. 2000 ;& Elshourbagy et al.. 2002]. In addition to its marked vasoactivity, there is substantial evidence suggesting a role for this factor in atherosclerosis. UII has also shown potent mitogenic effects on smooth muscle cells [Sauzeau et al. 2001], with synergistic effects observed when combined with mildly oxidized low-density lipoprotein (moxLDL), as well as with 5-HT (serotonin) [Watanabe et al. 2001]. Of note is the finding that UII stimulates hyperlipidemia in fish by enhancing depot lipase activity, and it channels glucose to free fatty acid synthesis [Sheridan et al. 1986]. Interestingly, Matsushita et al.[2001] observed increased

urinary levels of UII in patients with hypertensive renal glomerular disease compared to normotensive glomerular disease. They attributed the increase to glomerular arteriosclerosis, a vascular disorder very closely related to atherosclerosis.

The cognate receptor of UII is known to be UT, a seven transmembrane spanning G-protein coupled receptor [Mori et al. 1999 & Liu et al. 1999]. Abundant expression of the receptor was reported in the heart and pancreas of humans. [Ames et al.1999] Specifically it was found in the atria and ventricles of the heart, as well as in endothelial cells and smooth muscle cells of the aortae and coronary arteries [Ames et al. 1999] .

The biological activity of UII in the cardiovascular system led us to hypothesize that there is an up-regulation of UII in atherosclerosis. To test this, we qualitatively examined the expression of UII using immunohistochemistry in two common pathologies of atherosclerosis including carotid arterial stenosis and abdominal aortic atherosclerosis. We also quantitatively examined the expression, using real- time PCR, of both prepro-UII and it's cognate receptor UT in tissue samples obtained from patients who had surgery for either abdominal aortic aneurysms or carotid endarterectomies. Finally, we examined the profile of UII and UT expression in the leukocyte sub-populations.

3.4 Methods

3.4.1 Tissue samples

Samples were retrieved from male subjects with an age range of 60-80 years. Tissue samples used for immunohistochemistry were retrieved either at autopsy [carotid arteries (n=5), and abdominal aortae (n=4)], or freshly during surgery for carotid endarterectomy (n=3) or abdominal aortic aneurysymal repair (n=4). Samples from autopsy cases were collected a maximum of 8 hours after death. Samples were fixed in formalin, embedded in paraffin, and then cut using a microtome (5μm thick). Tissue samples used for RT-PCR were collected freshly at surgery (Guys and St. Thomas Hospital, London, England) for carotid endarterectomy (n=17), or abdominal aortic aneurysms repair (n=8). Normal human aortae (n=7) were obtained from the Anatomic Gift Foundation (White Oak, GA; USA). Samples were snap frozen in liquid nitrogen and stored at -80°C until further use.

3.4.2 Immunohistochemistry

Immunohistochemical staining for UII, Von Willebrand factor and smooth muscle cell actin was performed using the avidin-biotin peroxidase method. Paraffin sections were dewaxed in toluene for 20 minutes, and rehydrated through 100%, 90%, 70%, and 50% alcohol for two minutes each. All sections were then immersed in PBS solution for five minutes and then 3% hydrogen peroxide solution to block endogenous peroxidase activity for 30 minutes. The sections were then washed three times in PBS solution for five minutes. The sections

were permeabilized in 0.2% Triton in 0.1M PBS (pH 7.4) for 30 minutes and washed three times in PBS for five minutes. Sections were then incubated in 10% normal goat serum (NGS) for 30 minutes at room temperature after which they were incubated overnight at 4°C with the primary antibody. The sections were washed three times in PBS for five minutes following the cold storage, and incubated for 45 minutes with biotinylated goat-anti mouse-IgG (1:200) at room temperature. They were then washed three times again in PBS for five minutes, and incubated with the avidin-biotin-peroxidase complex (Vectastain Elite Kit, Vector Laboratories, Burlingame, CA, U.S.A.) for 45 minutes at room temperature. The sections were then washed in PBS for five minutes. Sites of immunostaining were visualized by developing sections in 0.025% diaminobenzidine and 0.03% peroxide for two to three minutes. The sections were then returned to the PBS solution and were then dehydrated through 50%, 70%, 90%, and 100% ethanol for two minutes each, and then cleared in toluene. Finally, the sections were mounted with Permount and glass cover slips and allowed to dry. The specificity of the immunostaining was confirmed using negative control experiments in which primary antibodies were substituted with NGS or pre-absorbed with UII antigen.

3.4.3 Isolation of human leukocytes

Human leukocytes were isolated from whole blood taken from healthy volunteers as previously described [Patel et al. 2001]. Specifically ~100 million cells from ~180 ml of whole blood. Monocytes were isolated from the leukocyte harvest using the

Graziani-Bowering et al. [2000] method. For monocyte-macrophage differentiation, monocytes were resuspended in RPMI 1640 (+10% human serum; type AB, sigma) culture medium at a density of 2.5 x 10^6/ml and seeded into 12-well tissue culture plates; medium was changed every 48 hours. For the generation of foam cells, macrophages were incubated in the presence of 100µg/ml oxLDL (Intracel) for a further three days [Patel et al. 2001]. Platelets were isolated using a counter current centrifugal elutriation method modified for platelet isolation by eluting platelets from the buffy coat at a flow rate of 9ml/min [Gibbs et al. 1997].

3.4.4 PCR analysis

Total RNA was extracted from human tissues and cells using Trizol reagent (Gibco BRL) according to the manufacturer's instructions. cDNA was reverse transcribed from DNAse I (Gibco BRL) treated total RNA using Superscript II reverse transcriptase (Gibco BRL) as previously described [Patel et al. 2001] A negative control reaction omitting the reverse transcriptase (-RT) was also performed for each DNase-treated RNA sample. 1 µl of each cDNA sample were analyzed for human preproU-II, human UT, and human GAPDH expression by real-time quantitative RT-PCR using the fluorescent TaqMan® 5'-nuclease assay as previously described [Patel et al. 2001]. Primers and probes utilized in this study have been described previously [Douglas et al. 2002]. Values for the leukocyte RT-PCR analysis are means of triplicate assays.

3.4.5 Statistical analysis

Data are presented as mean ± S.E. Individual groups were compared using one-way ANOVA with the Tukey post-Hoc test with the aid of a commercial software program (*SPSS 11.5*). A P value <0.05 was considered significant.

3.5 Results

3.5.1 Immunohistochemical analysis

Histological examination of the carotid arteries obtained at autopsies revealed the presence of a distinct immunoreactivity for U-II in the hyperplasic intima and in endothelial cells (figure. 1A). There was an intense U-II immunostaining in tissue samples obtained from carotid endarterectomies. Specifically, there was abundant staining in the myointimal cells of the hyperplasic intima, with less in the media (figure 1B). Also there was apparent immunoreactivity in the carotid endothelium. Furthermore, we observed UII staining was less abundant but still apparent in medial layers of all carotid artery samples.

In the normal aorta, there was an apparent U-II immunoreactivity only in endothelial cells (figure 1C). We also examined U-II immunoreactivity in atherosclerotic aortae collected at autopsy. In these samples, there was a large degree of inflammatory cell immunoreactivity in addition to specific endothelial cell staining, and some apparent medial immunoreactivity as well (figure 1D). Moreover, in tissue samples obtained from repair of abdominal aortic aneurysms, besides endothelial cells, we found a marked expression of U-II immunoreactivity in inflammatory cells (figure 1E).

In order to determine cellular phenotypes of cells immunoreactive for UII we performed colocalization studies using established cellular markers. Specifically we performed immunohistochemistry on serial sections with antibodies against Von Willebrand factor, a marker of endothelial cells, and with anti-α actin antibody a marker of smooth muscle cells and myofibroblasts and

compared these to serial sections immunoreactive for UII. From the serial sections we noted the co-existence of immunoreactivity for α-actin with that of UII, thus indicating UII expression in cells with the smooth muscle cell phenotype (figure 1G-H). We also demonstrated co-localization of Von Willebrand factor and UII in similar cells indicating UII expression in cells expressing an endothelial cell phenotype. Negative control sections showed no non-specific immunoreactivity (figure 1F).

3.5.2 RT-PCR analysis

3.5.2.1 Plaque analysis

Using real-time RT-PCR, it was possible to quantify the mRNA levels of both UII and UT in tissue samples from abdominal aortic aneurysms. These levels were expressed as the ratio of the copy number of the gene of interest to the copy number of the housekeeping gene, GAPDH. UII mRNA expression was increased in abdominal aortic aneurysms (0.22 ± 0.086) over normal aortae (0.019 ± 0.0063, p= 0.036, figure 2). UT mRNA was also significantly increased in abdominal aortic aneurysm samples compared to normal aortae (0.064 ± 0.023 vs. 0.0045 ± 0.0009; p= 0.031, figure 3).

We also evaluated the degree of UII and UT expression in tissue samples from carotid endarterectomies. However, since we did not have normal carotid arteries with which to compare these, conclusions may be suspect. Nevertheless assuming that normal aortic tissue samples have equivalent levels of UII and UT as normal carotid arteries, it was observed that UII mRNA expression was

increased in carotid endarterectomies (0.089 ± 0.031) compared to normal aortic tissue (0.019 ± 0.0063), but this increase was not significant. Again UT mRNA expression was also increased in carotid endarterectomies (0.025 ± 0.0092) compared to normal aortic tissue (0.0045 ± 0.0009), and again the increase was not significant.

3.5.2.2 Expression of UII and UT in human Leukocytes

Using real-time quantitative RT-PCR we evaluated the amount of UII and UT mRNA expression in human leukocyte sub-populations. Values are expressed as the ratio of the copy number of the gene of interest to the copy number of the GAPDH gene. The highest levels of UII mRNA were seen in the sub-population of lymphocytes (0.194 ± 0.030) when compared with monocytes (0.0255 ± 0.010), macrophages (0.00341 ± 0.0022), foam cells (0.00536 ± 0.0008), and platelets (0.0113 ± 0.0065; figure 4).

In contrast, UT mRNA levels were highest in the monocyte (0.00289 ± 0.00015) and macrophage (0.00181 ± 0.00014) populations but low in the lymphocyte (0.000142 ± 0.00007), and foam cell (0.000188 ± 0.00017) sub-populations (figure 5). UT mRNA was undetectable in the platelet fraction.

3.6 Discussion

Recent findings of UII activity in the cardiovascular system prompted us to determine if UII is up-regulated in atherosclerosis, the most prominent of cardiovascular disorders. Firstly, we examined the expression of UII in atherosclerotic lesions of both carotid arteries and of abdominal aortae. To do this we performed immunohistochemistry using anti-UII antibodies. We were able to demonstrate a large degree of UII immunoreactivity in atherosclerotic vessels of both carotid and aortic origin. In both types of vessels UII was most prominent in the hyperplasic intima of the lesion, often with a clear separation between intima and media. However, medial UII immunoreactivity was also observed in both carotids and aortae. Interestingly, we noted that normal segments of otherwise diseased vessels also exhibited UII immunoreactivity. This indicated that there may be a diffuse up-regulation of UII in the diseased state. To the best of our knowledge this is the first depiction of UII immunoreactivity in atherosclerotic plaques of carotid arteries and aortae. Importantly, the most prominent staining was found in the lesion, indicating a direct up-regulation in association with atherosclerotic plaques.

With these findings we then proceeded to determine quantitative measurements of UII, as well as, it's cognate receptor UT in tissue samples harvested from patients undergoing carotid endarterectomies and abdominal aortic aneurysm repair. We found that UII mRNA expression was significantly increased in abdominal aortic aneurysm tissue samples. Importantly, we found that UT mRNA was also significantly elevated in abdominal aortic aneurysms.

As noted, both UII and UT mRNA levels were also elevated in carotid endarterectomies compared to normal aorta. However, this did not reach statistical significance. Also, the biological significance of this is questionable at best since we were unable to compare the mRNA levels for either UII or UT from the diseased carotid endarterectomy tissue samples with the mRNA levels of normal carotid arteries. Nevertheless, the RT-PCR data on UII does reinforce the qualitative data observed with immunohistochemistry. In agreement with our findings, others have also demonstrated UT mRNA expression in human aortic tissue [Ames et al. 1999 & Matsushita et al. 2001]. In addition, Maguire et al.[2000] showed the presence of UT receptors in the aorta by UII radioligand binding activity.

The large degree of inflammatory cell staining observed by immunohistochemistry led us to quantitatively determine the levels of both UII and UT in the leukocyte sub-populations. We found that lymphocytes were by far the largest producers of UII, which is quite interesting in light of the fact that the role of lymphocytes in atherosclerosis is becoming increasingly more important [Pinderski et al. 2002 & Daugherty et al. 2002]. In contrast, monocytes and macrophages were the largest producers of UT, with relatively little expression in either foam cells, lymphocytes, or platelets. These findings suggest that UII may act in an autocrine or paracrine fashion in the setting of atherosclerosis.

It has recently been demonstrated that UII binding to UT activates Rho kinase [Sauzeau et al. 2001] and that Rho kinase in monocytes is involved in the regulation of plasminogen activator inhibitor-1 (PAI-1) synthesis [Ishibashi et al. 2002]. In addition to this, Rho activation has been implicated as the mediator in thrombin

induced suppression of endothelial nitric oxide synthase (eNOS) and the up-regulation of endothelin converting enzyme (ECE-1) [Eto et al. 2001]. It is tempting to speculate that UII may promote atherogenesis in part by down-regulation of eNOS and up-regulation of ECE-1 and PAI-1 via Rho kinase activation.

UII has been demonstrated as the most potent vasoconstrictor to date [Ames et al. 1999]. Therefore up-regulation of this factor has the potential to lead to vasospasm. In addition to its marked vasoactivity UII has been shown to act as a mitogenic factor for smooth muscle cells [Sauzeau et al. 2001 & Watanabe et al. 2001]. Hence, the up-regulation of UII in carotid and aortic atherosclerotic plaques may affect either the vessels vasoactivity or it may act primarily as a mitogenic factor or both. Studies aimed at using a selective UT antagonist will be needed to address the physiological significance of increased UII and UT expression in atherosclerotic carotids and aortae.

To conclude, here we have demonstrated a quantitative and qualitative increase in UII expression in both atherosclerotic carotid arteries and aortae. We also showed that UII expression was highest in lymphocytes whereas UT expression was most prominent in the monocyte/macrophage population. These findings suggest a possible role for UII and UT in the pathophysiology of atherosclerosis.

Figure Legends:

Figure 1: UII immunoreactivity in both carotid and aortic tissue samples (large arrows indicate endothelium and asterisks indicate intimal layer). (**A**), Shown here is a non-lesioned carotid artery collected at autopsy showing diffuse UII immunoreactivity within the thickened intimal layer (100X magnification). (**B**) UII immunoreactivity in endothelial cells and myointimal cells in the hyperplastic intima of a carotid endarterectomy sample (100X magnification). (**C**), Normal aorta with distinct endothelial UII immunoreactivity (200X magnification). (**D**), Diseased aortic segment obtained at time of autopsy showing intense UII immunoreactivity in endothelial and inflammatory cells (400X magnification). (**E**), Diseased aortic sample retrieved during abdominal aortic aneurysmal repair showing marked inflammatory cell infiltration with intense UII immunoreactivity (400X magnification). (**F**), A section of diseased aorta collected at autopsy incubated without primary antibody as negative control section (100X magnification). Consecutive sections of a carotid artery segment showing UII immunoreactivity (**G**, small arrows indicate identical cells in serial sections), and α-actin immunoreactivity (**H**), in smooth muscle cells of the hyperplasic intima (400X magnification).

Figure 1

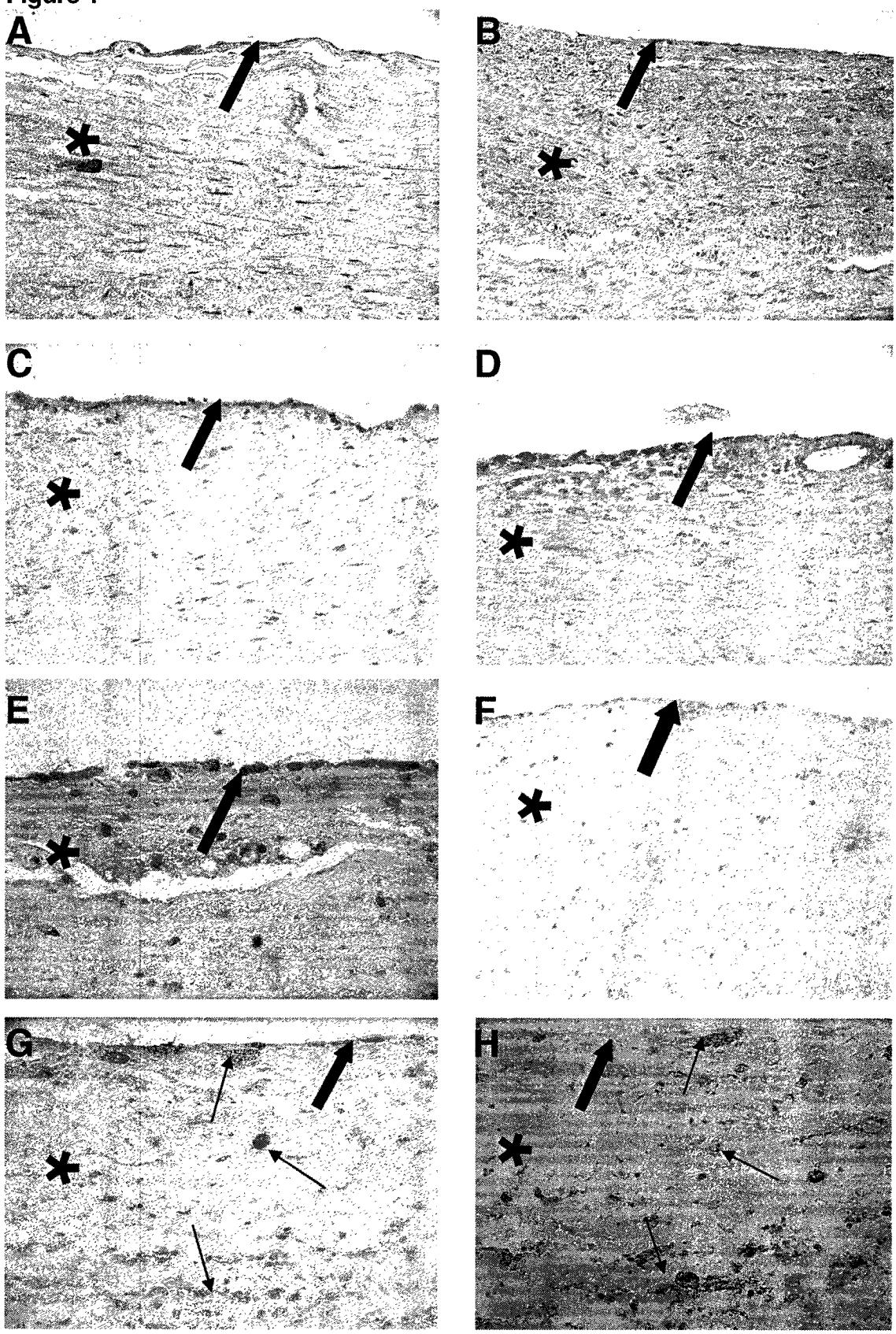

Figure 2: Relative levels of prepro-UII mRNA in normal aortic samples (n=7) compared with tissue samples retrieved from abdominal aortic aneurysm (AAA, n=8) and carotid endarterectomies (CE, n=17), normalized to GAPDH. The graph demonstrates that UII is significantly elevated in tissue samples from abdominal aortic aneurysms compared to normal aortae. (* indicates $p<0.05$).

Figure 2

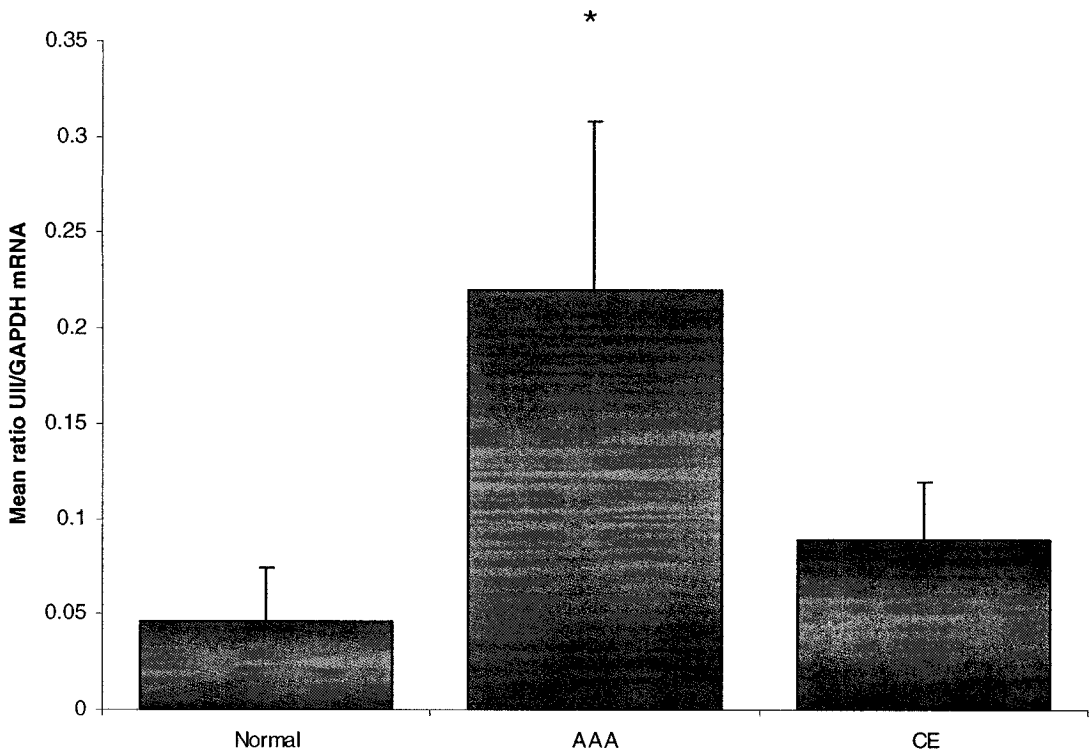
*
0.35
0.3
0.25
0.2
0.15
0.1
0.05
0
Mean ratio UII/GAPDH mRNA
Normal
AAA
CE

Figure 3: Relative levels of UT mRNA in normal aortic samples (n=7) compared with tissue samples retrieved from abdominal aortic aneurysm (AAA, n=8) and carotid endarterectomies (CE, n=17), normalized to GAPDH. The graph demonstrates that UT is significantly elevated in tissue samples from abdominal aortic aneurysms compared to normal aortic samples (* indicates $p<0.05$).

Figure 3

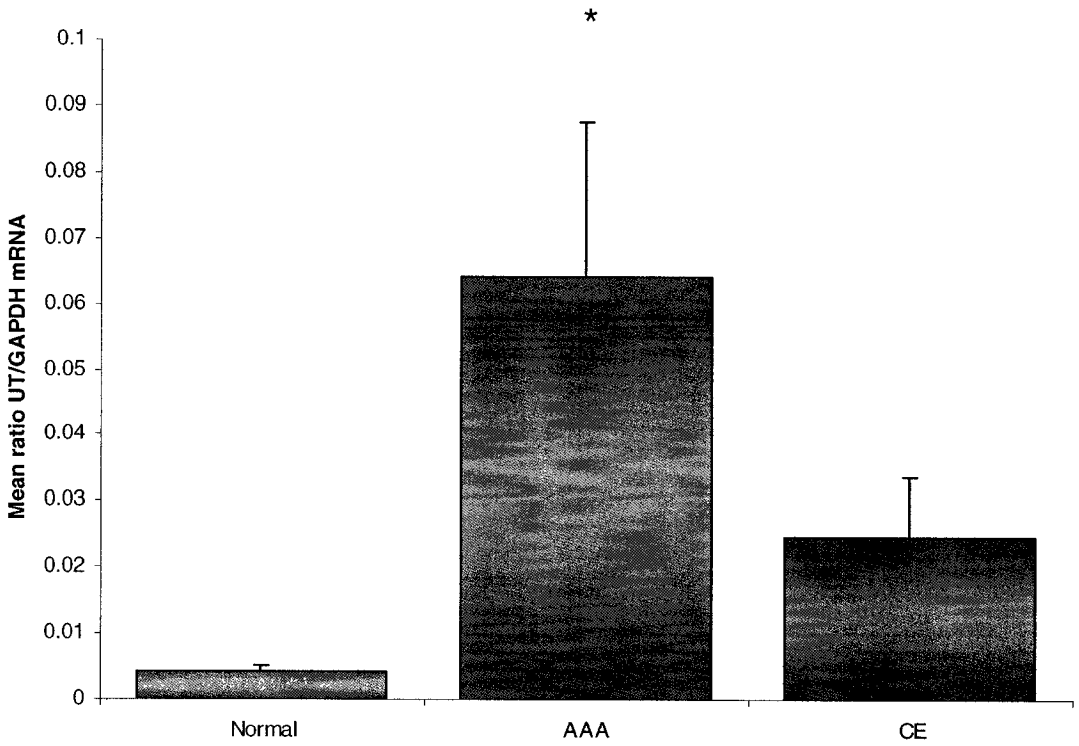
*
0.1
0.09
0.08
0.07
0.06
0.05
0.04
0.03
0.02
0.01
0
Mean ratio UT/GAPDH mRNA
Normal
AAA
CE

Figure 4: Relative levels of Prepro-UII mRNA in leukocyte sub-populations normalized to GAPDH. This graph demonstrates that UII levels are highest in lymphocytes.

Figure 4

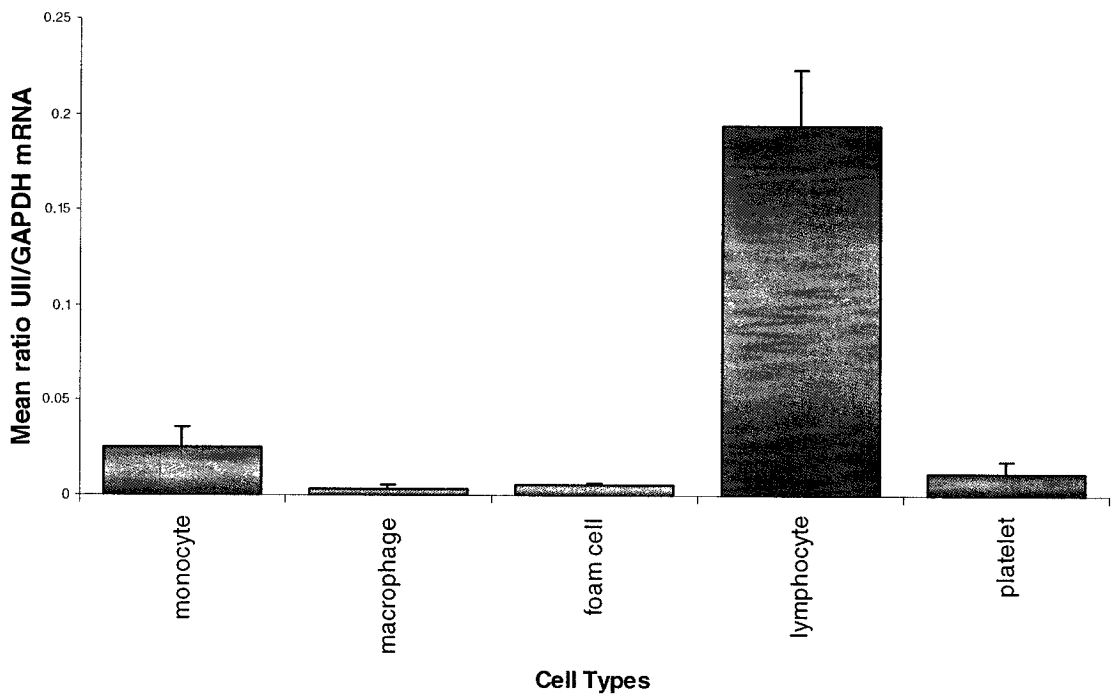
Mean ratio UII/GAPDH mRNA
0.25
0.2
0.15
0.1
0.05
0
monocyte
macrophage
foam cell
lymphocyte
platelet
Cell Types

Figure 5: Relative levels of UT mRNA in leukocyte sub-populations normalized to GAPDH. This graph demonstrates that UT mRNA is most abundant in the Monocyte/Macrophage population.

Figure 5

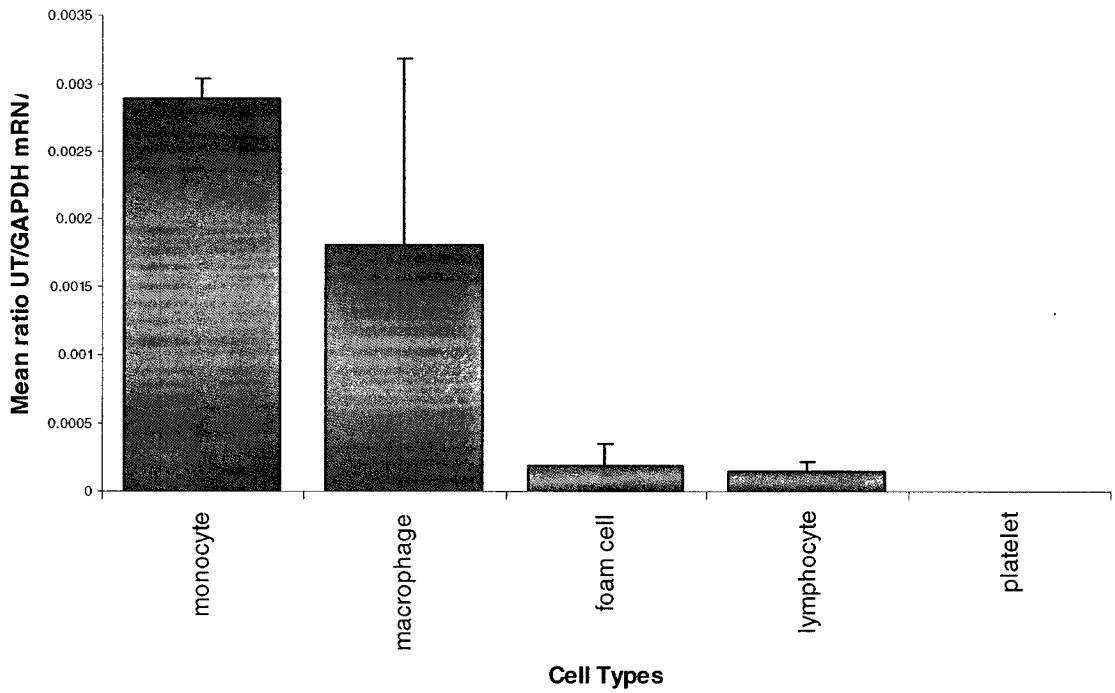
0.0035
0.003
0.0025
0.002
0.0015
0.001
0.0005
0
Mean ratio UT/GAPDH mRN
monocyte
macrophage
foam cell
lymphocyte
platelet
Cell Types

Chapter IV

Urotensin-II Receptor Knockout Increases Plasma Lipids and Atherosclerosis in ApoE Knockout Mice.

4.1 Preface

In the previous chapter we investigated the degree of UII and UT expression in human carotid and aortic atherosclerosis. We found that UII and UT mRNA levels were significantly increased in human atherosclerotic aortae. Thus here we aimed at determining whether UII/UT signaling has an effect in the pathophysiology of atherosclerosis by evaluating the effect of UT knockout in a well established mouse model of atherosclerosis. This work resulted in a manuscript submitted to the *Journal of Clinical Investigation*.

4.2 Abstract

Objective: Urotensin-II (UII) is a vasoactive peptide whose levels are elevated in cardiovascular disease. Based on our recent studies which demonstrated increased expression of UII and its receptor, UT, in human atherosclerosis, we sought to determine the effect of UT gene deletion in a mouse model of atherosclerosis.

Methods & Results: UT knockout (KO) mice were crossed with ApoE KO mice to develop UT/ ApoE double knockout (DKO) mice. At 6 weeks of age wild-type (WT), UT KO, ApoE KO, and DKO mice were placed on a high fat western type diet for 12 weeks. We evaluated the degree of atherosclerosis via an *en face* aortic presentation, and the quality of lesions via aortic plaque histology. In addition, serum total cholesterol and triglycerides were analyzed. Liver histology was also evaluated. Negligible atherosclerosis was observed in either WT or UT KO mice. ApoE KO mice showed apparent aortic atherosclerosis and hepatic steatosis. However, DKO mice exhibited significantly increased atherosclerosis compared to ApoE KO mice ($P<0.05$). This was associated with a significant increase in total serum cholesterol ($P<0.001$), serum triglycerides ($P<0.001$) and decrease in hepatic steatosis ($P<0.001$). Furthermore we carried out real time RT-PCR analysis on lipid uptake receptors, as well as the nuclear receptors involved in lipid metabolism. We found that ABCA1, SR-A1, SR-B1,as well as, LXR-α, PPAR-δ, and PPAR-γ were all significantly decreased in DKO mice compared to ApoE KO mice. Finally we performed Western blot analysis on LXR-α protein levels. Indeed, we found that DKO animals had significantly

reduced LXR-α protein levels compared to ApoE KO mice. DKO mice also exhibited hypertrophy of heart, kidneys, and spleen ($P<0.01$).

Conclusions: We demonstrate that UT gene deletion exacerbates hyperlipidemia in a mouse model of atherosclerosis leading to increased aortic lesion formation as well as exacerbation of other atherosclerotic disease sequelae. We propose that UT KO in an ApoE deficient background suppresses lipid uptake in the liver via the down regulation of nuclear receptor expression, which in turn attenuates lipid uptake receptor expression and therefore lipid uptake in the liver. Consequently this leads to an increase in hyperlipidemia and atherosclerotic lesion formation.

4.3 Introduction

Atherosclerosis, the primary cause of ischemic cardiomyopathy and ultimately a major contributing factor to death in the Western World today is obviously a huge burden on society and as such is the focus of a considerable amount of research. Urotensin-II (UII) is emerging as a prominent vasoactive factor in a variety of cardiovascular diseases including atherosclerosis. This was first suggested by Ames et al. [1999] who described UII immunoreactivity in human coronary atheroma. In addition, both Sauzeau et al.[2001] as well as Watanabe et al.[2001] demonstrated that UII induced smooth muscle cell proliferation, an integral step in the early development of atherosclerotic plaques. Interestingly, Watanabe et al.[2001] demonstrated a synergistic effect of UII on proliferation of SMCs when administered with oxidized LDL. This has potentially serious pathological implications since oxidized lipids are a major contributor to atherosclerotic lesion formation.

UII was found to be elevated in atherosclerotic arteries of human origin. In fact we were the first to show increased mRNA and protein levels of UII in atherosclerotic human aortae. [Bousette et al. 2004] Furthermore, we demonstrated that UT mRNA levels were also increased in diseased human aortae. Interestingly, Hassan et al.[2005] demonstrated that UII protein and mRNA levels were significantly increased in arteries of patients with coronary atherosclerosis compared to normal coronary arteries. Thus, these findings suggest a potential role for U-II in the pathogenesis of coronary atherosclerosis.

Our findings are supported by Maguire et al.[2004] who found prominent UII immunoreactivity in atherosclerotic plaques of coronary arteries as well as in the thickened intima of failed saphenous vein grafts of explanted human hearts. In addition to increased UII levels in atherosclerotic lesions, reports have demonstrated increased UII levels in plasma of patients with atherosclerotic disease. Heringlake et al. 2004 & Lapp et al. 2004

Interestingly, UT mRNA was shown to be significantly up-regulated in the aortae of ApoE KO mice, an established model for the study of atherosclerosis. Wang et al. 2005a In addition they also demonstrated significantly increased UII radioligand binding in these same aortae.

Thus, both UII and UT are up-regulated in atherosclerotic arteries of humans, and in aortae of ApoE KO mice. Also UII induces SMC proliferation alone and in a synergistic fashion with oxidized LDL, a major contributor to atherosclerosis. These data support the role of UII in atherosclerotic pathophysiology. Therefore based on these data we hypothesized that UT gene deletion would attenuate atherosclerotic burden in ApoE KO mice, a well established model of atherosclerosis.

4.4 Methods

4.4.1 Animals

The study utilized 4 strains including WT (C57BL6/J; ApoE $^{+/+}$, UT$^{+/+}$; n=54), UT KO (ApoE $^{+/+}$, UT $^{-/-}$; n=35), ApoE KO (ApoE $^{-/-}$, UT $^{+/+}$; n=11), and UT/ApoE double knockout mice (DKO, ApoE $^{-/-}$, UT $^{-/-}$; n=20). The generation of UT KO was previously described. [Behm et al., 2003] Briefly, gene targeting was performed in murine E14.1 ES cells, replacing the single coding exon of the UT receptor locus with a positive selection cassette containing the neomycin phosphotransferase gene driven by the phosphoglycerate kinase I promoter. The KO strategy resulted in the deletion of the whole UT open reading frame. These animals were backcrossed at least 10 times to the C57BL6/J background and then bred to homozygosity. The UT KO mice were then crossed with the ApoE KO to generate DKO mice. The ApoE KO mice were ordered from Taconic (B6.129P2-*Apoe*^{tm1Unc} N11). Genotypes were verified by PCR and gel electrophoresis (Table 1 and Figure 1).

4.4.2 Study design

Mice were bred and allowed to mature to 6 weeks of age at which point male mice were weighed and put on a high fat diet for a period of 12 weeks. The high fat diet (TD-88137, Harlan Teklad) consisted of 42% calories from fat with 0.15% cholesterol content. [Kuhlencordt et al. 2001] At the conclusion of the study period mice were fasted for 4 hours, weighed, and then sacrificed by exsanguination under anesthesia. We then harvested serum, the heart, the aorta, lungs, liver, kidneys,

and spleen. Each organ was weighed and then fixed in 10% formalin or flash frozen in liquid nitrogen and stored at –80 ° C.

4.4.3 Tissue Histology

Formalin fixed aortae were surgically cleaned of all adventitial fat and extraneous tissue. These aortae were then stained with sudan IV and pinned to a rubber surface for presentation. Flash frozen aortae were embedded in OCT freezing media for sectioning via the cryostat (10 μm thickness). Formalin fixed livers were embedded in paraffin, and cut (5μm). Sections were then stained with hematoxylin & eosin. For the liver 5 random photomicrographs were taken (100X magnification) from each animal. These photomicrographs were then downloaded into an image analysis program, *Image ProPlus*, which allowed for the quantification of hepatic steatosis in the livers.

4.4.4 Serum Lipids

Fasting blood samples were harvested at the time of sacrifice. Serum was then collected and stored at –20 ° C. These serum samples were then analyzed for serum total cholesterol using a cholesterol assay kit (BioVision, CA, USA) according to the manufacturer's instructions. Similarly, serum total glycerol (a surrogate for triglyceride levels) was determined using a triglyceride analysis kit (Sigma, St-Louis; Misouri). Protocol was carried out as per manufacturer's instructions.

4.4.5 Real Time RT-PCR analysis

Liver samples were retrieved from storage at -80 ° for RNA extraction using Trizol (Invitrogen, Ontario, Canada) and performed as per the manufacturer's instructions. RNA integrity was then verified for all samples by evaluating the clarity of the 28S and 18S bands and verifying that the bands were 28S>18S by gel electrophoresis. Following this, 2 μg of each RNA sample was reverse transcribed to synthesize cDNA using the Omniscript reverse transcriptase kit from Qiagen (Ontario, Canada). From this, 1 μl of cDNA was used to amplify target genes using specific primers (Table 1). Genes were amplified individually in the LightCycler (Roche, Montreal, Canada) using Quantitect SYBR Green reagent (Qiagen, Ontario, Canada) with the following amplification conditions: DNA polymerase activation, 15 minutes at 95 ° C followed by 40 cycles of denaturation, annealing and extension for 15 seconds at 94 ° C, 20 seconds at 50-60 ° C (depending on primer T_m) and 20-30 seconds at 72 ° C (depending on amplicon size), respectively. Primers were designed using PrimerQuest biotool [www.idtdna.com] (Table 1). All values for mRNA expression determined by RT-PCR are expressed as the ratio of the copy number of the mRNA transcript of interest to the copy number of the mRNA transcript of the housekeeping gene GAPDH. The copy number of mRNA transcript is determined by the threshold cycle of the PCR reaction for each sample. A homogeneous amplification of the products was rechecked by analyzing the melting curves of the amplified products.

4.4.6 Western Blotting

Western blotting was performed as previously described [Saito et al. 2002], with goat polyclonal anti-LXR-α antibody (1:300 dilution) and bovine anti-goat secondary antibody conjugated to horse peroxidase (1:5000 dilution). LXR-α levels were normalized to the housekeeping gene Histone H1 as previously described [Iankova et al. 2006] Protein bands were then quantified using arbitrary units (AU) with the image analysis program, *Image J.*

4.4.7 Statistical analyses

Multi-group comparisons were analyzed using ANOVA with the Tukey post-hoc test. Direct two group comparisons were carried out using the student's t-Test. A P value <0.05 was considered statistically significant. All statistical analyses were carried out using SPSS version 11.5.

4.5 Results

4.5.1 Lesion area fraction

Wild type C57BL/6 mice demonstrated negligible atherosclerosis following exposure to a high fat diet for 12 weeks (Figure 2A). Interestingly, UT KO animals also demonstrated negligible lesion formation. Conversely, ApoE KO mice exhibited apparent atherosclerosis especially in the aortic arch with few small lesions in the thoracic and abdominal aorta. Remarkably, DKO mice exhibited a significant 54% increase in lesion area fraction compared to ApoE KO mice (4.23 ± 0.41 % vs. 6.59 ± 0.59 %, $P<0.001$) (Figure 2B). Of note, two of eleven aortae analyzed from the DKO mice developed abdominal aortic aneurysms which was not observed in any other strain (Figure 3). The first of had such extensive atherosclerosis that >85% of the aorta was diseased. The second was not quite so extensively diseased but nonetheless ~20% of the aorta was encompassed with atherosclerotic lesions.

4.5.2 Lesion histology

As expected from the en face aortic analysis, lesions were absent from WT and UT KO aortic arches (Figure 4A-D). On the other hand ApoE KO and DKO animals both presented with lesions or varying sizes. Atherosclerotic plaques varied from Type 1 lesions exhibiting intimal thickening to type V lesions bearing large fatty cores with an overlying fibrous cap (Figure 4 E-H). All lesions had pronounced inflammatory infiltrates. No major histological differences in lesions

were noted between ApoE KO and DKO animals, however, the largest lesions were found in DKO animals.

4.5.3 Serum Lipids

Serum total cholesterol and serum triglycerides were measured. UT KO mice exhibited serum total cholesterol levels comparable to WT mice. As expected ApoE KO mice demonstrated a very significant increase in serum total cholesterol compared to wild type and UT KO animals ($P<0.001$) (Figure 5A), which is in accordance with levels reported by others. [Sukovich et al. 1998] Remarkably, DKO had even greater serum total cholesterol levels, which were significantly increased compared to all other strains including ApoE KO mice ($P=0.001$). Serum triglyceride analysis revealed that UT KO mice exhibited a small but significant increase in serum triglycerides compared to WT mice ($P<0.01$) (Figure 5B). Again, ApoE KO mice showed a very significant increase in serum triglycerides compared to WT and UT KO mice ($P<0.001$). Finally, DKO mice demonstrated triglyceride levels greater than all other strains including ApoE KO ($P=0.001$) (Figure 5B).

4.5.4 Gross anatomy

We measured body weight at the beginning and end of the 12-week study period. Interestingly, we found that UT KO mice had a significant reduction in body weight gain compared to WT mice ($P<0.001$) (Table 2) (Figure 6A). Of note, DKO mice experienced the least weight gain of all the strains. Specifically, DKO

mice had significantly lesser weight gain compared to WT mice and ApoE KO mice ($P<0.05$), but not compared to UT KO mice (Table 2) (Figure 6A).

We also measured organ weights at time of sacrifice. The organs included heart, right and left lungs, liver, right and left kidneys, and spleen. Interestingly, UT KO mice exhibited significantly reduced liver mass compared to WT mice ($P<0.01$) (Table 2) (Figure 6B), however, all other organs had comparable weights. Similarly to UT KO mice, DKO mice also had decreased liver weights, which was significant when compared to both WT and ApoE KO mice ($P<0.05$) (Table 2) (Figure 6B). Of note, DKO mice had significantly increased heart, right kidney, left kidney, and spleen weights compared to all other strains ($P<0.05$) (Table 2). This latter data is especially remarkable in light of the fact that these DKO mice had the least body weight gain.

4.5.5 Liver histology

The significant reduction in liver size in both UT KO and DKO mice led us to analyze liver histology. Analysis of H & E stained liver demonstrated that WT, UT KO, and ApoE KO mice had apparent hepatic steatosis (Figure 7A-C). In contrast, DKO mice had significantly reduced hepatic steatosis compared to all other strains ($P<0.001$) (Figure 7D-E).

4.5.6 Liver mRNA and Nuclear Protein Analysis:

The marked reduction in hepatic steatosis suggested that there may be an alteration in the expression of lipid uptake receptors. Therefore, we analyzed

mRNA levels from liver tissue of the 4 strains of mice. Specifically, we analyzed the mRNA levels of the LDL receptor (LDLR), the LDLR-related protein (LRP), the ATP binding cassette-A1 (ABCA1), scavenger receptor-A1 (SR-A1), and SR-B1. Expectedly, LRP, ABC-A1, SR-A1, and SR-B1 were all significantly elevated in ApoE KO mice ($P<0.05$) compared to both WT and UT KO mice (Table 3). Of note, LRP levels were also significantly elevated in DKO mice compared to WT and UT KO mice (Table 3). However, mRNA levels for ABC-A1, SR-A1, and SR-B1 were significantly reduced in DKO mice compared to ApoE KO mice ($P<0.05$) (Figure 8A-C) (Table 3). Although mRNA levels for these lipid uptake receptors were consistently reduced in the UT KO compared to WT mice, these values did not reach statistical significance (Table 3).

These lipid uptake receptors are believed to be transcriptionally regulated by a group of nuclear receptors including liver X receptor-α (LXR-α), as well as the peroxisome proliferator activated receptors (PPARs) α, δ, and γ. Therefore mRNA analysis on the latter receptors was evaluated. The results indicate that both LXR-α and PPAR-δ mRNA expression levels were significantly increased in ApoE KO mice compared to WT and UT KO mice ($P<0.01$). Importantly, there was a significant attenuation of the expression of LXR-α, PPAR-δ, and γ in DKO mice compared to ApoE KO mice (Figure 8D-F)($P<0.01$).

The significant reduction in LXR-α mRNA levels prompted us to evaluate LXR protein levels. Therefore we performed western blotting analysis for LXR protein expression on nuclear protein extracts from livers of the 4 mouse strains. We found that while WT and UT KO LXR-α levels were comparable yet

significantly less than in ApoE KO mice, DKO mice also had significantly reduced levels compared to ApoE KO mice ($P<0.05$) (Figure 9).

4.6 Discussion

This study demonstrates that UT gene deletion leads to increased atherosclerotic lesion formation only when on an ApoE KO genetic background. Indeed, UT KO alone in mice demonstrated negligible lesion formation following the administration of a high fat diet for 12 weeks. Interestingly, UT KO mice consistently presented with livers of lesser mass, whether on a WT or ApoE KO genetic background. In addition, while WT, UT KO and ApoE KO mice all exhibited apparent hepatic steatosis, this sequela of a high fat diet was significantly reduced in DKO mice. The substantial reduction in hepatic steatosis in DKO mice led us to investigate whether it affected serum lipid levels. Indeed, we found that DKO mice show exaggerated serum total cholesterol and serum triglycerides compared to ApoE KO mice. This observation is supported by the finding of a small but significant increase in serum triglycerides in UT KO mice compared to WT mice. The significantly elevated serum lipids in DKO animals may explain the significant increase in atherosclerotic burden compared to ApoE KO mice.

The liver is an integral organ in the regulation of lipid metabolism. Therefore it was of great interest to find that DKO mice exhibited significantly reduced liver mass and hepatic steatosis. Mice with UT KO alone did not have altered hepatic steatosis but did have significantly decreased liver size. This suggests that these phenomena may not be linked. Thus, the reduced steatosis only manifests itself in the absence of apolipoprotein E. The decreased steatosis is likely due to either a reduction in liver uptake of lipids or an increase in lipid

oxidation or export. However, if the decreased hepatic steatosis was a result of increased liver oxidation one would not expect to observe the exaggerated serum dyslipidemia as well as the multiple organ hypertrophy.

In order to determine if the decreased steatosis and associated hyperlipidemia was in fact a result of reduced lipid uptake we analyzed the mRNA expression of lipid transporters including the LDL receptor, LRP, ABCA1, SR-A1, and SR-B1. Interestingly, we found significant reductions in the mRNA levels of ABCA1, SR-A1, and SR-B1 in DKO mice. This is supported by several studies which show that scavenger receptor deficiency increases plasma cholesterol and aggravates atherosclerosis in hyperlipidemic mice. [Rigotti et al. 1997; Braun et al. 2002; de Winther et al. 1999] Furthermore, overexpression of SR-B1 led to a significant decrease in plasma HDL and non-HDL cholesterol levels, [Ueda et al. 1999] Therefore these latter studies support the present hypothesis in which attenuation of lipid uptake receptors, including the scavenger receptors SR-A1 and SR-B1, causes an increase in hyperlipidemia and exacerbates atherosclerosis in ApoE deficient mice.

To investigate whether the effect of UT deficiency plays a role upstream of the lipid uptake receptors we analyzed the expression of nuclear receptors known to regulate the transcriptional expression of the former. Of note, we found that the mRNA levels for LXR-α, PPAR-δ, and PPAR-γ were all significantly decreased in DKO mice compared to ApoE KO mice. Furthermore, we went on to demonstrate that protein levels for LXR-α were also significantly decreased in DKO mice compared to ApoE KO mice. Therefore the reduced levels of these

nuclear receptors involved in transcriptional regulation of lipid uptake receptors leads to the reduced expression of the latter, which in turn would account for reduced liver uptake of lipids and hence reduced hepatic steatosis. This is supported by a study which demonstrated that liver specific disruption of PPAR-γ attenuated hepatic steatosis. [Matsusue et al. 2003] The fact that hepatic steatosis was not altered in UT KO mice can be easily explained by the fact that these mice still express ApoE and therefore lipid uptake can still be mediated through this ligand.

Atherosclerosis is a multifactorial and multi organ disease. This fact is reiterated by the present study which shows that increased atherosclerosis in DKO mice is associated with hypertrophy of the heart, kidneys, and spleen. It is unlikely that the enlargement of all these organs in DKO mice is a direct effect of UT gene deletion, since UT KO mice have comparable organ weights to WT mice, save for the liver which is significantly smaller. Therefore the increase in serum lipids is a likely culprit. Indeed, ApoE KO mice have been shown to progressively develop endothelial dysfunction and hypertension which in turn induced cardiac hypertrophy.[Yang et al. 1999] Also aged, but not young, ApoE KO mice also exhibited significantly elevated aortic stiffness and this was associated with cardiac hypertrophy. [Wang et al. 2005b] Hence, the increased serum lipids in DKO mice could exacerbate endothelial dysfunction, vascular stiffness, and hypertension in these animals and thus cause the pronounced cardiac hypertrophy.

Of note was the unexpected finding of reduced body weight gain in both UT KO vs. WT animals; as well as in DKO mice vs. ApoE KO mice. Therefore,

UT gene deletion decreases body weight gain. Whether these alterations are due to reduced growth, appetite, and/or decreased fat deposition was not evaluated in this study. In light of this finding it is interesting to note that Bernard et al. [2005] recently demonstrated that a single nucleotide polymorphism in the UII promoter was associated with % body fat in a population of Hong Kong Chinese.

In conclusion, in the present study we show that UT gene deletion leads to a decreased body weight gain and liver size in mice with a wild-type genetic background fed a high fat diet. While UT deletion in an ApoE KO genetic background leads to significantly increased atherosclerotic lesion formation, serum lipids, and organ masses, as well as, a significant decrease in body weight gain, liver mass and hepatic steatosis. Furthermore we also demonstrated that DKO mice have significantly reduced expression of liver nuclear receptors, including LXR-α, PPAR-δ, and PPAR-γ, which in turn reduced the mRNA expression of liver lipid uptake receptors including SR-A1, and SR-B1.

These findings indicate that UII-UT signaling regulates genes involved in lipid metabolism in the liver, either directly or indirectly via an as of yet undefined peripheral factor.

Figure 1. Genotyping analysis.

DNA was isolated from WT mice (lanes 1-5), UT KO mice (lanes 6-10), ApoE KO mice (lanes 11-15), and DKO mice (lanes 16-20). This DNA was subjected to polymerase chain reaction (PCR) to amplify specific DNA segments with appropriate primers (Table 1). Amplicons were gel electrophoresed to verify appropriate amplicon sizes. Lanes 1,6,11,16: DNA Ladder: bands demonstrating amplicons of 500, 400, and 300 BP from the top. Lanes 2,7,12,17: Presence of band (155bp) indicates an ApoE (+/+) genotype. Lanes 3, 8, 13, 18: Presence of band (250bp) indicates ApoE (-/-), since forward primer recognizes sequence in ApoE gene while reverse primer recognizes sequence in NEO gene. Lanes 4, 9, 14, 19: Presence of band (199bp) indicates NEO (+/+), which is gene used to replace both knockout genes (i.e. ApoE and UT). Lanes 5, 10, 15, 20: Presence of band (138bp) indicates UT (+/+).

Figure 1

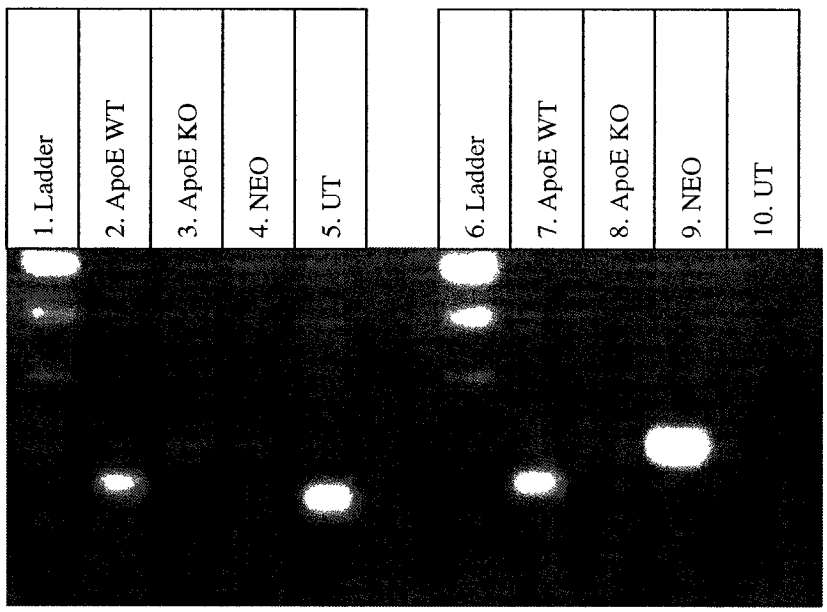
1. Ladder
2. ApoE WT
3. ApoE KO
4. NEO
5. UT
6. Ladder
7. ApoE WT
8. ApoE KO
9. NEO
10. UT

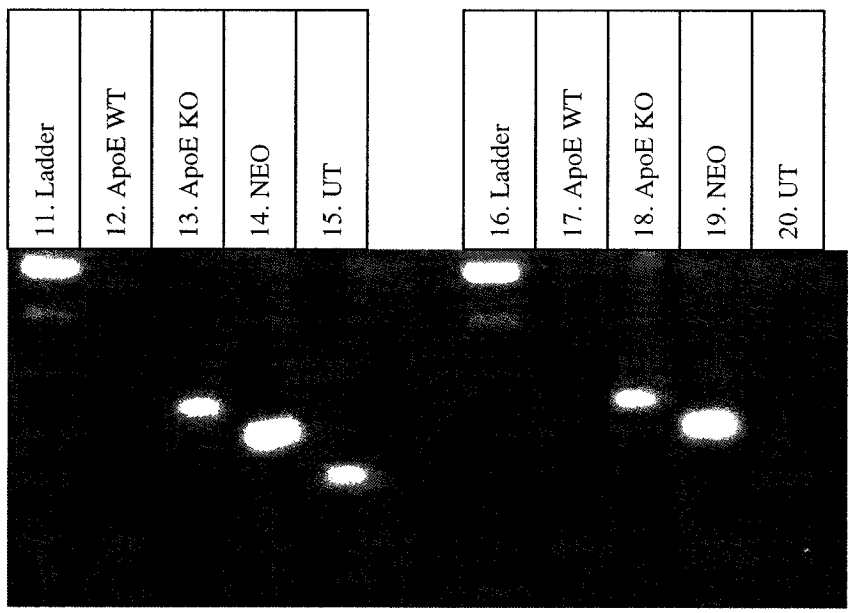
11. Ladder
12. ApoE WT
13. ApoE KO
14. NEO
15. UT
16. Ladder
17. ApoE WT
18. ApoE KO
19. NEO
20. UT

Figure 2. Aortic atherosclerosis. A, Representative photographs of aortae stained with Sudan IV. B, Graph demonstrating lesion area quantification. N=10,10, 6, and 9 for WT, UT KO, ApoE KO and DKO, respectively. * indicates $P<0.05$ vs. WT and UT KO; # indicates $P<0.05$ vs. ApoE KO.

Figure 2A

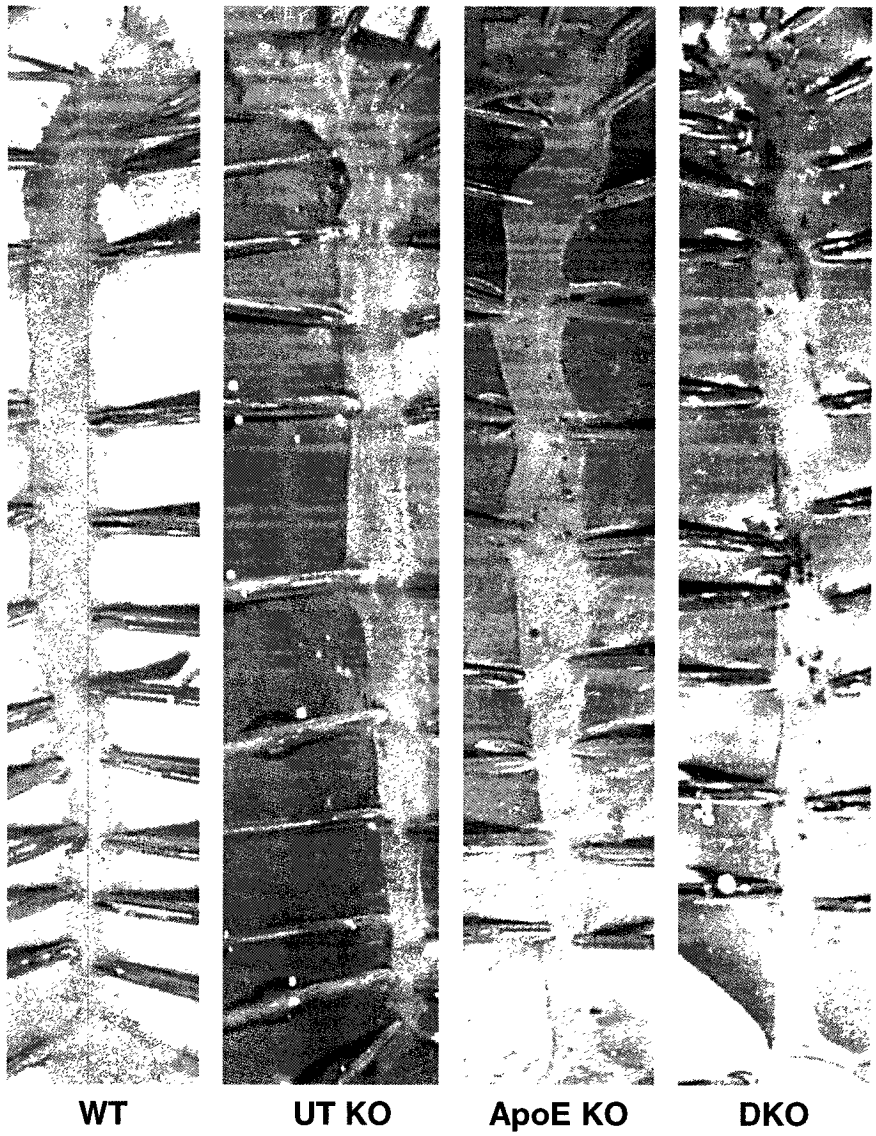
WT
UT KO
ApoE KO
DKO

B

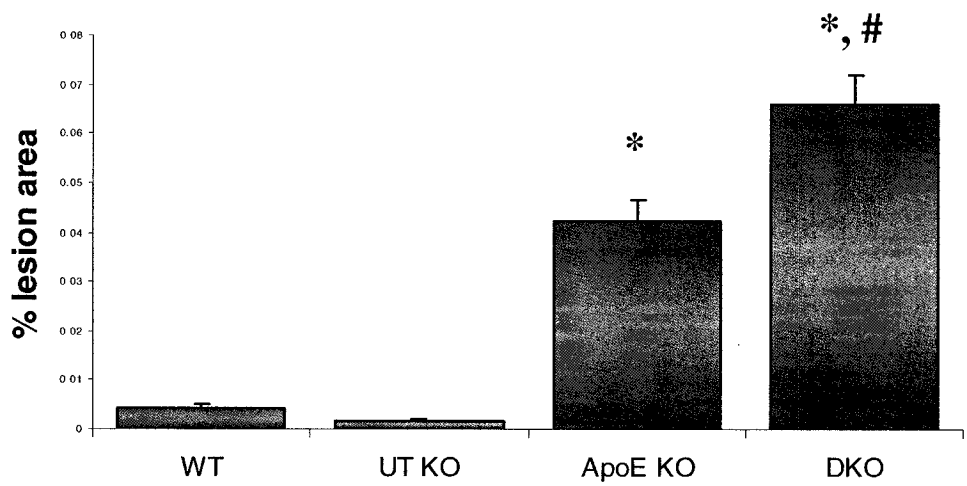
% lesion area
0.08
0.07
0.06
0.05
0.04
0.03
0.02
0.01
0
*
*, #
WT
UT KO
ApoE KO
DKO

Figure 3. Aortic aneurysms. Representative photographs of two aortae from DKO mice exhibiting aortic aneurysms (red arrow).

Figure 3

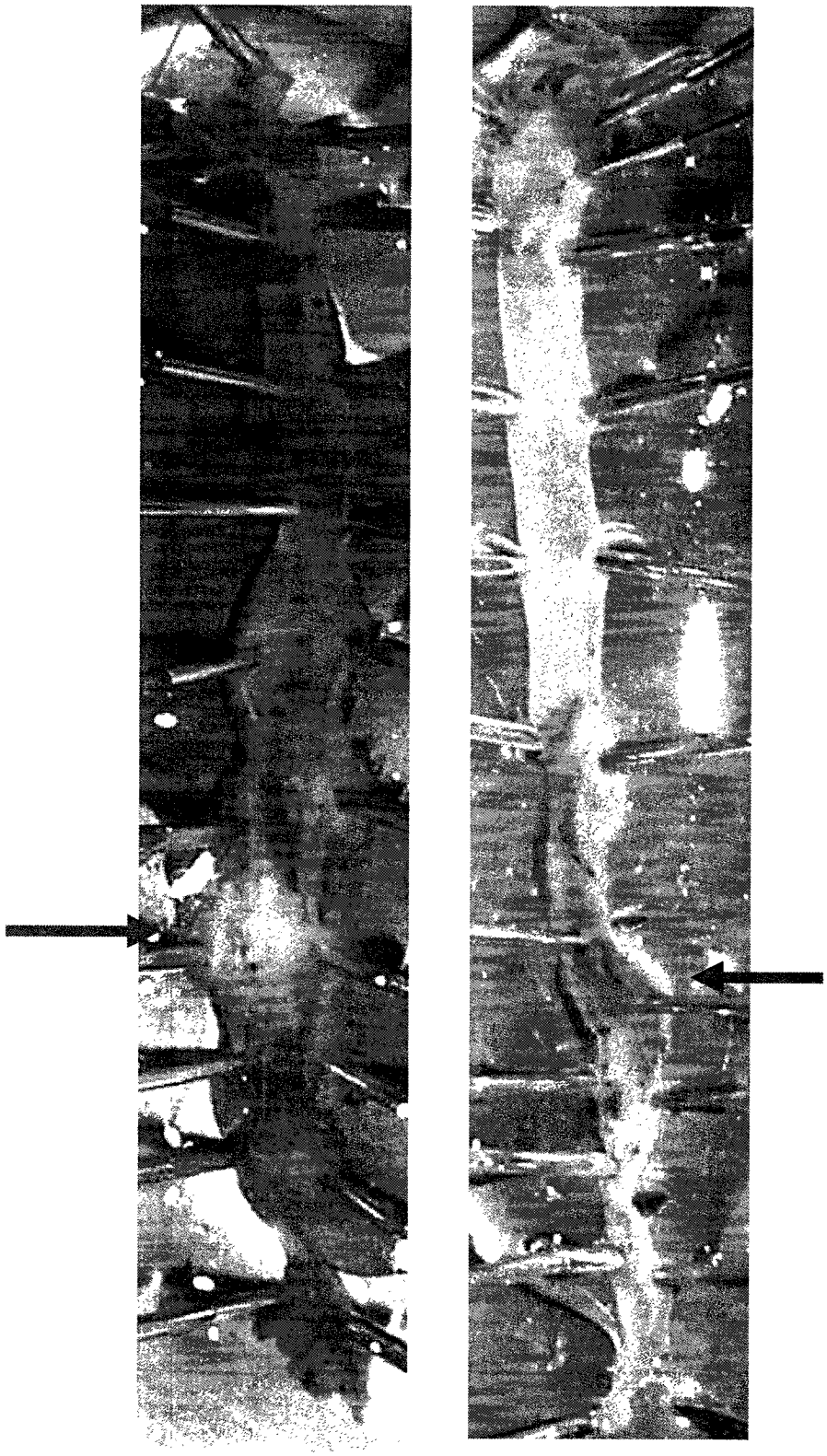

Figure 4. Aortic histology. Representative photomicrographs of Aortic cross-sections. Panel A demonstrates a WT aorta (100X magnification). Panel B is greater magnification of WT aorta (400X magnification). Panel C demonstrates a UT KO aorta (100X magnification). Panel D is greater magnification of UT KO aorta (400X magnification). Panel E demonstrates an ApoE KO aorta with type V lesion (100X magnification). Panel F is greater magnification of ApoE KO lesion clearly demonstrating a fatty core with overlying fibrous cap (200X magnification). Panel G demonstrates a DKO aorta with large type V lesions (100X magnification). Panel H is greater magnification of DKO lesion clearly demonstrating a fatty core with overlying fibrous cap (200X magnification).

Figure 4

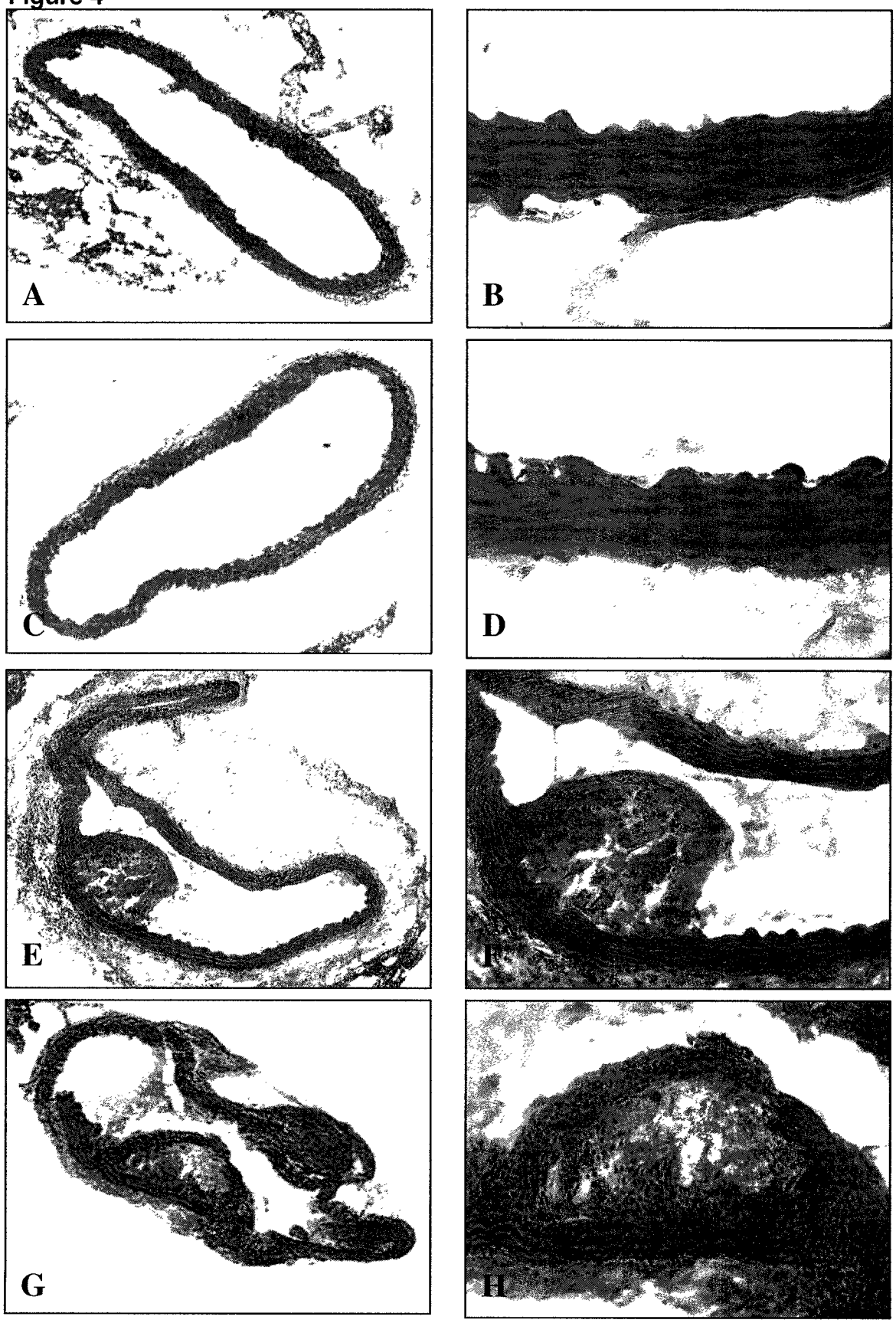

Figure 5. Serum lipid analysis. A, Graph demonstrating significantly elevated serum total cholesterol in ApoE KO mice (* indicates $P<0.001$ vs. WT and UT KO mice). Furthermore, DKO mice exhibited significantly elevated serum total cholesterol compared to all other strains (# indicates $P<0.001$). B, Graph demonstrating significantly elevated serum glycerol levels in UT KO vs WT (+ indicates $P<0.01$), ApoE KO vs. WT and UT KO (* indicates $P<0.001$) and DKO vs. all strains (# indicates $P<0.001$).

Figure 5A

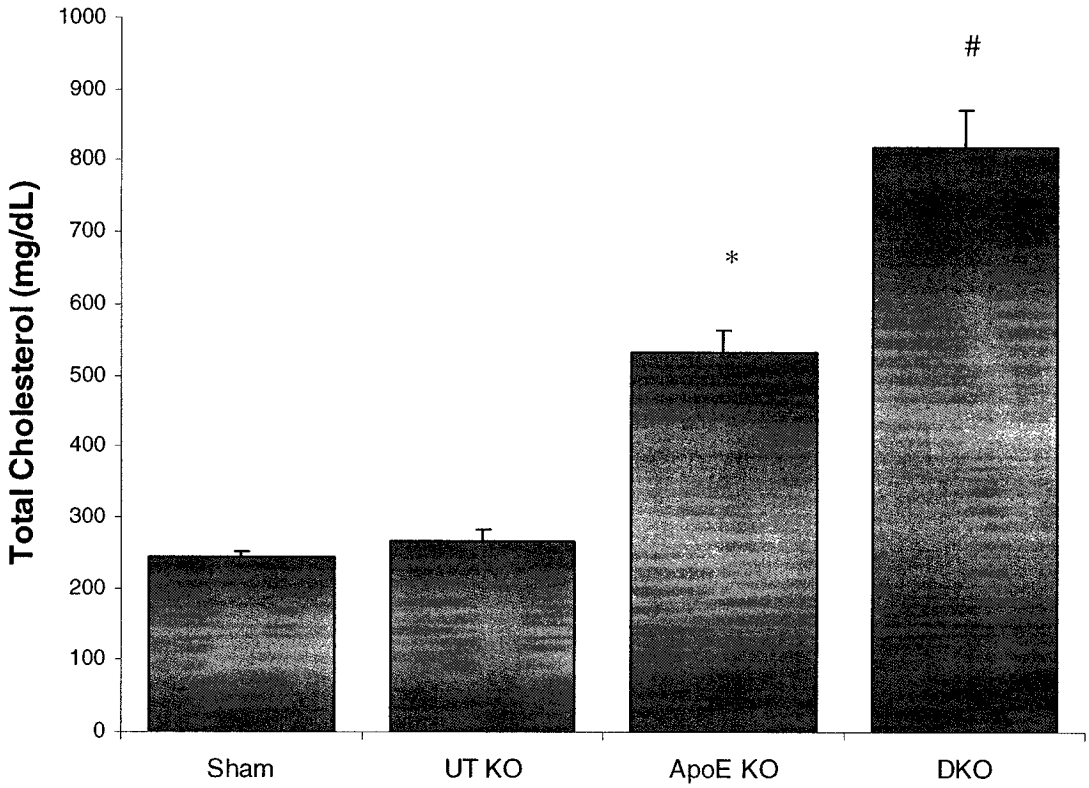
Total Cholesterol (mg/dL)
1000
900
800
700
600
500
400
300
200
100
0
#
*
Sham
UT KO
ApoE KO
DKO

B

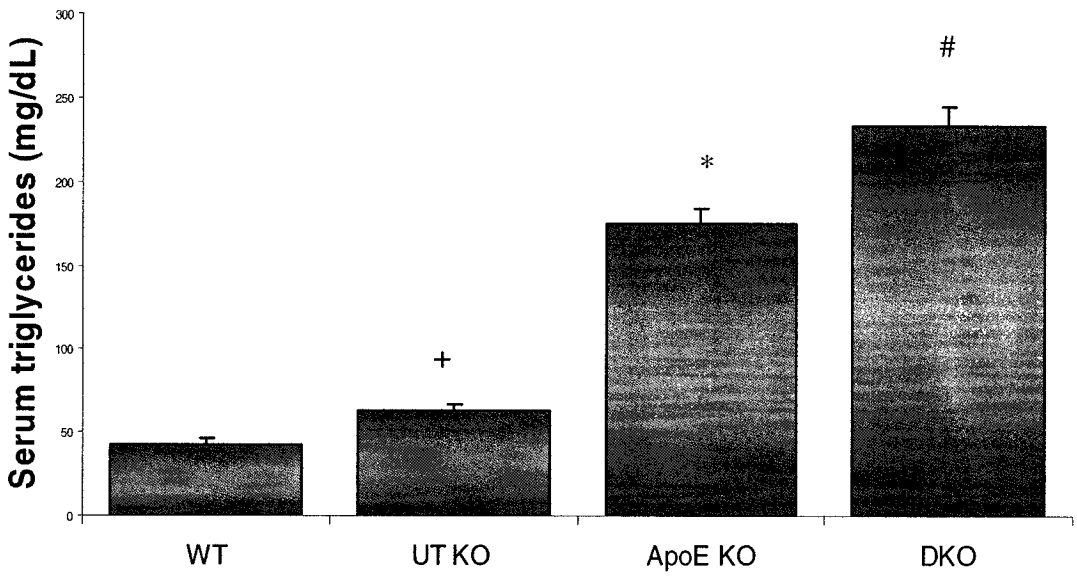
Serum triglycerides (mg/dL)
300
250
200
150
100
50
0
#
*
+
WT
UT KO
ApoE KO
DKO

Figure 6. Body weight gain and liver weight analysis. A, Graph demonstrating significantly reduced body weight gain in UT KO mice and DKO mice compared to WT mice (* indicates $P<0.001$) and ApoE KO (# indicates $P<0.05$) mice, respectively. B, Graph demonstrating significantly reduced liver mass in UT KO mice and DKO mice compared to WT mice (* indicates $P=0.001$) and ApoE KO (# indicates $P<0.05$) mice, respectively.

Figure 6A

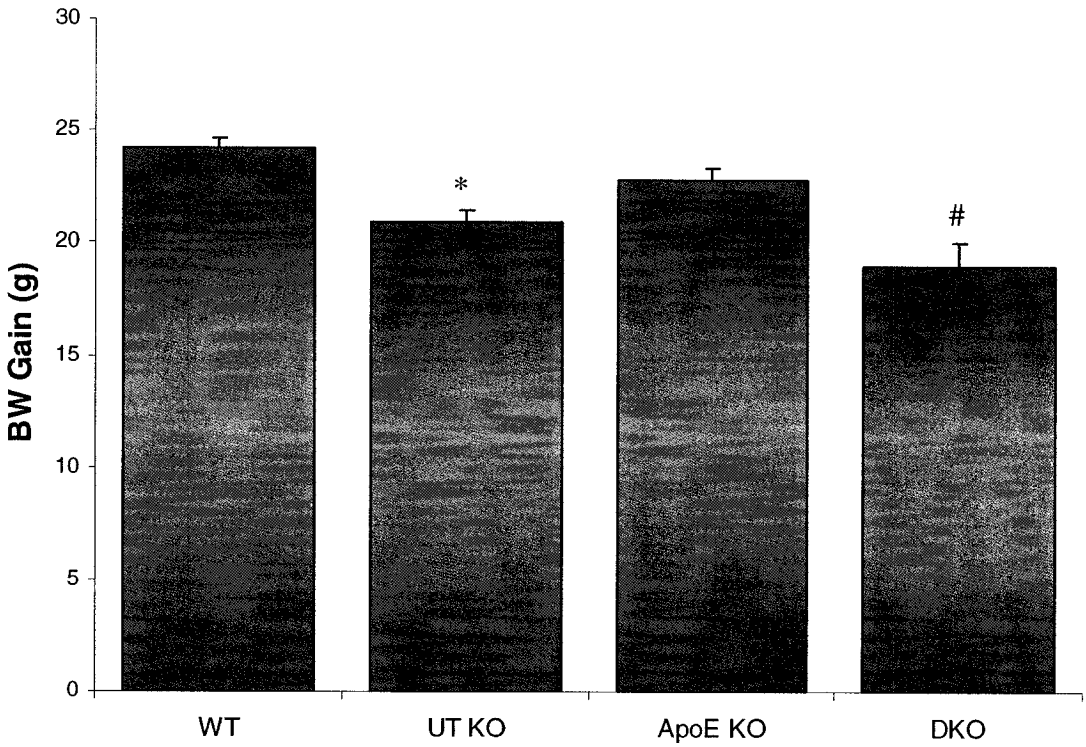
30
25
20
15
10
5
0
BW Gain (g)
*
#
WT
UT KO
ApoE KO
DKO

B

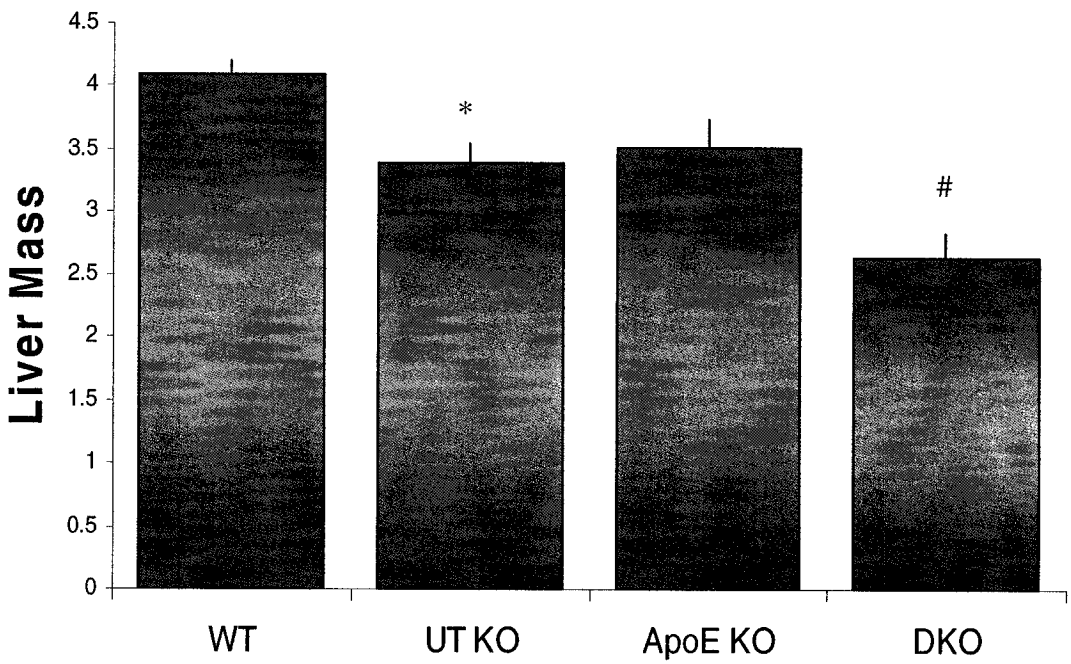
4.5
4
3.5
3
2.5
2
1.5
1
0.5
0
Liver Mass
*
#
WT
UT KO
ApoE KO
DKO

Figure 7. Liver steatosis. Representative photomicrographs of livers stained with hematoxylin & eosin demonstrating hepatic steatosis from (A), WT; (B), UT KO; (C), ApoE KO; and (D), DKO mice (100X magnification). E, Graph demonstrating significantly reduced hepatic steatosis in DKO mice compared to all other strains (* indicates $P<0.001$).

Figure 7

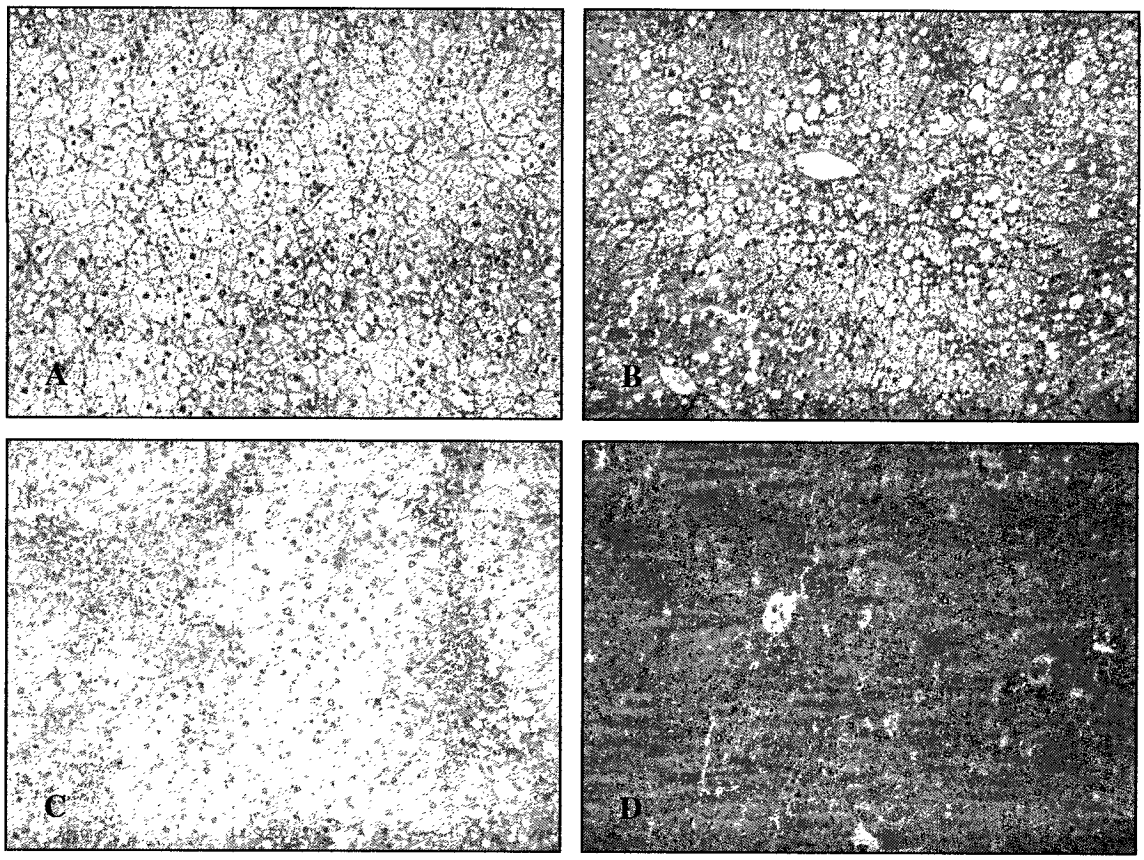
A
B
C
D

E

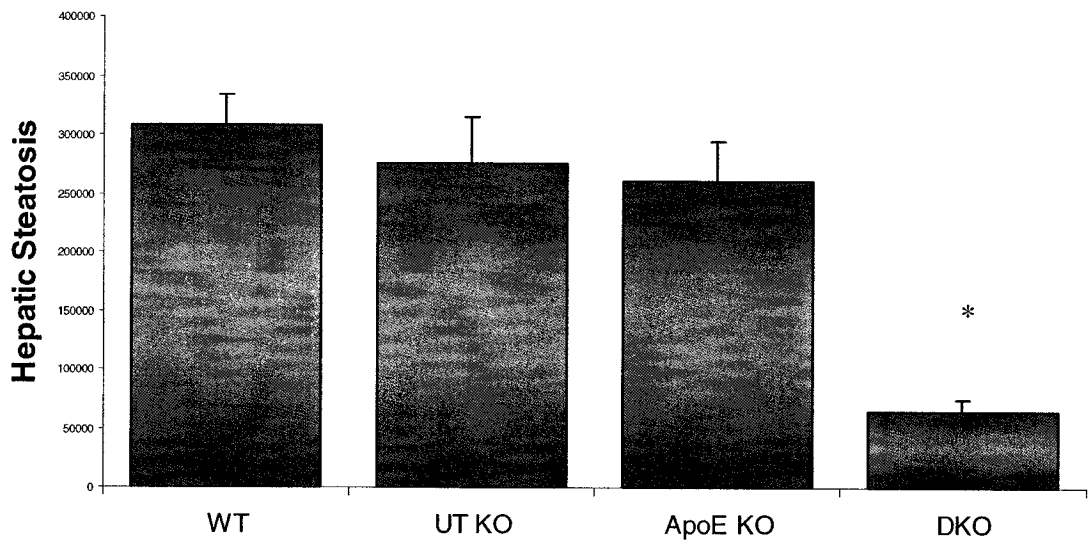
Hepatic Steatosis
400000
350000
300000
250000
200000
150000
100000
50000
0
*
WT
UT KO
ApoE KO
DKO

Figure 8. mRNA analysis Graphs demonstrating mRNA levels (normalized to GAPDH) for (A), ABCA1; (B), SR-A1; (C), SR-B1; (D),LXR-α; (E), PPAR-δ; and (F), PPAR-γ. (* indicates $P<0.05$ vs. WT and UTKO, # indicates $P<0.05$ vs. ApoE KO).

Figure 8

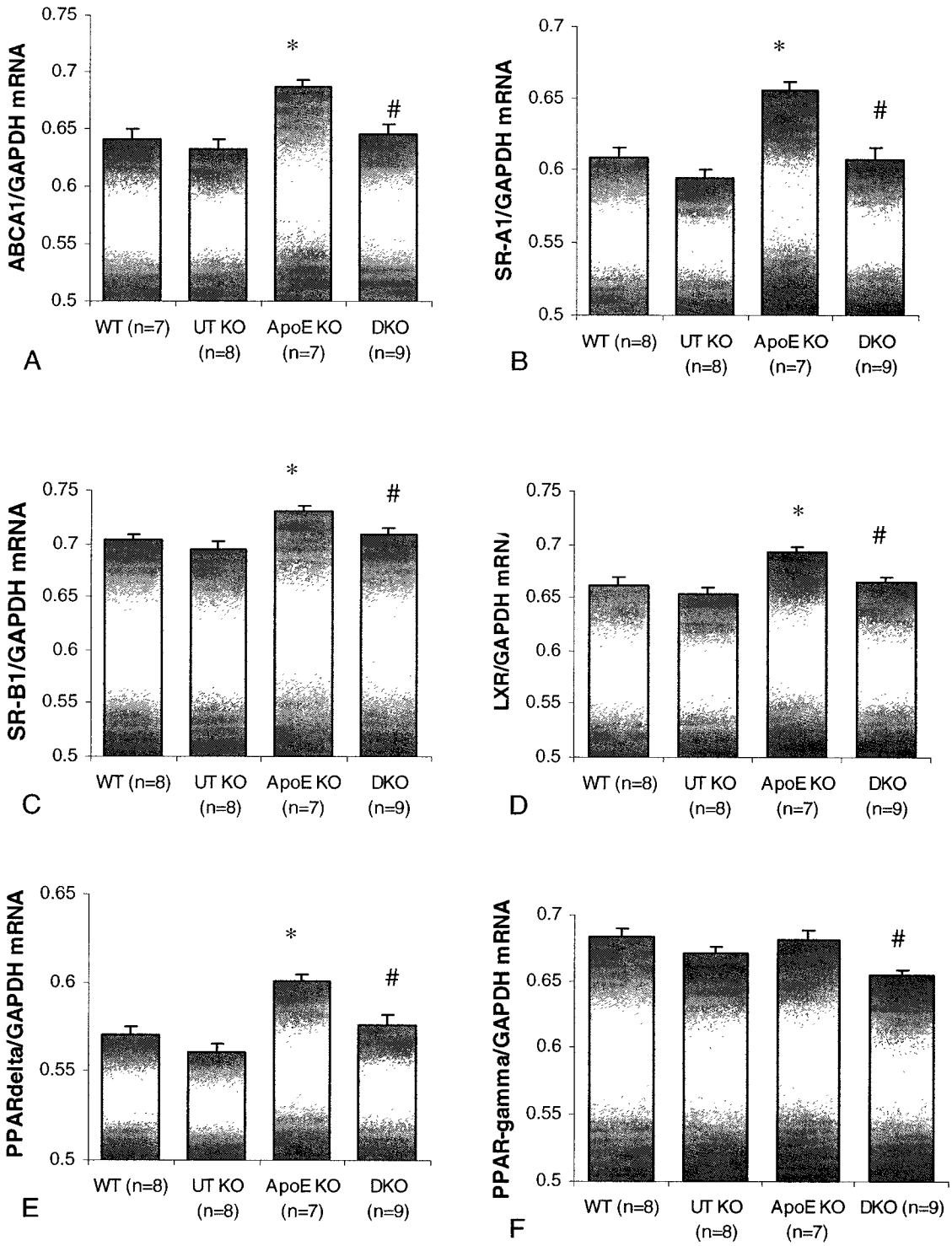
ABCA1/GAPDH mRNA
0.75
0.7
0.65
0.6
0.55
0.5
*
#
WT (n=7)
UT KO (n=8)
ApoE KO (n=7)
DKO (n=9)
A
SR-A1/GAPDH mRNA
0.7
0.65
0.6
0.55
0.5
*
#
WT (n=8)
UT KO (n=8)
ApoE KO (n=7)
DKO (n=9)
B
SR-B1/GAPDH mRNA
0.75
0.7
0.65
0.6
0.55
0.5
*
#
WT (n=8)
UT KO (n=8)
ApoE KO (n=7)
DKO (n=9)
C
LXR/GAPDH mRN
0.75
0.7
0.65
0.6
0.55
0.5
*
#
WT (n=8)
UT KO (n=8)
ApoE KO (n=7)
DKO (n=9)
D
PPARdelta/GAPDH mRNA
0.65
0.6
0.55
0.5
*
#
WT (n=8)
UT KO (n=8)
ApoE KO (n=7)
DKO (n=9)
E
PPAR-gamma/GAPDH mRNA
0.7
0.65
0.6
0.55
0.5
#
WT (n=8)
UT KO (n=8)
ApoE KO (n=7)
DKO (n=9)
F

Figure 9. LXR-α Western blotting. Representative Western blot for LXR-α and Histone H1 for mice groups. Graph demonstrating quantification of LXR-α blots normalized to nuclear housekeeping gene Histone H1. (* indicates $P<0.05$ vs. WT and UTKO, # indicates $P<0.05$ vs. ApoE KO)

Figure 9.

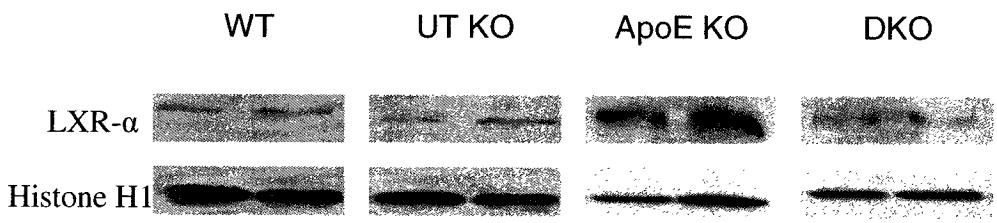
WT
UT KO
ApoE KO
DKO
LXR-α
Histone H1

A

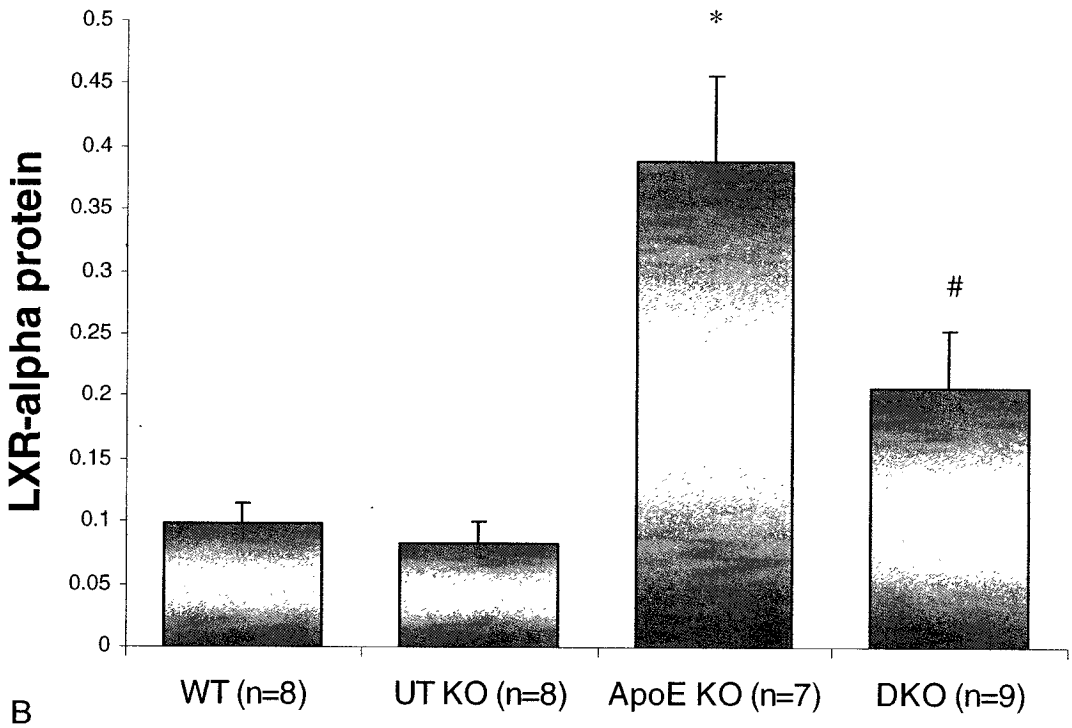
LXR-alpha protein
0.5
0.45
0.4
0.35
0.3
0.25
0.2
0.15
0.1
0.05
0
*
#
WT (n=8)
UT KO (n=8)
ApoE KO (n=7)
DKO (n=9)

B

Table 1; Genotyping and liver mRNA anlysis primers.

Gene	Primer Sequence
ApoE-F (WT)	GCCTAGCCGAGGGAGAGCCG
ApoE-R (WT)	TGTGACTTGGGAGCTCTGCAGC
ApoE-F (KO)	TTGGTGACCGCATCCGAGG
ApoE-R (KO)	GCCTCGTCCTGCAGTTCATTCA
NEO-F	CCATTCGACCACCAAGCGAAACA
NEO-R	CCATGATATTCGGCAAGCAGGCA
UT-F	CTCTTCTGGGCATGCTTTCTGC
UT-R	GATGCAGCTGTTGCCGTAAGTG
LDLR-F	AAT GAG GAG CAG CCA CAT GGT A
LDLR-R	TGT TGA TGT TCT TCA GCC GCC A
LRP-F	AGG AGC AGG TTG TTA GTC AGC A
LRP-R	ACT CGC CGC TTA TAC CAG AAC A
ABC-A1-F	TGA AGC CTG TCC AGG AGT TC
ABC-A1-R	ATG ACA AGG AGG ATG GAA GC
SR-A1-F	AAG AAC AAG CGC ACG TGG AA
SR-A1-R	ACC AGT TTG TCC AGT AAG C
SR-B1-F	TGC AGC TGA GCC TCT ACA TCA A
SR-B1-R	AAC CAC AGC AAC GGC AGA ACT A
LXR-F	TGA CTT TGC CAA ACA GCT C
LXR-R	AGC ATG ACT CGA TTG CAG AG
PPAR-α-F	AAT TTG CTG TGG AGA TCG G
PPAR-α-R	AGG TGT CAT CTG GAT GGT TGC
PPAR-δ-F	AGC CCA AGT TCG AGT TTG CTG
PPAR-δ-R	ACA GAA TGA TGG CCG CGA TGA A
PPAR-γ-F	AGG ACA TCC AAG ACA ACC TGC
PPAR-γ-R	TCT GCC TGA GGT CTG TCA TC
GAPDH-F	AAG AAG GTG GTG AAG CAG GCA
GAPDH-R	AGT TGC TGT TGA AGT CGC AGG A

Table 2, Body and Organ weights.

	WT	UT KO	ApoE KO	DKO
BW Gain (g)	24.2 ± 0.46	**20.9 ± 0.56 ***	22.8 ± 0.58	**18.9 ± 1.05 * #**
HW (g)	0.138± .002	0.135± .0025	0.146 ± .0045	**0.180± .0045* #**
RLW (g)	0.112 ± .0017	0.105 ± .0017	0.117 ± .0043	0.125 ± .0033 *
LLW (g)	0.052 ± .0008	0.050 ± .0009	0.056 ± .002	0.060 ± .002*
LW (g)	4.10± .106	**3.38 ± .162***	3.51 ± .231	**2.63 ± .192* #**
RKW (g)	0.174 ± .002	0.171 ± .003	0.187 ± .0058	**0.201 ± .0057 * #**
LKW (g)	0.168± .0025	0.166 ± .003	0.178± .0038	**0.202± .0021* #**
SW (g)	0.128 ± .0039	0.122 ± .0043	0.151 ± .0036	**0.189 ± .0128* #**

Table: Liver mRNA analysis

Genes	WT (n=8)	UT KO (n=8)	ApoE KO (n=7)	DKO (n=9)
LDLR	0.66 ± 0.007	0.65 ± 0.008	0.67 ± 0.007	0.65 ± 0.009
LRP	0.76 ± 0.005	0.77 ± 0.006	0.81 ± 0.003 *	0.80 ± 0.006 *
ABC-A1	0.64 ± 0.008	0.63 ± 0.009	0.69 ± 0.005 *	0.64 ± 0.009 #
SR-A1	0.61 ± 0.007	0.59 ± 0.007	0.66 ± 0.006 *	0.61 ± 0.008 #
SR-B1	0.70 ± 0.005	0.69 ± 0.007	0.73 ± 0.004 *	0.70 ± 0.006 #
LXR	0.66 ± 0.008	0.65 ± 0.006	0.69 ± 0.004 *	0.66 ± 0.005 #
PPAR-α	0.80 ± 0.006	0.79 0.005	0.82 ± 0.004	0.80 ± 0.005
PPAR-δ	0.57 ± 0.004	0.56 ± 0.005	0.60 ± 0.003 *	0.58 ± 0.005 #
PPAR-γ	0.68 ± 0.006	0.67 ± 0.005	0.68 ± 0.008	0.65 ± 0.004 #

(mRNA levels are normalized to GAPDH mRNA. LXR: Liver X Receptor; PPAR: Peroxisome Proliferator Activated Receptor; LDLR: Low Density Lipoprotein Receptor; LRP: Low Density Lipoprotein Receptor Related Peptide; ABC: ATP Binding Cassette transporter; SR: Scavenger Receptor. * indicates $P<0.05$ vs. WT & UT KO, # indicates $P< 0.05$ vs. ApoE KO)

5.0 General Discussion

The latter studies provide strong evidence of a pathophysiological role for urotensin-II in cardiovascular disease. Indeed, we showed that blockade of UII signaling with a selective UII receptor antagonist significantly attenuated mortality, cardiac dysfunction and hypertrophy in a well established model of CHF. Furthermore, treatment with the UII receptor antagonist was associated with a significant reduction in cardiac fibrosis. We proceeded to investigate the role of UII in atherosclerosis, the main underlying cause of ischemic cardiomyopathy. We showed that UII and UT expression was significantly elevated in human atherosclerosis of the carotid arteries and aortae. Following this we evaluated the effect of UT deficiency in a mouse model of atherosclerosis. We showed that UT gene deletion in an ApoE deficient genetic background exacerbated atherosclerosis of the mouse aorta. This was associated with significant increases in serum lipids as well as heart, kidney, and spleen hypertrophy, in addition to a significant reduction in body mass, liver mass, and hepatic steatosis.

The prominent effect of UII blockade on animals with CHF suggests it could be an important pharmacological target. Indeed, CHF amelioration with SB-611812 was comparable with previous studies using either endothelin receptor antagonists or angiotensin-converting enzyme inhibitors. Nguyen et al. 1998; Mulder et al. 1997; Pfeffer et al. 1991; Jain et al. 1994; Lapointe et al. 2002

In addition to a substantial attenuation of cardiac dysfunction, UII blockade also attenuated cardiac hypertrophy, an important characteristic of

CHF. Indeed we showed that UII receptor antagonism significantly reduced cardiomyocyte size and LV chamber dilatation. This finding is supported by other studies demonstrating hypertrophic effects of UII on cardiomyocytes in culture. Tzanidis et al., 2003 & Johns et al., 2004

The most significant improvements in cardiac dysfunction noted with the use of the UII receptor blocker were in diastolic parameters, specifically a reduction in LVEDP, RVSP, CVP and lung edema. It is increasingly being appreciated that diastolic dysfunction is associated not only with an increase in matrix deposition, most prominently collagen, but also on the type of collagens being produced. Several studies demonstrate that collagen type I is the major collagen type in cardiac fibrosis, as such there is an increase in the collagen type I to III ratio in disease. Marijianowski et al. 1995; Huang et al. 2004; Wei et al. 2004

Therefore, it is noteworthy that our findings show that, not only is fibrosis and collagen deposition attenuated with the use of the UII receptor antagonist, but the collagen type I to type III ratio was also decreased with treatment. This is supported by an interesting study by Kompa et al. [2004] who demonstrate that chronic infusion of UII in the rat led to a significant increase in LVEDP and in collagen type I to type III ratio. Our findings are further supported by the demonstration of UII induced expression of collagen type I, collagen type III, and fibronectin mRNA in cardiac fibroblasts. Tzanidis et al. 2003

Here we present strong evidence of UII's role in cardiac pathophysiology in CHF following coronary artery ligation. UII is thus poised

to be an important pharmacological target for the attenuation not only of cardiac dysfunction following an ischemic injury but also for the reduction in cardiac hypertrophy and fibrosis.

The leading cause of ischemic cardiomyopathy is atherosclerosis. As such we aimed to determine if UII expression is altered in human atherosclerosis and whether UII signaling plays a pathophysiological role in this disease. Indeed, we were the first to show that UII was increased in human atherosclerosis. Since then, several studies have been published supporting the evidence that UII is elevated in atherosclerosis. Specifically, several groups, including our own, have shown increased expression of UII in diseased coronary arteries, [Hassan et al. 2005; Maguire et al. 2004] and in plasma of patients with coronary artery disease. [Herringlake et al. 2004] UT is also elevated in aortae of hyperlipidemic mice. [Wang et al. 2005] Furthermore, UII has been shown to induce the activity and expression of acyl-CoA Cholesterol acyltransferase, an enzyme believed to play an important role in the accumulation of cholesterol in atherosclerotic plaques. [Watanabe et al. 2005]

The latter finding of elevated UII expression in human atherosclerosis led us to hypothesize that elevation of UII may promote this disease. Therefore, we aimed at determining the role UII plays in atherosclerosis by evaluating the effect of UT gene deletion in a mouse model of atherosclerosis. Surprisingly, we found that UT gene deletion led to an increase in atherosclerotic burden in ApoE deficient mice. Noteworthy, is the fact that this increase in disease was only noted in double knockout (DKO) mice, but

not in mice with UT KO alone. The increased atherosclerosis in these DKO mice was especially dramatic in two animals which developed aortic aneurysms.

In addition to the increase in atherosclerosis in mice deficient in both UT and ApoE we found that the livers in these animals had significantly reduced mass. This prompted the histological evaluation of these livers. Interestingly, we found that hepatic steatosis, a characteristic feature of mice fed a high fat diet, was significantly reduced in DKO mice. In addition, we also found that serum total cholesterol and serum triglycerides were significantly elevated in DKO mice. Analysis of lipid uptake receptor expression demonstrated that mRNA levels for scavenger receptor A1, and B1 were significantly reduced in DKO mice livers. Furthermore, we found that expression of liver transcriptional regulators, including LXR-α, PPAR-δ, and PPAR-γ, were also significantly attenuated in DKO mice. Therefore we propose that the mechanism of increased atherosclerosis in DKO mice is a result of attenuated lipid uptake and metabolism in the liver due to reduced lipid uptake receptor expression. This in turn led to increased plasma lipids, which in turn aggravated atherosclerosis.

Even in light of this data, it is still unknown whether or not UII signaling is vasculoprotective. This is because we cannot discern whether the altered disease levels in DKO mice were due to the lack of "protective" UII signaling or whether it was due to the elevated plasma lipids. However, one must consider that if in fact UII is vasculo-protective, why then, was there no

disease aggravation in the UT single KO mice. We, and others, have shown that UII and UT is elevated in atherosclerosis, however, whether this increased expression has a counter-regulatory role such as BNP in heart failure, or whether it is truly a modulator of atherosclerotic disease will need to be elucidated in future studies.

Noeworthy , is a study by Weisberg et al.[2005] who demonstrated attenuated hepatic steatosis and adiposity in a mouse model lacking the CCR2 gene. This is especially interesting in light of the fact that DKO mice also had significantly reduced body mass. Furthermore, CCR2 deficiency also led to significantly elevated plasma triglycerides, which was similarly noted in our DKO mice. However, atherosclerosis was not evaluated in the study by Weisberg et al. Nonetheless, deficiency of CCR2, a chemokine receptor produced some similar results as those found in our study and therefore investigation into functional similarities between these receptors may be warranted.

Of note is the fact that both body mass and liver masses were significantly decreased in mice with UT KO alone, yet there was no increase in atherosclerosis or organ hypertrophy. This suggests that the resultant increase in atherosclerosis and organ hypertrophy in DKO is due to the exaggerated hyperlipidemia. Indeed previous studies have demonstrated organ hypertrophy due to hyperlipidemia. Yang et al., 1999; Wang et al. 2005; Wellman et al., 1971; Kasiske et al., 1990

Here we provide initial evidence of altered lipid storage in the liver, thus making the liver an important research target for this mouse model. Alternatively, one must bear in mind that this may also be only a species specific development and may not be reproduced in humans. The ApoE KO mouse is merely a model of human atherosclerosis and not an exact replica of the disease. Indeed, mice do not normally express cholesterol ester transfer protein, a plasma glycoprotein believed to be integral to plasma lipid metabolism in humans. Therefore, deletion of the UT gene in mice may have unforeseen ramifications in the mouse model that are not duplicated in humans due to genomic differences.

To summarize, we have demonstrated that UII is elevated in human atherosclerosis, however we failed to show that deletion of the UT receptor is athero-protective. Although a mechanism was put forth regarding the cause of increased disease in DKO mice, it does not completely exclude the possibility that UII signaling is athero-protective. In contrast, we do conclusively demonstrate that UII antagonism is cardio-protective in a rat model of CHF.

Future studies should investigate which specific signaling pathways are activated in the heart by UII and how these converge to produce the pathophysiological sequelae associated with congestive heart failure including cardiac hypertrophy and fibrosis. Further studies with specific antagonists are also essential for the validation of UII as a pharmacological target. Furthermore, studies are needed to delineate the true vascular effect

of UII in atherosclerosis. Firstly the evaluation of lipid uptake in the periphery needs to be evaluated. Also it will be interesting to evaluate whether the UT upregulation in a transgenic model would demonstrate the reverse effect, i.e. decreased atherosclerosis. Future studies in this field are warranted.

In conclusion, we were the first to demonstrate a pathophysiological role for UII in cardiovascular diseases which may lead to a breakthrough in the management of CHF and may also give more insight into the pathogenesis of atherosclerosis.

6.0 Contribution of authors

Chapter 2:

The candidate carried out all of the research except for the animal surgery, drug administration, and hemodynamic analysis. The latter was carried out by Hu Fu.

Chapter 3:

The candidate performed the immunohistochemistry, writing of the text and RT-PCR data analysis. The cell culture and RT-PCR work was carried out by Dr. Lisa Patel.

Chapter 4:

The candidate carried out all research except for the tissue harvesting which was carried out by Wisam Al-Ramli and Hu Fu.

7.0 References

Abdelrahman AM, Pang CC. Involvement of the nitric oxide/L-arginine and sympathetic nervous systems on the vasodepressor action of human urotensin II in anesthetized rats. Life Sci. 2002 Jul 5;71(7):819-25.

Affolter JT, Newby DE, Wilkinson IB, Winter MJ, Balment RJ, Webb DJ. No effect on central or peripheral blood pressure of systemic urotensin II infusion in humans. Br J Clin Pharmacol. 2002 Dec;54(6):617-21.

Ames RS, Sarau HM, Chambers JK, Willette RN, Aiyar NV, Romanic AM, Louden CS, Foley JJ, Sauermelch CF, Coatney RW, Ao Z, Disa J, Holmes SD, Stadel JM, Martin JD, Liu WS, Glover GI, Wilson S, McNulty DE, Ellis CE, Elshourbagy NA, Shabon U, Trill JJ, Hay DW, Ohlstein EH, Bergsma DJ, Douglas SA. Human urotensin-II is a potent vasoconstrictor and agonist for the orphan receptor GPR14. Nature. 1999 Sep 16;401(6750):282-6. Erratum in: Nature 1999 Dec 23-30;402(6764):898.

Balat A, Pakir IH, Gok F, Anarat R, Sahinoz S. Urotensin-II levels in children with minimal change nephrotic syndrome. Pediatr Nephrol. 2005 Jan;20(1):42-5. Epub 2004 Nov 25.

Balat O, Aksoy F, Kutlar I, Ugur MG, Iyikosker H, Balat A, Anarat R. Increased plasma levels of Urotensin-II in preeclampsia-eclampsia: a new mediator in pathogenesis? Eur J Obstet Gynecol Reprod Biol 2005;120:33-8.

Baron MG. Postinfarction aneurysm of the left ventricle. Circulation. 1971 May;43(5):762-9.

Behm DJ, Herold CL, Ohlstein EH, Knight SD, Dhanak D, Douglas SA. Pharmacological characterization of SB-710411 (Cpa-c[D-Cys-Pal-D-Trp-Lys-Val-Cys]-Cpa-amide), a novel peptidic urotensin-II receptor antagonist. Br J Pharmacol. 2002 Oct;137(4):449-58.

Behm DJ, Harrison SM, Ao Z, Maniscalco K, Pickering SJ, Grau EV, Woods TN, Coatney RW, Doe CP, Willette RN, Johns DG, Douglas SA. Deletion of the UT receptor gene results in the selective loss of urotensin-II contractile activity in aortae isolated from UT receptor knockout mice. Br J Pharmacol 2003;139:464-72.

Behm DJ, Doe CP, Johns DG, Maniscalco K, Stankus GP, Wibberley A, Willette RN, Douglas SA. Urotensin-II: a novel systemic hypertensive factor in the cat. Naunyn Schmiedebergs Arch Pharmacol. 2004;369:274-80.

Behm DJ, Herold CL, Camarda V, Aiyar NV, Douglas SA. Differential agonistic and antagonistic effects of the urotensin-II ligand SB-710411 at

rodent and primate UT receptors. Eur J Pharmacol. 2004 May 25;492(2-3):113-6.

Beltrami AP, Urbanek K, Kajstura J, Yan SM, Finato N, Bussani R, Nadal-Ginard B, Silvestri F, Leri A, Beltrami CA, Anversa P. Evidence that human cardiac myocytes divide after myocardial infarction. N Engl J Med. 2001 Jun 7;344(23):1750-7.

Bernard MY Cheung, Raymond YH Leung, Yu Bun Man, Louisa YF Wong, Chu Pak Lau. Association of blood pressure and obesity with a single nucleotide polymorphism at 17P12. American Journal of Hypertension, Volume 18, Supplement 1, 2005, Page A79

Birker-Robaczewska M, Boukhadra C, Studer R, Mueller C, Binkert C, Nayler O. The expression of urotensin II receptor (U2R) is up-regulated by interferon-gamma. J Recept Signal Transduct Res 2003; 23: 289-305.

Bishop JE, Greenbaum R, Gibson DG, Yacoub M, Laurent GJ. Enhanced deposition of predominantly type I collagen in myocardial disease. J Mol Cell Cardiol. 1990 Oct;22(10):1157-65.

Bogoyevitch MA, Glennon PE, Andersson MB, et al. Endothelin-1 and fibroblast growth factors stimulate the mitogen-activated protein kinase signaling cascade in cardiac myocytes. The potential role of the cascade in the integration of two signaling pathways leading to myocyte hypertrophy. J Biol Chem. 1994;269(2):1110-9.

Bohm F, Pernow J. Urotensin II evokes potent vasoconstriction in humans in vivo. Br J Pharmacol. 2002 Jan;135(1):25-7.

Bottrill FE, Douglas SA, Hiley CR, White R. Human urotensin-II is an endothelium-dependent vasodilator in rat small arteries. Br J Pharmacol. 2000;130:1865-70.

Boucard AA, Sauve SS, Guillemette G, Escher E, Leduc R. Photolabelling the rat urotensin II/GPR14 receptor identifies a ligand-binding site in the fourth transmembrane domain. Biochem J. 2003 Mar 15;370(Pt 3):829-38.

Bousette N, Patel L, Douglas SA, Ohlstein EH, Giaid A. Increased expression of urotensin II and its cognate receptor GPR14 in atherosclerotic lesions of the human aorta. Atherosclerosis. 2004;176:117-23.

Bousette N, Hu F, Ohlstein EH, Dhanak D, Douglas SA, Giaid A. Urotensin-II blockade with SB-611812 attenuates cardiac dysfunction in a rat model of coronary artery ligation. J Mol Cell Cardiol. 2006;41:285-95.

Bousette N, Pottinger J, Ramli W, Ohlstein EH, Dhanak D, Douglas SA, Giaid A. Urotensin-II receptor blockade with SB-611812 attenuates cardiac remodeling in experimental ischemic heart disease. Peptides. 2006; [Epub ahead of print]

Braun A, Trigatti BL, Post MJ, Sato K, Simons M, Edelberg JM, Rosenberg RD, Schrenzel M, Krieger M. Loss of SR-BI expression leads to the early onset of occlusive atherosclerotic coronary artery disease, spontaneous myocardial infarctions, severe cardiac dysfunction, and premature death in apolipoprotein E-deficient mice. Circ Res 2002; 90:270-6.

Camarda V, Rizzi A, Calo G, Gendron G, Perron SI, Kostenis E, Zamboni P, Mascoli F, Regoli D. Effects of human urotensin II in isolated vessels of various species; comparison with other vasoactive agents. Naunyn Schmiedebergs Arch Pharmacol. 2002;365:141-9.

Camarda V, Guerrini R, Kostenis E, Rizzi A, Calo G, Hattenberger A, Zucchini M, Salvadori S, Regoli D. A new ligand for the urotensin II receptor. Br J Pharmacol. 2002 Oct;137(3):311-4.

Camarda V, Song W, Marzola E, Spagnol M, Guerrini R, Salvadori S, Regoli D, Thompson JP, Rowbotham DJ, Behm DJ, Douglas SA, Calo' G, Lambert DG. Urantide mimics urotensin-II induced calcium release in cells expressing recombinant UT receptors. Eur J Pharmacol 2004;498:83-6.

Camejo G, Fager G, Rosengren B, Hurt-Camejo E, Bondjers G. Binding of low density lipoproteins by proteoglycans synthesized by proliferating and quiescent human arterial smooth muscle cells. J Biol Chem. 1993 Jul 5;268(19):14131-7.

Camejo G, Olsson U, Hurt-Camejo E, Baharamian N, Bondjers G. The extracellular matrix on atherogenesis and diabetes-associated vascular disease. Atheroscler Suppl. 2002 May;3(1):3-9. Review.

Chana RS, Wheeler DC, Thomas GJ, Williams JD, Davies M. Low-density lipoprotein stimulates mesangial cell proteoglycan and hyaluronan synthesis. Nephrol Dial Transplant 2000;15:167-72.

Charles CJ, Rademaker MT, Richards AM, Yandle TG. Urotensin II: evidence for cardiac, hepatic and renal production. Peptides. 2005 Nov;26(11):2211-4. Epub 2005 Apr 19.

Chartrel N, Leprince J, Dujardin C, Chatenet D, Tollemer H, Baroncini M, Balment RJ, Beauvillain JC, Vaudry H. Biochemical characterization and immunohistochemical localization of urotensin II in the human brainstem and spinal cord. J Neurochem. 2004 Oct;91(1):110-8.

Chen YL, Chang YJ, Jiang MJ. Monocyte chemotactic protein-1 gene and protein expression in atherogenesis of hypercholesterolemic rabbits. Atherosclerosis. 1999 Mar;143(1):115-23.

Chen YH, Zhao MW, Yao WZ, Pang YZ, Tang CS. The signal transduction pathway in the proliferation of airway smooth muscle cells induced by urotensin II. Chin Med J (Engl). 2004 Jan;117(1):37-41.

Cheung BM, Leung R, Man YB, Wong LY. Plasma concentration of urotensin II is raised in hypertension. J Hypertens. 2004;22:1341-4.

Cittadini A, Casaburi C, Monti MG, Di Gianni A, Serpico R, Scherillo G, Saldamarco L, Vanasia M, Sacca L. Effects of canrenone on myocardial reactive fibrosis in a rat model of postinfarction heart failure. Cardiovasc Drugs Ther. 2002 May;16(3):195-201.

Cleutjens JP, Verluyten MJ, Smiths JF, Daemen MJ. Collagen remodeling after myocardial infarction in the rat heart. Am J Pathol. 1995 Aug;147(2):325-38.

Clozel M, Binkert C, Birker-Robaczewska M, Boukhadra C, Ding SS, Fischli W, Hess P, Mathys B, Morrison K, Muller C, Muller C, Nayler O, Qiu C, Rey M, Scherz MW, Velker J, Weller T, Xi JF, Ziltener P. Pharmacology of the urotensin-II receptor antagonist palosuran (ACT-058362; 1-[2-(4-benzyl-4-hydroxy-piperidin-1-yl)-ethyl]-3-(2-methyl-quinolin-4-yl)-urea sulfate salt): first demonstration of a pathophysiological role of the urotensin System. J Pharmacol Exp Ther. 2004 Oct;311(1):204-12. Epub 2004 May 14.

Clozel M, Hess P, Qiu C, Ding SS, Rey M. The Urotensin-II Receptor Antagonist Palosuran Improves Pancreatic and Renal Function in Diabetic Rats. J Pharmacol Exp Ther. 2006 Mar;316(3):1115-21. Epub 2005 Nov 2.

Conlon JM, O'Harte F, Smith DD, Tonon MC, Vaudry H. Isolation and primary structure of urotensin II from the brain of a tetrapod, the frog Rana ridibunda. Biochem Biophys Res Commun. 1992 Oct 30;188(2):578-83.

Coulouarn Y, Jegou S, Tostivint H, Vaudry H, Lihrmann I. Cloning, sequence analysis and tissue distribution of the mouse and rat urotensin II precursors. FEBS Lett. 1999 Aug 20;457(1):28-32.

Coulouarn Y, Lihrmann I, Jegou S, Anouar Y, Tostivint H, Beauvillain JC, Conlon JM, Bern HA, Vaudry H. Cloning of the cDNA encoding the urotensin II precursor in frog and human reveals intense expression of the urotensin II gene in motoneurons of the spinal cord. Proc Natl Acad Sci U S A. 1998 Dec 22;95(26):15803-8.

Cowley E, Thompson JP, Sharpe P, Waugh J, Ali N, Lambert DG. Effects of pre-eclampsia on maternal plasma, cerebrospinal fluid, and umbilical cord urotensin II concentrations: a pilot study. Br J Anaesth 2005;95:495-9.

Daugherty A, Rateri DL. T lymphocytes in atherosclerosis: the yin-yang of Th1 and th2 influence on lesion formation. Circ Res. 2002;90(10):1039-40.

de Winther MP, Gijbels MJ, van Dijk KW, van Gorp PJ, suzuki H, Kodama T, Frants RR, Havekes LM, Hofker MH. Scavenger receptor deficiency leads to more complex atherosclerotic lesions in APOE3Leiden transgenic mice. Atherosclerosis 1999; 144:315-21.

Dhanak, D., & Knight, S. D. (2001). Sulfonamide derivative urotensin-II receptor antagonists, preparation, pharmaceutical compositions, and therapeutic use. *PCT Int. Appl.* WO 2001045694.

Disa J, Floyd LE, Edwards RM, Douglas SA, Aiyar NV. Identification and characterization of binding sites for human urotensin-II in Sprague-Dawley rat renal medulla using quantitative receptor autoradiography. Peptides. 2005 Nov

Djordjevic T, BelAiba RS, Bonello S, Pfeilschifter J, Hess J, Gorlach A. Human urotensin II is a novel activator of NADPH oxidase in human pulmonary artery smooth muscle cells. Arterioscler Thromb Vasc Biol 2005;25:519-25.

Dobaczewski M, Bujak M, Zymek P, Ren G, Entman ML, Frangogiannis NG. Extracellular matrix remodeling in canine and mouse myocardial infarcts. Cell Tissue Res. 2006 Feb 22; [Epub ahead of print]

Douglas, S.A. and Ohlstein, E.H. (2000) Urotensin receptors. In The IUPHAR Compendium of Receptor Characterization and Classification (Girdlestone, D., ed.), pp. 365–372, IUPHAR Media, London

Douglas SA, Tayara L, Ohlstein EH, Halawa N, Giaid A. Congestive heart failure and expression of myocardial urotensin II. Lancet. 2002 Jun 8;359(9322):1990-7.

Douglas SA, Naselsky D, Ao Z, Disa J, Herold CL, Lynch F, Aiyar NV. Identification and pharmacological characterization of native, functional human urotensin-II receptors in rhabdomyosarcoma cell lines Br J Pharmacol. 2004; 142: 921-32.

Douglas SA, Dhanak D, Johns DG. From 'gills to pills': urotensin-II as a regulator of mammalian cardiorenal function. Trends Pharmacol Sci. 2004 Feb;25(2):76-85. Review.

Douglas SA, Behm DJ, Aiyar NV, Naselsky D, Disa J, Brooks DP, Ohlstein EH, Gleason JG, Sarau HM, Foley JJ, Buckley PT, Schmidt DB, Wixted WE, Widdowson K, Riley G, Jin J, Gallagher TF, Schmidt SJ, Ridgers L, Christmann LT, Keenan RM, Knight SD, Dhanak D. Nonpeptidic urotensin-II receptor antagonists I: in vitro pharmacological characterization of SB-706375. Br J Pharmacol. 2005;145:620-35.

Dschietzig T, Bartsch C, Pregla R, Zurbrugg HR, Armbruster FP, Richter C, Laule M, Romeyke E, Neubert C, Voelter W, Baumann G, Stangl K. Plasma levels and cardiovascular gene expression of urotensin-II in human heart failure. Regul Pept. 2002 Dec 31;110(1):33-8.

Elshourbagy NA, Douglas SA, Shabon U, Harrison S, Duddy G, Sechler JL, Ao Z, Maleeff BE, Naselsky D, Disa J, Aiyar NV. Molecular and pharmacological characterization of genes encoding urotensin-II peptides and their cognate G-protein-coupled receptors from the mouse and monkey. Br J Pharmacol. 2002 May;136(1):9-22.

Eto M, Barandier C, Rathgeb L, Kozai T, Joch H, Yang Z, Luscher TF. Thrombin suppresses endothelial nitric oxide synthase and upregulates endothelin-converting enzyme-1 expression by distinct pathways: role of Rho/ROCK and mitogen-activated protein kinase. Circ Res. 2001;89(7):583-90.

Filipeanu CM, Brailoiu E, Le Dun S, Dun NJ. Urotensin-II regulates intracellular calcium in dissociated rat spinal cord neurons. J Neurochem 2002;83:879-84.

Flohr S, Kurz M, Kostenis E, Brkovich A, Fournier A, Klabunde T. Identification of nonpeptidic urotensin II receptor antagonists by virtual screening based on a pharmacophore model derived from structure-activity relationships and nuclear magnetic resonance studies on urotensin II. J Med Chem. 2002 Apr 25;45(9):1799-805.

Frimm Cde C, Sun Y, Weber KT. Wound healing following myocardial infarction in the rat: role for bradykinin and prostaglandins. J Mol Cell Cardiol. 1996 Jun;28(6):1279-85.

Gardiner SM, March JE, Kemp PA, Davenport AP, Bennett T. Depressor and regionally-selective vasodilator effects of human and rat urotensin II in conscious rats. Br J Pharmacol. 2001;132:1625-9.

Gardiner SM, March JE, Kemp PA, Bennett T. Bolus injection of human UII in conscious rats evokes a biphasic haemodynamic response. Br J Pharmacol. 2004 Oct;143(3):422-30. Epub 2004 Aug 31.

Gartlon J, Parker F, Harrison DC, Douglas SA, Ashmeade TE, Riley GJ, Hughes ZA, Taylor SG, Munton RP, Hagan JJ, Hunter JA, Jones DN. Central effects of urotensin-II following ICV administration in rats. Psychopharmacology (Berl). 2001;155:426-33.

Gartlon JE, Ashmeade T, Duxon M, Hagan JJ, Jones DN. Urotensin-II, a neuropeptide ligand for GPR14, induces c-fos in the rat brain. Eur J Pharmacol 2004;493:95-8.

Gendron G, Simard B, Gobeil F Jr, Sirois P, D'Orleans-Juste P, Regoli D. Human urotensin-II enhances plasma extravasation in specific vascular districts in Wistar rats. Can J Physiol Pharmacol 2004;82:16-21.

Gendron G, Gobeil F Jr, Morin J, D'Orleans-Juste P, Regoli D. Contractile responses of aortae from WKY and SHR to vasoconstrictors. Clin Exp Hypertens 2004;26:511-23.

Gendron G, Gobeil F Jr, Belanger S, Gagnon S, Regoli D, D'Orleans-Juste P. Urotensin II-induced hypotensive responses in Wistar-Kyoto (Wky) and spontaneously hypertensive (Shr) rats. Peptides. 2005 Aug;26(8):1468-74.

Gibbs BF, Noll T, Falcone FH, Haas H, Vollmer E, Vollrath I, Wolff HH, Amon U. A three-step procedure for the purification of human basophils from buffy coat blood. Inflamm Res. 1997;46(4):137-42.

Gibson A, Wallace P, Bern HA. Cardiovascular effects of urotensin II in anesthetized and pithed rats. Gen Comp Endocrinol. 1986 Dec;64(3):435-9.

Gibson A. Complex effects of Gillichthys urotensin II on rat aortic strips. Br J Pharmacol. 1987 May;91(1):205-12.

Gibson A, Conyers S, Bern HA. The influence of urotensin II on calcium flux in rat aorta. J Pharm Pharmacol. 1988 Dec;40(12):893-5.

Giebing G, Tolle M, Jurgensen J, Eichhorst J, Furkert J, Beyermann M, Neuschafer-Rube F, Rosenthal W, Zidek W, van der Giet M, Oksche A. Arrestin-independent internalization and recycling of the urotensin receptor contribute to long-lasting urotensin II-mediated vasoconstriction. Circ Res. 2005;97:707-15.

Gong H, Wang YX, Zhu YZ, Wang WW, Wang MJ, Yao T, Zhu YC. Cellular distribution of GPR14 and the positive inotropic role of urotensin II in the myocardium in adult rat. J Appl Physiol. 2004;97:2228-35.

Gray GA, Jones MR, Sharif I. Human urotensin II increases coronary perfusion pressure in the isolated rat heart: potentiation by nitric oxide synthase and cyclooxygenase inhibition. Life Sci. 2001 Jun 1;69(2):175-80.

Graziani-Bowering GM, Filion LG. Down regulation of CD4 expression following isolation and culture of human monocytes.Clin Diagn Lab Immunol. 2000;7(2):182-91.

Grossman W, Jones D, McLaurin LP. Wall stress and patterns of hypertrophy in the human left ventricle. J Clin Invest. 1975 Jul;56(1):56-64.

Gruson D, Rousseau MF, Ahn SA, van Linden F, Ketelslegers JM. Circulating urotensin II levels in moderate to severe congestive heart failure: Its relations with myocardial function and well established neurohormonal markers. Peptides. 2005

Hassan GS, Chouiali F, Saito T, Hu F, Douglas SA, Ao Z, Willette RN, Ohlstein EH, Giaid A. Effect of human urotensin-II infusion on hemodynamics and cardiac function. Can J Physiol Pharmacol 2003;81:125-8.

Hassan GS, Douglas SA, Ohlstein EH, Giaid A. Expression of urotensin-II in human coronary atherosclerosis Peptides. 2005; 26: 2464-72.

He YH, Hong JM, Guo HS, Wei JR, Chen H, Zuo HH, Li ZL. Effects of urotensin II on cultured cardiac fibroblast proliferation and collagen type I mRNA expression. Di Yi Jun Yi Da Xue Xue Bao. 2004 May;24(5):505-8.

Heller J, Schepke M, Neef M, Woitas R, Rabe C, Sauerbruch T. Increased urotensin II plasma levels in patients with cirrhosis and portal hypertension. J Hepatol. 2002 Dec;37(6):767-72.

Heringlake M, Kox T, Uzun O, Will B, Bahlmann L, Klaus S, Eleftheriadis S, Armbruster FP, Franz N, Kraatz E. The relationship between urotensin II plasma immunoreactivity and left ventricular filling pressures in coronary artery disease. Regul Pept 2004;121:129-36.

Herold CL, Behm DJ, Buckley PT, Foley JJ, Wixted WE, Sarau HM, Douglas SA. The neuromedin B receptor antagonist, BIM-23127, is a potent antagonist at human and rat urotensin-II receptors. Br J Pharmacol. 2003;139:203-7.

Hillier C, Berry C, Petrie MC, O'Dwyer PJ, Hamilton C, Brown A, McMurray J.

Effects of urotensin II in human arteries and veins of varying caliber. Circulation. 2001;103:1378-81.

Hirsch AT, Dzau VJ, Creager MA. Baroreceptor function in congestive heart failure: effect on neurohumoral activation and regional vascular resistance. Circulation. 1987 May;75(5 Pt 2):IV36-48. Review.

Hood SG, Watson AM, May CN. Cardiac actions of central but not peripheral urotensin II are prevented by beta-adrenoceptor blockade. Peptides. 2005 Jul;26(7):1248-56.

Horie S, Tsurumaki Y, Someya A, Hirabayashi T, Saito T, Okuma Y, Nomura Y, Murayama T. Involvement of cyclooxygenase-dependent pathway in contraction of isolated ileum by urotensin II. Peptides. 2005 Feb;26(2):323-9.

Horie S, Yasuda S, Tsurumaki Y, Someya A, Saito T, Okuma Y, Nomura Y, Hirabayashi T, Murayama T. Contraction of isolated guinea-pig ileum by urotensin II via activation of ganglionic cholinergic neurons and acetylcholine release. Neuropharmacology. 2003 Dec;45(7):1019-27.

Hurt E, Bondjers G, Camejo G. Interaction of LDL with human arterial proteoglycans stimulates its uptake by human monocyte-derived macrophages. J Lipid Res. 1990 Mar;31(3):443-54.

Iankova I, Petersen RK, Annicotte JS, Chavey C, Hansen JB, Kratchmarova I, Sarruf D, Benkirane M, Kristiansen K, Fajas L. Peroxisome proliferator-activated receptor gamma recruits the positive transcription elongation factor b complex to activate transcription and promote adipogenesis. Mol Endocrinol 2006; 20:1494-505.

Ishibashi T, Nagata K, Ohkawara H, Sakamoto T, Yokoyama K, Shindo J, Sugimoto K, Sakurada S, Takuwa Y, Teramoto T, Maruyama Y. Inhibition of Rho/Rho-kinase signaling downregulates plasminogen activator inhibitor-1 synthesis in cultured human monocytes. Biochim Biophys Acta. 2002;1590(1-3):123-30.

Ishihata A, Sakai M, Katano Y. Vascular contractile effect of urotensin II in young and aged rats: influence of aging and contribution of endothelial nitric oxide. Peptides. 2006 Jan;27(1):80-6. Epub 2005 Sep 12.

Ishihata A, Ogaki T, Aita T, Katano Y. Role of prostaglandins in urotensin II-induced vasodilatation in the coronary arteries of aged rats. Eur J Pharmacol. 2005 Oct 31;523(1-3):119-26.

Itoh H, Itoh Y, Rivier J, Lederis K. Contraction of major artery segments of rat by fish neuropeptide urotensin II. Am J Physiol. 1987 Feb;252(2 Pt 2):R361-6.

Itoh H, McMaster D, Lederis K. Functional receptors for fish neuropeptide urotensin II in major rat arteries. Eur J Pharmacol. 1988 Apr 27;149(1-2):61-6.

Iwanaga Y, Kihara Y, Hasegawa K, Inagaki K, Yoneda T, Kaburagi S, Araki M, Sasayama S. Cardiac endothelin-1 plays a critical role in the functional deterioration of left ventricles during the transition from compensatory hypertrophy to congestive heart failure in salt-sensitive hypertensive rats. Circulation. 1998 Nov 10;98(19):2065-73.

Johns DG, Ao Z, Naselsky D, Herold CL, Maniscalco K, Sarov-Blat L, Steplewski K, Aiyar N, Douglas SA. Urotensin-II-mediated cardiomyocyte hypertrophy: effect of receptor antagonism and role of inflammatory mediators. Naunyn Schmiedebergs Arch Pharmacol. 2004;370:238-50.

Joyal D, Huynh T, Aiyar N, Guida B, Douglas S, Giaid A. Urotensin-II levels in acute coronary syndromes. Int J Cardiol. 2006 Mar 22;108(1):31-5.

Kasiske, BL, O'Donnell, MP & Schmitz, PG, et al: Renal injury of diet-induced hypercholesterolemia in rats. Kidney Int 1990 37:880–891

Katano Y, Ishihata A, Aita T, Ogaki T, Horie T. Vasodilator effect of urotensin II, one of the most potent vasoconstricting factors, on rat coronary arteries. Eur J Pharmacol. 2000 Aug 18;402(1-2):R5-7.

Kinney WA, Almond Jr HR, Qi J, Smith CE, Santulli RJ, de Garavilla L, Andrade-Gordon P, Cho DS, Everson AM, Feinstein MA, Leung PA, Maryanoff BE. Structure-function analysis of urotensin II and its use in the construction of a ligand-receptor working model. Angew Chem Int Ed Engl. 2002 Aug 16;41(16):2940-4.

Kompa AR, Thomas WG, See F, Tzanidis A, Hannan RD, Krum H. Cardiovascular role of urotensin II: effect of chronic infusion in the rat. Peptides. 2004; 25:1783-8.

Kruger S, Graf J, Kunz D, Stickel T, Merx MW, Hanrath P, Janssens U. Urotensin II in patients with chronic heart failure. Eur J Heart Fail. 2005 Jun;7(4):475-8.

Kuhlencordt PJ, Gyurko R, Han F, Scherrer-Crosbie M, Aretz TH, Hajjar R, Picard MH, Huang PL. Accelerated atherosclerosis, aortic aneurysm formation, and ischemic heart disease in apolipoprotein E/endothelial nitric

oxide synthase double-knockout mice. Circulation. 2001 Jul 24;104(4):448-54.

Langham RG, Kelly DJ, Gow RM, Zhang Y, Dowling JK, Thomson NM, Gilbert RE. Increased expression of urotensin II and urotensin II receptor in human diabetic nephropathy. Am J Kidney Dis. 2004 Nov;44(5):826-31.

Lapp H, Boerrigter G, Costello-Boerrigter LC, Jaekel K, Scheffold T, Krakau I, Schramm M, Guelker H, Stasch JP. Elevated plasma human urotensin-II-like immunoreactivity in ischemic cardiomyopathy. Int J Cardiol 2004;94:93-7.

Li L, Yuan WJ, Pan XJ, Wang WZ, Qiu JW, Tang CS. Effect of urotensin II on the nitric oxide production in neonatal rat cardiomyocytes Sheng Li Xue Bao. 2002 Aug 25;54(4):307-10.

Li L, Yuan WJ, Su DF. Effects of rat urotensin II on coronary flow and myocardial eNOS protein expression in isolated rat heart. Acta Pharmacol Sin. 2004 Nov;25(11):1444-9.

Li J, Wang J, Russell FD, Molenaar P. Activation of calcineurin in human failing heart ventricle by endothelin-1, angiotensin II and urotensin II. Br J Pharmacol. 2005;145:432-40.

Lim M, Honisett S, Sparkes CD, Komesaroff P, Kompa A, Krum H. Differential effect of urotensin II on vascular tone in normal subjects and patients with chronic heart failure. Circulation. 2004;109:1212-4.

Lin Y, Tsuchihashi T, Matsumura K, Abe I, Iida M. Central cardiovascular action of urotensin II in conscious rats. J Hypertens. 2003;21:59-65.

Lin Y, Tsuchihashi T, Matsumura K, Fukuhara M, Ohya Y, Fujii K, Iida M. Central cardiovascular action of urotensin II in spontaneously hypertensive rats.
Hypertens Res. 2003;26:839-45.

Lin L, Ding WH, Jiang W, Zhang YG, Qi YF, Yuan WJ, Tang CS. Urotensin-II activates L-arginine/nitric oxide pathway in isolated rat aortic adventitia. Peptides. 2004;25:1977-84.

Liu Q, Pong SS, Zeng Z, Zhang Q, Howard AD, Williams DL Jr, Davidoff M, Wang R, Austin CP, McDonald TP, Bai C, George SR, Evans JF, Caskey CT. Identification of urotensin II as the endogenous ligand for the orphan G-protein-coupled receptor GPR14. Biochem Biophys Res Commun. 1999;266:174-8.

Lu Y, Zou CJ, Huang DW, Tang CS. Cardiovascular effects of urotensin II in different brain areas. Peptides2002;23:1631-5.

Ludmer PL, Selwyn AP, Shook TL, Wayne RR, Mudge GH, Alexander RW, Ganz P. Paradoxical vasoconstriction induced by acetylcholine in atherosclerotic coronary arteries. N Engl J Med 1986;315:1046-51.

MacLean MR, Alexander D, Stirrat A, Gallagher M, Douglas SA, Ohlstein EH, Morecroft I, Polland K. Contractile responses to human urotensin-II in rat and human pulmonary arteries: effect of endothelial factors and chronic hypoxia in the rat. Br J Pharmacol. 2000 May;130(2):201-4.

Maguire JJ, Kuc RE, Davenport AP. Orphan-receptor ligand human urotensin II: receptor localization in human tissues and comparison of vasoconstrictor responses with endothelin-1. Br J Pharmacol. 2000 Oct;131(3):441-6.

Maguire JJ, Kuc RE, Wiley KE, Kleinz MJ, Davenport AP. Cellular distribution of immunoreactive urotensin-II in human tissues with evidence of increased expression in atherosclerosis and a greater constrictor response of small compared to large coronary arteries. Peptides. 2004 Oct;25(10):1767-74.

Marijianowski MM, Teeling P, Mann J, Becker AE. Dilated cardiomyopathy is associated with an increase in the type I/type III collagen ratio: a quantitative assessment. J Am Coll Cardiol 1995; 25: 1263–1272

Matsumoto Y, Abe M, Watanabe T, Adachi Y, Yano T, Takahashi H, Sugo T, Mori M, Kitada C, Kurokawa T, Fujino M. Intracerebroventricular administration of urotensin II promotes anxiogenic-like behaviors in rodents. Neurosci Lett. 2004;358:99-102.

Matsushita M, Shichiri M, Imai T, Iwashina M, Tanaka H, Takasu N, Hirata Y. Co-expression of urotensin II and its receptor (GPR14) in human cardiovascular and renal tissues. J Hypertens. 2001 Dec;19(12):2185-90.

Matsushita M, Shichiri M, Fukai N, Ozawa N, Yoshimoto T, Takasu N, Hirata Y. Urotensin II is an autocrine/paracrine growth factor for the porcine renal epithelial cell line, LLCPK1. Endocrinology. 2003;144:1825-31.

Matsusue K, Haluzik M, Lambert G, Yim SH, Gavrilova O, Ward JM, Brewer B Jr, Reitman ML, Gonzalez FJ. Liver-specific disruption of PPARgamma in leptin-deficient mice improves fatty liver but aggravates diabetic phenotypes. J Clin Invest 2003; 111:737-47

McMurray JJ, Ray SG, Abdullah I, Dargie HJ, Morton JJ. Plasma endothelin in chronic heart failure. Circulation. 1992 Apr;85(4):1374-9.

Mori M, Sugo T, Abe M, Shimomura Y, Kurihara M, Kitada C, Kikuchi K, Shintani Y, Kurokawa T, Onda H, Nishimura O, Fujino M. Urotensin II is the endogenous ligand of a G-protein-coupled orphan receptor, SENR (GPR14). Biochem Biophys Res Commun. 1999 Nov;265(1):123-9.

Mori M, Fujino M. Urotensin II-related peptide, the endogenous ligand for the urotensin II receptor in the rat brain. Peptides. 2004 Oct;25(10):1815-8. Review.

Mukherjee D, Sen S. Collagen phenotypes during development and regression of myocardial hypertrophy in spontaneously hypertensive rats. Circ Res. 1990 Dec;67(6):1474-80.

Napoli C, D'Armiento FP, Mancini FP, Postiglione A, Witztum JL, Palumbo G, Palinski W. Fatty streak formation occurs in human fetal aortas and is greatly enhanced by maternal hypercholesterolemia. Intimal accumulation of low density lipoprotein and its oxidation precede monocyte recruitment into early atherosclerotic lesions.J Clin Invest. 1997 Dec 1;100(11):2680-90.

Nishikawa N, Masuyama T, Yamamoto K, et al. Long-term administration of amlodipine prevents decompensation to diastolic heart failure in hypertensive rats. J Am Coll Cardiol 2001; 38: 1539-45.

Ng LL, Loke I, O'Brien RJ, Squire IB, Davies JE. Plasma urotensin in human systolic heart failure. Circulation. 2002 Dec 3;106(23):2877-80.

Nothacker HP, Wang Z, McNeill AM, Saito Y, Merten S, O'Dowd B, Duckles SP, Civelli O. Identification of the natural ligand of an orphan G-protein-coupled receptor involved in the regulation of vasoconstriction. Nat Cell Biol. 1999 Oct;1(6):383-5.

Ohsako S, Ishida I, Ichikawa T, Deguchi T. Cloning and sequence analysis of cDNAs encoding precursors of urotensin II-alpha and -gamma. J Neurosci. 1986 Sep;6(9):2730-5.

Onan D, Pipolo L, Yang E, Hannan RD, Thomas WG. Urotensin II promotes hypertrophy of cardiac myocytes via mitogen-activated protein kinases. Mol Endocrinol. 2004;18:2344-54.

Ovcharenko E, Abassi Z, Rubinstein I, Kaballa A, Hoffman A, Winaver J. Renal effects of human urotensin-II in rats with experimental congestive heart failure. Nephrol Dial Transplant 2006;21:1205-11.

Patacchini R, Santicioli P, Giuliani S, Grieco P, Novellino E, Rovero P, Maggi CA. Urantide: an ultrapotent urotensin II antagonist peptide in the rat aorta. Br J Pharmacol. 2003;140:1155-8.

Patel L, Charlton SJ, Chambers JK, Macphee CH. Expression and functional analysis of chemokine receptors in human peripheral blood leukocyte populations. Cytokine. 2001;14(1):27-36.

Paysant J, Rupin A, Simonet S, Fabiani JN, Verbeuren TJ. Comparison of the contractile responses of human coronary bypass grafts and monkey arteries to human urotensin-II. Fundam Clin Pharmacol. 2001;15:227-31.

Pearson D, Shively JE, Clark BR, Geschwind II, Barkley M, Nishioka RS, Bern HA. Urotensin II: a somatostatin-like peptide in the caudal neurosecretory system of fishes. Proc Natl Acad Sci U S A. 1980 Aug;77(8):5021-4.

Pinderski LJ, Fischbein MP, Subbanagounder G, Fishbein MC, Kubo N, Cheroutre H, Curtiss LK, Berliner JA, Boisvert WA. Overexpression of Interleukin-10 by Activated T Lymphocytes Inhibits Atherosclerosis in LDL Receptor-Deficient Mice by Altering Lymphocyte and Macrophage Phenotypes. Circ Res. 2002;90(10):1064-71.

Proulx CD, Simaan M, Escher E, Laporte SA, Guillemette G, Leduc R. Involvement of a cytoplasmic-tail serine cluster in urotensin II receptor internalization. Biochem J. 2005 Jan 1;385(Pt 1):115-23.
Qi J, Du J, Tang X, Li J, Wei B, Tang C. The upregulation of endothelial nitric oxide synthase and urotensin-II is associated with pulmonary hypertension and vascular diseases in rats produced by aortocaval shunting. Heart Vessels 2004;19:81-8.

Rakowski E, Hassan GS, Dhanak D, Ohlstein EH, Douglas SA, Giaid A. A role for urotensin II in restenosis following balloon angioplasty: use of a selective UT receptor blocker. J Mol Cell Cardiol. 2005; 39: 785-91.

Rdzanek A, Filipiak KJ, Karpinski G, Grabowski M, Opolski G. Exercise urotensin II dynamics in myocardial infarction survivors with and without hypertension. Int J Cardiol. 2005

Richards AM, Nicholls MG, Lainchbury JG, Fisher S, Yandle TG. Plasma urotensin II in heart failure. Lancet. 2002;360:545-6.

Rigotti A, Trigatti BL, Penman M, Rayburn H, Herz J, Krieger M. A targeted mutation in the murine gene encoding the high density lipoprotein (HDL) receptor scavenger receptor class B type I reveals its key role in HDL metabolism. Proc Natl Acad Sci U S A. 1997; 94:12610-5.

Roberts WC. Preventing and arresting coronary atherosclerosis Am Heart J 1995;130:580-600.

Rossowski WJ, Cheng BL, Taylor JE, Datta R, Coy DH. Human urotensin II-induced aorta ring contractions are mediated by protein kinase C, tyrosine kinases and Rho-kinase: inhibition by somatostatin receptor antagonists. Eur J Pharmacol. 2002 Mar 8;438(3):159-70.

Russell FD, Molenaar P, O'Brien DM. Cardiostimulant effects of urotensin-II in human heart in vitro. Br J Pharmacol. 2001 Jan;132(1):5-9.

Russell FD, Meyers D, Galbraith AJ, Bett N, Toth I, Kearns P, Molenaar P. Elevated plasma levels of human urotensin-II immunoreactivity in congestive heart failure. Am J Physiol Heart Circ Physiol. 2003;285:H1576-81.

Russell FD, Kearns P, Toth I, Molenaar P. Urotensin-II-converting enzyme activity of furin and trypsin in human cells in vitro. J Pharmacol Exp Ther. 2004;310:209-14.

Russell FD, Molenaar P. Investigation of signaling pathways that mediate the inotropic effect of urotensin-II in human heart. Cardiovasc Res. 2004;63:673-81.

Sabbah HN, Sharov VG, Lesch M, Goldstein S. Progression of heart failure: a role for interstitial fibrosis. Mol Cell Biochem. 1995 Jun 7-21;147(1-2):29-34.

Sadoshima J, Xu Y, Slayter HS, et al. Autocrine release of angiotensin II mediates stretch-induced hypertrophy of cardiac myocytes in vitro. Cell 1993;75:977-984

Saetrum Opgaard O, Nothacker H, Ehlert FJ, Krause DN. Human urotensin II mediates vasoconstriction via an increase in inositol phosphates. Eur J Pharmacol. 2000 Oct 13;406(2):265-71.

Saito T, Hu F, Tayara L, Fahas L, Shennib H, Giaid A. Inhibition of NOS II prevents cardiac dysfunction in myocardial infarction and congestive heart failure. Am J Physiol Heart Circ Physiol 2002;283: H339–45.

Sakurai T, Yanagisawa M, Masaki T. Molecular characterization of endothelin receptors. Trends Pharmacol Sci 1992;3:103-8.

Salonen R, Salonen JT. Determinants of carotid intima-media thickness: a population-based ultrasonography study in eastern Finnish men. J Intern Med 1991;229:225-31.

Sauzeau V, Le Mellionnec E, Bertoglio J, Scalbert E, Pacaud P, Loirand G. Human urotensin II-induced contraction and arterial smooth muscle cell proliferation are mediated by RhoA and Rho-kinase. Circ Res. 2001 Jun 8;88(11):1102-4.

Schwartz SM, deBlois D, O'Brien ER. The intima. Soil for atherosclerosis and restenosis. Circ Res. 1995 Sep;77(3):445-65. Review.

See F, Kompa A, Martin J, Lewis DA, Krum H. Fibrosis as a therapeutic target post-myocardial infarction. Curr Pharm Des. 2005;11(4):477-87. Review.

Shenouda A, Douglas SA, Ohlstein EH, Giaid A. Localization of urotensin-II immunoreactivity in normal human kidneys and renal carcinoma. J Histochem Cytochem. 2002 Jul;50(7):885-9.

Sheridan MA, Bern HA. Both somatostatin and the caudal neuropeptide, urotensin II, stimulate lipid mobilization from coho salmon liver incubated in vitro. Regul Pept. 1986;14:333-44.

Shi L, Ding W, Li D, Wang Z, Jiang H, Zhang J, Tang C. Proliferation and anti-apoptotic effects of human urotensin II on human endothelial cells. Atherosclerosis 2005

Silvestre RA, Rodriguez-Gallardo J, Egido EM, Marco J. Inhibition of insulin release by urotensin II--a study on the perfused rat pancreas. Horm Metab Res. 2001 Jun;33(6):379-81.

Silvestre RA, Egido EM, Hernandez R, Leprince J, Chatenet D, Tollemer H, Chartrel N, Vaudry H, Marco J. Urotensin-II is present in pancreatic extracts and inhibits insulin release in the perfused rat pancreas. Eur J Endocrinol. 2004 Dec;151(6):803-9.

Simpson CM, Penny DJ, Stocker CF, Shekerdemian LS. Urotensin-II is elevated in children with congenital heart disease. Heart. 2005 Nov 24
Sondermeijer B, Kompa A, Komesaroff P, Krum H. Effect of exogenous urotensin-II on vascular tone in skin microcirculation of patients with essential hypertension. Am J Hypertens. 2005 Sep;18(9 Pt 1):1195-9.

Song W, Abdel-Razik AE, Lu W, Ao Z, Johns DG, Douglas SA, Balment RJ, Ashton N. Urotensin II and renal function in the rat Kidney Int. 2006; 69: 1360-8.

Stary HC, Blankenhorn DH, Chandler AB, Glagov S, Insull W Jr, Richardson M, Rosenfeld ME, Schaffer SA, Schwartz CJ, Wagner WD, et al. A definition of the intima of human arteries and of its atherosclerosis-prone regions. A

report from the Committee on Vascular Lesions of the Council on Arteriosclerosis, American Heart Association. Circulation. 1992 Jan;85(1):391-405. Review.

Stirrat A, Gallagher M, Douglas SA, Ohlstein EH, Berry C, Kirk A, Richardson M, MacLean MR. Potent vasodilator responses to human urotensin-II in human pulmonary and abdominal resistance arteries.Am J Physiol Heart Circ Physiol 2001;280:H925-8.

Sugo T, Murakami Y, Shimomura Y, Harada M, Abe M, Ishibashi Y, Kitada C, Miyajima N, Suzuki N, Mori M, Fujino M. Identification of urotensin II-related peptide as the urotensin II-immunoreactive molecule in the rat brain. Biochem Biophys Res Commun 2003;310:860-8.

Sukovich DA, Kauser K, Shirley FD, DelVecchio V, Halks-Miller M, Rubanyi GM. Expression of interleukin-6 in atherosclerotic lesions of male ApoE-knockout mice: inhibition by 17beta-estradiol. Arterioscler Thromb Vasc Biol. 1998;18(9):1498-505.

Sun Y, Zhang JQ, Zhang J, Ramires FJ. Angiotensin II, transforming growth factor-beta1 and repair in the infarcted heart. J Mol Cell Cardiol. 1998 Aug;30(8):1559-69.

Suzuki S, Wenyi Z, Hirai M, Hinokio Y, Suzuki C, Yamada T, Yoshizumi S, Suzuki M, Tanizawa Y, Matsutani A, Oka Y. Genetic variations at urotensin II and urotensin II receptor genes and risk of type 2 diabetes mellitus in Japanese. Peptides. 2004 Oct;25(10):1803-8.

Takahashi K, Totsune K, Murakami O, Arihara Z, Noshiro T, Hayashi Y, Shibahara S. Expression of urotensin II and its receptor in adrenal tumors and stimulation of proliferation of cultured tumor cells by urotensin II. Peptides 2003;24:301-6.

Takahashi K, Totsune K, Murakami O, Shibahara S. Expression of urotensin II and urotensin II receptor mRNAs in various human tumor cell lines and secretion of urotensin II-like immunoreactivity by SW-13 adrenocortical carcinoma cells Peptides. 2001; 22: 1175-9.

Tamura K, Okazaki M, Tamura M, Isozumi K, Tasaki H, Nakashima Y. Urotensin II-induced activation of extracellular signal-regulated kinase in cultured vascular smooth muscle cells: involvement of cell adhesion-mediated integrin signaling. Life Sci. 2003 Jan 17;72(9):1049-60.

Tasaki K, Hori M, Ozaki H, Karaki H, Wakabayashi I. Mechanism of human urotensin II-induced contraction in rat aorta. J Pharmacol Sci. 2004 Apr;94(4):376-83.

Tomanek RJ, Palmer PJ, Peiffer GL, Schreiber KL, Eastham CL, Marcus ML. Morphometry of canine coronary arteries, arterioles, and capillaries during hypertension and left ventricular hypertrophy. Circ Res. 1986 Jan;58(1):38-46.

Thompson JP, Watt P, Sanghavi S, Strupish JW, Lambert DG. A comparison of cerebrospinal fluid and plasma urotensin II concentrations in normotensive and hypertensive patients undergoing urological surgery during spinal anesthesia: a pilot study. Anesth Analg. 2003;97:1501-3.

Tostivint H, Joly L, Lihrmann I, Parmentier C, Lebon A, Morisson M, Calas A, Ekker M, Vaudry H. Comparative genomics provides evidence for close evolutionary relationships between the urotensin II and somatostatin gene families. Proc Natl Acad Sci U S A. 2006 Feb 14;103(7):2237-42. Epub 2006

Totsune K, Takahashi K, Arihara Z, Sone M, Ito S, Murakami O. Increased plasma urotensin II levels in patients with diabetes mellitus. Clin Sci (Lond). 2003 Jan;104(1):1-5.

Totsune K, Takahashi K, Arihara Z, Sone M, Murakami O, Ito S, Kikuya M, Ohkubo T, Hashimoto J, Imai Y. Elevated plasma levels of immunoreactive urotensin II and its increased urinary excretion in patients with Type 2 diabetes mellitus: association with progress of diabetic nephropathy. Peptides. 2004 Oct;25(10):1809-14.

Tzanidis A, Hannan RD, Thomas WG, Onan D, Autelitano DJ, See F, Kelly DJ, Gilbert RE, Krum H. Direct actions of urotensin II on the heart: implications for cardiac fibrosis and hypertrophy. Circ Res 2003;93:246-53..

Ueda Y, Royer L, Gong E, Zhang J, Cooper PN, Francone O, Rubin EM. Lower plasma levels and accelerated clearance of high density lipoprotein (HDL) and non-HDL cholesterol in scavenger receptor class B type I transgenic mice. J Biol Chem 1999; 274:7165-71

Vergura R, Camarda V, Rizzi A, Spagnol M, Guerrini R, Calo' G, Salvadori S, Regoli D. Urotensin II stimulates plasma extravasation in mice via UT receptor activation. Naunyn Schmiedebergs Arch Pharmacol. 2004 Nov;370(5):347-52.

Wang (a) ZJ, Shi LB, Xiong ZW, Zhang LF, Meng L, Bu DF, Tang CS, Ding WH. Alteration of vascular urotensin II receptor in mice with apolipoprotein E gene knockout. Peptides. 2006; 27:858-63.

Wang (b) YX. Cardiovascular functional phenotypes and pharmacological responses in apolipoprotein E deficient mice. Neurobiol Aging. 2005 Mar;26(3):309-16. Review.

Wang H, Mehta JL, Chen K, Zhang X, Li D. Human urotensin II modulates collagen synthesis and the expression of MMP-1 in human endothelial cells. J Cardiovasc Pharmacol 2004;44:577-81.

Wang ZJ, Shi LB, Xiong ZW, Zhang LF, Meng L, Bu DF, Tang CS, Ding WH. Alteration of vascular urotensin II receptor in mice with apolipoprotein E gene knockout. Peptides. 2005

Watanabe T, Pakala R, Katagiri T, Benedict CR. Synergistic effect of urotensin II with mildly oxidized LDL on DNA synthesis in vascular smooth muscle cells. Circulation. 2001 Jul 3;104(1):16-8.

Watanabe T, Pakala R, Katagiri T, Benedict CR. Synergistic effect of urotensin II with serotonin on vascular smooth muscle cell proliferation. J Hypertens 2001 ;19:2191-6.

Watanabe T, Koba S, Katagiri T, Pakala R, Benedict CR.Lsophosphatidylcholine potentiates the mitogenic effect of various vasoactive compounds on rabbit aortic smooth muscle cells. Jpn Heart J 2002;43:409-16.

Watanabe T, Suguro T, Kanome T, Sakamoto Y, Kodate S, Hagiwara T, Hongo S, Hirano T, Adachi M, Miyazaki A. Human urotensin II accelerates foam cell formation in human monocyte-derived macrophages. Hypertension. 2005 Oct;46(4):738-44. Epub 2005 Sep 19.

Watson AM, Lambert GW, Smith KJ, May CN. Urotensin II acts centrally to increase epinephrine and ACTH release and cause potent inotropic and chronotropic actions. Hypertension. 2003;42:373-9.

Wei S, Chow LT, Sanderson JE. Effect of carvedilol in comparison with metoprolol on myocardial collagen postinfarction. J Am Coll Cardiol 2000;36:276–81.

Weisberg SP, Hunter D, Huber R, Lemieux J, Slaymaker S, Vaddi K, Charo I, Leibel RL, Ferrante AW Jr. CCR2 modulates inflammatory and metabolic effects of high-fat feeding. J Clin Invest 2006;116:115-24.

Wellman, KF & Volk, BW: Renal changes in experimental hypercholesterolemia in normal and subdiabetic rabbits. II. Long-term studies. Lab Invest 1971 24:144–155

Wenyi Z, Suzuki S, Hirai M, Hinokio Y, Tanizawa Y, Matsutani A, Satoh J, Oka Y. Role of urotensin II gene in genetic susceptibility to Type 2 diabetes mellitus in Japanese subjects. Diabetologia. 2003 Jul;46(7):972-6. Epub 2003 Jun 27.
Wilkinson IB, Affolter JT, de Haas SL, Pellegrini MP, Boyd J, Winter MJ, Balment RJ, Webb DJ. High plasma concentrations of human urotensin II do not alter local or systemic hemodynamics in man. Cardiovasc Res. 2002 Feb 1;53(2):341-7.

Williams KJ, Scalia R, Mazany KD, et al. Rapid restoration of normal endothelial functions in genetically hyperlipidemic mice by a synthetic mediator of reverse lipid transport. Arterioscler Thromb Vasc Biol. 2000; 20:1033–1039.

Yang R, Powell-Braxton L, Ogaoawara AK, et al.
Hypertension and endothelial dysfunction in apolipoprotein E knockout mice. ArteriosclerThromb Vasc Biol. 1999;19:2762–2768.

Yki-Jarvinen H.
Fat in the liver and insulin resistance.
Ann Med. 2005;37(5):347-56. Review.

ZAINO EC, TABOR SH. CARDIAC HYPERTROPHY IN ACUTE MYOCARDIAL INFARCTION. A STUDY BASED ON 100 AUTOPSIED CASES. Circulation. 1963 Dec;28:1081-3.

Zhang Y, Li J, Cao J, Chen J, Yang J, Zhang Z, Du J, Tang C.
Effect of chronic hypoxia on contents of urotensin II and its functional receptors in rat myocardium. Heart Vessels. 2002 Jan;16(2):64-8.

Zhang AY, Chen YF, Zhang DX, Yi FX, Qi J, Andrade-Gordon P, de Garavilla L, Li PL, Zou AP. Urotensin II is a nitric oxide-dependent vasodilator and natriuretic peptide in the rat kidney. Am J Physiol Renal Physiol 2003;285:F792-8.

Zoccali C, Mallamaci F, Tripepi G, Cutrupi S, Pizzini P, Malatino L. Urotensin II is an inverse predictor of incident cardiovascular events in end-stage renal disease Kidney Int. 2006; 69:1253-8.

8.0 Manuscript reprints, animal ethics certificates, and copyright waiver forms.

Available online at www.sciencedirect.com
SCIENCE DIRECT
Journal of Molecular and Cellular Cardiology 41 (2006) 285–295
Journal of Molecular and Cellular Cardiology
www.elsevier.com/locate/yjmcc

Original article

Urotensin-II blockade with SB-611812 attenuates cardiac dysfunction in a rat model of coronary artery ligation

Nicolas Bousette [a], Fu Hu [a], Eliot H. Ohlstein [b], Dashyant Dhanak [c], Stephen A. Douglas [b], Adel Giaid [a,*]

[a] *Division of Cardiology, Montreal General Hospital, McGill University Health Center, Suite L3-109, 1650 Cedar Avenue, Montreal, Quebec, Canada H3G 1A4*
[b] *The Cardiovascular and Urogenital-CEDD, GlaxoSmithKline, King of Prussia, PA 19406, USA*
[c] *Microbial, Musculoskeletal and Proliferative Diseases CEDD, GlaxoSmithKline, Collegeville, PA 19426, USA*

Received 22 March 2006; received in revised form 10 May 2006; accepted 11 May 2006
Available online 22 June 2006

Available online at www.sciencedirect.com
SCIENCE DIRECT
Journal of Molecular and Cellular Cardiology 41 (2006) 285–295
Journal of Molecular and Cellular Cardiology
www.elsevier.com/locate/yjmcc

Original article

Urotensin-II blockade with SB-611812 attenuates cardiac dysfunction in a rat model of coronary artery ligation

Nicolas Bousette [a], Fu Hu [a], Eliot H. Ohlstein [b], Dashyant Dhanak [c], Stephen A. Douglas [b], Adel Giaid [a,*]

[a] *Division of Cardiology, Montreal General Hospital, McGill University Health Center, Suite L3-109, 1650 Cedar Avenue, Montreal, Quebec, Canada H3G 1A4*
[b] *The Cardiovascular and Urogenital-CEDD, GlaxoSmithKline, King of Prussia, PA 19406, USA*
[c] *Microbial, Musculoskeletal and Proliferative Diseases CEDD, GlaxoSmithKline, Collegeville, PA 19426, USA*

Received 22 March 2006; received in revised form 10 May 2006; accepted 11 May 2006
Available online 22 June 2006

Abstract

Expression of urotensin II (UII) is significantly elevated in the hearts of patients with congestive heart failure (CHF). Recent reports have also shown increased plasma levels of UII in patients with CHF, and these levels correlated with the severity of disease. We therefore hypothesized that blockade of UII signaling would improve cardiac function in a rat model of CHF. CHF was induced in rats by ligating the left coronary artery. Animals were randomized to either treatment with a specific UT receptor antagonist, SB-611812 (30 mg/kg/day, UID by gavage), or vehicle, starting either 30 min prior to coronary ligation (early treatment) or 10 days after ligation (delayed treatment). Treatment drug or vehicle wa administered daily thereafter for 8 weeks. We measured cardiac function and evaluated the levels of mRNA expression for mediators of CHF. In addition, we evaluated UII and UT protein levels using immunohistochemistry and Western blotting. Cardiomyocyte hypertrophy was evaluated by measuring cardiomyocyte cross-sectional area. Animals with CHF showed increased UII and UT expression as evidenced by immunohistochemistry and Western blotting. Treatment with the SB-611812 significantly reduced overall mortality, left ventricular end-diastolic pressure by 72%, lung edema by 71%, right ventricular systolic pressure by 92%, central venous pressure by 59%, cardiomyocyte hypertrophy by 54%, and ventricular dilatation by 79% ($P < 0.05$). Therefore, blockade of the UT receptor reduced mortality and improved cardiac function in this model of myocardial infarction and CHF, suggesting an important role for UII in the pathogenesis of this condition.

Keywords: Myocardial infarction; Hemodynamics; Receptors; SB-611812

1. Introduction

Urotensin-II (UII) a relatively novel peptide, originally isolated from fish spinal cords, has prompted some substantial interest in the field of cardiovascular medicine. In humans, UII binds to a 389 amino acid G-protein coupled receptor termed UT [1]. The G-protein associated with the UT receptor is of the Gq class, which is the same class of G-proteins that bind to angiotensin, endothelin, and α-adrenoceptors. UII induced both endothelium-independent vasoconstriction and endothelium-dependent vasorelaxation, the order and magnitude of which were dependent on the species tested and anatomical location [2–4]. UII also exerted inotropic effects on the isolated human atrial trabeculea [5], mitogenic effects on smooth muscle cells [6,7], and induced collagen and fibronectin synthesis by cardiac fibroblasts [8]. In fact, the latter study also showed that UII induced hypertrophy of rat neonatal cardiomyocytes. Bolus injection of UII into cynomolgus monkeys resulted in the development of cardiovascular collapse [1].

The heart is one of the tissues with the highest degree of UT expression, further supporting its role in cardiovascular physiology [1]. We have previously demonstrated increased myocardial expression of UII in CHF patients, and this increase was significantly correlated with the increase in left ventricular end-diastolic dimension (LVEDD) [9]. Our findings were followed by several reports of increased plasma levels of UII in CHF [10,11]. Of note, is the finding of increased plasma level of UII which correlated with left ventricular end-diastolic pressure [11]. Recently, Johns et al. demonstrated in a model of

* Corresponding author. Fax: +1 514 934 8448.
E-mail address: adel.giaid@mcgill.ca (A. Giaid).

0022-2828/$ - see front matter © 2006 Elsevier Inc. All rights reserved.
doi:10.1016/j.yjmcc.2006.05.008

CHF in the rat that cardiac ventricular mRNA expression of U-II and UT receptor was increased [12]. In addition, this study demonstrated that a competitive peptidic UT receptor antagonist, BIM-23127, inhibited U-II-induced hypertrophy in H9c2 cardiomyocytes.

Based on the cardiovascular actions of UII and our own findings in CHF patients, we hypothesized that UII is upregulated in an experimental CHF model of myocardial infarction, and that UT receptor antagonism may lead to improvement in cardiac function and structure. Thus, we utilized a nonpeptidic selective UT antagonist SB-611812 to block UII/UT signaling. We have previously demonstrated the effectiveness of this antagonist in attenuating UII induced neointimal hyperplasia in a rat model of balloon angioplasty-mediated restenosis [13]. In the following study, SB-611812 was administered to rats prior and after coronary artery ligation; and evaluated for its effects on mortality, infarct size, hemodynamics, and gene expression.

2. Methods

2.1. Details of SB-611812

SB-611812, an arylsulfonamide UT antagonist (2,6-dichloro-*N*-(4-chloro-3-{[2-(dimethylamino)ethyl]oxy}phenyl)-4-(trifluoromethyl)benzenesulfonamide), was synthesized at GlaxoSmithKline, King of Prussia, PA [14]. SB-611812, potently binds the rat recombinant UT receptor (K_i 121 nM) and antagonizes UII in both isolated vascular tissue (rat aortic contraction) and cell-based (inhibition of $[Ca2+]_i$-mobilization in rat UT-HEK293 cells) assays (pA2s of 6.59 and 6.60, respectively). SB-611812 has approximately 100% bioavailability and has 4–5 h half life in the rat by oral gavage. Specificity of SB-611812 was demonstrated by the fact that pretreatment of the rat isolated aorta with 10 μM SB-611812 (which is 40-fold higher concentration than the pA_2 of this compound in the aortic vasoactivity bioassay) did not inhibit the contraction induced by KCl, Phenylephrine, Endothelin-I, or Angiotensin-II. In a separate study, we found that 1 nM exogenous UII induced a significant increase in renal vascular resistance which was 90% inhibited with the dose utilized in the present study (30 mg/kg/day) (data not shown). Dosing experiments in healthy animals showed no acute or chronic effects for the drug on either hemodynamics or cardiac function. This compound was a generous gift from GlaxoSmithKline.

2.2. Study groups

Throughout the study, male Lewis rats weighing ~250 g obtained from Charles River laboratories were used. Animals were initially divided into a sham group (n = 9) and a myocardial infarction (MI) group. The MI group was further subdivided randomly into 5 groups including: MI only group (n = 22), an MI + treatment group (day 0) in which treatment was administered by gavage (30 mg/kg/day; once a day) 30 min prior to surgery (n = 22); MI + vehicle group (day 0) in which the drug vehicle (0.1% methylcellulose) was administered by gavage 30 min prior to surgery (n = 28); MI + treatment group (day 10) in which treatment was administered by gavage 10 days after surgery (n = 12); MI + vehicle group (day 10) in which the drug vehicle (0.1% methylcellulose) was administered by gavage 10 days after surgery (n = 15). Animals were administered either drug, SB-611812, or vehicle once a day for the duration (8 weeks) of the study period.

All animals receiving a coronary ligation underwent a left thoracotomy followed by dissection of the pericardial sac and exposure of the left anterior ventricular free wall. The left anterior descending coronary artery (LAD) was then visualized and a suture was placed in the myocardium surrounding the LAD and the suture was ligated. Pallor of the anterior free wall was verified before wound closure. The sham group underwent the same procedure except the suture was not ligated but was cut at both ends at the epicardial border. Eight weeks after surgery, animals were anesthetized and cardiac function and hemodynamic measurements were recorded. Experiments were performed in accordance with the Guide for the Care and Use of Laboratory Animals (National Institutes of Health Publication 86 to 23, revised 1996), and with approval of the Animal Care Committee of the McGill University Health Center.

2.3. Hemodynamic and cardiac function measurements

Rats were catheterized via the carotid artery. The polyethylene tubing (PE50 from Intramedic, Montreal, Canada) catheter (0.58 mm), which was connected to a pressure transducer measured systolic arterial pressure (Psyst.), diastolic arterial pressure (Pdiast.), and mean arterial pressure (MAP). The catheter was then passed into the left ventricle for measurements of left ventricular end-systolic pressure (LVESP), left ventricular end-diastolic pressure (LVEDP), +dP/dt (the first derivative of the rate in positive pressure change in the ventricle), and −dP/dt (the first derivative of the rate in negative pressure change in the ventricle). The latter may not be accurately reflected using the fluid-filled catheter system employed here. Central venous pressure and right ventricular systolic pressure (RVSP) were determined by inserting a catheter into the right atrium and ventricle through the jugular vein.

2.4. Tissue collection

Animals were sacrificed by exsanguination, and the hearts were collected and snap frozen in liquid nitrogen and stored at −80 °C, or fixed in 4% paraformaldehyde and embedded in paraffin for histological and immunohistochemical analysis. Lungs were also harvested and weighed. They were allowed to dry in a 40 °C oven for 1 week and weighed again until there were three consecutive identical weights. These values were then used to calculate the lung wet/dry weight ratio.

2.5. Infarct analysis

Heart tissue embedded in paraffin was cut at 5 μm slices and stained with the histological stain, Masson's trichrome which

allowed one to discern infarct from noninfarcted myocardial tissue. Following this, pictures were taken of the sections and downloaded into an image analysis program for infarct size analysis (Image ProPlus, Media Cybernetics, CA, USA). Infarct size was documented as percentage of infarct area compared to total left ventricular area in representative sections. All sections were examined in a blinded fashion.

2.6. Assessment of cardiomyocyte hypertrophy and ventricular dilatation

Myocyte cross-sectional area analysis was carried out by taking photomicrographs of the endocardial region of heart sections stained with hematoxylin and eosin (at 400× magnification). These photomicrographs (4/animal; sham $n = 6$, vehicle $n = 8$, and treatment $n = 8$) were then analyzed by the image analysis program, Image ProPlus. The latter enables the users to demarcate individual myocytes and quantify their area using arbitrary units. Ventricular dilatation was expressed as LV chamber area. Analysis was carried out by determining the intrachamber area of the LV from histological sections cut in the transverse plane using Image ProPlus.

2.7. Immunohistochemistry

Immunohistochemical staining for UII and UT was performed using the avidin–biotin peroxidase method as previously described [15]. The rabbit polyclonal anti-rat UII antibody utilized in this study has been previously described in detail [9]. The rabbit polyclonal anti-rat/human UT antibodies were developed at Covance research products Inc. (Denver, PA). We utilized 1/400 dilutions of sera for both anti-UII and anti-UT antibodies. Negative control sections were incubated with the antisera:antigens mixture or a normal serum only.

2.8. Real-time RT-PCR

Left ventricular myocardial samples (for n values see Table 2) were retrieved from storage for RNA extraction using Trizol (Invitrogen, Ontario, Canada) and performed as per the manufacturer's instructions. RNA integrity was then verified for all samples by evaluating the clarity of the 28S and 18S bands and verifying that the bands were 28S > 18S by gel electrophoresis. Following this, 2 μg of each RNA sample was reverse transcribed to synthesize cDNA using the Omniscript reverse transcriptase kit from Qiagen (Ontario, Canada). From this, 1 μl of cDNA was used to amplify target genes using specific primers (Table 1). Genes were amplified individually in the LightCycler (Roche, Montreal, Canada) using Quantitect SYBR Green reagent (Qiagen, Ontario, Canada) with the following amplification conditions: DNA polymerase activation, 15 min at 95 °C followed by 40 cycles of denaturation, annealing and extension for 15 s at 94 °C, 20 s at 50–60 °C (depending on primer T_m), and 20–30 s at 72 °C (depending on amplicon size), respectively. Primers were designed using PrimerQuest biotool [http://www.idtdna.com] (Table 1). All values for mRNA expression determined by RT-PCR are expressed as the ratio of the copy number of the mRNA transcript of interest to the copy number of the mRNA transcript of the housekeeping gene RPL32. The copy number of mRNA transcript is determined by the threshold cycle of the PCR reaction for each sample. This threshold cycle is the cycle at which cDNA replication begins to amplify exponentially, and is therefore an indicator of the levels of starting template. RPL32 levels are expressed as the inverse of threshold cycle. A homogeneous amplification of the products was rechecked by analyzing the melting curves of the amplified products.

Table 1
Primer sequences

	Primer sequences
AT-1 F:	5′ CCG TGA CTG TGA ATT TGC TG 3′
AT-1 R:	5′ GGA ATG TAT TTC AGA AGC TGG AG 3′
BNP F:	5′ ACA GCT CTC AAA GGA CCA 3′
BNP R:	5′ ATC CGG TCT ATC TTC TGC 3′
cTnI F:	5′ CTG ACC CAG AAG ATC TAT GAC 3′
cTnI R:	5′ TCC TTC TTC ACC TGC TTG A 3′
RPL32 F:	5′ ATC CTG ATG CCC AAC ATT GGT TAC 3′
RPL32 R:	5′ GTT GCA CAT CAG CAG CAC TTC CAG 3′
UT F:	5′ GGG CAT GGT GGG AAA TGT A 3′
UT R:	5′ AGA CGT ACA TGG AGG CCG AG 3′

AT-1, angiotensin type 1 receptor; BNP, brain natriuretic peptide; cTnI, cardiac troponin-I; RPL32, ribosomal protein L32; UT, UII Receptor.

2.9. Western blotting

Western blotting was performed as previously described [16], with rabbit polyclonal anti-rat UII antibody (1:400 dilution); or with rabbit polyclonal anti-rat/human UT antibodies (1:400 dilution). The UT Western blot was repeated three times with three different rabbit anti-rat/human UT antibodies raised against three different UT epitopes. Equal protein loading conditions were utilized. Protein concentrations were determined using the Bio-Rad modified Bradford protein assay. Protein bands were then quantified using arbitrary units (AU) with the image analysis program, Image ProPlus (Media Cybernetics, CA, USA).

2.10. Statistical analysis

All parameters were evaluated using either one-way ANOVA test (with the Tukey post hoc test), Student's t test (for two group comparisons), or Kaplan–Meier analysis for mortality, with the aid of the statistical program SPSS 11.5. A P value of <0.05 was considered statistically significant.

3. Results

3.1. Characteristics of the MI/CHF model

Several anatomical and functional parameters were evaluated in the CHF model including hemodynamics, cardiac function, heart and lung weights, and also mRNA expression

of markers and mediators of CHF. There was no difference between the MI only and the MI + vehicle groups in all hemodynamic and structural parameters investigated, suggesting no effect of vehicle on any of these parameters. There was a significant increase in LVEDP (165%), RVSP (19%), CVP (98%), and a significant decrease in ±dP/dt (32%) in vehicle-treated MI rats compared to sham rats (Table 3). There was a significant increase in the heart weight to body weight ratio (36%; $P < 0.05$) (Table 3), cardiomyocyte hypertrophy (61%; $P < 0.005$), ventricular dilatation (110%; $P < 0.001$), as well as the lung wet-to-dry weight ratio in the vehicle group compared to the sham group (11%; $P < 0.001$) (Table 3). LVSP was decreased (15%) compared to the sham group but this did not reach statistical significance (Table 3). There was no significant difference in systolic and diastolic blood pressure, mean arterial pressure, and heart rate between the two groups (Table 3).

The mRNA expression of both BNP and AT-1 was significantly increased in the vehicle-treated MI group compared to the sham group (9% and 8%, respectively; $P < 0.05$) (Table 2). Conversely, cardiac troponin I (cTnI) levels were significantly decreased in the vehicle-treated MI group compared to the sham group (7%; $P < 0.005$) (Table 2).

3.2. Increased myocardial expression of UII in heart failure

Immunohistochemistry revealed the presence of little to no UII expression in cardiomyocytes and only weak UII expression in intramyocardial vascular smooth muscle cells of normal hearts (Fig. 1A). Also, no UII expression was observed in endothelial cells of the myocardial vasculature. In contrast, there was strong expression of UII in CHF animals. Especially in the surviving cardiomyocytes and myofibroblasts of the endocardial region of the infarcted left ventricle (Figs. 1B–C). Immunoreactivity was strong in the viable left ventricle, particularly at the peri-infarct border zone (Figs. 1D–E). Also, there was abundant expression of UII in intramyocardial vessels of the left ventricle (Fig. 1F). In the right ventricle of CHF animals, moderate expression of UII in cardiomyocytes and intramyocardial smooth muscle cells was observed (Fig. 1G). The ventricular septa only showed weak UII expression. All negative control sections showed no immunoreactivity for UII (Fig. 1H).

Table 2
Relative expression of UT, BNP, AT-1, and cTnI to RPL32 in the study groups

Genes	Sham ($n = 8$)	Vehicle ($n = 12$)	SB611812 ($n = 8$)
RPL32 ($1/C_t$)	0.059 ± 0.09	0.060 ± 0.09	0.060 ± 0.14
UT LV	0.519 ± 0.217	0.591 ± 0.028	N/A
UT RV	0.525 ± 0.024	0.563 ± 0.016[a]	N/A
BNP	0.938 ± 0.014	1.021 ± 0.008[a]	1.022 ± 0.011[a]
AT-1	0.522 ± 0.009	0.560 ± 0.008[a]	0.576 ± 0.015[a]
cTnI	1.21 ± 0.02	1.13 ± 0.03[a]	1.16 ± 0.06

RPL32 (ribosomal protein L32); Ct (threshold cycle); UT (urotensin-II receptor), LV (left ventricle), RV (right ventricle), BNP (brain natriuretic peptide), AT-1 (angiotensin type 1 receptor), cTnI (cardiac troponin I).
[a] Indicates $P < 0.05$ vs. sham.

UII protein level was quantified using Western blot analysis. Here we show that the level of UII protein expression is significantly increased in the hearts, specifically, the left ventricles of CHF animals compared to sham operated controls (1705 ± 103 Arbitrary Units (AU) vs. 1346 ± 96 AU; $P < 0.05$) (Figs. 2A–B). Rat prepro-UII consists of 123 amino acid residues with a predicted molecular weight of 13.7 kDa. In accordance with this, the Western blot shows a band corresponding to protein with a molecular weight of approximately 14 kDa.

3.3. Increased myocardial expression of UT in heart failure

There was moderate diffuse UT immunoreactivity in the normal control hearts (Fig. 3A). Specifically, UT immunoreactivity was seen in cardiomyocytes, vascular and endocardial endothelial cells, and in vascular smooth muscle cells. In animals with myocardial infarction, like UII, UT protein expression was much more pronounced in the viable cardiomyocytes within the infarct region although perhaps to a slightly lesser degree compared to UII (Figs. 3B–D). In addition, pronounced immunoreactivity was observed in the endocardial endothelium, especially in the infarct region (Figs. 3B–D). Interestingly, there was marked and intense UT immunoreactivity in the myocardial vasculature, both in the infarcted and noninfarcted zones (Figs. 3E–F). The vascular UT immunoreactivity was stronger in small vessels. The interventricular septum showed diffuse immunoreactivity though it was less intense than the right ventricle of CHF animals which showed diffuse, yet pronounced immunoreactivity (Fig. 3G). Right ventricular vasculature also exhibited UT immunoreactivity although this was less intense than in the infarcted LV. There was no detectable immunoreactivity in negative control sections in which the primary anti-sera were omitted or preabsorbed with the antigen (Fig. 3H).

Western blot analysis was also performed to determine UT protein content. Interestingly, the band corresponding to UT at 60 kDa was comparable between normal and CHF hearts (Figs. 2C–D). However, there were two bands at approximately 150 and 200 kDa which were significantly increased in the CHF hearts compared to the normal controls. Specifically, the band at ~200 kDa was significantly increased [1241 ± 164 AU vs. 356 ± 56 AU; $P < 0.001$] in CHF hearts compared to normal hearts. Interestingly, the band at ~150 kDa was virtually nonexistent in normal hearts while it was quite prominent in CHF hearts. This indicates that UT forms either a hetero- or homo-oligomeric complex in heart failure. The specificity for UT was verified by the presence of these bands using three different antibodies raised against three different epitopes of UT (data not shown).

Subsequently, we quantified UT mRNA content by RT-PCR in the left and right ventricles of control and CHF animals (Table 2). UT mRNA was increased in the left ventricle of the CHF compared to the control animals; however, it did not reach statistical significance. UT mRNA was significantly increased in the right ventricle of CHF animals compared to that of control animals ($P < 0.05$).

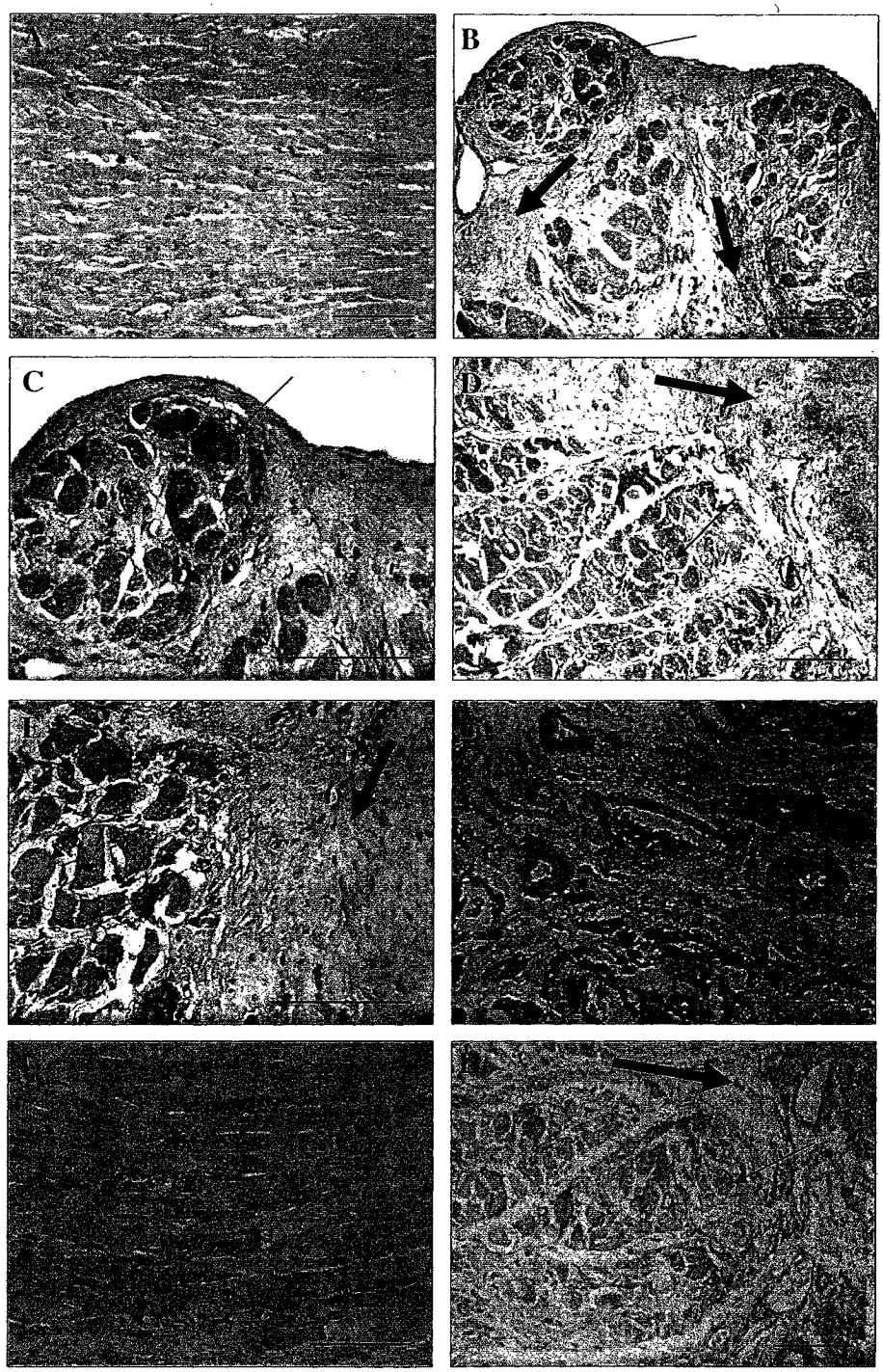

Fig. 1. Representative photomicrographs of UII immunohistochemistry. Panel A demonstrates weak diffuse UII immunoreactivity of left ventricular myocardium of normal rats (200× magnification). Panel B shows intense UII immunoreactivity in surviving cardiomyocytes (thin arrow) in the endocardial region of the left ventricle of an infarcted (thick arrow) myocardium (200× magnification). Panel C is a greater magnification of the same section as panel B (thin arrow indicating surviving cardiomyocyte; 400× magnification). Panel D demonstrates intense immunoreactivity in the viable cardiomyocytes (thin arrow) in the border zone of the peri-infarct region of the left ventricle of CHF animals (thick arrow indicates scar region; 200× magnification). Panel E is greater magnification of panel D (thi arrow indicating viable myocardium and thick arrow indicating infarcted tissue; 400× magnification). Panel F shows strong UII immunoreactivity of the microvasculature (dashed arrows) in the infarcted myocardium (400× magnification). Panel G demonstrates moderate diffuse UII immunoreactivity in the right ventricle of CHF animals (300× magnification). Panel H is a negative control demonstrating no immunoreactivity of the same section as panel D (thin arrow indicating viable myocardium and thick arrow indicating scar tissue) when the primary serum is omitted. All sections were counterstained with hematoxylin. Scale bars represent 75 μm.

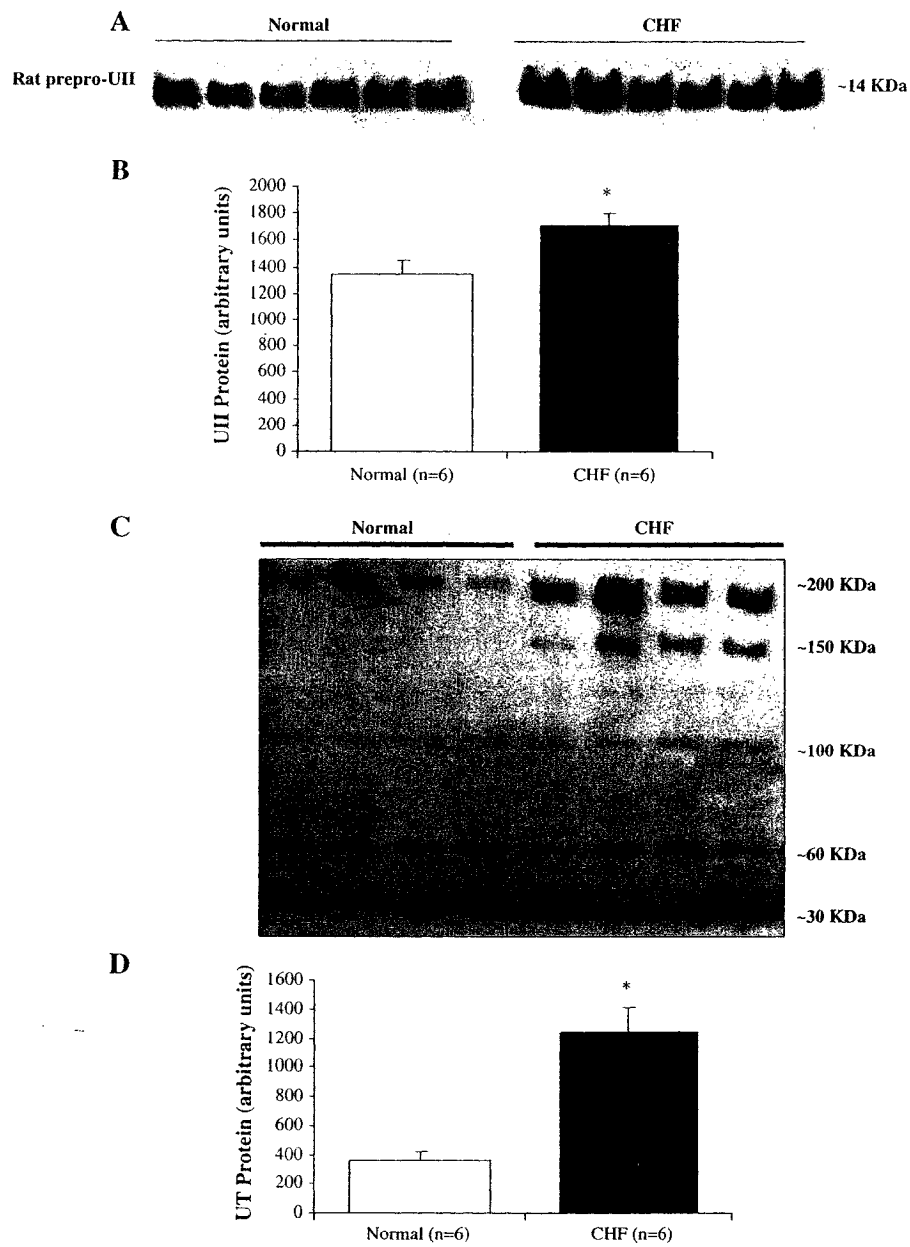

Fig. 2. Prepro-UII and UT protein quantification. (A) Representative Western blot demonstrating prepro-UII protein levels with a molecular weight of 13.7 kDa from left ventricular protein homogenates of normal and CHF hearts. (B) Graph demonstrating quantification of UII Western blot. * indicates $P < 0.05$. (C) Representative Western blot demonstrating UT protein levels from left ventricular protein homogenates of normal and CHF hearts. Bands represent proteins with molecular weights of ~30 kDa, ~60 kDa, ~100 kDa, ~150 kDa, ~200 kDa. (D) Graph demonstrating quantification of UT Western blot. * indicates $P < 0.05$.

3.4. *Effect of UT receptor antagonist: early treatment (day 0)*

Early treatment with SB-611812, in which the drug was administered 30 min prior to coronary ligation, significantly reduced overall (0 h–8 weeks) mortality compared to the vehicle-treated MI group ($P = 0.024$; Fig. 4). Infarct analysis demonstrated a small, nonsignificant, decrease in infarct size in the treatment group compared to the vehicle group ($P = 0.14$). However, treatment (starting on day 0) led to a significant (54%) reduction in cardiomyocyte hypertrophy ($P < 0.01$) (Table 3) and ventricular dilatation (79%; Fig. 5; $P < 0.001$). Early treatment with SB-611812 also significantly improved cardiac function and reduced lung edema (Fig. 6 and Table 3). Specifically, the treatment group had a significantly reduced LVEDP (72%; $P < 0.001$) and RVSP (92%; $P < 0.05$) compared to the vehicle group. CVP was also significantly reduced in the treatment compared to the vehicle group (58%; $P < 0.05$). The UT receptor antagonist also significantly improved the degree of lung edema as determined by the wet-to-dry weight ratio of the lungs (71%, $P < 0.001$). Heart weight to body weight ratio was also improved by treatment but this did not reach statistical significance ($P = 0.099$).

Cardiac contractility indices ±dP/dt showed improvement compared to vehicle but this did not reach statistical significance (Table 3). There was no notable effect for the drug on either systolic or diastolic or mean arterial pressure nor was there a difference in heart rate in the treatment grou compared to the vehicle group.

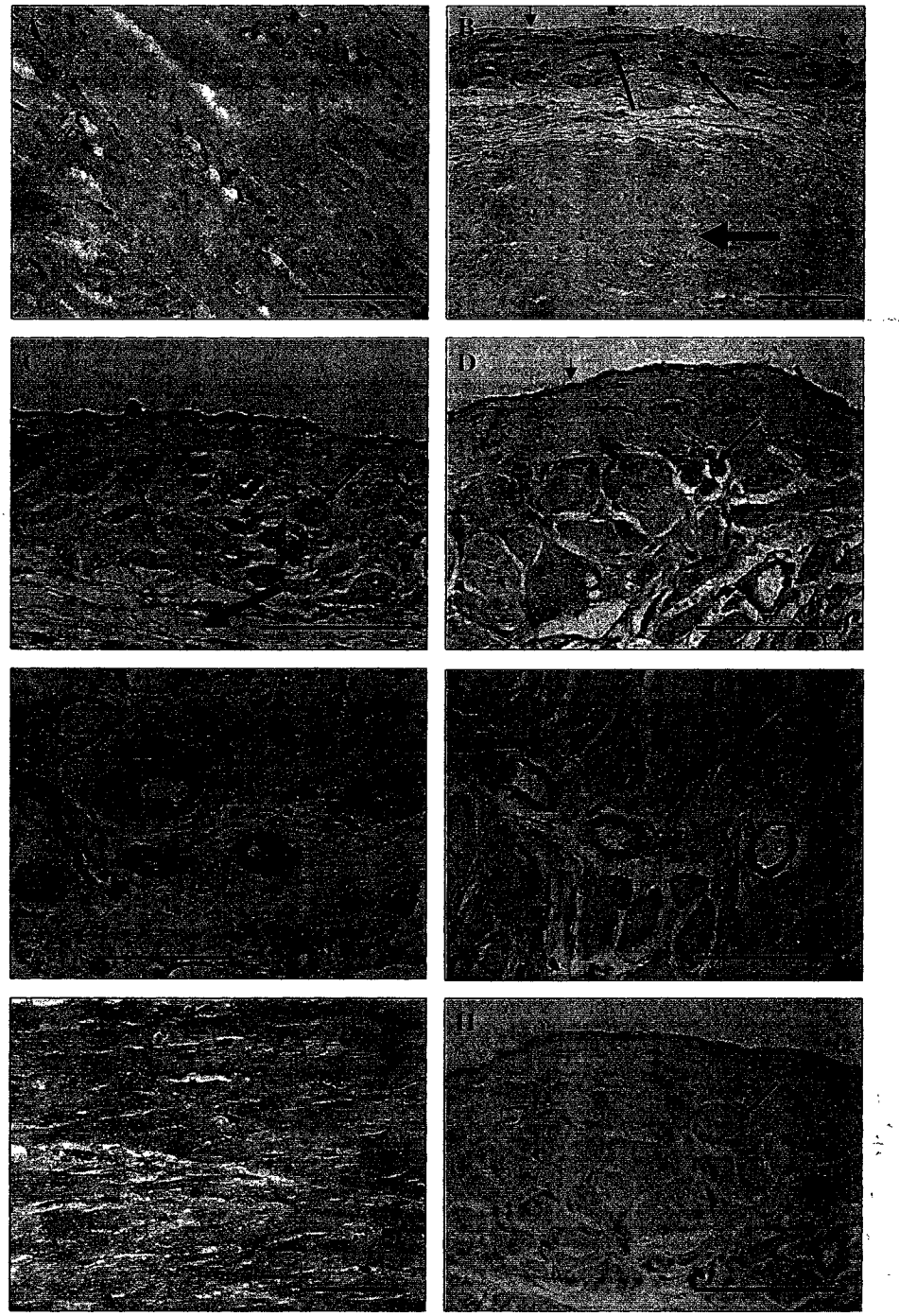

Fig. 3. Representative photomicrographs of UT immunohistochemistry. Panel A demonstrates moderate diffuse UT immunoreactivity of left ventricular myocardium of normal rats (300× magnification). Panel B shows strong UT immunoreactivity in the endocardial region of the left ventricle of a CHF animal, with staining in the endocardial endothelium (short arrows), and viable cardiomyocytes (long thin arrow, thick arrow indicates infarct scar; 200× magnification). Panel C is a greater magnification of the same section as panel B demonstrating strong UT immunoreactivity in both the endocardial endothelial cells (short arrows) and the surviving cardiomyocytes (long thin arrows) in the endocardial region of the left ventricle (thick arrow indicates infarct scar; 400× magnification). Panel D demonstrates inten immunoreactivity in the viable cardiomyocytes (long thin arrow), endothelial cells (short arrow), and microvasculature (dashed arrow) in the infarct zone of the lef ventricle of a CHF animal (400× magnification). Panels E and F show intense UT immunoreactivity in the microvasculature (dashed arrows) of both the infarct and peri-infarct zone respectively (400× magnification). Panel G demonstrates moderate to strong diffuse UT immunoreactivity in the right ventricle of CHF animals (300× magnification). Panel H is a negative control demonstrating no immunoreactivity of the same section as panel D (thin arrow indicating viable myocardium and dashed arrow indicating myocardial vessel) when the primary serum is omitted. All sections were counterstained with hematoxylin. Scale bars represent 75 μm.

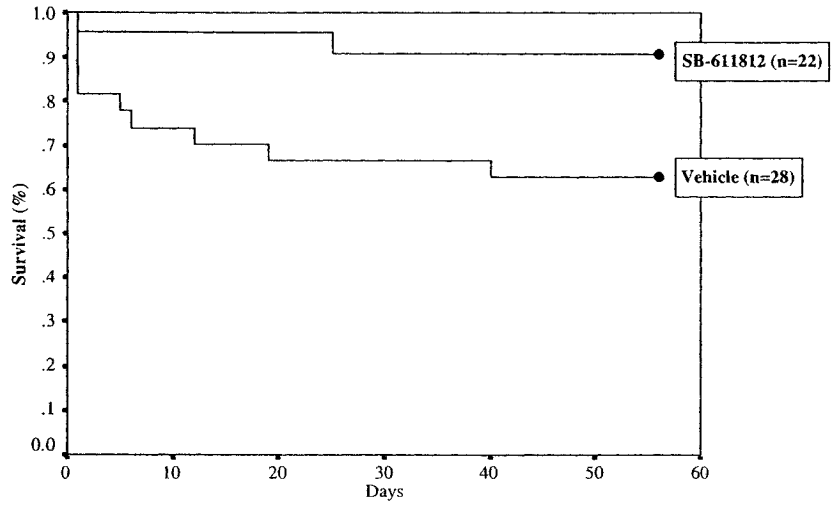

Fig. 4. Kaplan–Meier survival plot. A survival plot demonstrating a significant reduction in overall mortality in only the SB-611812 group in which treatment started on day 0 (2/22), compared to vehicle-treated animals (10/28) started at the same time as the treatment group ($P = 0.024$).

3.5. Sub-study: effect of delayed treatment (day 10)

Two additional groups, which were given either the antagonist or vehicle starting on day 10 post-MI were also evaluated. Similarly to the group in which treatment was administered on day 0, delayed SB-611812 administration resulted in a significant reduction in LVEDP (10.38 ± 1.65 mm Hg vs. 19.4 ± 2.25 mm Hg; $P < 0.01$). Also, both RVSP and CVP were significantly reduced in the treatment group compared to the vehicle group (22.37±3.33 mm Hg vs. 33.67 ± 2.23 mm Hg and 3.87 ± 0.515 mm Hg vs. 7.11 ± 0.655 mm Hg, respectively; $P < 0.05$). Furthermore, there was a significant reduction in lung wet-to-dry weight ratio (4.77 ± 0.067 vs. 5.01 ± 0.072; $P < 0.05$). There was no significant difference between treatment and vehicle (started on day 10) for other parameters including LVSP, ±dP/dt, MAP, or heart weight to body weight ratio. Infarct sizes were slightly smaller in treatment group compared to vehicle group; however, this was not statistically significant (38.2 ± 2.7 vs. 32.1 ± 2.7; $P = 0.15$).

Table 3
Hemodynamic parameters, cardiac function, heart weight, and lung edema for the three study groups

Parameters	Sham ($n = 9$)	Vehicle ($n = 16$)	SB611812 ($n = 17$)
LVEDP (mm Hg)	7.18 ± 0.91	19.0 ± 1.06[a]	10.6 ± 1.10[b]
RVSP (mm Hg)	27.3 ± 0.78	32.6 ± 0.79[a]	27.7 ± 1.50[b]
CVP (mm Hg)	3.78 ± 0.28	7.47 ± 0.56[a]	5.31 ± 0.62[b]
+dP/dt	4050 ± 273	2765 ± 241[a]	3162 ± 184[a]
−dP/dt	4210.0 ± 258.1	2870 ± 249[a]	3183 ± 206[a]
LVSP (mm Hg)	108.1 ± 4.59	91.8 ± 4.89	92.1 ± 4.48
Psystolic (mm Hg)	103.9 ± 4.54	95.1 ± 5.76	98.8 ± 4.85
Pdiastolic (mm Hg)	65.89 ± 4.48	70.7 ± 5.59	72.9 ± 4.53
MAP (mm Hg)	78.4 ± 3.85	78.8 ± 5.60	81.5 ± 4.29
HW/BW% (g/g)	0.241 ± 0.008	0.300 ± 0.016[a]	0.267 ± 0.005
Lung wet/dry ratio	4.62 ± 0.055	5.13 ± 0.064[a]	4.77 ± 0.066[b]
Infarct size	N/A	38.2% ± 2.2	33.06% ± 1.7
CM Area (AU)	199,977 ± 8324	321,897 ± 10,390[a]	256,382 ± 7705[b]
Chamber area (AU)/ body weight (g)	39.8 ± 4.9	82.1 ± 6.2[a]	48.4 ± 4.9[b]

LVSP (left ventricular systolic pressure), Psystolic (systolic blood pressure), Pdiastolic (diastolic blood pressure), MAP (mean arterial pressure), LVEDP (left ventricular end-diastolic pressure), RVSP (right ventricular systolic pressure), CVP (central venous pressure), +dP/dt (the first derivative of the rate in positive pressure change in the ventricle), −dP/dt (the first derivative of the rate in negative pressure change in the ventricle), HW/BW (heart weight to body weight ratio), lung wet:dry weight ratio, infarct size, CM Area AU (cardiomyocyte area in arbitrary units).

[a] Indicates $P < 0.05$ vs. sham.

[b] Indicates $P < 0.05$ vs. vehicle.

4. Discussion

The present study demonstrated increased expression of UII and UT in the myocardium of rats with CHF secondary to myocardial infarction. Hence based on these findings, the efficacy of UII blockade using a specific UT antagonist, SB-611812 was evaluated in the rat CHF model. This is the first in vivo study demonstrating the efficacy of UT blockade in an experimental model of CHF using a selective nonpeptidic UT receptor antagonist, SB-611812. This antagonist is highly selective for the UT receptor and is devoid of any agonist activity, which has been a hindrance with previous UT antagonists described in the literature [17]. Importantly, SB-611812 led to a decrease in mortality. However, due to the small number of animals in this study, we must use caution when interpreting the survival benefit of this drug. In addition to the reduced mortality, treatment showed an improvement in CHF as evidenced by significantly reduced LVEDP, lung edema, RVSP, and CVP when compared to the control group receiving only the drug vehicle, methylcellulose. These findings demonstrate an important role for UII in cardiovascular function and structure, and suggest a potential therapeutic significance for selective UT antagonism in the treatment of CHF.

Comparison of SB-611812 with other receptor antagonists in similar models indicates a large therapeutic potential for this antagonist. Of note, endothelin receptor antagonists have

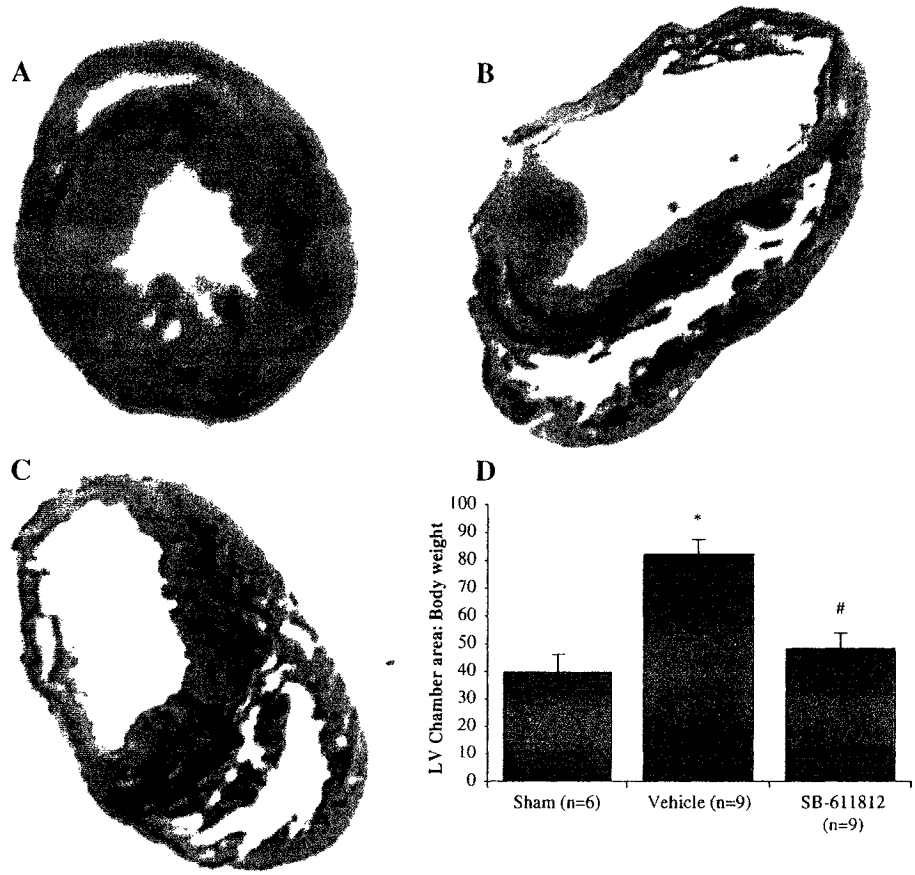

Fig. 5. Analysis of left ventricular chamber area. Representative photomicrographs of transversely cut hearts from sham (A), vehicle (B), and SB-611812 (started on day 0) (C) groups stained with Mason's trichrome. (D) Graph representing quantification left ventricular chamber area/body weight ratio in sham (n = 6), Vehicle (n = 9), and treatment (n = 9) groups. * indicates $P < 0.05$ vs. sham; # indicates $P < 0.05$ vs. vehicle.

actually shown increased mortality and adverse ventricular remodeling following coronary ligation in the rat when administered early after infarction; however, delayed administration of the antagonists significantly improved cardiac function and survival [18,19]. Interestingly, our study demonstrates that there is no detrimental effect of early UT antagonism following myocardial infarction.

On the other hand, the use of angiotensin converting enzyme (ACE) inhibitors showed an improvement in cardiac function similar to the one reported here for the UT antagonist SB-611812 [20–22]. Although drug efficacies cannot be directly compared in such a manner because of variations in study parameters, it can still be appreciated that SB-611812 improves cardiac dysfunction associated with coronary artery ligation in a manner that is comparable to other therapeutic modalities including ACE inhibition which is a mainstay in cardiovascular therapy today.

The loss of functional contractile units following MI causes a reduction in pumping capacity of the heart. As a compensatory mechanism, the heart dilates to increase stroke volume. Here we show that treatment led to a significant reduction in ventricular dilatation compared to vehicle treated animals. Ventricular dilatation increases wall stress and the heart compensates by increasing cardiomyocyte size. Indeed, cardiac hypertrophy is an important prognostic determinant in heart disease and thus its attenuation is an important therapeutic mechanism. This study demonstrates that CHF in the rat is associated with a significant increase in cardiac hypertrophy and that treatment with SB-611812 significantly attenuated this hypertrophy. This finding is supported by others who showed that UII induced cardiomyocyte hypertrophy [8,12]. Recently, Johns et al. showed that the UII-induced cardiomyocyte hypertrophy was inhibited with the administration of a competitive peptidic UT receptor antagonist, BIM-23127 [12].

Previous studies have suggested that UII does not have a spare receptor reserve [23], therefore UII activity is regulated, at least in part, by altering the UII receptor expression. Therefore, in addition to demonstrating increased UII expression in heart failure which is well established in a variety of cardiovascular diseases, we also sought to evaluate if UT is differentially expressed in CHF. We demonstrated that UT protein expression is significantly increased using immunohistochemistry and Western blotting. Rat UT has a molecular weight (MW) of 42.7 kDa. However, this protein has several glycosylation sites and as such has been demonstrated to have a MW ~60 kDa [24]. Interestingly, we found using Western blotting, that the bands corresponding to ~60 kDa proteins were comparable

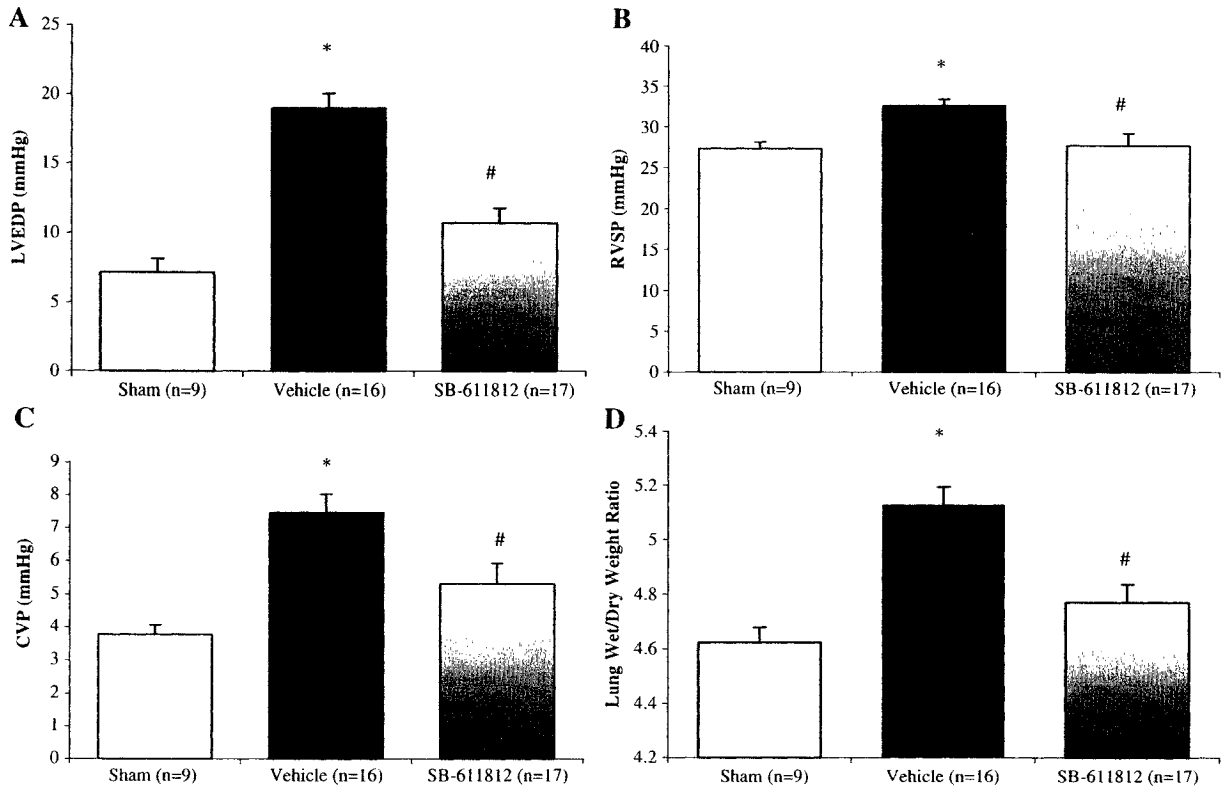

Fig. 6. Effect of UT receptor blockade on cardiac function and lung edema. Panel A demonstrates a significant reduction in LVEDP in the treatment (started on day 0) npared to the vehicle group. Similarly, panels B and C show a significant reduction in RVSP and CVP, respectively, in the treatment (started on day 0) compared to ..ie vehicle group. Panel D shows a significant reduction in lung wet-to-dry weight ratio in the treatment (started on day 0) compared to the vehicle group. * indicates $P < 0.05$ vs. sham; # indicates $P < 0.05$ vs. vehicle.

between normal and CHF hearts. However, there were two bands corresponding to proteins of MW of ~150 kDa and ~200 kDa that were significantly increased in CHF hearts. Notably, these same bands were seen with all three different antibodies raised against three different UT epitopes indicating UT specificity. Therefore, the high molecular weight proteins are likely homo- or hetero-protein oligomers. Oligomerization of G-protein coupled receptors is actually quite a prominent phenomenon and is now known to affect receptor specificity, pharmacology, and trafficking [25].

In conclusion, we have demonstrated, in a rat model of CHF induced by coronary ligation, up-regulation of myocardial UII and UT, and that blocking the UT receptor pathway with the specific UT antagonist SB-611812 leads to decreased mortality and improved parameters of cardiac function including decreased LVEDP, lung edema, RVSP and CVP, and reduces cardiac hypertrophy and dilatation. These findings suggest that SB-611812 shows substantial therapeutic potential for the treatment of myocardial infarction and CHF.

cknowledgments

This work was supported by grants from the Canadian Institute of Health and Research and the Quebec Heart and Stroke Foundation.

Appendix A. Supplementary data

Supplementary data associated with this article can be found, in the online version, at doi:10.1016/j.yjmcc.2006.05.008.

References

[1] Ames RS, Sarau HM, Chambers JK, Willette RN, Aiyar NV, Romanic AM, et al. Human urotensin-II is a potent vasoconstrictor and agonist for the orphan receptor GPR14. Nature 1999;401:282–6.

[2] Camarda V, Rizzi A, Calo G, Gendron G, Perron SI, Kostenis E, et al. Effects of human urotensin II in isolated vessels of various species; comparison with other vasoactive agents. Naunyn Schmiedeberg's Arch Pharmacol 2002;365:141–9.

[3] Bohm F, Pernow J. Urotensin II evokes potent vasoconstriction in humans in vivo. Br J Pharmacol 2002;135:25–7.

[4] Douglas SA, Sulpizio AC, Piercy V, Sarau HM, Ames RS, Aiyar NV, et al. Differential vasoconstrictor activity of human urotensin-II in vascular tissue isolated from the rat, mouse, dog, pig, marmoset and cynomolgus monkey. Br J Pharmacol 2000;131:1262–74.

[5] Russell FD, Molenaar P, O'Brien DM. Cardiostimulant effects of urotensin-II in human heart in vitro. Br J Pharmacol 2001;132: 5–9.

[6] Sauzeau V, Le Mellionnec E, Bertoglio J, Scalbert E, Pacaud P, Loirand G. Human urotensin II-induced contraction and arterial smooth muscle cell proliferation are mediated by RhoA and Rho-kinase. Circ Res 2001; 88:1102–4.

[7] Watanabe T, Pakala R, Katagiri T, Benedict CR. Synergistic effect of urotensin II with serotonin on vascular smooth muscle cell proliferation. J Hypertens 2001;9:2191–6.

[8] Tzanidis A, Hannan RD, Thomas WG, Onan D, Autelitano DJ, See F, et al. Direct actions of urotensin II on the heart: implications for cardiac fibrosis and hypertrophy. Circ Res 2003;93:246–53.
[9] Douglas SA, Tayara L, Ohlstein EH, Halawa N, Giaid A. Congestive heart failure and expression of myocardial urotensin II. Lancet 2002;359: 1990–7.
[10] Richards AM, Nicholls MG, Lainchbury JG, Fisher S, Yandle TG. Plasma urotensin II in heart failure. Lancet 2002;360:545–6.
[11] Lapp H, Boerrigter G, Costello-Boerrigter LC, Jaekel K, Scheffold T, Krakau I, et al. Elevated plasma human urotensin-II-like immunoreactivity in ischemic cardiomyopathy. Int J Cardiol 2004;94:93–7.
[12] Johns DG, Ao Z, Naselsky D, Herold CL, Maniscalco K, Sarov-Blat L, et al. Urotensin-II-mediated cardiomyocyte hypertrophy: effect of receptor antagonism and role of inflammatory mediators. Naunyn Schmiedeberg's Arch Pharmacol 2004;370:238–50.
[13] Rakowski E, Hassan GS, Dhanak D, Ohlstein EH, Douglas SA, Giaid A. A role for urotensin II in restenosis following balloon angioplasty: use of a selective UT receptor blocker. J Mol Cell Cardiol 2005;9:785–91.
[14] Dhanak D, Knight SD. Sulfonamide derivative urotensin-II receptor antagonists, preparation, pharmaceutical compositions, and therapeutic use. PCT Int. Appl. WO 2001045694; 2001.
[15] Giaid A, Yanagisawa M, Langleben D, Michel RP, Levy R, Shennib H, et al. Expression of endothelin-1 in the lungs of patients with pulmonary hypertension. N Engl J Med 1993;328:1732–9.
[16] Saito T, Hu F, Tayara L, Fahas L, Shennib H, Giaid A. Inhibition of NOS II prevents cardiac dysfunction in myocardial infarction and congestive heart failure. Am J Physiol, Heart Circ Physiol 2002;283:H339–45.
[17] Behm DJ, Herold CL, Camarda V, Aiyar NV, Douglas SA. Differential agonistic and antagonistic effects of the urotensin-II ligand SB-710411 at rodent and primate UT receptors. Eur J Pharmacol 2004; 492:113–6.
[18] Nguyen QT, Cernacek P, Calderoni A, Stewart DJ, Picard P, Sirois P, et al. Endothelin A receptor blockade causes adverse left ventricular remodeling but improves pulmonary artery pressure after infarction in the rat. Circulation 1998;98:2323–30.
[19] Mulder P, Richard V, Derumeaux G, Hogie M, Henry JP, Lallemand F, et al. Role of endogenous endothelin in chronic heart failure: effect of long-term treatment with an endothelin antagonist on survival, hemodynamics, and cardiac remodeling. Circulation 1997;96:1976–82.
[20] Pfeffer JM. Progressive ventricular dilation in experimental myocardial infarction and its attenuation by angiotensin-converting enzyme inhibition. Am J Cardiol 1991;68:17D–25D.
[21] Jain P, Korlipara G, Mallavarapu C, Sikand V, Lillis O, Cohn PF. Effects of captopril therapy after late reperfusion on left ventricular remodeling after experimental myocardial infarction. Am Heart J 1994;4 Pt 1:756–63.
[22] Lapointe N, Blais Jr C, Adam A, Parker T, Sirois MG, Gosselin H, et al. Comparison of the effects of an angiotensin-converting enzyme inhibitor and a vasopeptidase inhibitor after myocardial infarction in the rat. J Am Coll Cardiol 2002;39:1692–8.
[23] Douglas SA, Dhanak D, Johns DG. From 'gills to pills': urotensin-II as a regulator of mammalian cardiorenal function. Trends Pharmacol Sci 2004; 25:76–85.
[24] Boucard AA, Sauve SS, Guillemette G, Escher E, Leduc R. Photolabelling the rat urotensin II/GPR14 receptor identifies a ligand-binding site in the fourth transmembrane domain. Biochem J 2003;370:829–38.
[25] Prinster SC, Hague C, Hall RA. Heterodimerization of g protein-coupled receptors: specificity and functional significance. Pharmacol Rev 2005; 57:289–98.

PEPTIDES XXX (2006) XXX–XXX

available at www.sciencedirect.com

ScienceDirect

journal homepage: www.elsevier.com/locate/peptides

Urotensin-II receptor blockade with SB-611812 attenuates cardiac remodeling in experimental ischemic heart disease

Nicolas Bousette [a], *Julia Pottinger* [a], *Wisam Ramli* [a], *Eliot H. Ohlstein* [b], *Dashyant Dhanak* [c], *Stephen A. Douglas* [b], *Adel Giaid* [a,*]

[a] *Division of Cardiology, Montreal General Hospital, McGill University Health Center, Suite L3-109, 1650 Cedar Avenue, Montreal, Quebec H3G 1A4, Canada*

[b] *The Cardiovascular and Urogenital-CEDD, GlaxoSmithKline, King of Prussia, PA 19406, USA*

[c] *Microbial, Musculoskeletal and Proliferative Diseases CEDD, GlaxoSmithKline, Collegeville, PA 19426, USA*

ARTICLE INFO

Article history:
Received 26 May 2006
Received in revised form
28 June 2006
Accepted 29 June 2006

Keywords:
Rat
Myocardial infarction
Fibrosis
Collagen
Urotensin-II

ABSTRACT

It is now well established that urotensin-II (UII) levels are increased in several cardiovascular diseases. We previously demonstrated that UII and the UII receptor (UT) protein levels are significantly increased in the hearts of both humans and rats with congestive heart failure (CHF). We have also recently demonstrated that UII blockade, with a selective UII antagonist, improves heart function in a rat model of ischemic CHF. Here, we evaluated the attenuation of cardiac remodeling associated with UII antagonism in the same rat model of ischemic CHF. Animals were administered a specific UT receptor antagonist, SB-611812 (30 mg/kg/day, gavage), or vehicle 30 min prior to coronary artery ligation followed by daily treatment for 8 weeks. Myocardial interstitial fibrosis was analyzed by Masson's trichrome and picrosirius red staining. RT-PCR analysis was utilized for mRNA expression studies. We used Western blotting to assess levels of collagen types I and III. Mitogenic activity of UII on cultured neonatal cardiac fibroblasts was also evaluated. Following coronary ligation, SB-611812 significantly attenuated both myocardial and endocardial interstitial fibrosis, and reduced collagen type I:III ratio ($P < 0.01$). UII induced proliferation of cardiac fibroblasts and this mitogenic effect was significantly inhibited with 1 μM of SB-611218 ($P < 0.05$). We demonstrate here that selective blockade of UT reduces diastolic dysfunction by decreasing myocardial fibrosis post-coronary ligation in vivo, and inhibits UII-mediated fibroblast proliferation in vitro.

1. Introduction

Urotensin-II is a small peptide with pleiotropic effects reminiscent of endothelin-1. UII binds a G-protein coupled receptor which activates a variety of intracellular signaling molecules [16,18]. UII and its receptor, UT, are widely expressed throughout the body particularly in the cardiovascular system [1,5]. We have previously demonstrated increased expression of UII and UT in the heart of patients with end-stage congestive heart failure due to either dilated or ischemic cardiomyopathy [4]. In the same study we showed that UII levels were significantly correlated with left ventricular end-diastolic dimension and

* *Corresponding author*. Tel.: +1 514 934 1934x43841; fax: +1 514 934 8344.
E-mail address: adel.giaid@mcgill.ca (A. Giaid).

0196-9781/$ – see front matter © 2006 Elsevier Inc. All rights reserved.
doi:10.1016/j.peptides.2006.06.011

inversely correlated with ejection fraction. In addition to the significantly elevated UII protein expression we also found that UII binding sites, a surrogate marker to UT levels, was significantly increased in end stage heart failure tissue independent of the etiology of cardiac disease. The increased expression of UII and UT in failing hearts is further supported by several studies demonstrating increased plasma levels of UII in patients with CHF [9,11,14,15].

In addition, we have recently demonstrated that both UII and UT were significantly up-regulated in a model of congestive heart failure following coronary ligation in the rat. Blockade of UII signaling using a selective UII antagonist, SB-611812 improved heart function and attenuated cardiac hypertrophy and ventricular dilatation [2].

The most notable improvement in cardiac function was related to diastolic parameters including an attenuation of left ventricular end diastolic pressure, lung edema, right ventricular systolic pressure and central venous pressure. This suggested that UII blockade resulted in reduced myocardial stiffness.

Fibrosis, a fundamental characteristic of cardiac remodeling following infarction, increases myocardial stiffness in large part by interstitial collagen deposition. Interestingly UII, has been previously shown to have a pro-fibrotic effects. For example, Tzanidis et al. demonstrated that UII induced collagen type I, collagen type III, and fibronectin mRNA expression in rat neonatal cardiac fibroblasts [19]. Furthermore, Wang et al. demonstrated that UII induced collagen type I mRNA and protein while decreasing expression and activity of matrix metalloptroteinase-1 (MMP-1) in endothelial cells [20].

Thus, UII is elevated in heart failure and has been shown to induce extracellular matrix protein expression in vitro, however, the effects of UII on cardiac fibroblast growth remains to be elucidated. Therefore, the aim of the present study was to evaluate the effect of UT blockade on myocardial fibrosis in our previously established rat model of CHF and on neonatal cardiac fibroblast growth in culture.

2. Methods

2.1. *Details of SB-611812*

SB-611812, an arylsulfonamide UT antagonist (2,6-dichloro-*N*-(4-chloro-3-{[2-(dimethylamino)ethyl]oxy}phenyl)-4-(trifluoromethyl)benzenesulfonamide), was synthesized at GlaxoSmithKline, King of Prussia, PA [3]. Selectivity and characteristics of this small molecule have been previously described [2,13].

2.2. *MI protocol*

Throughout the study male Lewis rats weighing ~250 g obtained from Charles River laboratories were used. Animals were divided into three groups including a sham group ($n = 9$), an MI + treatment group ($n = 17$), and an MI + vehicle group ($n = 16$). Animals were blindly randomized to either treatment or vehicle administration.

Under general anesthesia animals were subjected to ligation of the left anterior descending (LAD) coronary artery or sham operation as previously described [2]. The treatment group received the first dose of the UT antagonist, SB-611812 (30 mg/kg/day; by gavage), 30 min prior to coronary ligation and then daily subsequently [2]. The vehicle group underwent the same protocol as the treatment group except that they received just the drug vehicle (0.1% methylcellulose) instead of the treatment drug. Daily administration of either drug or vehicle was carried out for the duration of the study (8 weeks). Analyses of hemodynamic, cardiac function, and lung edema were carried out as previously described [2]. Experiments were performed in accordance with the Guide for the Care and Use of Laboratory Animals (National Institutes of Health Publication 86 to 23, revised 1996), and with approval of the Animal Care Committee of the McGill University Health Center.

2.3. *Tissue collection*

Eight weeks after surgery, animals were anaesthetized before exsanguination. The hearts were harvested and dissected in which a transverse slice of approximately 2–3 mm was taken in the center of the infarction or in the midline between the base of the heart and the apex for sham rats. This slice was fixed in 4% paraformaldehyde and embedded in paraffin for histological analysis. The rest of the myocardium was dissected to separate the left ventricle, interventricular septum, right ventricle and atria. These myocardial specimens were then snap frozen in liquid nitrogen and stored at −80 °C.

2.4. *Histology*

All hearts were sectioned across the ventricles (cut in transverse fashion) for histological analyses. The extent of fibrosis in both the viable left ventricle and infarcted region was quantified using Masson's trichome stained heart sections. Specifically, for analysis of fibrosis in the viable left ventricle, six random photomicrograghs were taken in the viable left ventricular myocardium at 400× magnification for each animal. The extent of fibrosis in these photomicrographs was then quantified by *Image ProPlus* in a blinded manner. For analysis of fibrosis within the infarcted region, three photomicrographs from each animal were taken and blue staining was quantified. Histological assessment of fibrillar collagen deposition using picrosirius red staining was also carried out. The latter was evaluated (in both viable myocardium and in the infarct region) in same fashion as with that of the Masson's trichrome stained heart sections described above.

2.5. *Western blotting*

Protein samples were assayed with specific antibodies against collagen type I, collagen type III (Santa-Cruz Biotechnology, CA), as previously described [17]. Sample protein concentration was determined using the modified Bradford assay (Bio-Rad, Ont., Canada) and equal protein loading conditions were utilized. Protein bands were then quantified using arbitrary units (AU) with the image analysis program, *Image ProPlus* (Media Cybernetics, CA, USA).

2.6. *Real time RT-PCR*

Left ventricular myocardial samples (for *n* values see Table 1) were retrieved from storage for RNA extraction using Trizol

Please cite this article as: Nicolas Bousette et al., Urotensin-II receptor blockade with SB-611812 attenuates cardiac remodeling in experimental ischemic heart disease, Peptides (2006), doi:10.1016/j.peptides.2006.06.011.

Table 1 – Relative expression of genes associated with CHF determined by RT-PCR

Genes	Sham ($n = 8$)	Vehicle ($n = 12$)	SB-611812 ($n = 8$)
Collagen type I	0.864 ± 0.012	0.948 ± 0.014*	0.927 ± 0.025
Collagen type III	0.910 ± 0.007	1.013 ± 0.015*	0.994 ± 0.021*
Fibronectin	0.782 ± 0.004	0.837 ± 0.011*	0.820 ± 0.014
MMP-2	0.383 ± 0.005	0.395 ± 0.006	0.392 ± 0.007
MMP-9	0.493 ± 0.007	0.529 ± 0.013	0.536 ± 0.019
MMP-14	0.674 ± 0.004	0.691 ± 0.008	0.681 ± 0.010
TIMP-1	0.695 ± 0.005	0.748 ± 0.007*	0.739 ± 0.012*
TIMP-2	0.884 ± 0.004	0.919 ± 0.006	0.901 ± 0.008
TIMP-3	0.804 ± 0.005	0.799 ± 0.008	0.786 ± 0.012

MMP, matrix metalloproteinase; TIMP, tissue inhibitor of MMP.
* Indicates $P < 0.05$ vs. sham.

(Invitrogen, Ont., Canada) and performed as per the manufacturer's instructions. PCR methodology was previously described [2]. Primers were designed using PrimerQuest biotool [www.idtdna.com] (Table 2). All values for mRNA expression determined by RT-PCR are expressed as the ratio of the copy number of the mRNA transcript of interest to the copy number of the mRNA transcript of the housekeeping gene RPL32. A homogeneous amplification of the products was verified by melting curve analysis of the amplified products.

Table 2 – Primer sequences

Collagen type I F	5′-GCA ACA GTC GAT TCA CCT ACA GCA-3′
Collagen type I R	5′-AAT GTC CAA GGG AGC CAC ATC-3′
Collagen type III F	5′-AGA AGT CTC TGA AGC TGA TGG-3′
Collagen type III R	5′-GCT CCA TTC ACC AGT TGT-3′
Fibronectin F	5′-CAG TGG CAG AAA GAG TAT CTC G-3′
Fibronectin R	5′-GTA TAC TGG TTG TAG GTG TGG-3′
MMP-2 F	5′-GGG TCT ATT CTG CCA GCA CTC-3′
MMP-2 R	5′-CTC CAG AAC TTG TCT CCT GCA A-3′
MMP-9 F	5′-TCT CGA ATC ACG GAG GAA-3′
MMP-9 R	5′-TTT GCG CCC AGA GAA GAA-3′
MMP-14 F	5′-GAT TGA TGC AGC TCT CTT CTG-3′
MMP-14 R	5′-CCT TCC CAG ACT TTG ATG-3′
RPL32 F	5′-ATC CTG ATG CCC AAC ATT GGT TAC-3′
RPL32 R	5′-GTT GCA CAT CAG CAG CAC TTC CAG-3′
TIMP-1 F	5′-GTA AAG ACC TAT AGT GCT GGC TG-3′
TIMP-1 R	5′-GAG GAT CTG ATC TGT CCA CAA-3′
TIMP-2 F	5′-GGT CAC AGA GAA GAG CAT CAA TG-3′
TIMP-2 R	5′-GTC CTC GAT GTC AAG AAA CTC-3′
TIMP-3 F	5′-GAT CAA GTC CTG CTA CTA CTT GC-3′
TIMP-3 R	5′-CGT AGT GTT TGG ACT GAT AGC-3′

MMP, matrix metalloprotease; RPL32, ribosomal protein L32; TIMP, tissue inhibitors of MMPs.

2.7. *Fibroblast culture and proliferation assay*

The effect of SB-611218 on UII-stimulated ventricular fibroblast proliferation was investigated in rat cardiac fibroblasts that were purchased from Cell applications (CA, USA). Initially, cardiac fibroblasts from passage 5 were plated at an equal density of 10^4 cells/well in a 96 well plate in Dulbecco's Modified Eagle Medium (DMEM) with 10% bovine serum media (with 50 U/ml penicillin, 50 μg/ml streptomycin) for 48 h (37 °C) followed by serum starvation in DMEM/0.01% bovine serum albumin (BSA) media (with 50 U/ml penicillin, 50 μg/ml streptomycin) for 48 h. Following this, cells were incubated with either DMEM/10% serum media, DMEM/0.01% BSA media, DMEM/0.01% BSA media with either 1 pM, 1 nM, 100 nM rat UII (Peptide Institute, Osaka, Japan), or DMEM/0.01% BSA media with 100 nM UII + 1 μM SB-611812, for 48 h. Proliferation was quantified using the colorimetric BrDU ELISA proliferation assay from Roche (Montreal, Canada). Protocol was carried out as per manufacturer's instructions.

2.8. *Statistical analysis*

All parameters were evaluated using either one-way ANOVA test (with the Tukey post hoc test) or Student's t-test (for two group comparisons) with the aid of the statistical program *SPSS* 11.5. A P value of <0.05 was considered statistically significant.

3. Results

Cardiac function and hemodynamic data for the three study groups are presented in Table 3. Histological evaluation of hearts from rats treated with the UII antagonist, SB-611812 showed a significant attenuation in cardiac fibrosis. Specifically, Mason's trichrome analysis demonstrated significantly increased interstitial fibrosis in the non-infarct zone of the left ventricle of vehicle compared to sham animals (113,640 ± 4615 versus 52,747 ± 3737 arbitrary units; $P < 0.001$). In the same zone, the SB-611812-treated group had significantly reduced interstitial fibrosis compared to the vehicle group (86,928 ± 6031 versus 113,640 ± 4615; $P = 0.004$) (Fig. 1). In the infarct zone, there was no difference in the extent of fibrosis

Please cite this article as: Nicolas Bousette et al., Urotensin-II receptor blockade with SB-611812 attenuates cardiac remodeling in experimental ischemic heart disease, Peptides (2006), doi:10.1016/j.peptides.2006.06.011.

Table 3 – Cardiac function and hemodynamic parameters for the three study groups

Parameters	Sham ($n = 9$)	Vehicle ($n = 16$)	SB-611812 ($n = 17$)
LVEDP (mmHg)	7.2 ± 0.91	19.0 ± 1.06*	10.6 ± 1.10#
RVSP (mmHg)	27.3 ± 0.78	32.6 ± 0.79*	27.7 ± 1.50#
CVP (mmHg)	3.78 ± 0.28	7.47 ± 0.56*	5.31 ± 0.62#
+dP/dt	4050 ± 273	2765 ± 241*	3162 ± 184*
−dP/dt	4210 ± 258	2870 ± 249*	3183 ± 206*
LVSP (mmHg)	108.1 ± 4.59	91.8 ± 4.89	92.1 ± 4.48
$P_{systolic}$ (mmHg)	103.9 ± 4.5	95.1 ± 5.7	98.8 ± 4.8
$P_{diastolic}$ (mmHg)	65.9 ± 4.4	70.7 ± 5.5	72.9 ± 4.5
MAP (mmHg)	78.4 ± 3.8	78.8 ± 5.6	81.5 ± 4.3
Lung edema	4.62 ± 0.05	5.13 ± 0.06*	4.77 ± 0.07#

LVEDP, left ventricular end-diastolic pressure; RVSP, right ventricular systolic pressure; CVP, central venous pressure; +dP/dt, the first derivative of the rate in positive pressure change in the ventricle; −dP/dt, the first derivative of the rate in negative pressure change in the ventricle; LVSP, left ventricular systolic pressure; $P_{systolic}$, systolic blood pressure; $P_{diastolic}$, diastolic blood pressure; MAP, mean arterial pressure; lung edema was determined from lung wet-to-dry weight ratio.
* indicates $P < 0.05$ vs. sham.
# indicates $P < 0.05$ vs. vehicle.

between vehicle and SB-611812 treated groups (265,851 ± 11,749 versus 267,511 ± 9277).

Similarly, analysis of picrosirius red staining demonstrated that the non-infarct zone of the left ventricle of vehicle group exhibited significantly increased collagen deposition compared to sham animals (152,416 ± 32,426 versus 29,702 ± 3765; $P = 0.003$). In the same region, the SB-611812 treated group exhibited significantly reduced picrosirius red staining compared to the vehicle group (74,398 ± 9141 versus 152,416 ± 32,426; $P = 0.03$) (Fig. 2). Picrosirius red staining in the infarct region was comparable between vehicle and treatment groups (521,311 ± 18,690 versus 495,798 ± 24,481).

The marked attenuation of cardiac fibrosis in SB-611812 treated rats led us to quantify specific collagen types. Analysis of the protein levels for collagen types I and III indicated a significant reduction (83%) in the collagen type I:III ratio in the SB-611812 treated group compared to the vehicle group ($P < 0.05$) (Fig. 3A and D). This significant decrease in collagen I:III ratio was the result of a significant decrease in collagen type I in treated animals compared to untreated ($P < 0.05$)

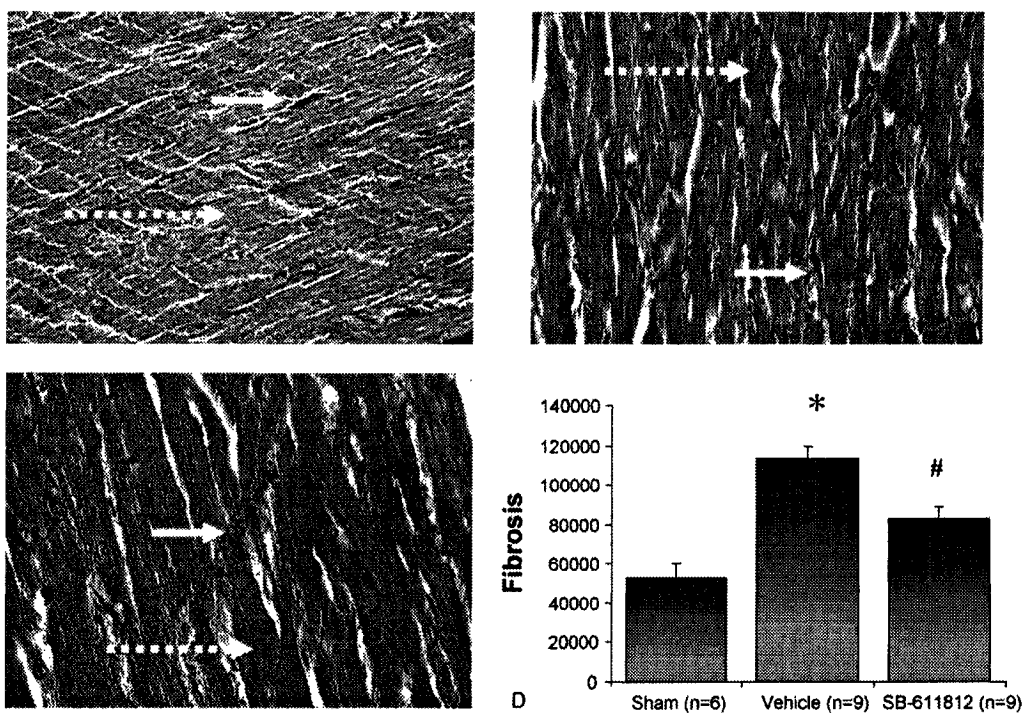

Fig. 1 – Analysis of interstitial fibrosis. Representative photomicrographs of viable left ventricle from sham (A), vehicle (B), and treatment (C) groups stained with Mason's trichrome. Short arrow indicates interstitial fibrosis (stained blue). Dashed long arrow indicates viable cardiomyocytes (stained red). (D) Graph representing quantification of interstitial fibrosis in sham ($N = 6$), Vehicle ($N = 9$), and treatment ($N = 9$) groups. (*) Indicates $P < 0.001$ vs. sham; (#) indicates $P = 0.004$ vs. vehicle. (For interpretation of the references to color in this figure legend, the reader is referred to the web version of the article.)

Please cite this article as: Nicolas Bousette et al., Urotensin-II receptor blockade with SB-611812 attenuates cardiac remodeling in experimental ischemic heart disease, Peptides (2006), doi:10.1016/j.peptides.2006.06.011

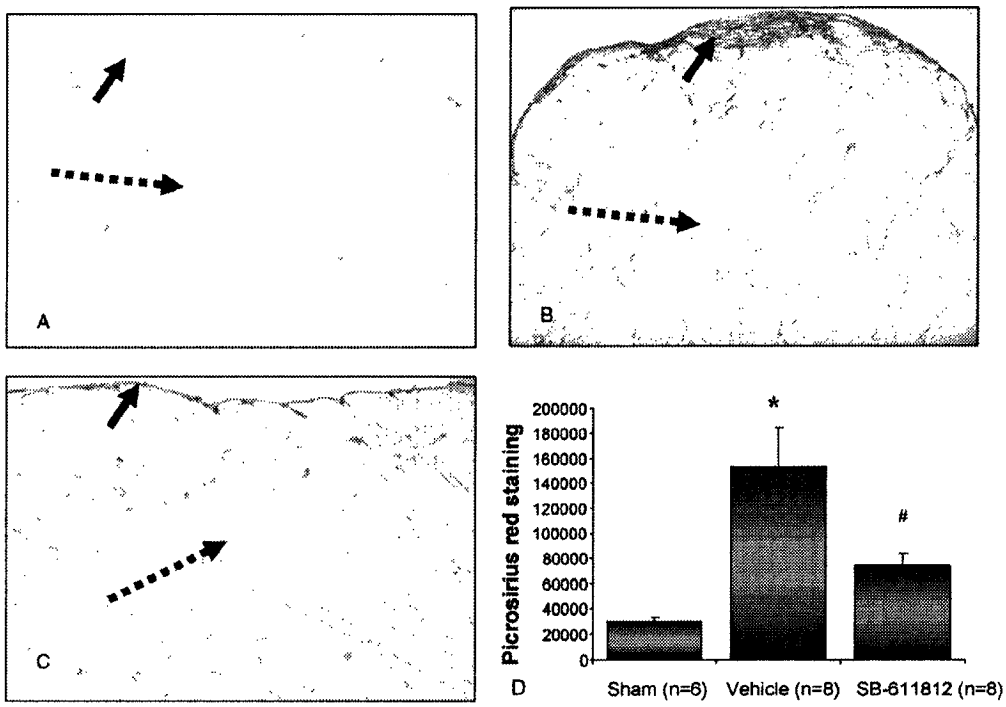

Fig. 2 – Analysis of collagen deposition. Representative photomicrographs of viable left ventricle from sham (A), vehicle (B), and treatment (C) groups stained with picrosirius red. Short arrow indicates endocardial collagen deposition (stained red). Dashed long arrow indicates viable cardiomyocytes (stained yellow). (D) Graph representing quantification of collagen deposition in sham ($N = 6$), vehicle ($N = 9$), and treatment ($N = 9$) groups. (*) Indicates $P = 0.003$ vs. sham; (#) indicates $P = 0.037$ vs. vehicle. (For interpretation of the references to color in this figure legend, the reader is referred to the web version of the article.)

(Fig. 3B), and a non-significant decrease in collagen type III protein levels (Fig. 3C).

We also evaluated mRNA expression levels for the extracellular matrix proteins collagen type I, collagen type III and fibronectin. Interestingly, collagen type I and fibronectin mRNA levels were reduced in the treatment group however this did not reach statistical significance (Table 1). We also evaluated the mRNA levels for matrix metalloproteinases (MMP) and tissue inhibitors of MMPs (TIMPs). Selective blockade of UT with SB-611812 had no effect on the levels of these factors (Table 1).

3.1. *Fibroblast proliferation assay*

UII demonstrated potent low efficacy mitogenic effects on cardiac fibroblasts as it significantly induced proliferation of these cells at 1 nM UII and 100 nM UII following incubation for 48 h ($P < 0.05$) (Fig. 4). The potency of UII is underscored by the fact that it tended to induce proliferation even at 1 pM UII, although this did not reach statistical significance ($P = 0.076$). Administration of the UT antagonist SB-611812 at a concentration of 1 μM completely inhibited the 100 nM UII-induced neonatal cardiac fibroblast proliferation ($P < 0.01$).

4. Discussion

It is now well established that the urotensin system is widely expressed in the myocardium, and it can modulate the physiologic and pathologic states of this system. Here, we sought to determine some of the mechanism involved in our recent findings of improved myocardial function in a rat model of ischemic CHF. Our data showed that the improvement in cardiac function observed with SB-611812 treatment was the result of attenuated cardiac remodeling following infarction. Indeed, we have demonstrated here that blockade of UII with SB-611812 led to a significant decrease in myocardial and endocardial fibrosis as well as a reduction in collagen deposition. Furthermore, we show that UII has a mitogenic effect of cardiac fibroblasts which may contribute to myocardial fibrosis post-coronary ligation.

There is evidence that collagen type I is more rigid while collagen type III has more elastic properties [10]. Therefore an increase in the ratio of collagen type I:III, as occurs in heart failure [7,21], would increase the rigid type collagen to the elastic type collagen thus explaining the increased myocardial stiffness observed in CHF. In fact Nishikawa et al. showed that a decrease in LVEDP, following amlodipine administration was associated with a decrease in the collagen type I:III ratio [12]. Interestingly, Kompa et al. demonstrated that chronic infusion of UII in the rat led to a 40% increase in LVEDP and that this was associated with a significant increase in the collagen type I:III ratio [8]. Here, we show that the treatment with the UT receptor antagonist SB-611812 led to a significant decrease in LVEDP (Table 3) and the collagen type I:III ratio. This difference in ratio was due to a significant decrease in collagen type I protein levels and a non-significant decrease in collagen type

Please cite this article as: Nicolas Bousette et al., Urotensin-II receptor blockade with SB-611812 attenuates cardiac remodeling in experimental ischemic heart disease, Peptides (2006), doi:10.1016/j.peptides.2006.06.011

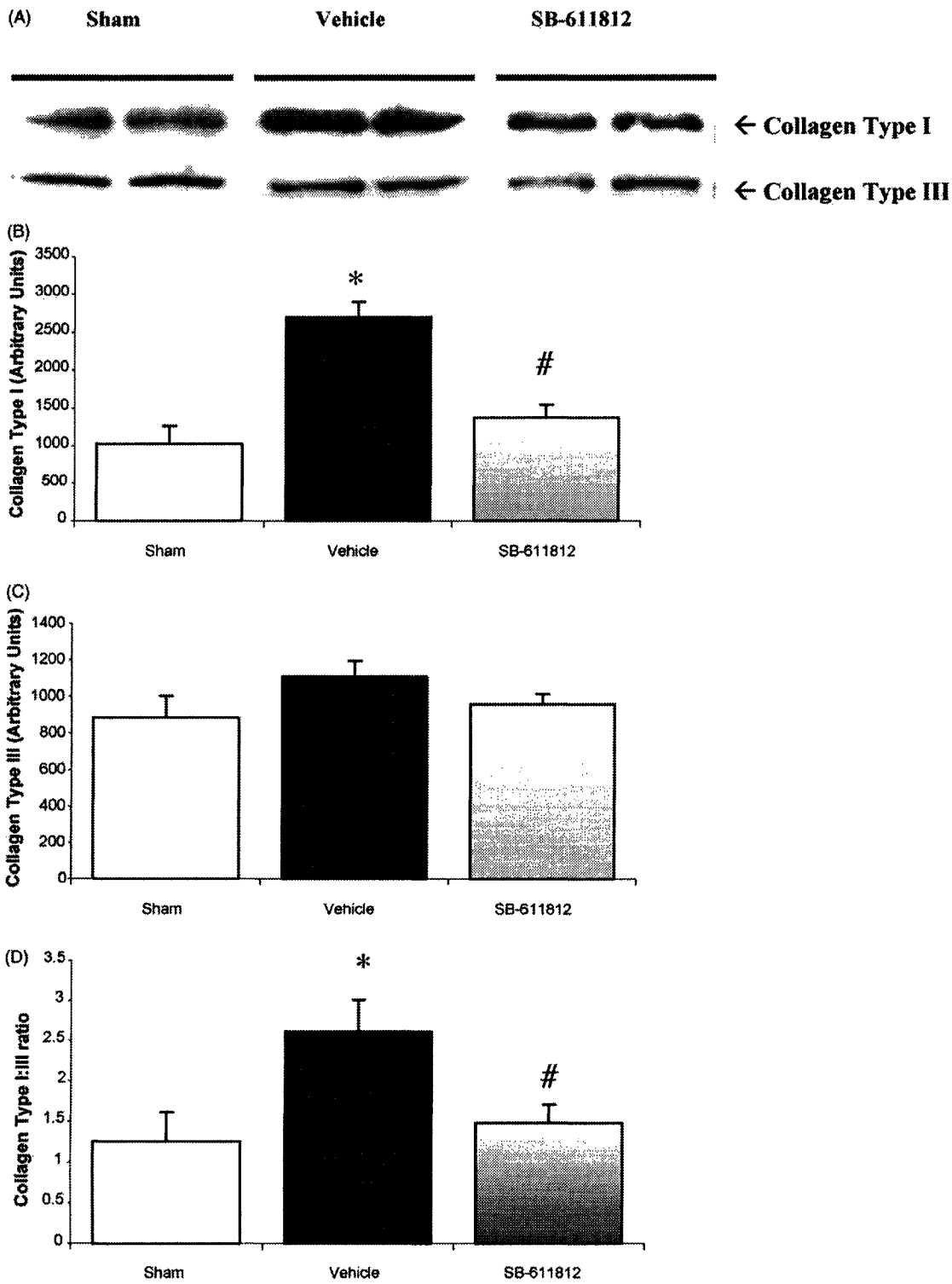

Fig. 3 – Effect of SB-611812 of collagen protein expression. Panel A, representative Western blots demonstrating collagen types I and III protein levels in the sham, vehicle and SB-611812 treatment groups. Panel B, a graph demonstrating the quantification of collagen type I protein levels in the sham ($n = 6$), vehicle ($n = 8$) and SB-611812 ($n = 9$) treatment groups. Panel C, a graph demonstrating quantification of collagen type III protein levels in the sham ($n = 6$), vehicle ($n = 8$) and SB-611812 ($n = 9$) treatment groups. Panel D, a graph demonstrating collagen type I:III ratio in the sham ($n = 6$), vehicle ($n = 8$) and SB-611812 ($n = 9$) treatment groups. (#) Indicates $P < 0.05$ vs. vehicle; (*) indicates $P < 0.05$ vs. sham.

Please cite this article as: Nicolas Bousette et al., Urotensin-II receptor blockade with SB-611812 attenuates cardiac remodeling in experimental ischemic heart disease, Peptides (2006), doi:10.1016/j.peptides.2006.06.011.

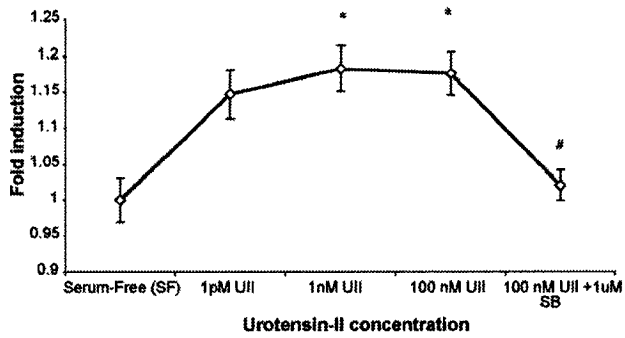

Fig. 4 – Urotensin-II induced rat fibroblast proliferation is inhibited by SB-611812. Dose–response graph demonstrating that UII acted as a potent, low efficacious, mitogen for rat neonatal cardiac fibroblasts, which significantly increased proliferation at 1 nM and 100 nM UII. Antagonism with 1 μM SB-611812 inhibited this effect at the highest UII concentration. (*) Indicates $P < 0.05$ vs. serum-free media; (#) indicates $P < 0.01$ vs. 100 nM UII.

III protein levels in the treatment compared to the vehicle group.

These findings are further supported by the demonstration of reduced reactive fibrosis in the viable myocardium as determined by Masson's trichrome staining as well as reduced endocardial collagen deposition as evidenced by reduced picrosirius red staining in the treatment group compared to the vehicle group. The mechanism of SB-611812 mediated inhibition of collagen type I synthesis will require further studies. In addition, it is of interest that collagen type I and fibronectin mRNA levels of the treatment group were not significantly different from the control sham group.

Myocardial fibrosis, a prominent characteristic of ventricular remodeling in CHF, is the result of increased deposition of extracellular matrix (ECM) proteins including collagens and fibronectin [21]. Notably, Tzanidis et al. have demonstrated UII induced collagen production from cardiac fibroblasts [19]. Also Wang et al. utilizing an endothelial cell culture, found that UII increased expression of collagen type I mRNA and protein and conversely decreased the expression of MMP-1 mRNA and protein as well as decreased the activity of MMP-1 [20]. UII activity in cardiac fibroblasts was further substantiated by He et al. who demonstrated UII induced proliferation of cardiac fibroblasts [6]. We also sought to determine if UII possessed mitogenic activity in neonatal cardiac fibroblasts. To this end, we show that UII induced cardiac fibroblast proliferation. Furthermore, we complimented these findings by demonstrating that UII induced proliferation of rat cardiac fibroblasts was inhibited with the use of the UT antagonist SB-611812.

In summary, we have unraveled here some of the mechanism involved in the improvement in cardiac dysfunction in ischemic heart disease. Specifically, selective UT antagonism with SB-611812 reduced myocardial fibrosis and collagen deposition in vivo, and reduced myocardial fibroblast proliferation in vitro. These findings suggest an important therapeutic role for UT antagonists in cardiac remodeling and fibrosis.

Acknowledgements

This work was supported by grants from the Canadian Institute of Health and Research and the Quebec Heart and Stroke Foundation. We also thank Fu Hu for his technical assistance with surgical protocols.

REFERENCES

[1] Ames RS, Sarau HM, Chambers. et al. Human urotensin-II is a potent vasoconstrictor and agonist for the orphan receptor GPR14. Nature 1999;401:282–6.
[2] Bousette N, Hu F, Ohlstein EH, Dhanak D, Douglas SA, Giaid A. Urotensin-II blockade with SB-611812 attenuates cardiac dysfunction in a rat modal of coronary artery ligation. J Mol Cell Cardiol 2006;41:285–95.
[3] Dhanak D, Knight SD. Sulfonamide derivative urotensin-II receptor antagonists, preparation, pharmaceutical compositions, and therapeutic use. PCT Int Appl WO 2,001,045,694 2001.
[4] Douglas SA, Tayara L, Ohlstein EH, Halawa N, Giaid A. Congestive heart failure and expression of myocardial urotensin II. Lancet 2002;359:1990–7.
[5] Elshourbagy NA, Douglas SA, Shabon U, Harrison S, Duddy G, Sechler JL, et al. Molecular and pharmacological characterization of genes encoding urotensin-II peptides and their cognate G-protein-coupled receptors from the mouse and monkey. Br J Pharmacol 2002;136:9–22.
[6] He YH, Hong JM, Guo HS, Wei JR, Chen H, Zuo HH, et al. Effects of urotensin II on cultured cardiac fibroblast proliferation and collagen type I mRNA expression. Di Yi Jun Yi Da Xue Xue Bao 2004;24:505–8 [Chinese].
[7] Huang Y, Hunyor SN, Jiang L, Kawaguchi O, Shirota K, Ikeda Y, et al. Remodeling of the chronic severely failing ischemic sheep heart after coronary microembolization: functional, energetic, structural, and cellular responses. Am J Physiol Heart Circ Physiol 2004;286:H2141–50.
[8] Kompa AR, Thomas WG, See F, Tzanidis A, Hannan RD, Krum H. Cardiovascular role of urotensin II: effect of chronic infusion in the rat. Peptides 2004;25:1783–8.
[9] Lapp H, Boerrigter G, Costello-Boerrigter LC, Jaekel K, Scheffold T, Krakau I, et al. Elevated plasma human urotensin-II-like immunoreactivity in ischemic cardiomyopathy. Int J Cardiol 2004;94:93–7.
[10] Marijianowski MM, Teeling P, Mann J, Becker AE. Dilated cardiomyopathy is associated with an increase in the type I/type III collagen ratio: a quantitative assessment. J Am Coll Cardiol 1995;25:1263–72.
[11] Ng LL, Loke I, O'Brien RJ, Squire IB, Davies JE. Plasma urotensin in human systolic heart failure. Circulation 2002;106:2877–80.
[12] Nishikawa N, Masuyama T, Yamamoto K, et al. Long-term administration of amlodipine prevents decompensation to diastolic heart failure in hypertensive rats. J Am Coll Cardiol 2001;38:1539–45.
[13] Rakowski E, Hassan GS, Dhanak D, Ohlstein EH, Douglas SA, Giaid A. A role for urotensin II in restenosis following balloon angioplasty: use of a selective UT receptor blocker. J Mol Cell Cardiol 2005;39:785–91.
[14] Richards AM, Nicholls MG, Lainchbury JG, Fisher S, Yandle TG. Plasma urotensin II in heart failure. Lancet 2002;360:545–6.
[15] Russell FD, Meyers D, Galbraith AJ, Bett N, Toth I, Kearns P, et al. Elevated plasma levels of human urotensin-II

immunoreactivity in congestive heart failure. Am J Physiol Heart Circ Physiol 2003;285:H1576–81.
[16] Saetrum Opgaard O, Nothacker H, Ehlert FJ, Krause DN. Human urotensin II mediates vasoconstriction via an increase in inositol phosphates. Eur J Pharmacol 2000;406:265–71.
[17] Saito T, Hu F, Tayara L, Fahas L, Shennib H, Giaid A. Inhibition of NOS II prevents cardiac dysfunction in myocardial infarction and congestive heart failure. Am J Physiol Heart Circ Physiol 2002;283: H339–45.
[18] Tasaki K, Hori M, Ozaki H, Karaki H, Wakabayashi I. Mechanism of human urotensin II-induced contraction in rat aorta. J Pharmacol Sci 2004;94: 376–83.
[19] Tzanidis A, Hannan RD, Thomas WG, Onan D, Autelitano DJ, See F, et al. Direct actions of urotensin II on the heart: implications for cardiac fibrosis and hypertrophy. Circ Res 2003;93:246–53.
[20] Wang H, Mehta JL, Chen K, Zhang X, Li D. Human urotensin II modulates collagen synthesis and the expression of MMP-1 in human endothelial cells. J Cardiovasc Pharmacol 2004;44:577–81.
[21] Wei S, Chow LT, Sanderson JE. Effect of carvedilol in comparison with metoprolol on myocardial collagen postinfarction. J Am Coll Cardiol 2000;36:276–81.

Please cite this article as: Nicolas Bousette et al., Urotensin-II receptor blockade with SB-611812 attenuates cardiac remodeling in experimental ischemic heart disease, Peptides (2006), doi:10.1016/j.peptides.2006.06.011.

ELSEVIER

Atherosclerosis 176 (2004) 117–123

ATHEROSCLEROSIS

www.elsevier.com/locate/atherosclerosis

Increased expression of urotensin II and its cognate receptor GPR14 in atherosclerotic lesions of the human aorta

Nicolas Bousette[a], Lisa Patel[b], Stephen A. Douglas[b], Eliot H. Ohlstein[b], Adel Giaid[a,*]

[a] *Montreal General Hospital, Suite L3-109, 1650 Cedar Avenue, Montreal, Que., Canada H3G 1A4*
[b] *The Cardiovascular and Urogenital Drug Discovery Group, GlaxoSmithKline, PA, USA*

Received 31 January 2003; received in revised form 1 March 2004; accepted 29 March 2004

Available online 26 June 2004

Abstract

Urotensin II (U-II), a novel vasoactive peptide, possesses a wide range of cardiovascular effects. U-II binds a seven transmembrane spanning G-protein coupled receptor termed GPR14. In the present study, we have characterized U-II expression in both carotid and aortic atherosclerotic plaques. Using immunohistochemistry we demonstrated U-II immunoreactivity in endothelial, smooth muscle and inflammatory cells of both carotid and aortic plaques, with a clear propensity for intimal staining. Using quantitative real-time RT-PCR we observed both increased U-II and GPR14 mRNA expression in tissue extracts from abdominal aortic aneurysms. We also extended our PCR analysis to include leukocyte expression of U-II and GPR14. We found that lymphocytes were by far the largest producers of U-II mRNA. In contrast monocytes and macrophages were the largest producers of GPR14 mRNA, with relatively little expression in foam cells, lymphocytes, and platelets. Our findings qualitatively and quantitatively demonstrate increased expression of U-II in atherosclerosis with a large degree of inflammatory cell involvement. These findings suggest a possible role for U-II in the pathophysiology of atherosclerosis.

Keywords: Endothelial cells; Inflammatory cells; RT-PCR; Immunohistochemistry

1. Introduction

Atherosclerosis, the leading cause of myocardial infarction and stroke, generally affects muscular and elastic arteries. Of these, carotid arteries and aortae are common targets. Many vasoactive factors are now known to play an important role in the pathophysiology of atherosclerosis. A novel vasoactive peptide, termed Urotensin-II (U-II), has been shown to have many properties reminiscent of endothelin-1. Human U-II is an 11 amino acid peptide [1], with a molecular weight of ~1388 [2]. Expression of U-II has been shown throughout the cardiovascular, nervous and urogenital systems [3–6]. We have recently shown increased myocardial expression of U-II in patients with congestive heart failure [5]. Others have reported expression of U-II in the heart and aorta of man, monkeys and mice [2,7]. Pharmacologic studies have shown that U-II is the most potent vasoconstrictor peptide isolated to date, however the vasoactive properties of U-II depend on the anatomical site and the type of species [3,4,7]. In addition to its marked vasoactivity, there is substantial evidence suggesting a role for this factor in atherosclerosis. U-II has also shown potent mitogenic effects on smooth muscle cells, with synergistic effects observed when combined with mildly oxidized low-density lipoprotein (moxLDL), as well as with 5-HT (serotonin) [8–10]. Of note is the finding that U-II stimulates hyperlipidemia in fish by enhancing depot lipase activity, and it channels glucose to free fatty acid synthesis [11]. Interestingly Matsushita et al. observed increased urinary levels of U-II in patients with hypertensive renal glomerular disease compared to normotensive glomerular disease [2]. They attributed the increase to glomerular arteriosclerosis, a vascular disorder very closely related to atherosclerosis.

The cognate receptor of U-II is known to be GPR 14, a seven transmembrane spanning G-protein coupled receptor [12,13]. Abundant expression of the receptor was

* Corresponding author. Tel.: +1 514 934 1934x43841; fax: +1 514 934 8448.
E-mail address: adel.giaid@mcgill.ca (A. Giaid).

0021-9150/$ – see front matter
doi:10.1016/j.atherosclerosis.2004.03.023

reported in the heart and pancreas of humans [3]. Specifically it was found in the atria and ventricles of the heart, as well as in endothelial cells and smooth muscle cells of the aortae and coronary arteries [3]. The biological activity of U-II in the cardiovascular system led us to hypothesize that there is an up-regulation of U-II in atherosclerosis. To test this, we qualitatively examined the expression of U-II using immunohistochemistry in two common pathologies of atherosclerosis including carotid arterial stenosis and abdominal aortic atherosclerosis. We also quantitatively examined the expression, using real-time PCR, of both prepro-U-II and it's cognate receptor GPR14 in tissue samples obtained from patients who had surgery for either abdominal aortic aneurysms or carotid endarterectomies. Finally, we examined the profile of U-II and GPR14 expression in the leukocyte sub-populations.

2. Materials and methods

2.1. Tissue samples

Samples were retrieved from male subjects with an age range of 60–80 years.

Tissue samples used for immunohistochemistry were retrieved either at autopsy [carotid arteries ($n = 5$), and abdominal aortae ($n = 4$)], or freshly during surgery for carotid endarterectomy ($n = 3$) or abdominal aortic aneurysmal repair ($n = 4$). Samples from autopsy cases were collected a maximum of 8 h after death. Samples were fixed in formalin, embedded in paraffin, and then cut using a microtome (5 μm thick). Tissue samples used for RT-PCR were collected freshly at surgery (Guys and St. Thomas Hospital, London, England) for carotid endarterectomy ($n = 17$), or abdominal aortic aneurysms repair ($n = 8$). Normal human aortae ($n = 7$) were obtained from the Anatomic Gift Foundation (White Oak, GA, USA). Samples were snap frozen in liquid nitrogen and stored at −80 °C until further use.

2.2. Immunohistochemistry

Immunohistochemical staining for U-II, Von Willebrand factor and smooth muscle cell actin was performed using the avidin-biotin peroxidase method [14]. Paraffin sections were dewaxed in toluene for 20 min, and rehydrated through 100, 90, 70, and 50% alcohol for 2 min each. All sections were then immersed in PBS solution for 5 min and then 2% hydrogen peroxide solution to block endogenous peroxidase activity for 30 min. The sections were then washed three times in PBS solution for 5 min. The sections were permeabilized in 0.2% Triton in 0.1 M PBS (pH 7.4) for 30 min and washed three times in PBS for 5 min. Sections were then incubated in 10% normal goat serum (NGS) for 30 min at room temperature after which they were incubated overnight at 4 °C with the primary antibody. The sections were washed three times in PBS for 5 min following the cold storage, and incubated for 45 min with biotinylated goat-anti mouse-IgG (1:200) at room temperature. They were then washed three times again in PBS for five minutes, and incubated with the avidin-biotin-peroxidase complex (Vectastain Elite Kit, Vector Laboratories, Burlingame, CA, USA) for 45 min at room temperature. The sections were then washed in PBS for 5 min. Sites of immunostaining were visualized by developing sections in 0.025% diaminobenzidine and 0.03% peroxide for 2–3 min. The sections were then returned to the PBS solution and subsequently immersed in cold running tap water for 5 min. The sections were then dehydrated through 50, 70, 90, and 100% ethanol for 2 min each, and then cleared in toluene. Finally, the sections were mounted with Permount and glass cover slips and allowed to dry. The specificity of the immunostaining was confirmed using negative control experiments in which primary antibodies were substituted with NGS or pre-absorbed with U-II antigen.

2.3. Isolation of human leukocytes

Human leukocytes were isolated from whole blood taken from healthy volunteers as previously described [15]. Specifically ~100 million cells from ~180 ml of whole blood. Monocytes were isolated from the leukocyte harvest using the Graziani-Bowering method [16]. For monocyte-macrophage differentiation, monocytes were resuspended in RPMI 1640 (+10% human serum; type AB, sigma) culture medium at a density of 2.5×10^6/ml and seeded into 12-well tissue culture plates; medium was changed every 48 h. For the generation of foam cells, macrophages were incubated in the presence of 100 μg/ml oxLDL (Intracel) for a further 3 days [15]. Platelets were isolated using a counter current centrifugal elutriation method modified for platelet isolation by eluting platelets from the buffy coat at a flow rate of 9 ml/min [17].

2.4. Taqman analysis

Total RNA was extracted from human tissues and cells using Trizol reagent (Gibco BRL) according to the manufacturer's instructions. cDNA was reverse transcribed from DNAse I (Gibco BRL) treated total RNA using Superscript II reverse transcriptase (Gibco BRL) as previously described [15]. A negative control reaction omitting the reverse transcriptase (−RT) was also performed for each DNase-treated RNA sample. One microgram of each cDNA sample were analyzed for human preproU-II, human GPR14, and human GAPDH expression by real-time quantitative RT-PCR using the fluorescent TaqMan® 5′-nuclease assay as previously described [15]. Primers and probes utilized in this study have been described previously [5]. Values for the leukocyte RT-PCR analysis are means of triplicate assays.

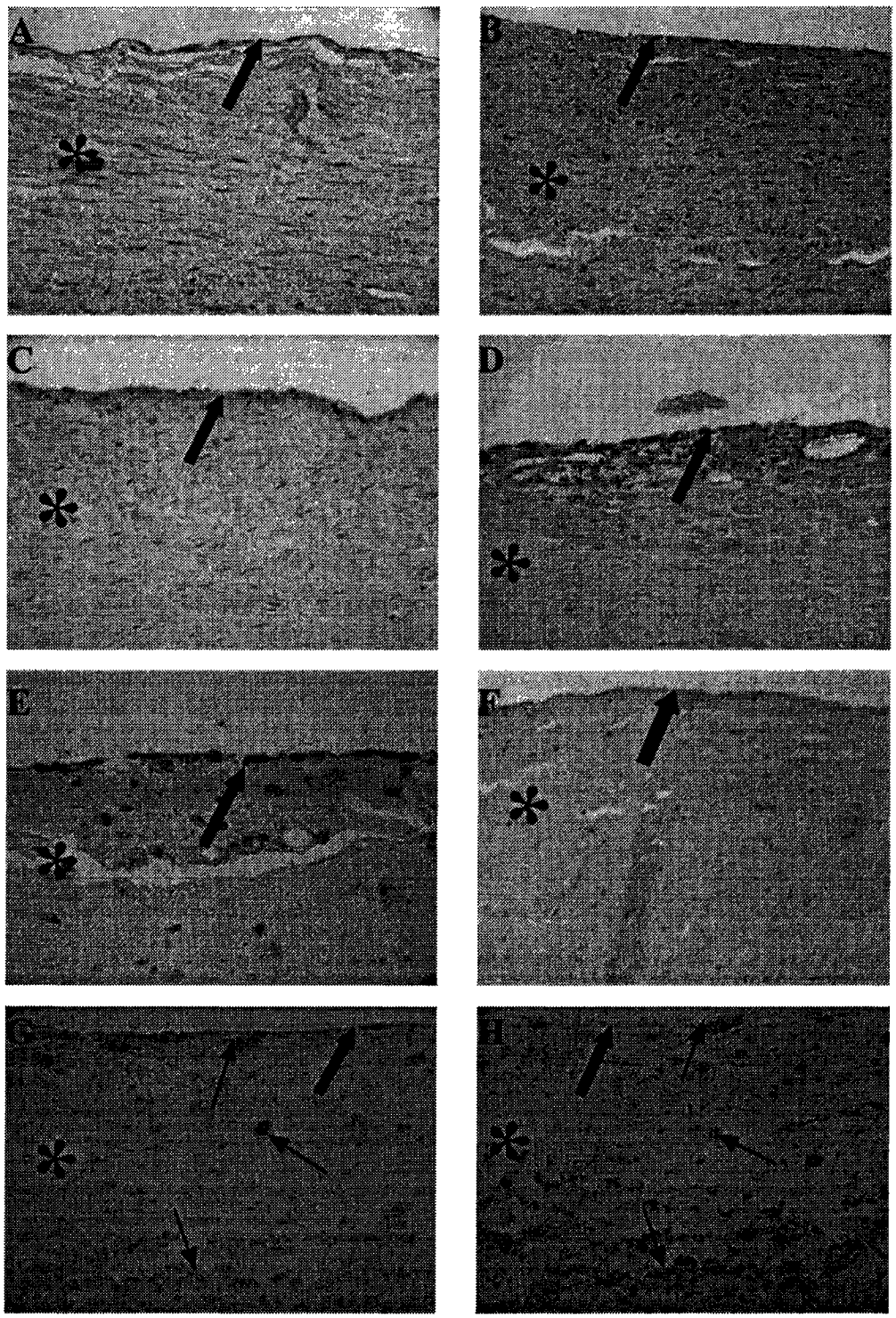

Fig. 1. U-II immunoreactivity in both carotid and aortic tissue samples (large arrows indicate endothelium and asterisks indicate intimal layer). (A) Shown here is a moderately atherosclerotic carotid artery collected at autopsy showing diffuse U-II immunoreactivity within the thickened intimal layer (100× magnification). (B) U-II immunoreactivity in endothelial cells and myointimal cells in the hyperplastic intima of a carotid endarterectomy sample (100× magnification). (C) Normal aorta with distinct endothelial U-II immunoreactivity (200× magnification). (D) Diseased aortic segment obtained at time of autopsy showing intense U-II immunoreactivity in endothelial and inflammatory cells (400× magnification). (E) Diseased aortic sample retrieved during abdominal aortic aneurismal repair showing marked inflammatory cell infiltration with intense U-II immunoreactivity (400× magnification). (F) A section of diseased aorta collected at autopsy incubated without primary antibody as negative control section (100× magnification). Consecutive sections of a carotid artery segment showing U-II immunoreactivity. (G, Small arrows indicate identical cells in serial sections), and α-actin immunoreactivity (H), in smooth muscle cells of the hyperplasic intima (400× magnification).

2.5. Statistical analysis

Data are presented as mean ± S.E. Individual groups were compared using one-way Anova with the aid of a commercial software program (SPSS 11.5). A P value <0.05 was considered significant.

3. Results

3.1. Immunohistochemical analysis

Histological examination of the carotid arteries obtained at autopsies revealed the presence of a distinct immunoreactivity for U-II in the hyperplasic intima and in endothelial cells (Fig. 1A). There was an intense U-II immunostaining in tissue samples obtained from carotid endarterectomies. Specifically, there was abundant staining in the myointimal cells of the hyperplasic intima, with less in the media (Fig. 1B). Also there was apparent immunoreactivity in the carotid endothelium. We observed U-II staining was less abundant but still apparent in medial layers of all carotid artery samples.

In the normal aorta, there was an apparent U-II immunoreactivity only in endothelial cells (Fig. 1C). We have also examined U-II immunoreactivity in atherosclerotic aortae collected at autopsy. In these samples, there was a large degree of inflammatory cell immunoreactivity in addition to specific endothelial cell staining, and some apparent medial immunoreactivity as well (Fig. 1D). Moreover, in tissue samples obtained from repair of abdominal aortic aneurysms, beside endothelial cells, we found a marked expression of U-II immunoreactivity in inflammatory cells (Fig. 1E).

In order to determine cellular phenotypes of cells immunoreactive for U-II we performed colocalization studies using established cellular markers. Specifically we performed immunohistochemistry on serial sections with antibodies against Von Willebrand factor, a marker of endothelial cells, and with anti-α actin antibody a marker of smooth muscle cells and myofibroblasts and compared these to serial sections immunoreactive for U-II. From the serial sections we noted the co-existance of immunoreactivity for

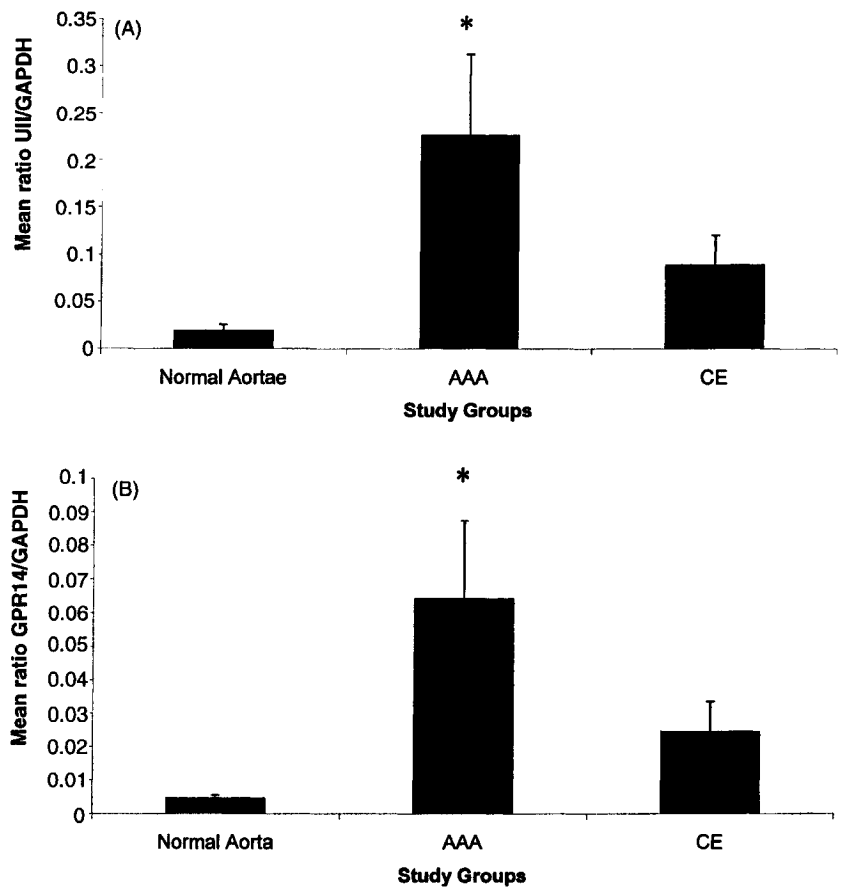

Fig. 2. Relative levels of prepro-U-II (A) and GPR 14 (B) in normal aortic samples ($n = 7$) compared with tissue samples retrieved from abdominal aortic aneurysm (AAA, $n = 8$) and carotid endarterectomies (CE, $n = 17$), normalized to GAPDH. The graph demonstrates that U-II is significantly elevated in tissue samples from abdominal aortic aneurysm compared to normal aortae. Also it demonstrates that GPR 14 is significantly elevated in tissue samples from abdominal aortic aneurismal repair compared to normal aortic samples. The symbol (*) indicates $P < 0.05$.

α-actin with that of U-II, thus indicating U-II expression in cells with the smooth muscle cell phenotype (Fig. 1G–H). We also demonstrated co-localization of Von Willebrand factor and U-II in similar cells indicating U-II expression in cells expressing an endothelial cell phenotype. Negative control sections showed no non-specific immunoreactivity (Fig. 1F).

3.2. RT-PCR analysis

3.2.1. Plaque analysis

Using real-time RT-PCR, it was possible to quantify the mRNA levels of both U-II and GPR14 in tissue samples from abdominal aortic aneurysms. These levels were expressed as the ratio of the copy number of the gene of interest to the copy number of the housekeeping gene, GAPDH. U-II mRNA expression was increased in abdominal aortic aneurysms over normal aortae ($P = 0.036$, Fig. 2A). GPR14 was also significantly increased in abdominal aortic aneurysm samples compared to normal aortae ($P = 0.031$, Fig. 2B). We also evaluated the degree of U-II and GPR14 expression in tissue samples from carotid endarterectomies. However, since we did not have normal carotid arteries with which to compare these, conclusions may be suspect. Nevertheless assuming that normal aortic tissue samples have equivalent levels of U-II and GPR14 as normal carotid arteries, it was observed that U-II mRNA expression was increased in carotid endarterectomies compared to normal aortic tissue, but this increase was not significant. Again GPR14 mRNA expression was also increased in carotid endarterectomies compared to normal aortic tissue, and again the increase was not significant.

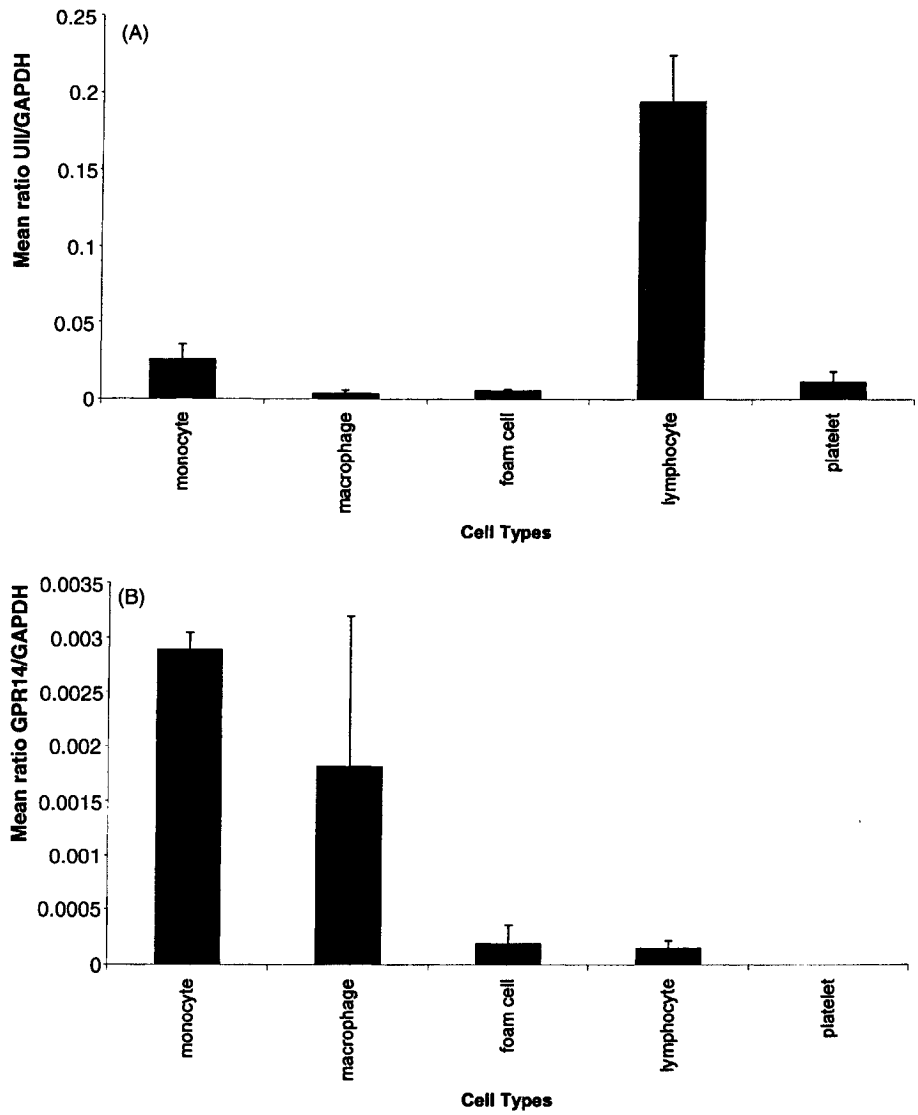

Fig. 3. Relative levels of Prepro-U-II mRNA (A) and GPR 14 mRNA (B) in leukocyte sub-populations normalized to GAPDH. This graph demonstrates that U-II levels are highest in lymphocytes whereas GPR14 is most abundant in the monocyte/macrophage population.

3.2.2. Expression of U-II and GPR14 in human leukocytes

Using real-time quantitative RT-PCR we evaluated the amount of U-II and GPR14 mRNA expression in human leukocyte sub-populations. Values are expressed as the ratio of the copy number of the gene of interest to the copy number of the GAPDH gene. The highest levels of U-II mRNA were seen in the sub-population of lymphocytes when compared with monocytes, macrophages, foam cells, and platelets (Fig. 3A). In contrast, GPR14 mRNA levels were highest in the monocyte and macrophage populations but low in the lymphocyte, and foam cell sub-populations (Fig. 3B). GPR14 mRNA was undetectable in the platelet fraction.

4. Discussion

Recent findings of U-II activity in the cardiovascular system prompted us to determine if U-II is up-regulated in atherosclerosis, the most prominent of cardiovascular disorders. Firstly, we examined the expression of U-II in atherosclerotic lesions of both carotid arteries and of abdominal aortae. To do this we performed immunohistochemistry using anti-U-II antibodies. We were able to demonstrate a large degree of U-II immunoreactivity in atherosclerotic vessels of both carotid and aortic origin. In both types of vessels U-II was most prominent in the hyperplasic intima of the lesion, often with a clear separation between intima and media. Though, medial U-II immunoreactivity was also observed in both carotids and aortae. Interestingly, we noted that normal segments of otherwise diseased vessels also exhibited U-II immunoreactivity. This indicated that there may be a diffuse up-regulation of U-II in the diseased state. To the best of our knowledge this is the first depiction of U-II immunoreactivity in atherosclerotic plaques of carotid arteries and aortae. Importantly, the most prominent staining was found in the lesion, indicating a direct up-regulation in association with atherosclerotic plaques.

With these findings we then proceeded to determine quantitative measurements of U-II, as well as it's cognate receptor GPR14 in tissue samples harvested from patients undergoing carotid endarterectomies and abdominal aortic aneurysm repair. We found that U-II mRNA expression was significantly increased in abdominal aortic aneurysm tissue samples. Importantly, we found that GPR14 mRNA was also significantly elevated in abdominal aortic aneurysms. As noted, both U-II and GPR14 mRNA levels were also elevated in carotid endarterectomies compared to normal aorta. However, this did not reach statistical significance. Also, the biological significance of this is questionable at best since we were unable to compare the mRNA levels for either U-II or GPR14 from the diseased carotid endarterectomy tissue samples with the mRNA levels of normal carotid arteries. Nevertheless, the RT-PCR data on U-II does reinforce the qualitative data observed with immunohistochemistry. In agreement with our findings, others have also demonstrated GPR14 mRNA expression in human aortic tissue [2,3]. In addition, Maguire et al. showed the presence of GPR14 receptors in the aorta by U-II radioligand binding activity [4].

The large degree of inflammatory cell staining observed by immunohistochemistry led us to quantitatively determine the levels of both U-II and GPR14 in the leukocyte sub-populations. We found that lymphocytes were by far the largest producers of U-II, which is quite interesting in light of the fact that the role of lymphocytes in atherosclerosis is becoming increasingly more important [18,19]. In contrast monocytes and macrophages were the largest producers of GPR14, with relatively little expression in either foam cells, lymphocytes, and platelets. These findings suggest that U-II may act in an autocrine or paracrine fashion in the setting of atherosclerosis.

In addition to its marked vasoactivity U-II has been shown to act as a mitogenic factor for smooth muscle cells [8–10]. Hence, the up-regulation of U-II in carotid and aortic atherosclerotic plaques may affect either the vessels vasoactivity or it may act primarily as a mitogenic factor or both. Studies aimed at using a selective GPR14 antagonist will be needed to address the physiological significance of increased U-II and GPR14 expression in atherosclerotic carotids and aortae.

To conclude, here we have demonstrated both a quantitative and qualitative increase in U-II expression in both atherosclerotic carotid arteries and aortae. We also showed that U-II expression was highest in lymphocytes whereas GPR 14 expression was most prominent in the monocyte/macrophage population. These findings suggest a possible role for U-II and GPR14 in the pathophysiology of atherosclerosis.

References

[1] Coulouarn Y, Lihrmann I, Jegou S, et al. Cloning of the cDNA encoding the urotensin II precursor in frog and human reveals intense expression of the urotensin II gene in motoneurons of the spinal cord. Proc Natl Acad Sci USA 1998;95(26):15803–8.

[2] Matsushita M, Shichiri M, Imai T, et al. Co-expression of urotensin II and its receptor (GPR14) in human cardiovascular and renal tissues. J Hypertens 2001;19(12):2185–90.

[3] Ames RS, Sarau HM, Chambers JK, et al. Human urotensin-II is a potent vasoconstrictor and agonist for the orphan receptor GPR14. Nature 1999;401(6750):282–6.

[4] Maguire JJ, Kuc RE, Davenport AP. Orphan-receptor ligand human urotensin II: receptor localization in human tissues and comparison of vasoconstrictor responses with endothelin-1. Br J Pharmacol 2000;131(3):441–6.

[5] Douglas SA, Tayara L, Ohlstein EH, Halawa N, Giaid A. Congestive heart failure and expression of myocardial urotensin II. Lancet 2002;359(9322):1990–7.

[6] Shenouda A, Douglas SA, Ohlstein EH, Giaid A. Localization of urotensin-II immunoreactivity in normal human kidneys and renal carcinoma. J Histochem Cytochem 2002;50(7):885–9.

[7] Elshourbagy NA, Douglas SA, Shabon U, et al. Molecular and pharmacological characterization of genes encoding urotensin-II peptides and their cognate G-protein-coupled receptors from the mouse and monkey. Br J Pharmacol 2002;136(1):9–22.

[8] Sauzeau V, Le Mellionnec E, Bertoglio J, et al. Human urotensin II-induced contraction and arterial smooth muscle cell proliferation are mediated by RhoA and Rho-kinase. Circ Res 2001;88(11): 1102–4.
[9] Watanabe T, Pakala R, Katagiri T, Benedict CR. Synergistic effect of urotensin II with mildly oxidized LDL on DNA synthesis in vascular smooth muscle cells. Circulation 2001;104(1):16–8.
[10] Watanabe T, Pakala R, Katagiri T, Benedict CR. Synergistic effect of urotensin II with serotonin on vascular smooth muscle cell proliferation. J Hypertens 2001;19(12):2191–6.
[11] Sheridan MA, Plisetskaya EM, Bern HA, Gorbman A. Effects of somatostatin-25 and urotensin II on lipid and carbohydrate metabolism of coho salmon, Oncorhynchus kisutch. Gen Comp Endocrinol 1987;66(3):405–14.
[12] Mori M, Sugo T, Abe M, et al. Urotensin II is the endogenous ligand of a G-protein-coupled orphan receptor, SENR (GPR14). Biochem Biophys Res Commun 1999;265(1):123–9.
[13] Liu Q, Pong SS, Zeng Z, et al. Identification of urotensin II as the endogenous ligand for the orphan G-protein-coupled receptor GPR14. Biochem Biophys Res Commun 1999;266(1):174–8.
[14] Giaid A, Yanagisawa M, Langleban D, et al. Expression of endothelin-1 in lungs of patients with pulmonary hypertension. N Engl J Med 1993;328:1732–9.
[15] Patel L, Charlton SJ, Chambers JK, Macphee CH. Expression and functional analysis of chemokine receptors in human peripheral blood leukocyte populations. Cytokine 2001;14(1):27–36.
[16] Graziani-Bowering GM, Filion LG. Down regulation of CD4 expression following isolation and culture of human monocytes. Clin Diagn Lab Immunol 2000;7(2):182–91.
[17] Gibbs BF, Noll T, Falcone FH, et al. A three-step procedure for the purification of human basophils from buffy coat blood. Inflamm Res 1997;46(4):137–42.
[18] Pinderski LJ, Fischbein MP, Subbanagounder G, et al. Overexpression of interleukin-10 by activated T lymphocytes inhibits atherosclerosis in LDL receptor-deficient mice by altering lymphocyte and macrophage phenotypes. Circ Res 2002;90(10): 1064–71.
[19] Daugherty A, Rateri DL. T lymphocytes in atherosclerosis: the yin-yang of Th1 and th2 influence on lesion formation. Circ Res 2002;90(10):1039–40.